AN INVESTIGATION INTO SURFACE FINISH IMPROVEMENT OF SMALL PLASTIC PARTS MANUFACTURED THROUGH ADDITIVE MANUFACTURING

JOSEPH NSENGIMANA

Thesis submitted in fulfilment of the requirements for the degree

MAGISTER TECHNOLOGIAE:

ENGINEERING: MECHANICAL

in the

Department of Mechanical and Mechatronics Engineering
Faculty of Engineering and Information Technology

at the

Central University of Technology, Free State

Supervisor: Dr. JG van der Walt, D Tech Eng: Mech. (Central University of Technology)
Co-supervisor: Dr. E Pei, PhD, MSc. (Brunel University London, UK)

BLOEMFONTEIN
September 2015

DEDICATION

I dedicate this dissertation to my wife, VIRGINIE MUKANTABANA as well as to my sons BOGDAN, BODGAR & JOSHUA. To all who inspired me to leave a legacy of service to others.

DECLARATION WITH REGARD TO INDEPENDENT WORK

I, **JOSEPH NSENGIMANA**, passport number [redacted] and student number [redacted], do hereby declare that this research project submitted to the Central University of Technology, Free State for the Degree **MAGISTER TECHNOLOGIAE: ENGINEERING: MECHANICAL**, is my own independent work; and complies with the Code of Academic Integrity, as well as other relevant policies, procedures, rules and regulations of the Central University of Technology, Free State; and has not been submitted before to any institution by myself or any other person in fulfilment (or partial fulfilment) of the requirements for the attainment of any qualification.

______________________	27.09.2015
SIGNATURE OF STUDENT	**DATE**

Central University of Technology, Free State

ACKNOWLEDGEMENTS

First of all I would like to give thanks to God Almighty from whom every good and perfect gift comes. He gave me the spiritual, mental and physical strength to complete this study.

I would like to thank my supervisor Dr. Kobus van der Walt and co-supervisors Dr. Eujin Pei for their help, advice and time.

My thanks are addressed to my wife Virginie Mukantabana and to my sons who understandably, accepted my long absence from home for the success of this research project.

Without the support of the Centre for Rapid Prototyping and Manufacturing (CRPM), the Product Development Technology Station (PDTS), Rwanda Education Board (REB), University of Rwanda-College of Science and Technology (UR-CST), Central University of Technology, Free State (CUT) and De Montfort University (DMU), the success of this research project would not have been possible. Thanks to these centres and institutions.

Last but not least I would like to thank my colleagues for their help, support and motivation in this undertaking.

ABSTRACT

Nowadays, Additive Manufacturing (AM), also known as 3D printing finds wide application in automotive, aerospace and medical fields. Functional additive manufactured parts must satisfy dimensional accuracy as well as to provide an acceptable quality of surface finish. However the dimensional accuracy of additive manufactured parts are affected by many process variables including accuracy of tessellation from Computer Aided Design (CAD) model, slicing algorithm, data transfer, device motion resolution, powder granulometry, beam offset, process parameters and shrinkage. The surface finish of additive manufactured parts is often poor due to the layer-by-layer manufacturing process of AM. The degree of this so called "stair-stepping" is dependent on the type of AM process and layer thickness used. Different post processing techniques can be used to improve the surface finish. Six post processing techniques were investigated in this study to improve the surface finish of small test pieces that were additive manufactured in nylon polyamide, Alumide® and Acrylonitrile Butadiene Styrene (ABS) plastic materials. The techniques include tumbling, shot peening, Computer Numerical Control (CNC) machining, spray painting, undercoat and hand finishing and chemical treatment by dissolving the surface of the test pieces. A Laser Sintering (LS) process was used to manufacture the nylon polyamide and Alumide® test pieces while Fused Deposition Modelling (FDM) was used for the ABS test pieces. A Coordinate Measuring Machine (CMM) also known as Touch probe scan machine was used for assessment of the dimensional accuracy of post processed test pieces compared to the geometry of the "as built" test pieces. The Chi-square test (χ^2) and the test for differences in deviation range proportions were used to establish the level of significance of differences between '"as built" and each post processing technique. It was shown that there exists a significant difference between deviation range proportions as one compares the "as built" to any one of the six considered post processing techniques. For all the three investigated materials, hand finishing technique produced the best improvement of surface finish though this technique was generally characterized by a lack of consistency in distribution of uniform deviation ranges across individual surfaces as well as across entire test pieces. The spray painting improved the surface finish and was found to be consistent in distribution of uniform deviation ranges across individual surfaces as well as across

entire test pieces. However this technique led to significant positive deviation ranges from the geometry of the "as built" test piece, thus affecting negatively the dimensional accuracy of the "as built" test piece. On one hand, despite the rounding of the sharp corners and the removal of small protrusions, tumbling and shot peening techniques, without affecting negatively the dimensional accuracy of the test piece, it was found that tumbling and shot peening are the optimal post processing techniques to improve the surface finish of relatively wide surfaces of Laser Sintered nylon and Alumide® test pieces. On the other hand, it was realized that tumbling or shot peening technique should not be applied to ABS test pieces as, in addition to the negative effects of the two techniques on nylon and Alumide® test pieces, tumbling and shot peening damage heavily the surfaces of ABS pieces. Chemical treatment by immersion into acetone bath was found to be the optimal technique for improvement of the surface finish of Fused Deposition Modelled ABS test pieces. Though through CNC machining the surface finish of nylon, Alumide® and ABS test pieces was improved, a relatively high standard deviation in surface finish across the entire test piece was observed. In addition to this, excessive negative deviation ranges were observed on the machined surfaces. This can be attributed to a single error during the calibration of the machine or the setting of the cutting parameters which led to the excessive negative deviation ranges from the geometry of the "as built" test piece. The consideration of individual cutting parameters for each surface inclination angle would reduce the standard deviation and eliminate the risk of excessive negative deviation ranges across the entire test piece. However, this approach would lead to excessive machining time, thus increasing the cost of the process. Finally, it was realized that CNC machining is not an appropriate technique to improve the surface finish of small plastic parts with complex shapes in the form of various inclination angles and small entities such as small conical features, round cavities and protrusions.

TABLE OF CONTENTS

LIST OF ACRONYMS AND ABBREVIATIONS

2D: Two Dimensional

3D: Three Dimensional

3DP: Three Dimensional Printing

ABS: Acrylonitrile Butadiene Styrene

AM: Additive Manufacturing

ASM: American Society for Metals

CAD: Computer Aided Design

CNC: Computer Numerical Control

CRPM: Centre for Rapid Prototyping and Manufacturing

DMLS: Direct Metal Laser Sintering

DTM: Desk Top Manufacturing

EBM: Electron Beam Melting

EOS: Electro Optical Systems

FDM: Fused Deposition Modelling

LENS: Laser Engineering Net Shaping

LOM: Laminated Object Manufacturing

LS: Laser Sintering

PDTS: Product Development Technology Station

SLA: Stereolithography

SLM: Selective Laser Melting

SLS: Selective Laser Sintering

SRMT: Surface Roughness Measuring Tester

STL: Standard Tessellation Language

UK: United Kingdom

LIST OF FIGURES

LIST OF TABLES

CHAPTER 1: GENERAL INTRODUCTION

1.1 Foreword

Additive Manufacturing (AM) or also known as 3D printing was developed as early as 1987 by 3D-Systems™ (Wohlers & Gornet 2011). AM covers a number of processes where a part is fabricated through a layer-wise construction method. For all AM processes the part first needs to be designed in a Computer Aided Design (CAD) software package. The virtual part is sliced using dedicated software to create a slice file which is sent to the AM machine for manufacturing of the part (Chua & Leong 2010: 4). AM has been successful applied in biomedical, automotive and aerospace industries (Zarringhalam, Hopkinson, Kamperman & de Vlieger 2006). For low volume and customised production, as compared to injection moulding technology, AM has proved to be economically efficient due to the reduced lead time and the flexibility in manufacturing of parts of any complexity in shape (Nancharaiah, Ranga & Ramachandra 2010: 106, Mireles et al. 2011: 185, Goodridge, Tuck & Hague 2012: 230 and Douglas & Stanley 2014). However the surface finish of AM parts is poor, mainly due to the layer-wise construction method which results in a "stair-step" effect on the surfaces of parts as shown in Figure 1.1.

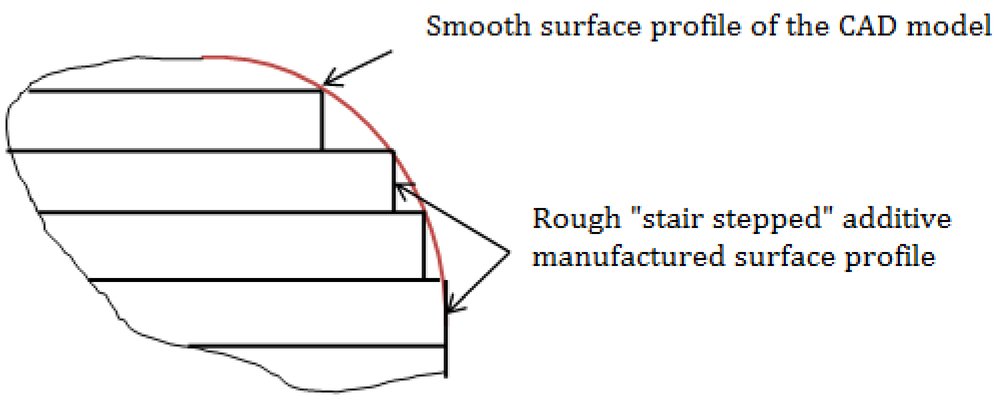

Figure 1.1: Stair step effect

From a design point of view, the improved surface finish of a part offers important benefits such as a good aesthetic appearance and an increase of mechanical properties of the manufactured part.

The purpose of this study is to investigate different post processing techniques in order to improve the surface finish of additive manufactured parts. This study will only focus on improving the surface finish of plastic test pieces manufactured through AM, more specifically in nylon polyamide and Acrylonitrile Butadiene Styrene (ABS). In addition to this, the surface finish improvement of a composite material (50% nylon / 50% aluminium) developed by Electro Optical Systems (EOS) named Alumide® will be investigated. The study focuses on these materials because they are most often used to manufacture plastic parts through the AM process. Polyamide 12 (Nylon 12) covers 95% of the polymer materials mostly used in Laser Sintering (LS) technology (Goodridge et al. ibid.: 236) while ABS thermoplastic material is one of the basic materials most often used in the Fused Deposition Modelling (FDM) process (Marcincinova & Kuric 2012; 25). The focus is also extended to Alumide® material because of the high stiffness and the semi metallic appearance properties of parts manufactured through LS of Alumide® which led it to be used in applications such as jewellery, wind tunnel models, and injection moulding tool inserts (De Beer et al. 2012: 4)

1.2 Problem statement

An inherent shortcoming of AM processes is the steps that are created between the layers as the parts are manufactured layer-by-layer. This “stair-step” effect affects the aesthetic appearance of the manufactured prototypes especially on surfaces with a shallow curve that was manufactured in the horizontal plane as shown in Figure 1.2.

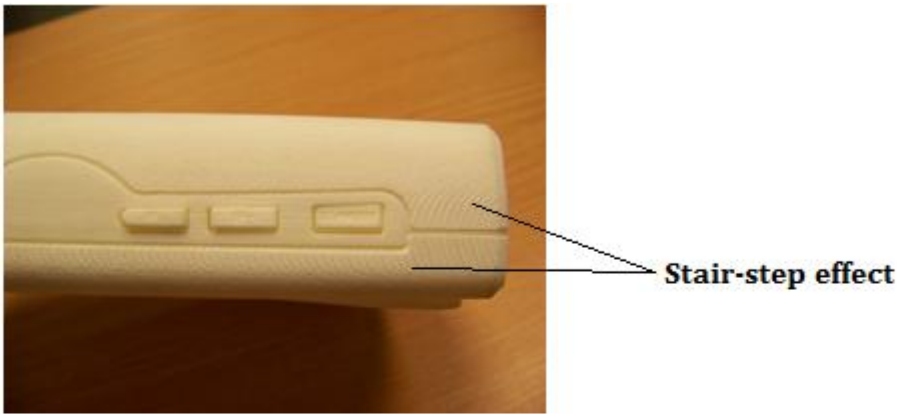

Figure 1.2: Prototype showing stair-step effect

The step height depends on the type of the AM process and machine fabrication parameters, the accuracy of tessellation algorithm and on the type of material that is processed; and may vary from 17 µm up to 200 µm. No literature could be found on the improvement of the surface finish of parts fabricated by LS in Alumide® or nylon polyamides as feed-stock materials and very little on parts fabricated by FDM in ABS.

1.3 Hypothetical resolution

The surface finish of nylon polyamide and Alumide® parts manufactured through LS and ABS parts manufactured through FDM can be improved through surface finishing techniques without influencing the geometrical accuracy of the parts negatively.

1.4 Purpose of the study

The purpose of this study is to find an optimal surface finishing improvement technique for small nylon polyamide and Alumide® test pieces manufactured through LS and ABS test pieces manufactured through FDM. Recommendations in this regards will be compiled and made available to service bureau's that manufactures prototypes.

1.5 Objectives of the study

The following three objectives are to be achieved in this study:

i. The assessment of the dimensional accuracy of six post processing techniques applied to LS of nylon and Alumide® and FDM of ABS test pieces
ii. The measurements of surface finish of the various finishing processes
iii. The recommendation of the best finishing process as a function of material and AM process.

1.6 Importance of the study

The determination of an optimal technique to improve the surface finish of small nylon and Alumide® parts manufactured through LS, and ABS parts fabricated through FDM will add value to the AM prototyping industry through making aesthetically pleasing prototypes possible, which will be more representative of the component when manufactured through its end-manufacturing process such as for example injection moulding.

1.7 Methodology

In this research, the following six post processing techniques to improve the surface finish of small plastic test pieces manufactured through AM were investigated.

i. Tumbling: Vibrating the test pieces together with small abrasive stones wetted by a soapy liquid.

ii. Shot peening: Blasting the test pieces with small stainless steel balls propelled by compressed air.

iii. CNC machining: Removing a thin layer of material from the surfaces of the test pieces through Computer Numerical Control (CNC) machining.

iv. Spray painting: Spraying primer coats followed by one layer of a silver paint onto the test pieces.

v. Undercoat and hand finishing: Applying MS epoxy primer undercoats and hand finishing by sanding to the test pieces.

vi. Chemical dissolving: Dissolving the surface of the test pieces with formic, resorcinol and nitric acids and with acetone.

A small test piece was designed in CAD to highlight the weaknesses and strengths of each surface finishing process. The test piece has angled surfaces varying from 10° to 90° in 10° increments to show the effect of stair stepping at different angles and how each surface finishing process improve this. Four standard test pieces were manufactured for each surface finishing technique in nylon polyamide, Alumide® and ABS materials. In addition to this, one test piece was manufactured in each material that would serve as reference test piece. The test pieces for CNC machining was designed slightly over sized by 0.72 x 0.72 x 0.36 mm^3 to allow the removing of a thin layer from the surfaces of the test piece. The LS test pieces were manufactured at the Centre for Rapid Prototyping and Manufacturing (CRPM) at the Central University of Technology (CUT), Free State while the FDM test pieces were manufactured at De Montfort University (DMU) in the United Kingdom. Depending on the expertise and the availability of technological facilities, the first three post processing techniques for surface finish of the test pieces were performed at CUT while the last three processes were performed at DMU. The surface finish of the reference (as built) and post processed parts were measured at CUT. For assessment of the dimensional accuracy of

AM processes and the post processing techniques, the “as built” test piece and one post processed test piece for each material were scanned by means of a touch probe scanner at CUT. An overview of the experimental procedure is presented in Figure 1.3 through a flow chart diagram.

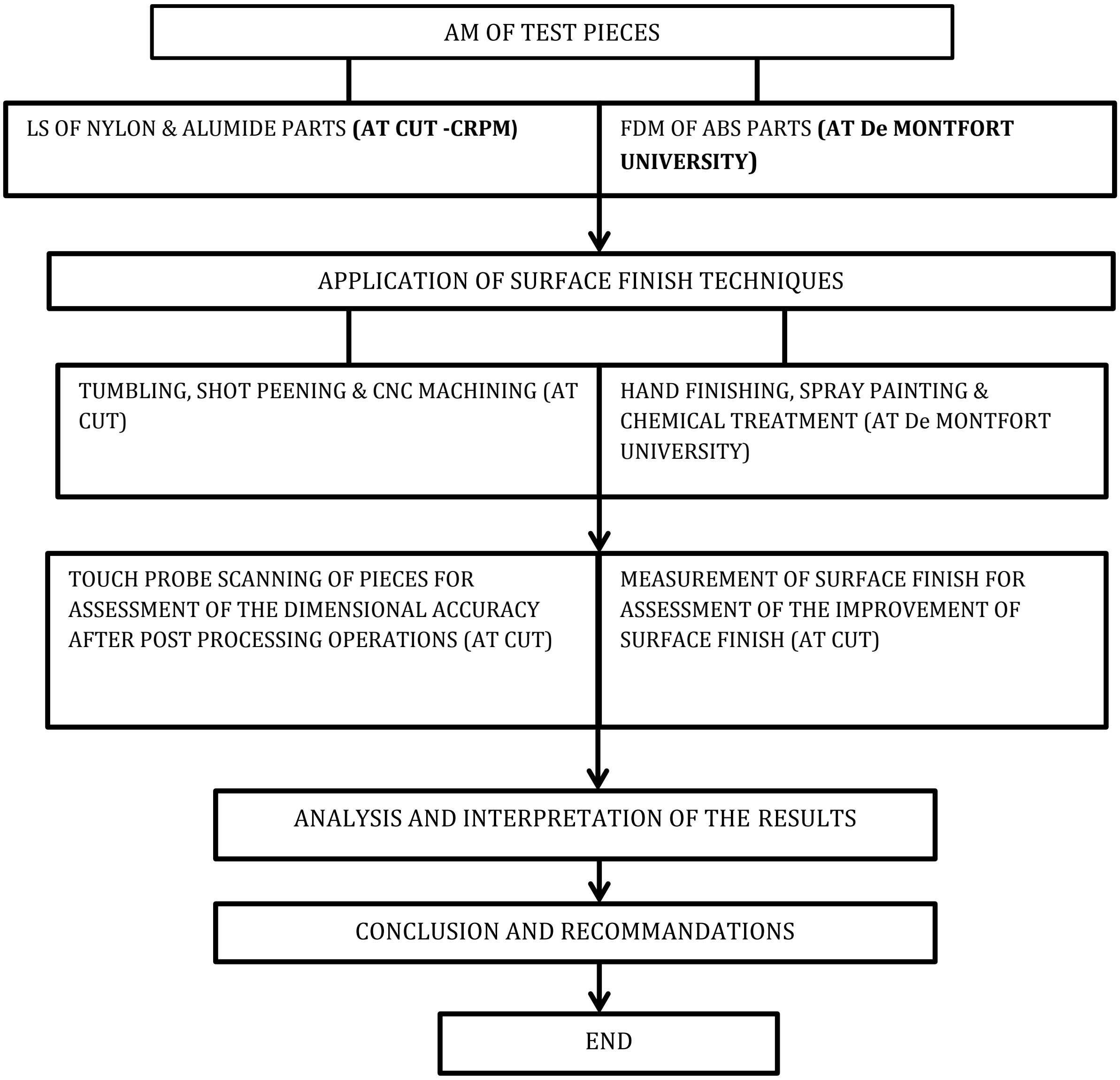

Figure 1.3: Flow chart of activities

The geometry of the “as built” test pieces were compared to the original CAD design to determine the deviations from the CAD dimensions. The geometry of the post processed test pieces were compared to the geometry of the “as built” test pieces to determine the effect of the post processing techniques on the geometry of the test pieces. Data from the touch probe scan were compared and visually displayed using GeoMagic Qualify®

software. The level of significance of frequency differences in dimensional deviation ranges between the “as built” and the post processed test pieces were evaluated using statistical categorical data analysis methods.

CHAPTER 2: PRODUCT DEVELOPMENT AND RAPID PROTOTYPING

2.1 Introduction

For businesses to survive in today's competitive environment, manufacturing companies experience immense pressure to produce products in shorter product development cycles. New product development begins with an analysis of the market where the customer needs are identified. The second phase is to conceptualize the modification of the existing design or the creation of totally new product. At this stage the product idea is formulated, drafted and designed with all engineering specifications to satisfy the customers' needs. The finalization of theoretical design with the use of existing CAD software packages is followed by the manufacturing of the physical product, which finally is to be delivered to the market for sales. Referring to Pugh's new product development model, Figure 2.1 summarizes the main steps involved in the New Product Development cycle.

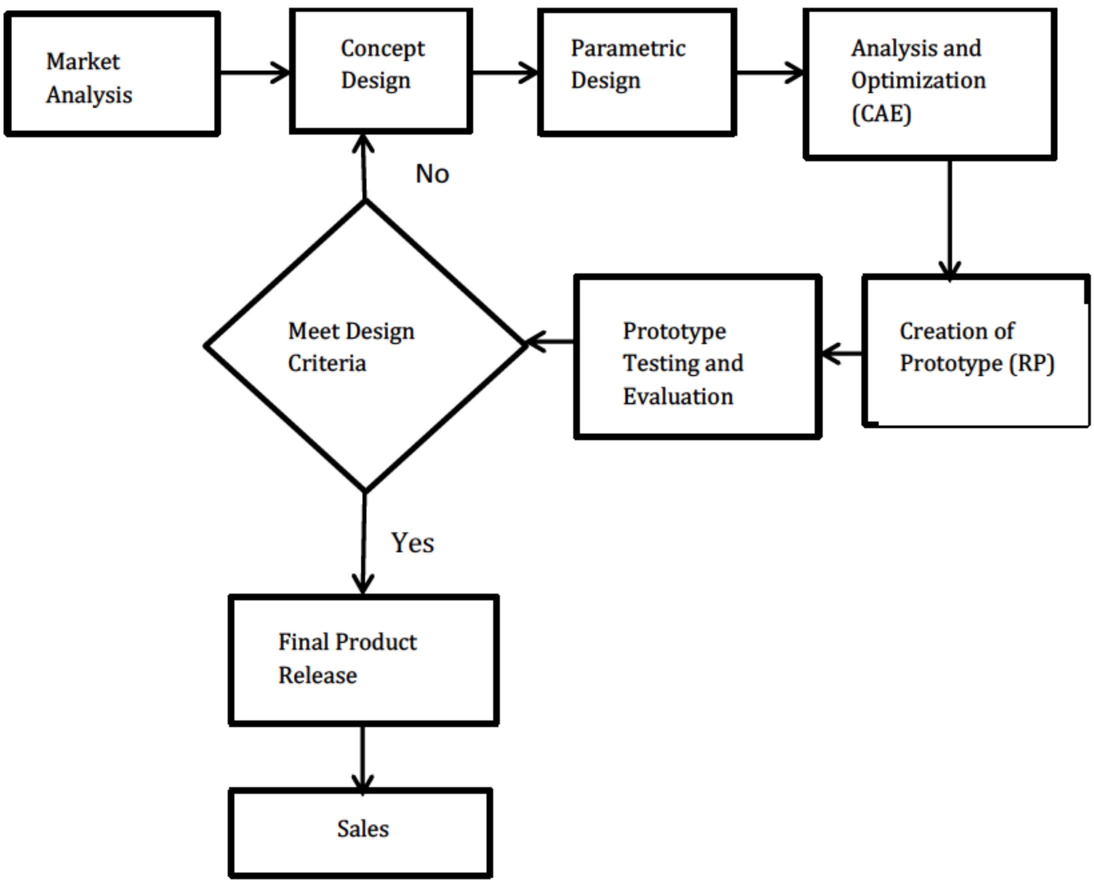

Figure 2.1: Flow chart of the new product development cycle (Kaufui & Aldo 2012: 2)

Each one of these four product development stages may be a long process requiring enough time and investment in terms of skilled personnel to organize and / or execute the work; tooling and equipment.

2.2 New Product Development

In a competitive market, the process of new product development may be challenging as the designer must balance both time and the costs involved for the development of the new product. At an early stage the designer has more chance to influence the design, whereas little information is available for decision making. The information is generated through the process of trying, analysing, evaluating, experimenting, demonstrating, verifying, and validating. At a later stage, there is plenty information available for decision making but with a little chance to influence the design through changes. For example a feature that is complex to manufacture but adds little to the product's market value may go undiscovered until it is too late to change it. It is reported that the excessive time required for new product development is one of the big problems encountered by Small and Medium Enterprises (SME) when they enter the competitive global market (Mohammadjafari, Shamsuddin, Siti & Zayandenroodi 2011: 11844, Ocloo, Akaba & Worwui-Brown 2014: 290).

2.3 Prototyping during the Design Process

The product development process encounters many obstacles that can potentially lead to failure of the project. The earlier these obstacles are discovered, the potential of costs escalating is reduced and deadlines can be met for product launch. Prototyping enables product developers to make necessary changes earlier in the process, thus facilitating iteration leading to improvement in features and functionality of the design.

A prototype can be defined as an approximation of a product (or a system) or its components in some form for a definite purpose in its implementation (Iliescu et al. 2009).

Manual prototyping by professional model makers has been traditionally used by the industry and in most cases, it is time-consuming and inaccurate. It also requires a skilled workforce which can be difficult to staff and train. According to Raghunath and Pandey 2007, the second phase of prototyping started around mid-1970s, when a 3D soft prototype model could be stressed in a virtual environment, simulated and tested with exact material and other properties, but with limited ability to assess the functional performance of the final product. The third phase of prototyping is Rapid Prototyping (RP) which emerged in the 1980s with the rapid growth of CAD (Kamrani & Nasr, 2006).

AM is a process of fabricating objects from 3D model data, usually layer-upon-layer as opposed to conventional traditional subtractive method where a prototype is obtained by removing material from a block. The use of AM allows the design of a product to be realized in its physical form (Nancharaiah et al. 2010, Chua et al. 2010, Behnam 2011 and Koike 2011). It provides true CAD design verification, because digital data is used directly to fabricate cost effective prototypes. A prototype that requires undercuts, overhangs, cores, and inner passages can be built with high accuracy. With a tangible prototype, designers can visualize potential problems and solutions, refining the product as early as possible in the design processes. The use of AM facilitates communication, streamlines the design review process, enables meaningful feedback from different departments, and speeds up the overall product development cycle (Chen & Cheng 1999).

2.4 Additive Manufacturing Technologies

AM allows parts to be produced directly from a 3D CAD model with little need for human intervention. Although several AM technologies exist, all of them have five common steps:

i. To create a digital 3D model using a CAD package.
ii. To convert the CAD model into Standard Tessellation Language (STL) format. This format reduces the part to a set of triangles by tessellating it. The advantage of the STL format is that most CAD systems support it, and it simplifies the part geometry by reducing it to its most basic components. The disadvantage is that the part loses some resolution, as only triangles, and not true arcs, splines, etc., now represent it. However, the errors introduced by these approximations are acceptable as long as they are less than the inaccuracy inherent in the manufacturing process.
iii. To slice STL into thin cross section layers of a typical thickness of 75 to 250 µm (Paul & Baskaran 1996: 169). These sections represent the two dimensional contours that the AM process will generate, when stacked

upon one another, the original three-dimensional part. This sectioning approach is common to all currently available AM processes. Obviously, the thinner the sections, the more accurate the part and more the time required to build the part.

iv. To construct the model one layer upon another.

v. To clean and to finish the model. This involves removing the part from the machine and detaching any supports depending on process (Tanay et al. 2013, Daneshmand, Aghanajafi & Shahverdi 2013: 426).

Table 2.1 presents a summary of the AM technologies most often highlighted in literature, to produce prototypes and end-used parts for specific applications.

Table 2.1: Summary of the most used AM technologies (Mousah 2011:7)

AM technology	**Commer-cially available since**	**Used material**	**Source of energy**	**Suitable usability**	**Accuracy (mm)**
Stereo-lithography (SLA)	1987	Liquid based: Photopolymer (acrylic and epoxy resin)	Ultraviolet laser	Form and fit models	<±0.05
Laser Sintering (LS)	1987	Powder based: fine polymeric, metallic and ceramic powder	CO_2 Laser	Form, fit and functional	0.05 to 0.1
Laminated Object Manufacturing (LOM)	1990	Solid based: Foils (papers, polymers, metals and ceramics)	CO_2 laser beam	Form, fit and functional models	±0.1 (paper) and ±0.15 (plastic)
Fused Deposition Modelling (FDM)	1991	Solid based: thermoplastic filaments.	Thermal energy	Functional	±0.127

AM technology	Commer-cially available since	Used material	Source of energy	Suitable usability	Accuracy (mm)
Laser Engineering Net Shaping (LENS)	1990	Powder based: Metals, stainless steel alloys, Titanium carbide, ceramics, Inconel and Functional Grade Material (FGM)	Neodymium doped Yttrium Aluminium Garnet (Nd:YAG) laser beam	Functional	Good in x-y plane (±0.05) Poor in z-direction (0.4)
Electron Beam Melting (EBM)	1997	Powder based: Metal powder (Ti6AI4V, Ti6AI4V ELI, Titanium Grade 2, Cobalt – Chrome, ASTM F 75)	Electron beam	Functional	±0.4
3D Printing (3DP)	1998	Powder based: Thermoplastics, cement, cast sand, plaster, and corn starch. Binding liquid: various resins, cyanoacrylates as infiltrating materials.	Printing head jetting glue	Form model not suitable for fit model	±5.08
Polyjet	2000	Liquid based: Photopolymer resins	Printing head jetting resin	Form and fit models	0.015 in x-y plane and 0.04 in z-direction

For the purpose of this study, the LS and FDM technologies are thoroughly described below.

2.4.1 Laser Sintering

Laser Sintering was developed at the University of Texas in Austin and commercialized by DTM Corporation between 1987 and 1992. DTM was purchased by 3D Systems in 2002 (Liron 2005). In 1994, the German company Electro Optical Systems (EOS) commercialized a machine that they named EOSINT based on LS technology (Kumar 2003; Wohlers & Gornet ibid.).

As shown in Figure 2.2, LS is a process in which powdered material is fused by the application of laser energy to produce parts. A CAD model is first tessellated and sliced into layers of 50-300 μm (Raghunath & Pandey ibid.: 1). The laser beam in continuous or pulse mode generates the heat for scanning and joining powder in a predetermined sizes and shapes of layers. Fine polymeric powder with particle sizes of between 20 to 100 μm diameter, like polystyrene, polycarbonate, polyamide (nylon) or Alumide®, is spread on the substrate using a recoating system.

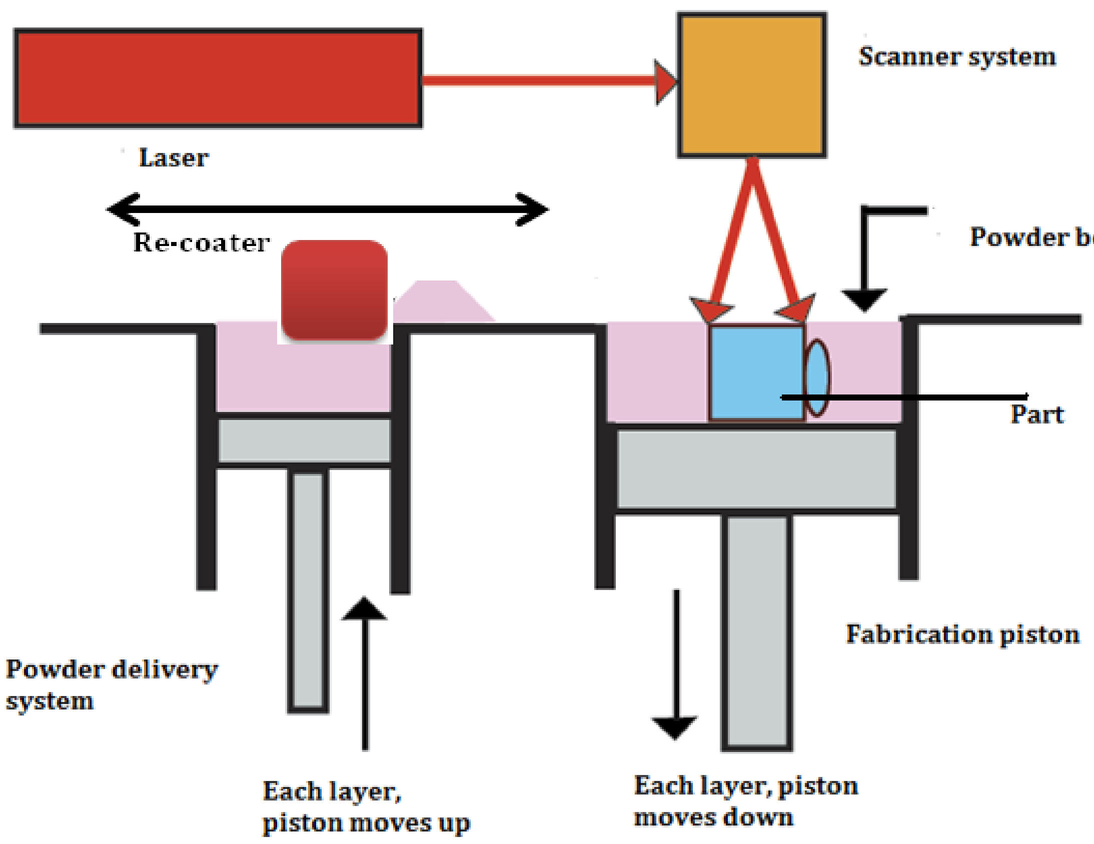

Figure 2.2: Laser Sintering process

The temperature of the entire bed is raised just below the melting point of the powder by infrared heating in order to minimize thermal distortion (curling) and facilitate fusion to the previous layer. The laser is modulated in such a way that only those grains, which are in direct contact with the beam are sintered.

Once laser scanning cures a slice, the bed is lowered and powder feed chamber is raised so that a covering of powder can be spread evenly over the build area by the recoater. The process is repeated until the part is complete. In this process support structures are not required as the un-sintered powder supports the part. The un-sintered powder is cleaned away and can be recycled once the model is complete. A wide range of materials such as plastics, metals, combination of metals and polymers, and combination of metals and ceramics can be used in LS process (Srivastava, Parida and Pandey 2010). It is also possible to use composites or reinforced polymers i.e. polyamides with fiberglass. They could also be reinforced by metals like copper. The disadvantages of the LS process are that the accuracy is limited by the size of particles of the materials used, oxidation needs to be avoided by executing the process in inert gas atmosphere (Kaufi & Aldo ibid.).For polymers, the process has to take place at constant temperature near the melting point of the material necessitating the material to cool before parts can be removed to prevent warpage.

2.4.2 Fused Deposition Modelling

Commercialized by Stratasys in 1991 (Liron 2005, Chua, Leong & Lim 2010 & Musah 2011), FDM is a process which creates models where each layer is built by deposition of molten thermoplastic or wax material in the form of a filament available on spools or cartridge in the case of Dimension or Prodigy FDM machines (Daneshmand, Aghanajafi & Shahverdi 2013: 428). The molten filament is extruded through a heated nozzle as shown in Figure 2.3. The CAD model is saved in STL file format, sliced and then sent to the FDM hardware for modelling (Anoop, Vedansh, Saurav & Siba 2011; Singh & Kumar 2014). The FDM machine's nozzle is heated and a thin filament of molten plastic is deposited on the building platform according to the first layer of the slice file. Since the air surrounding the head is maintained at a temperature which is below the material's melting point, the exiting material quickly solidifies. The extrusion nozzle which follows the tool path controlled by a Computer Aided Manufacturing software package can move in both horizontal (XY plane) and in vertical (Z-axis) directions.

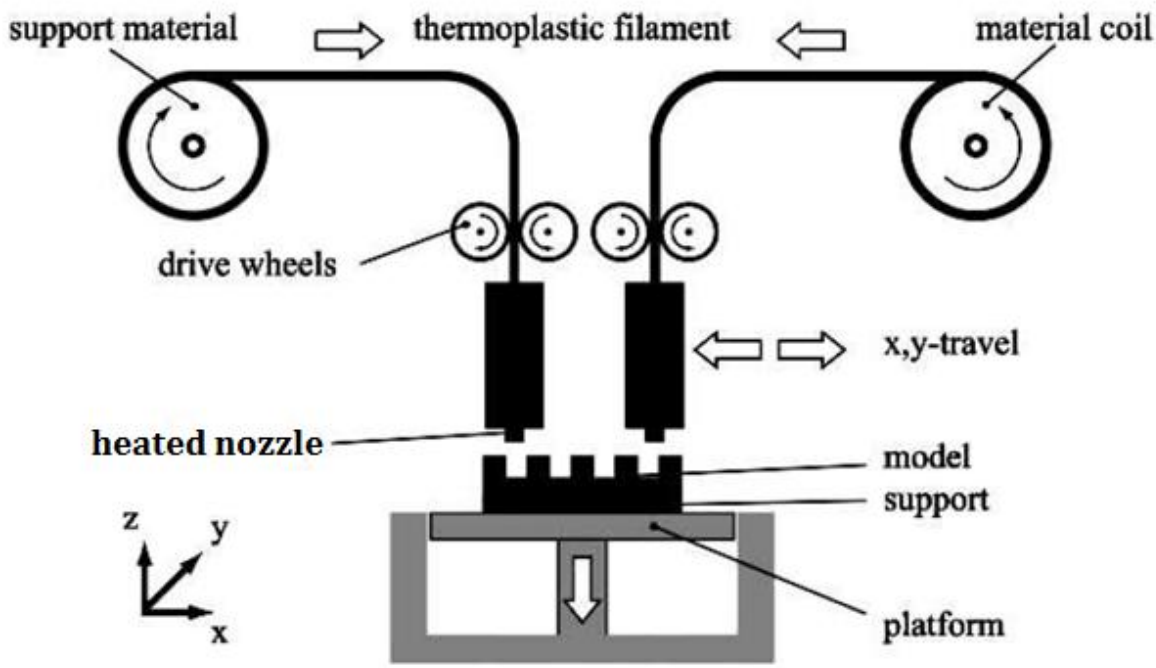

Figure 2.3: Fused Deposition Modelling process (Mousah 2011: 11)

When the first layer is completed, the building platform is lowered by one layer thickness and the next layer is deposited and the process continues in that manner until the entire part is built. Support structures which are built during the process can be removed manually; or when water soluble supports are employed they may simply be dissolved with the latter approach being most valuable with more complicated geometries (Daneshmand & Aghanajafi. 2012: 127). After the removal of the supports, the FDM part can be viewed as a laminate composite structure with vertically stacked layers of bonded fibers or rasters (Ziemian, C., Sharma & Ziemian, S., 2012: 160). While the surface finish of FDM models is generally rougher than that of models produced using Stereolithography (SLA), the end product is typically more robust and durable (Philips Plastics Corporation 2009, Equbal et al 2010: 1261 & Daneshmand et al. ibid.: 426) The build rate is typically twice faster as compared with SLA and can be approximated at 6.35 mm vertically per hour (Matthew, Sunjay & Richard 2003: 243.). FDM printers support the use of ABS plastics which are also frequently used in medical and automotive applications. Materials such as Polycarbonate (PC), Methyl methacrylate Acrylonitrile-Butadiene Styrene (ABSi), Polyphenyl sulfone (PPSF) and other blends of ABS (ABS-M30, ABS M30i, ABS-Plus, ABS-PC and ABS-P400) are also used by FDM technology (Mireles et al. ibid.: 185).

2.4.3 Conclusion

In this chapter, the challenges encountered in new product development process for low volume production has been described. The most used AM processes have been reviewed to highlight their main characteristics in terms of the type and the form of the used materials; the type of the energy used to fuse or sinter the material; the possible achievable dimensional accuracy; and finally in terms of suitable usability of the end product: form model, fit model or functional model. The further progress of this work is focusing on investigation of the surface finish of small plastic parts manufactured from nylon and Alumide® through LS process; and the surface finish of small plastic parts from ABS materials, produced through the FDM process.

CHAPTER 3: LASER SINTERING OF NYLON AND ALUMIDE® AND FUSED DEPOSITION MODELLING OF ABS

3.1 LS process of nylon

3.1.1 Overview and application of nylon

Nylon is a generic name commonly used for all synthetic polyamides. The first publication on basic principle of synthesis of nylon which is known as polycondensation appeared in 1929. In 1935 in a DuPont Laboratory (USA), Wallace H. Carothers invented the original nylon on the basis of the synthesis of poly (hexamethylene adipamide); followed by the issue of the first patent for the production of synthetic polyamide in 1937. In 1938, DuPont produced and commercialized Nylon 6/6 for toothbrush filaments and Nylon 6 was first produced at IG Farbenindustrie in Germany by P. Schlack (Nexant Inc. 2009: 1).

Nylons are commonly identified by the numbers corresponding to the number of Carbon atoms in the monomers. The family of nylons consists of several different types. Nylon 6/6, nylon 6, nylon 6/10, nylon 6/12, nylon 11, nylon 12, and nylon 6-6/6 copolymers are the most common (ASM International 1988 & Nexant Inc. ibid.).

Nylons are characterized by the following advantageous properties:

- Resistance to chemicals: oils, greasy, solvents and bases
- Fire resistance
- Good drawability and good appearance
- Outstanding fatigue to repeated impact and abrasion
- Low coefficient of friction and creep resistance
- High tensile strength and toughness
- Thermo-stability: Nylon retains properties over a wide temperature range from -60 to 110°C
- Good processability: Nylon can be processed through a number of techniques including injection moulding, extrusion, blow moulding, monomer casting, solution coating, fluidized-bed, electrostatic coating or forming (Nexant Inc. ibid.).

The main drawback of nylon is its high moisture absorption. This results in the change of dimensions and mechanical properties of parts manufactured using nylon material.

3.1.2 LS process and nylon

LS technology was first used mainly on polymers and nylon to create prototypes for audio-visual help and fit- to- form tests. With the advancement of RP technologies, the production of form or fit models was expanded to functional model parts produced from plastics, metals, combination of metals and polymers, or combination of metals and ceramics (Kumar 2003: 43). Though LS can use a wide range of materials, ±95% of LS production processes of rapid prototypes and functional parts that are based on polymers, involves polyamide -12 i.e typical nylon grade (Kruth, Levy, Schindel, Craeghs & Yasa, 2008: 2; Goodridge et al. 2012: 236). As compared to other polymers, nylon 12 has an advantage of presenting a wide processing window i.e the range of process parameters that could be successfully used in combination. In order to obtain high mechanical properties of LS of nylon 12, an optimum processing temperature exists, but a deviation of several degrees can generally be allowed, which is not tolerated by other polymers such as nylon 11 or Ultra-High- Molecular-Weight Polyethylene (UHMWPE). The slight deviation of ±2°C from the processing temperature of such materials can result in distortion and curling of corners and edges of the part, which hinders the deposition of the subsequent layers (Goodridge et al. ibid.: 242).

The parameters that vary in LS process are powder size and size distribution, powder density, ratio of powders mixture, scan size, laser fill scan spacing, laser fill power, laser beam speed, pulse size, pulse frequency, part-bed temperature, layer thickness, build orientation. Bacchewar et al. 2007 found that in the LS process, the build orientation and the layer thickness are the most significant factors influencing the surface roughness for the upward oriented faces whereas surface roughness of the downward faces are also influenced by the laser power.

The measurable properties of laser sintered parts are yield and tensile strength, elongation, Young's modulus, hardness, surface finish, line width, layer thickness, shrinkage, porosity, wear resistance rate and density (Kumar ibid.: 44, Caulfield, McHugh & Lohfeld 2007: 478).

In commercial practices, it is not economical to use only the virgin powder to build SL parts. The mixture of the virgin and used powders is recommended in order to compensate the high purchasing cost of the virgin powder and to minimize the waste. Gornet, Davis, Starrs & Mulloy [n.d] conducted a study to characterize DuraForm™

which is a nylon-based thermoplastic, to determine the process stability on the melt index, scanning calorimetry, mechanical properties and surface finish of LS process when the powder is subjected to multiple heating up to seven times. The visual qualitative evaluation indicated that the surface finish was excellent for the first three builds; acceptable for the next two builds and not acceptable after the fifth reuse of the powder. The main reason was found to be the degradation of physical and chemical characteristics of the powder due to the repeated heating cycles.

Kruth et al. ibid. reviewed the materials that were successfully processed or being investigated in LS. They noted that the LS process has an advantage of reusing the powder for further fabrication. However for polymers, a long exposure to heat causes a non-constant consolidation conditions and a shift in melting temperature, causing a drop in powder flowability and a rise in melt viscosity, thus preventing a good sintering quality. These given reasons could be the potential source of rough surface after a certain number of cycles of the used powder. The use of a mixture of 70% virgin and 30% re-used powder was recommended in order to remediate this problem. Therefore, the "refresh rate" i.e the percentage of the material that can be reused must be efficiently monitored in order to achieve a low production cost without compromising the desired mechanical properties, surface finish and dimensional accuracy of the LS parts.

Pham, Dotchev & Yusoff 2008 investigated the significance of the Mass Flow Rate (MFR) on the surface quality of laser sintered nylon PA2200 (PA12) parts. It was confirmed that MFR index is a very sensitive indicator of the change in powder properties and provides a relatively fast and inexpensive method of measuring the rate of the powder degradation due to LS process. It was found that the higher MFR, the better powder quality and vice versa. It was observed that the powder with a lower MFR produced poor rough surface finish known as "orange peel" texture and a higher shrinkage. They recommended a consideration of a MFR higher than (25 to 27) g/10 min when mixing and blending used and new PA2200 powders in order to produce parts with acceptable surface finish without "orange peel" texture (Pham, Dotchev & Yusoff 2008: 2175).

Goodridge et al. report that the density, the surface quality and the accuracy of LS produced parts were found to increase with the decrease of the powder particle sizes. However the particles of diameter smaller than 45 µm can make difficult the spreading of the powder due to static forces. Indeed, the particles of small size joint together at faster rate, thus putting them at risk of unwanted sintering adjacent to desired area which affects negatively the accuracy of the part. Consequently, for LS of macro-parts, the recommended optimal range for particle size being 45 to 90 μm (Goodridge et al. ibid.: 237). The surface finish is also influenced by the level of sphericity of the powder. Powder with a spherical consistency would have an ability to flow over the rotating roller or the recoating blade, and packing becomes efficient due to the reduction of the surface area to volume ratio, thus rendering the surface finish of LS part smoother.

The shrinkage of LS polymers is another significant concern. It is mentioned that the shrinkage of nylon during crystallization hinders the production of dimensional accurate parts (Zarringhalam et al. 2006: 172). The degree of shrinkage which depends on the specific type of the polymer, is mainly affected by the build temperature, the temperature gradient in the powder bed (the greater is the temperature gradient, greater is the shrinkage), laser parameter, the cooling rate and the size and geometry of the part (Goodridge et al. ibid.: 252). To compensate for shrinkage, a scaling factor is applied in each direction of the STL file (Singh, Sachdeva & Sharma 2012: 62).

3.2 LS process of Alumide®

3.2.1 Overview and application of Alumide®

During the EuroMold of December 2003, EOS GmbH released a new material known as Alumide®. Alumide® is a blend of Nylon (polyamide 12) powder and grey aluminium powder. This powder reduces the strength and flexibility of the nylon, thus making Alumide® to be suitable for fabrication of brittle stiff parts with metallic appearance. Alumide® is used to manufacture automotive parts for small production runs and for the production of illustrative models for educational and jig manufacturing purposes (De Beer & Booysen 2005: 389). The LS parts manufactured from Alumide® possesses the following properties:

- Excellent dimensional accuracy
- Well balanced ratio density and stiffness
- Increased thermal conductivity
- Good machinability
- Easy post processing by grinding, polishing or coating (EOS GmbH 2014).

3.2.2 LS process and Alumide®

Toyota Motorsport GmbH (TMG) used Alumide® in the LS process to build various test components for their Formula 1 cars, as well as components to be used in wind tunnel tests. Due to its metallic appearance with a good surface finish, De Beer & Booysen 2005 also reported that in one project, an on-board camera dummy for test-runs and qualifying was built by using Alumide® and an excellent dimensional accuracy was obtained.

For the execution of a tender at the South American market, Technimark, an industrial partner to CUT, developed parts used to hold electronic devices and Printed Circuit (PC) boards of pre-paid electrical meters. The company had four injection mould halves manufactured with inserts in Alumide® as a tooling medium. As compared to conventional tooling method used for the first generation of pre-paid electrical meters, the new approach reduced the mould cost from US$7 765 to US$1 984. Based on the showed performances of the Alumide® developed inserts in term of wear and crack resistance, it was recommended that Alumide® has the potential to serve as an alternative material for rapid tooling (De Beer, Booysen, Barnard & Truscott 2005).

During the LS process, the scanning of a layer of a part is generally done in two steps: scanning the contour and fill-in scanning of the part. As the optimal order of the two steps depends on the type of the material to be laser sintered, Goodridge recommends that it is better to contour the Alumide® at the end; whereas the nylon must be contoured at the beginning in order to produce a better surface finish of the part (Goodridge et al. ibid.: 249).

Combrinck, Booysen, Van der Walt & de Beer 2012 evaluated the effectiveness of using Alumide® in terms of dimensional accuracy, surface roughness and overall production cost for manufacturing of rapid tooling inserts for injection moulds. As a case study, DMLS in maraging tool steel and LS in Alumide® were compared. Due to the layer thicknesses of 0.15 mm in the case of LS, and 0.02 mm for DMLS machine, the surface finish of LS process was rougher compared to the DMLS process and not acceptable for inserts for injection moulding, thus hand finishing was required. The dimensional accuracy of LS Alumide® inserts was found to be acceptable as per CAD drawings. The overall cost of the production was reduced from US$13 471 for DMLS, to US$3 784 for

LS Alumide®, thus rendering the later the best alternative for production of inserts for injection moulds when small production runs are concerned.

De Beer et al. 2012 used Alumide® powder to manufacture jewellery of different shapes on an EOS Formiga LS machine. They realized that from an aesthetic point of view and to prevent the surfaces of the jewellery from trapping dirt, the surface finish of Alumide® is not suitable for this purpose. In order to improve the surface finish, they used tumbling in an abrasive media to polish the jewellery and smooth surfaces resulting in a metallic lustre on surfaces.

The surface finish of Alumide® parts obtained through the LS process can be improved by grinding, polishing, filing or coating (Urednik 2013, EOS GmbH ibid.).

To the best knowledge of the author, not much work has been done in the direction of a comparative study of the above post processing techniques along with tumbling, shot peening, CNC machining or chemical treatment to dissolve the surface, for improvement of the surface finish of Alumide® parts manufactured through the LS process. There is a need to carry out such a comparative study in order to find an optimal surface finish improvement technique for Alumide® parts manufactured through the LS process.

3.3 FDM process of ABS

3.3.1 Overview and application of ABS

Acrylonitrile Butadienne Styrene (ABS) resins belong to a very versatile family of engineering thermoplastics produced by combining three monomers: Acrylonitrile, Butadienne and Styrene. Acrylonitrile contributes to heat resistance, and surface hardness of the system, Butadienne contributes to toughness and impact resistance and the Styrene component contributes to the processability, rigidity and strength. The proportions can vary from 15 to 35% Acrylonitrile, 5 to 30% Butadienne and 40 to 60% Styrene (Ziemian et al. ibid.: 162). Stabilizers, lubricants, colorants and other additives can be added to the system, and while it makes the production of ABS very complex, it allows great flexibility in the product property design. As a result of the unique morphology of ABS, hundreds of different products have been developed and are available commercially.

Injection moulding and extrusion are two processing techniques used for fabrication of ABS.materials The main difference between the two processes is that for injection moulding of ABS products, the melt viscosity is significantly low as compared to ABS-extruded products (ASM International ibid.).

ABS-materials exhibit the following advantageous engineering properties:

- Excellent impact strength at room and at very low temperatures (-40°C)
- The Deflection Temperature Under Load (DTUL) of ABS is sufficient to allow its use in a broad range of application in the temperature range of 110 to 120°C for short exposure time
- Excellent performance under tensile test and creep resistance for long period of time as compared to other plastic materials
- Good resistant to acids, (except concentrated oxidizing acids), alkalies, salts, essential oils, and a wide range of food and pharmaceutical products.

However, ABS products are attacked by many solvents including ketones and esters. ABS plastics are flammable when exposed to high temperature. The electrical insulating of ABS plastics is relatively good, and these plastics are suitable for secondary insulating applications.

3.3.2 FDM process and ABS

ABS plastics have been one of the most popularly used materials for the FDM process. It is reported that the FDM produced ABS P400 parts with compressive strength ranging between 17 and 19 MPa, which equivalent to (80 to 90)% of the strength of injection moulded ABS P400 parts, thus making the FDM manufactured parts to be used not only as prototypes but also for functional testing models (Chua & Leong 2003: 130, Daneshmand et al. ibid.: 428, Novakova & Novak 2012: 412). As shown in Figure 3.1, build orientation, layer thickness, raster angle, raster width, air gap and speed of deposition are the process parameters that mostly affect mechanical properties, dimensional accuracy and surface finish of FDM parts (Anita, Alunachalam & Radhakrishna. 2001: 388, Anoop, Ohdar & Mahapatra 2009).

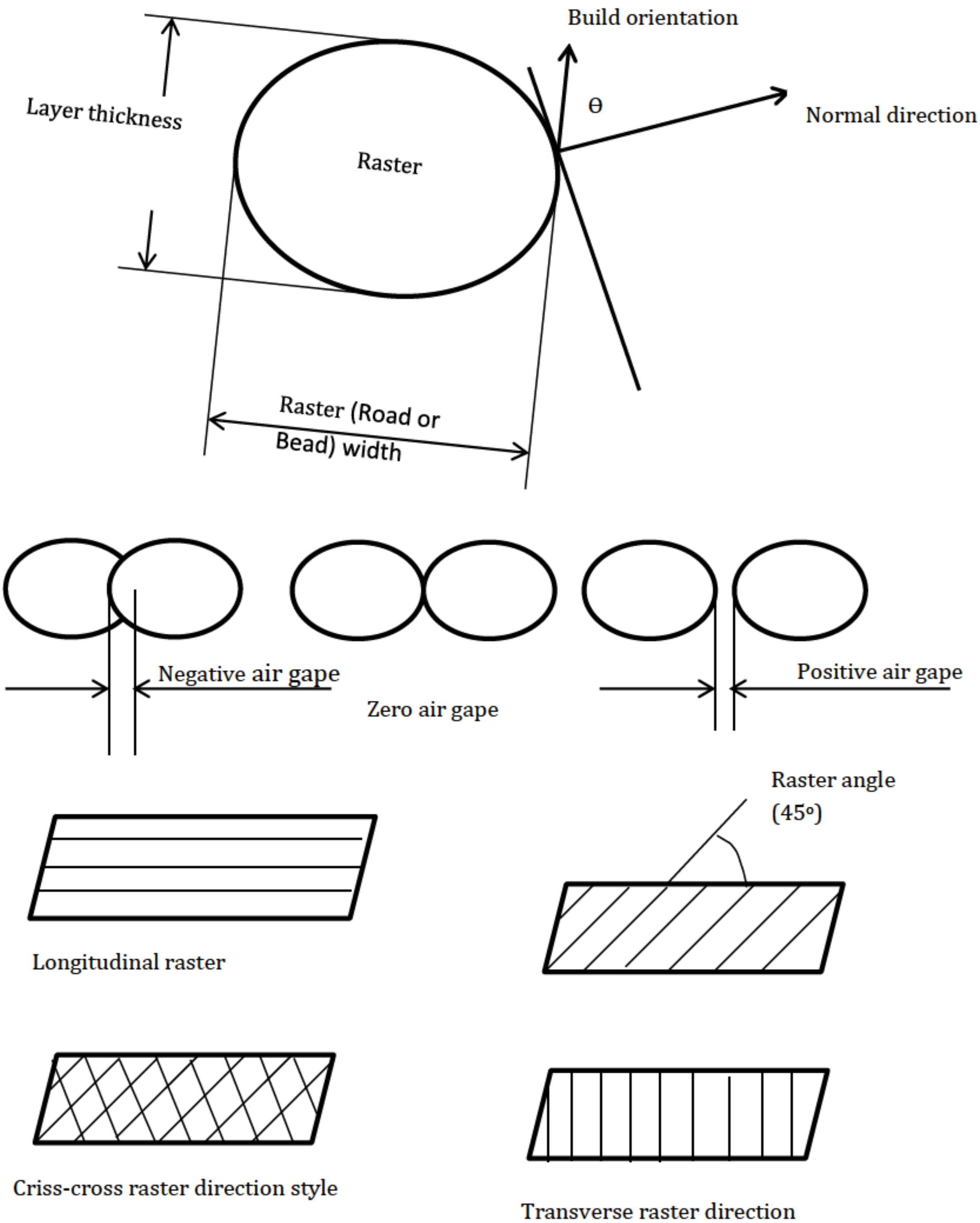

Figure 3.1: FDM process parameter

The shrinkage due to the solidification process of additive manufactured parts affects negatively the dimensional and the form accuracy of the fused deposition modelled ABS parts. Using the Taguchi method, Anoop, Ohdar & Mahapatra 2009 investigated the significance of the process parameters along with their interactions on the dimensional accuracy of FDM processed ABSP400 parts. A prismatic CAD model of 80 mm length, 10 mm width and 4 mm thick was designed, followed by the building of the test parts through FDM process with ABSP400 material. It was found that the shrinkage is dominant along the length and width of the part whereas the thickness is always more than the desired CAD dimensions. They concluded the following:

i. For minimizing the percentage change in length, higher layer thickness (0.254 mm), 0° built orientation angle, maximum raster angle (60°), medium raster width (0.4564 mm) and maximum air gap (0.008 mm) are desirable.

ii. For minimizing the percentage change in width, the medium raster angle (30°) and air gap (0.004 mm) will give desirable results.

iii. For minimizing the percentage change in thickness, the lower values of layer thickness (0.127 mm), built orientation angle (0°), raster angle (0°), higher value of raster width (0.5064 mm) and medium value of air gap are recommended (Anoop et al. ibid.: 4251).

From the Design of Experiments (DOE) and Analysis of Variance (ANOVA) method, Nancharaiah, Ranga & Ramachandra 2010 found that the layer thickness and the road width affect greatly the dimensional accuracy and the quality of the surface finish of ABS parts obtained through FDM process. Furthermore, the air gap showed to have more effect on the dimensional accuracy and little influence on the surface finish (Nancharaiah et al. 2010: 111).

The presence of porosity characterizes the ABS parts fabricated through FDM process, thus limiting their end use in areas of low fluid pressure, in order to avoid catastrophic failure of the plastic vessels such as water pipes and tanks, heat exchangers for air dehumidification and water recovery, hermetic housing for biomedical devices like defibrillators or pacemaker. Mireles et al. 2011 investigated two sealing methods namely, brushing and vacuum infiltration, of FDM fabricated parts from ABS M30 material. The aim of the study was to obtain impermeable end use parts by eliminating voids and reinforcing the bonds of FDM layers. Eleven sealants i.e Miniwax sanding sealer, Thompson’s water sealer, Polyurethane oil base, Polyurethane water base, DEFT clear Woos Finish lacquer, IPS Weld-on 3 Cement, BJB TC-1614 epoxy, Stycast W19+Catalysti 9 epoxy, West Marine penetrating epoxy, West System 109 + 209 Hardener epoxy and Hysol E-30HP, were used for sealing by brushing method. Only five sealers namely, Miniwax sanding sealer, Polyurethane oil base, BJB TC-1614 epoxy, Stycast W19+Catalysti 9 epoxy and West System 109 + 209 Hardener epoxy, were investigated for vacuum infiltration sealing methods. It was found that the sealing by brushing and infiltration with BJB TC-1614 epoxy as a post-processing method of a multi-feature FDM part fabricated from ABS M30 material had notable results. Individually, brushing and vacuum infiltration allowed the test part to repeatedly hold a fluid pressure of 276 kPa and 138 kPa respectively, for at least a period of 5 minutes. As compared to other applied sealing methods, the mean absolute dimensional change between the non-treated and the brushed/infiltrated part caused by application of BJB TC-1614 epoxy was minimal (0.231 mm for brushing and 0.104 mm for vacuum infiltration) and the application of epoxies produced the greatest change in dimensions. It is also noted that if precaution is taken, all sealants showed to produce a desirable aesthetic results with exception to West Marine penetrating epoxy which displayed notable accumulation during the drying process, resulting in unappealing surfaces (Mireles et al. ibid.: 194-195).

CHAPTER 4: ADDITIVE MANUFACTURING AND SURFACE FINISH

4.1 Stair step effect and surface finish

Despite the significant progress made in material flexibility and mechanical performances of AM, a relatively poor surface finish, when compared to the surface finish of traditional fabrication methods, still presents a major limitation in all types of AM processes (Lamikiz, Sanchez, Lopez de Lacalle & Arana 2007, Chen & Lu 2013). Mechanical properties are critically important in the area of AM where the stiffness, strength and surface finish must be sufficient to meet in-service loading and operation requirements. The properties of additive manufactured parts must be comparable to those of parts manufactured through traditional methods in order to make the Solid Freeform Fabrication (SFF) based processes competitive (Caulfield et al. ibid.: 477). The surface quality is greatly influenced by the"stair-step"effect, which is the stepped approximation by layers of curved and inclined surfaces such is shown in Figure 4.1 a-c. This effect is present, to a greater or lesser degree, in all additive layer manufacturing processes (Yasa & Kruth 2011; Giovanni, Liang, Richard & Kenneth 2013).

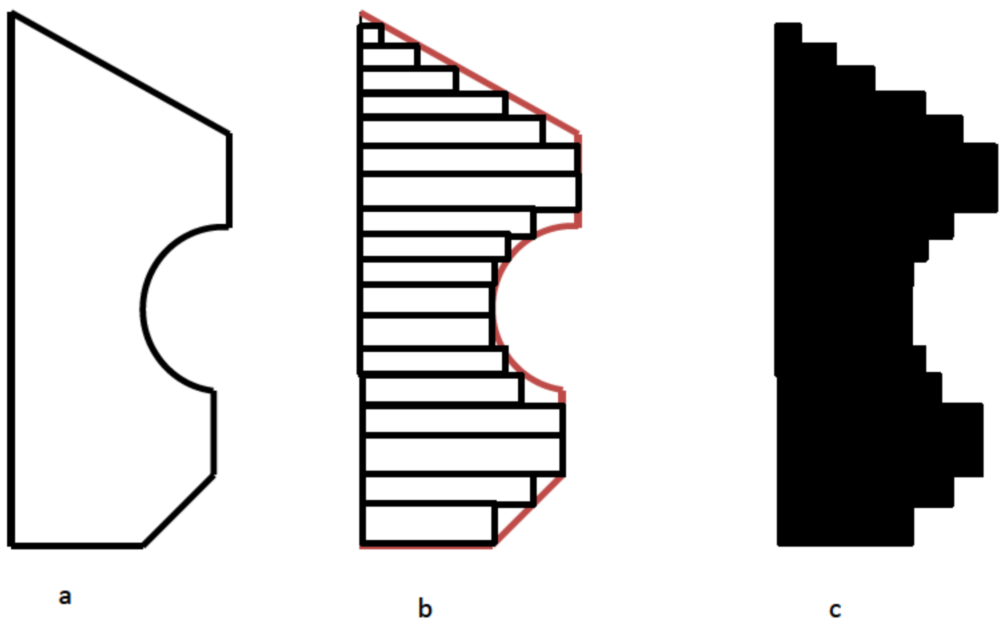

Figure 4.1: Stair step effect: CAD surface profile (a), Layer slices (b), Additive Manufactured profile (c)

Due to the "stair step effect", there are always geometric gaps between the CAD model and the fabricated surface profiles of the part. This effect which is the major cause of a poor surface finish in AM can be minimized by reducing the layer thickness, but this will increase the net build time to generate the part, thus implying a high cost of manufacturing. Other sources of a poor surface finish are chordal effect (Figure 4.2a), burrs which remain on the surface of the part after detaching it from the support structures in the cases of SLA process (Figure 4.2b); and errors due to the starting and the ending of deposition in the case of FDM process. The chordal error is induced when STL files are generated from the CAD model whereby all curved surfaces are approximated as a series of triangles, hence leading to a non-smooth surface (Pandey, Reddy & Dhande 2003a & b). A big resolution of STL file will also affect negatively the good appearance of AM parts.

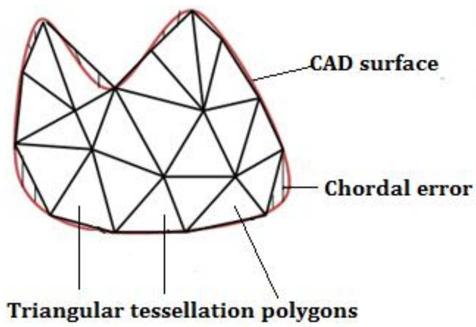

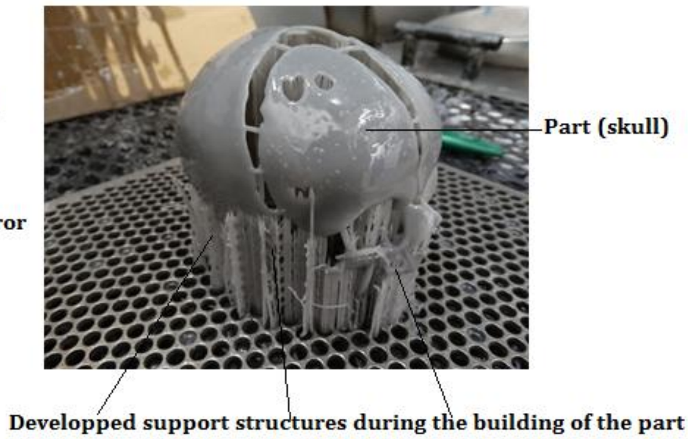

a b

Figure 4.2: Chordal effect (a), Skull fabricated through SLA process with support structures to be detached during the cleaning process (b)

A rough solution to this problem is to add a positive offset to the surface, build the prototype and then perform surface finishing operations to bring it back to the original dimensions (Vasudevarao, Prakash & Handerson [n.d.]). The difficulties encountered in finishing undercuts and small recesses are limitations of using the above approach. It is advisable that before the tessellated model can be sent to AM equipment for building, the validity of all the tessellated triangles in the model must be checked. Depending on the nature of the invalidity of facets (triangles), an appropriate repair of tessellation algorithm is to be applied to the design. A good surface finish of parts is a concern since it can affect the part accuracy, reduce the post processing cost and improve the functionality of the part (Vijay, Danaiah & Rajesh 2011). Post processing techniques can be used to improve the surface finish of AM parts. These processes may however also increase the overall production time, thus defeating the main goal of using RP. Post processing techniques may lead to the loss of dimensional accuracy of the part. These treatments should therefore be minimized to avoid negative effects on the geometry of the part compared to the original CAD.

4.2 Prediction of surface finish of parts manufactured through AM

At an initial stage of AM, the surface finish can be theoretically predicted in advance in order to achieve an optimal process planning. The one-dimensional surface finish can be represented by the level of irregularities or deviations $y(x)$ of the actual surface profile from a reference or fiducial line- ox as indicated in Figure 4.3.

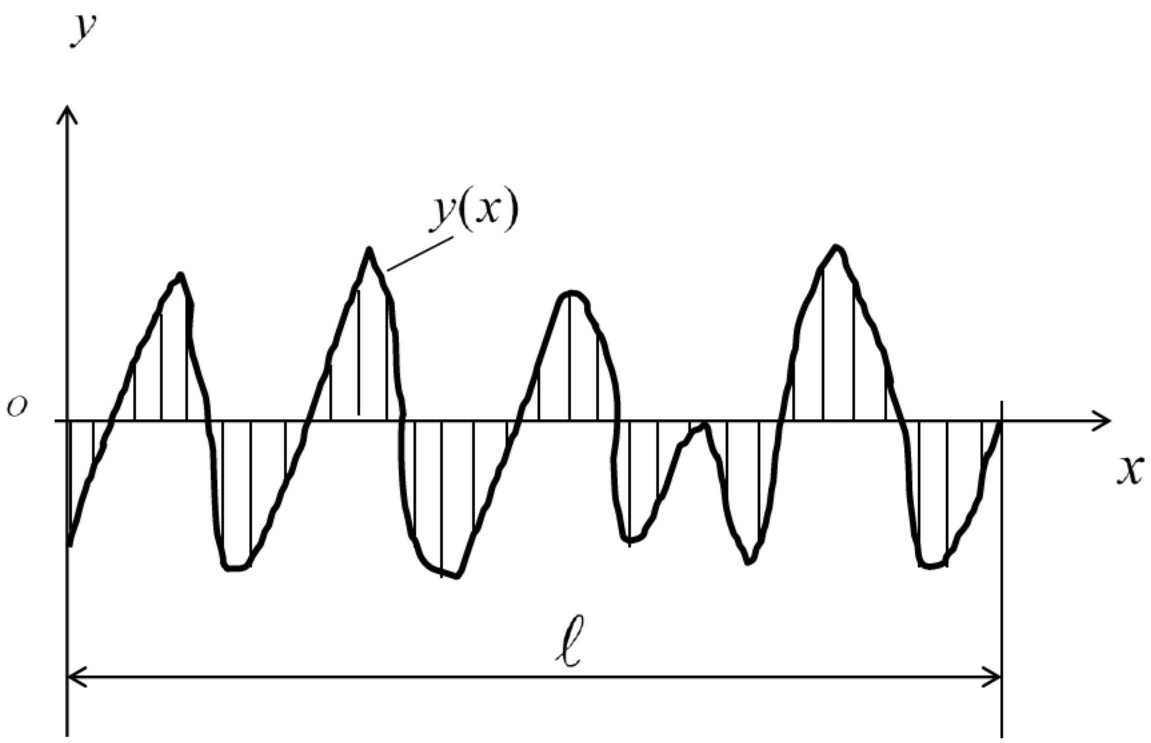

Figure 4.3: One dimensional surface finish representation

The one dimensional average surface roughness R_a is defined as follows:

$$R_a = \frac{1}{\ell}\int_0^{\ell} |y(x)| dx \tag{4.1}$$

ℓ -is the length of the profile through which the surface roughness is evaluated

$y(x)$-the level of deviations of the surface heights from the fiducial line- ox .

For a given layer thickness L , it has been shown that the surface roughness is dictated largely by the surface angle ϴ, that the normal to each particular surface makes with the vertical direction as illustrated by Figure 4.4.

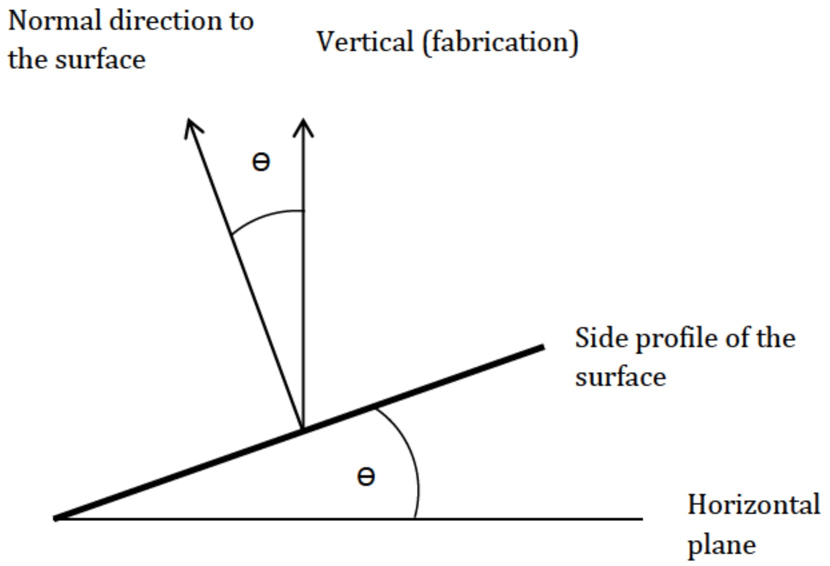

Figure 4.4: Surface angle and fabrication direction

Considering a surface profile of length W , inclined at an angle θ from the horizontal direction, covered by two consecutive layers, the surface irregularities of the profile of the part obtained through AM with a layer thickness L , can be illustrated as shown in Figure 4.5.

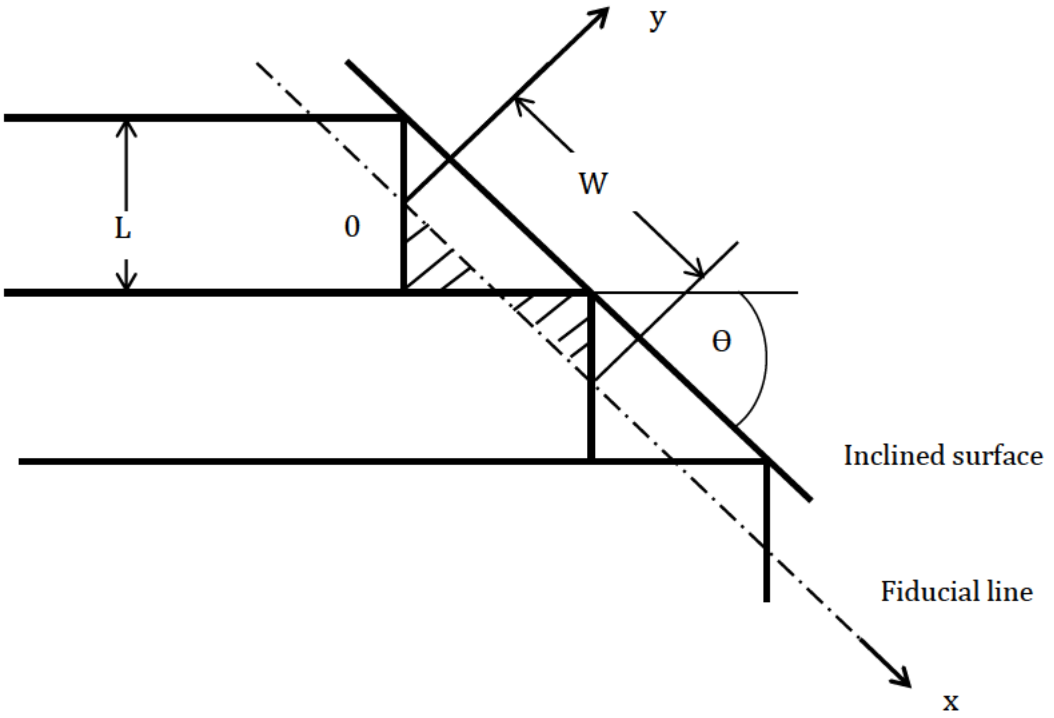

Figure 4.5: Surface finish of AM process

Applying eq. (4.1), the average surface roughness, denoted by R_a is determined by the following relationship:

$$R_a = \frac{1}{W}\int_0^W |y(x)|dx \tag{4.2}$$

Evaluating the surface area between the fiducial line and the actual profile obtained from AM for the two consecutive layers, the surface roughness R_a is given by:

$$R_a = \frac{1}{\frac{L}{\sin\theta}}\left(\frac{L^2}{4\tan\theta}\right) = \frac{L\sin\theta}{4\tan\theta} = \frac{L\sin\theta\cos\theta}{4\sin\theta} = \frac{L\cos\theta}{4}$$

$$R_a = \frac{L|\cos\theta|}{4},\ 0\leq\theta\leq 180° \tag{4.3}$$

Eq. (4.3) shows that the surface roughness is influenced by the layer thickness L and the surface angle θ. With a fixed constant layer thickness L, as the surface angle increases from 0 to 90°, the surface finish decreases and the theoretical minimum surface roughness, Ra=0 being expected at vertical planes where Θ=90° as indicated in Figure 4.6.

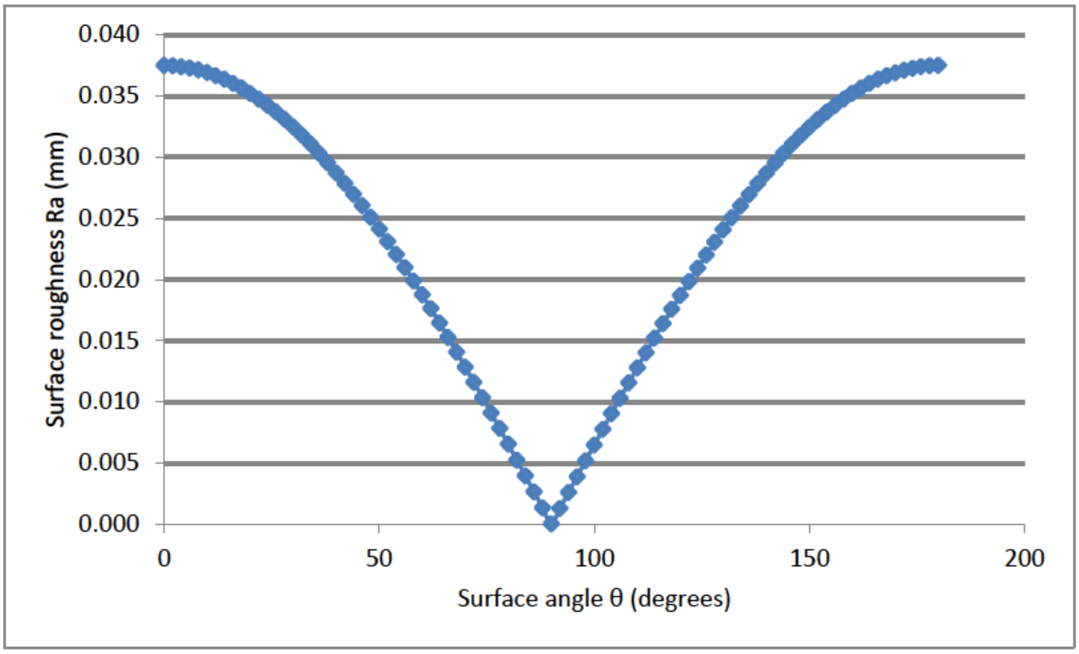

Figure 4.6: Variation of the surface roughness with surface angle

Reeves and Cobb [n.d.] validated eq. (4.3) by developing a series of test samples, an example of which is shown in Figure 4.7 to evaluate the surface finish of a SLA processed part. The benchmark consists of a range of angled surfaces in 2° increments where 0° represents the up facing whereas 180° is the down facing surface.

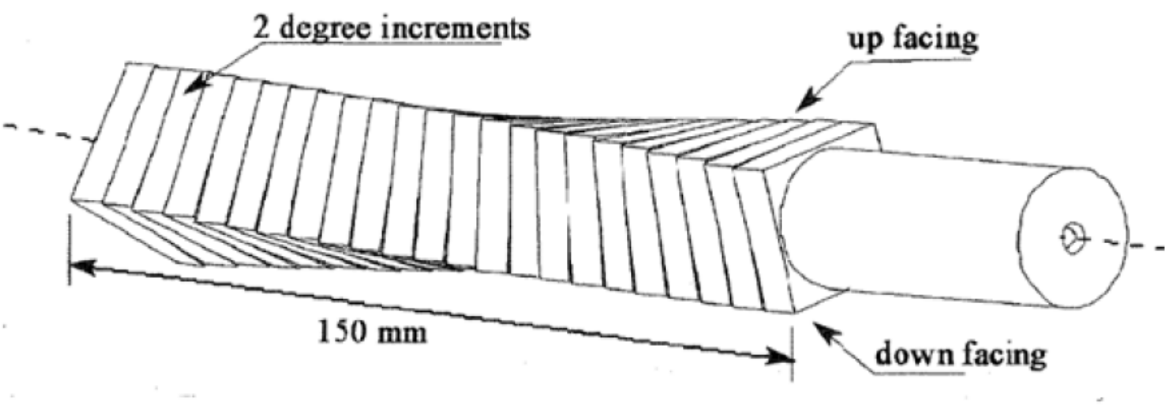

Figure 4.7: Test sample geometry used to determine SLA surface roughness

Source: Reeves & Cobb [n.d.]

The measured surface roughness decreased as the surface angle increases from 0 to 90°, and the minimum surface roughness has been measured at faces with surface angles in the vicinity of 90°. For the faces located at angles from 90 to 180°, the surface finish increases but not in a symmetrical manner; the planes at 100 to 150° showing better surface finish than expected.

The surface profile angle ϕ which depends on the material properties in AM can be illustrated as shown in Figure 4.8.

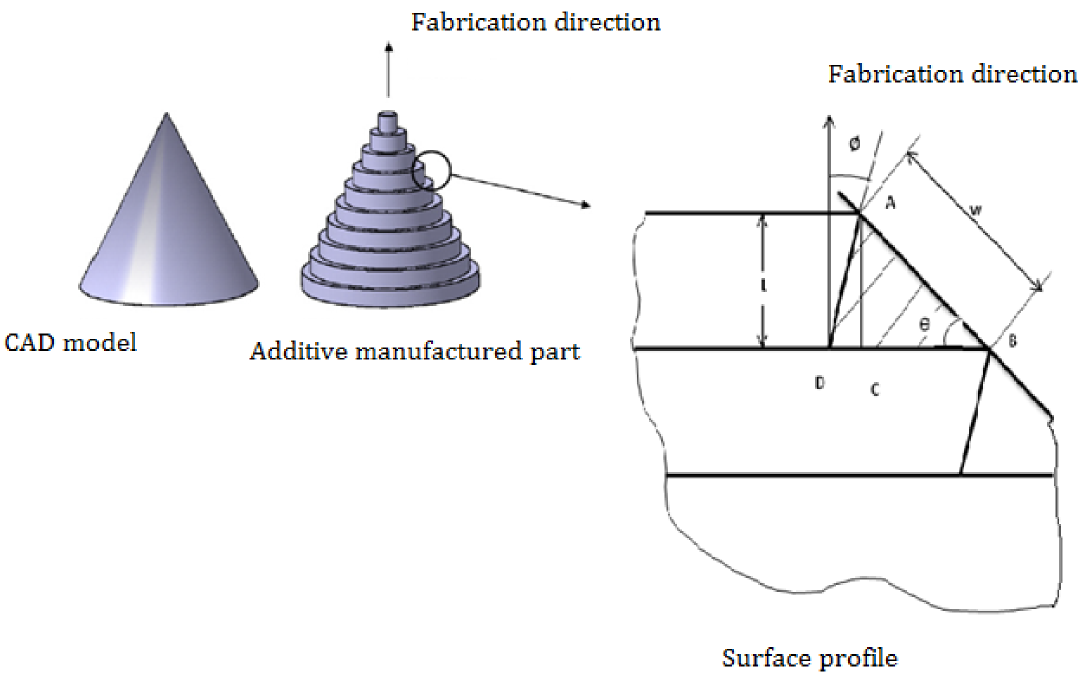

Figure 4.8: Surface profile angle in AM process (Daekeon, Hochan & Seokhee 2008)

From Figure 4.8,

$BD = BC + CD$ - is the step width and W - is the distance between consecutive step edges.

The surface finish R_a is defined as the ratio between the area S of the triangle ABD, and the distance W between consecutive step edges.

$$R_a = \frac{S}{W} \tag{4.4}$$

$$R_a = \frac{AC}{2W}(CD + BC) \tag{4.5}$$

$$BC = \frac{L}{\tan\theta},\ CD = L\tan\phi \text{ and } W = \frac{L}{\sin\theta} \tag{4.6}$$

$AC = L$ -is the layer thickness;

ϕ -is the surface profile angle and

θ -is the inclination angle of the surface with the horizontal.

Replacing (4.5) into (4.4), we have

$$R_a = \frac{L}{2}\left(L\tan\varphi + \frac{L}{\tan\theta}\right)\frac{\sin\theta}{L}$$

$$R_a = \frac{L}{2}\left(\frac{\sin\varphi}{\cos\varphi} + \frac{\cos\theta}{\sin\theta}\right)\sin\theta$$

$$R_a = \frac{L}{2}\left(\frac{\sin\varphi\sin\theta}{\cos\varphi} + \cos\theta\right)$$

$$R_a = \frac{L}{2}\left(\frac{\sin\varphi\sin\theta + \cos\varphi\cos\theta}{\cos\varphi}\right)$$

Finally,

$$R_a = \frac{L}{2}\left|\frac{\cos(\theta-\varphi)}{\cos\varphi}\right|, 0 < \theta < 180^o \tag{4.7}$$

For a given AM machine, the layer thickness L is a constant and the surface profile angle ϕ which depends on the material properties can vary from 5° to 15°, and also can be fixed as a constant for a given AM process. For the layer thickness $L = 0.150mm$ and surface profile angle $\phi = 10^o$, the theoretical surface roughness distribution for AM models is shown by Figure 4.9.

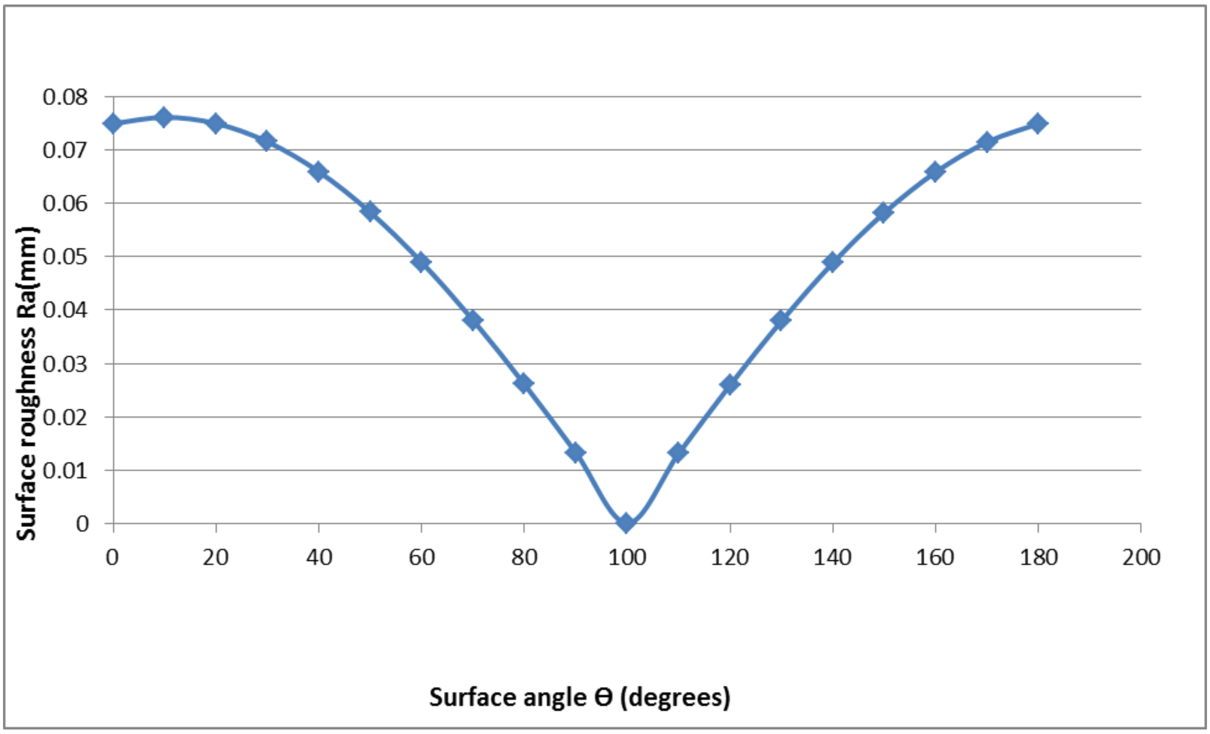

Figure 4.9: Theoretical distribution of surface finish with the surface angle for a surface profile angle of 10°

With the above prediction, the surface finish R_a is almost equal to zero at angles Θ closer to 90° and attains the lowest value (R_a=0) on a down facing surface located at angle Θ=100°.

Campbell, Martorelli & Lee 2002, based on the research done by Reeves & Cobb, developed an algorithm to enable the AM model users, to visualize and optimize the different surface roughness values within a CAD system, and thereafter to optimize the build orientation of the part. Table 4.1 shows the scope of the limitations of their investigation.

Table 4.1: Investigated processes and findings

AM system	Used material	Layer thickness (μm)	Assessment of the prediction as compared to eq. (4.3)
SLA 350	Epoxy 5190	100	For up facing surfaces from 0 to 90° and down facing surfaces from 150 to 180°, the trend of the curve of Ra is as per the prediction of eq. (4.3) but the measured values are greater than the predicted values as per eq. (4.3). For down facing surfaces between 90 and 150°, the trend of the curve is as predicted, but the measured Ra values are 10 μm less than the prediction as per eq. (4.3)
Actua2100 (Jetting process)	Thermo Jet 45	100	On up facing faces, the surface finish can be reasonably predicted with the measured values less than the calculated as per eq. (4.3). For down facing surfaces, the measured values are worse and with a trend to oscillate randomly, therefore not easy to predict.
FDM 1650	ABS 400	253	For up facing surface from 0 to 45°, the surface roughness varies randomly and it is difficult to predict. For faces at 45 to 180°, the surface finish was reasonably predictable and the measured Ra values were less than the calculated with exception in the range of 75 to 110°.
LOM 1015	MRP 014	114	With large oscillations, the trend of the measurements follows quite reasonably the trend of the theoretical curve within 10 μm for the most part of the curve.
Z402(3DP process)	ZP11 (starch based)	175	The surface roughness was unpredictable. With the least variation of measurements lying between 12 and 23 μm, the trend does not follow the theoretical curve, thus not showing the effect of the surface angle, and also suggesting that the effect of build orientation has a less importance in this process.

Based on the fact that there was no common applicable method for all investigated AM processes whereby a designer could predict quantitatively the surface finish on a particular area prior to the fabrication of the part, Campbell, Martorelli & Lee ibid. proposed an algorithm for visualization of the surface roughness. Implementing the system using the AutoLisp language within AutoCAD 14 and incorporating it in STL file, the algorithm allowed displaying ranges of colours to represent surface roughness with an increment of 5 μm. Areas of unacceptable surface roughness can be identified and an alternative build orientation can be determined by checking all possible orientations by rotating the digital model about X and Y axes at 5° intervals until surface finish requirements are satisfied.

Eq. (4.7) is only based on the geometry of the AM process and does not take into account unpredictable roughness characteristics, such as support removal burrs and other process parameters such as build orientation, laser power, beam speed and hatch spacing (distance between consecutive laser scans). This is one of the causes of the existence of gaps between the theoretical prediction and the actual measured distribution of the surface roughness. Moreover, the visualisation prediction of the surface finish of the part prior to its fabrication proposed by Campbell, Martorelli & Lee contained discontinuous roughness distribution over several partial areas on the surface of the test model.

To more correctly predict the surface roughness on faces at intermediate face between two faces with known surface roughness, Daekeon, Hochan & Seokhee 2008 proposed a new calculation based on an interpolation method.

$$R(\theta) = R(\theta_p) + \frac{R(\theta_n) - R(\theta_p)}{\theta_n - \theta_p}(\theta - \theta_p) \tag{4.8}$$

θ -the actual intermediate surface angle

θ_p -the surface angle of the previous face

θ_n -the surface angle of the next face

$R(\theta)$ -the predicted surface roughness at angle θ

$R(\theta_p)$ and $R(\theta_n)$ -the measured roughness values at previous and next faces at surface angles θ_p and θ_n respectively.

The interpolation of empirical roughness is based on discrete number of measurements meaning that, a large number of measurements are required to achieve a high resolution. In order to obtain reasonable calculated results with the minimum number of measured roughness values, the error analysis in relation with calculating the roughness values by changing the number of the measured roughness was used. For the total surface angle range from 0 to 180°, by fixing the surface angle intervals or increments of 3°, 6° and 9° corresponding to 60, 30, and 20 measurements respectively, it was found that, with exception of some specific values and some small intervals of surface angles, the measurement error could be less than 2 µm. It was concluded that reasonable calculated results can be achieved if the number of measured roughness is over 60 measurement points. Using this approach, the surface roughness values could be calculated at surface angles that were difficult or even impossible to measure. More importantly, the actual surface roughness distribution could be reasonably reflected with a minimum number of roughness data.

The proposed prediction methodology was applied to an industrial skull model composed of 116,961 facets produced through LS and FDM processes. The predicted roughness values were less than 35 μm near the mouth, nose, and forehead of the model, which indicates that the FDM roughness distribution curve was properly reflected in the prediction (Daekeon et al. ibid.: 670).

It is traditionally considered that the built edge profiles of deposited slices of AM part are of a rectangular shape. On the basis of their microscopic study of a Solid Ground Cured (SGC) part, Pandey, Reddy & Dhande 2003a, realised that due to the curing of raw material, hence uncontrolled flow of the molten material, the built edge profiles of deposited slices are comparable to a parabola with a sharp vertex instead of being approximated to a rectangular shape (Pandey, Reddy & Dhande ibid: 64). For FDM manufactured parts, a deterministic formula to predict the surface roughness was proposed.

$$R_a = (69.28 \text{ } to \text{ } 72.36)\frac{L}{\cos\theta}, \text{ in } \mu\text{m}. \quad (4.9)$$

L - the layer thickness in mm and θ - the build orientation angle.

For optimization of the minimum layer thickness and the minimum build time, adaptive slicing methods were studied. From eq. (4.9), by fixing a surface roughness R_a value and applying the appropriate algorithm, a required layer thickness is calculated as follows:

$$L = \frac{R_a \times \cos\theta}{70.82} \quad (4.10)$$

It was concluded that for other AM processes, the developed formula can be applied by adopting an appropriate coefficient of proportionality to $\left(\frac{L}{\cos\theta}\right)$ expression.

Daekeon, Jin-Hwe, Soonman, Jungil & Seokhee 2009 noticed that due to the mechanism of building a part by FDM which is based on the melting of a filament, the surface profile from FDM process must differ from the surface profile obtained from other AM processes. The cross-section shape of the deposited filament being close to an elliptic curve, they formulated a mathematical model of surface roughness in FDM by assuming the filament profile as an elliptic curve (Figure 4.10). Using the traditional method of computing the surface roughness R_a as per eq. (1), a mathematical model to predict the surface roughness for FDM parts was developed. The layer thicknesses of 0.178 mm and 0.254 mm were used and Reeves & Cobb's specimen was used with an angle increment of 3°. Figure 4.11, shows the validation of the theoretical developed method when it was compared to the empirical measurements of surface roughness on different angles for a layer thickness of 0.178 mm.

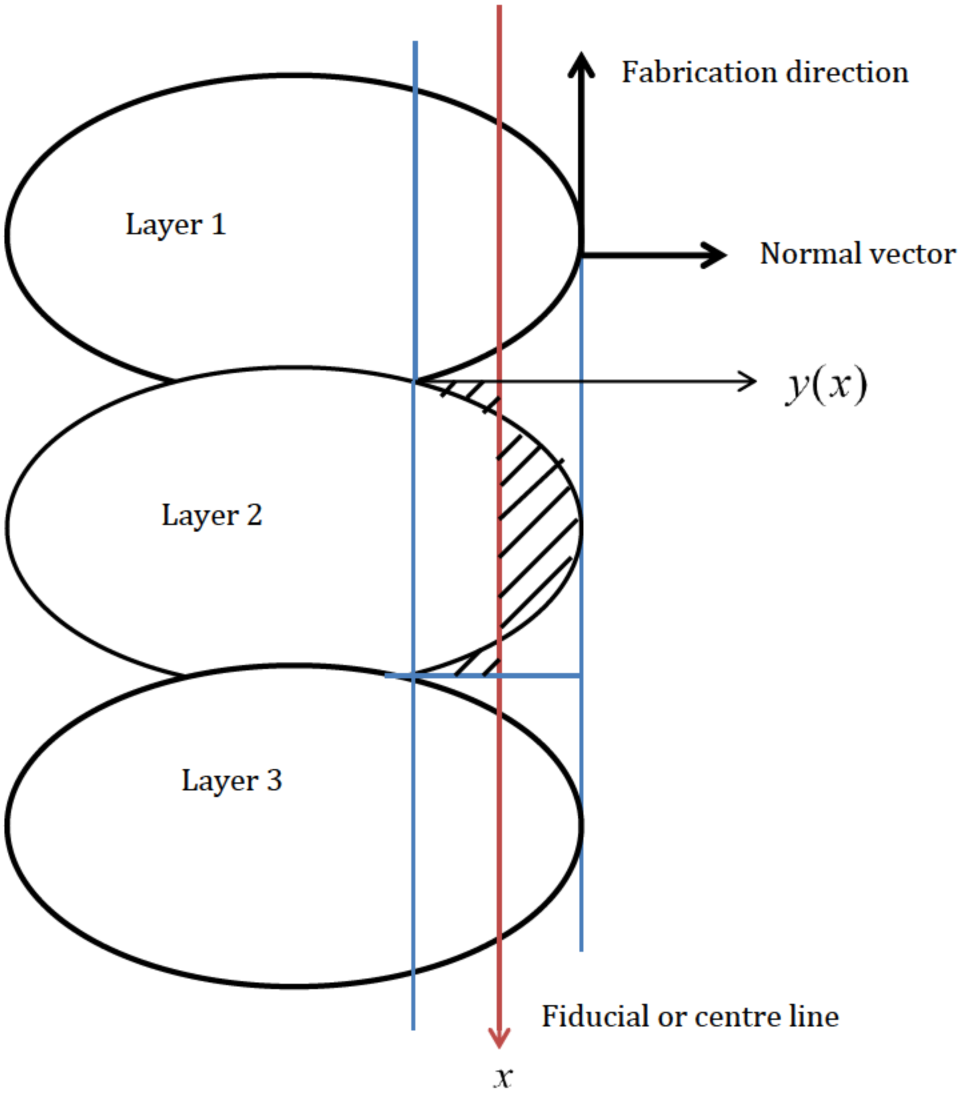

Figure 4.10: Elliptical curve method for prediction of surface roughness of FDM parts

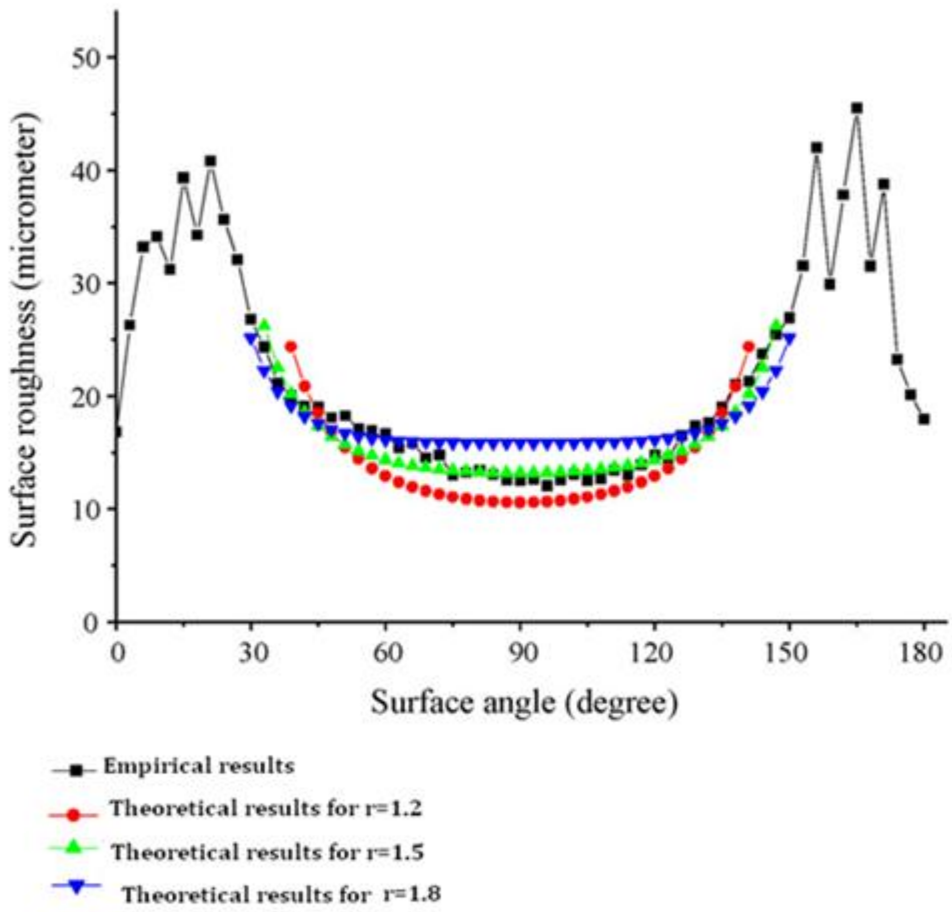

Figure 4.11: Empirical and computed surface roughness Ra for a layer thickness of 0.178 mm for various section shapes of filament (Source: Daekeon, Jin-Hwe et al. 2009)

The validity of the new proposed analytical approach for prediction of surface roughness of FDM parts was proved and it was recommended that it can be used to achieve advanced process planning in AM (Daekeon, Jin-Hwe et al. 2009: 5600).

Optimal build orientations of the parts have been investigated as a solution to improve the surface finish obtained through AM. Chen & Lu 2013 investigated the effect of the build orientation on surface finish of a crank and a slider mechanism built using VeroGrey™ material on Objet Eden 350 machine with a layer thickness of 16 µm. For the transverse build orientation, surface finish, Ra, of 3.122 µm and 8.502 µm were obtained when the measurement is made in axial and transverse directions respectively. For the axial build orientation, the surface finish was 14.787 µm in axial direction and 8.675 µm in transverse direction. It was concluded that when layer thicknesses are getting thinner with ever developing AM technologies, the build orientation is no longer a major factor that influence the surface finish of the part, instead, it is found that the scanning orientation on layers has more influence on the surface finish (Chen & Lu ibid.: 378).

4.3 Improvement of surface finish

As presented in Section 4.2, extensive research has been conducted to predict the surface roughness of AM parts. The measured surface finish values however appeared to be greater than the predicted values and not acceptable for the desired surface quality of the end-use parts. For industrial applications, the improvement of surface finish of additive manufactured parts during the building process and/or by post processing techniques is still a great necessity.

In the case of the FDM process, it has been shown that the optimal selection of process parameters such as layer thickness, deposited bead width, air gap, build orientation and model temperature, can reduce the effect of surface roughness. It has been established that the layer thickness, the build orientation and the interaction between these two parameters have a significant effect of the surface finish of FDM parts.

Adaptive slicing algorithm which consists of using various layer thicknesses instead of one constant slice thickness was used with subsequent Abrasive Flow Machining (AFM). AFM is a surface finishing process where abrasive particles in fluid state flow under pressure through the workpiece to remove burrs thus improving the surface finish of the part. Using AFM a surface roughness of 1.27 µm Ra was obtained. The main limitation was the lack of control on pressure distribution in the viscous media, which may cause the uneven removal of material from the additive manufactured part, through the brittle fracture mechanism (William & Melton 1998). An improvement of surface roughness was obtained through adaptive slicing algorithm followed by CNC machining of the part with a ball end mill cutter. It was realized that the accessibility of intricate features and details to the ball end mill cutter was the main limitation to that technique (Kulkarni & Dutta 2000).

In cases where small cutting forces are suitable to machine the staircase of parts manufactured by the FDM process, Pandey, Reddy & Dhandi 2003b, designed and used Hot Cutter Machining (HCM). The use of HCM is based on the fact that the ABS material softens when it comes into contact with a hot edge, thus involving very low cutting forces for the removal of material. HCM allows access to intricate detail of parts manufactured through AM where conventional turning, drilling, milling or grinding processes cannot be performed to improve surface roughness. An improvement of surface finish from 100 to 0.5 µm R_a could be achieved through the process (Pandey, Reddy & Dhandi 2003b: 325).

Hand finishing which consists of three main steps: priming, polishing and cosmetic spraying; is time consuming and not efficient for a high number of small parts. In order to overcome the drawback of the manual surface finish process, Schmid, Simon & Levy 2009 used a Rosler vibratory grinding machine with different ceramic medias, to improve the surface finish of Duraform PA12 and Duraform HST (fibre-reinforced plastic) parts manufactured through the LS process. The investigation was carried for 4 h, 8 h and 12 h. They found that the surface roughness of all tested parts was around R_a=2 µm with equal standard deviation and the period of 8 h delivered the best surface finish. Furthermore, they applied on PA12 a dip coating in silicon, polyurethane and vinyl-acrylpolymers solutions to increase the water tightness of the parts. The dip coating in silicon and vinyl-acrylpolymers showed desirable results for enhancement of water tightness (Schmid et al. 2009: 7-8).

Galantucci, Lavecchia & Percoco 2009 investigated the improvement of surface finish of ABS parts through chemical treatment by dissolving the surface using dimethyl-ketone (acetone). An experiment was conducted on 24 square base prism specimens of 18 mm x 18 mm x 8 mm of sizes by immersion into a bath of 90% of acetone and 10% of water for a period of 5 minutes. After immersion, all specimens were kept at a room temperature in vacuum atmosphere for a period of 1 hour. For the top surfaces, the roughness was improved from (17.2-11.8) µm R_a to (4.6-2.2) µm R_a, while for the side surfaces, an improvement from (18.8-16.2) µm R_a to (8.7-5.8) µm R_a was observed. The dimensional accuracy was also checked and it was noticed that all specimens shrank by less than 1%, while the weight was increased by 1% due to the absorption of the liquid.

Daneshmand & Aghanajafi 2012 studied the aerodynamic coefficient of a wind tunnel model manufactured through FDM. The nose and the tail of the model were manufactured from ABS-M30 material with layer thickness of 0.180 mm. The obtained surface roughness was 16 µm R_a. A chromium coating was applied to the surfaces through electroplating, and the roughness decreased to 0.832 µm R_a, thus improving the aerodynamic coefficient (Daneshmand & Aghanajafi ibid.: 126). Daneshmand, Aghanajafi & Shahverdi 2013 carried out research aiming to introduce a 3D printing process using a high performance composite material Zp 150 and FDM technology with ABS-M30, as methods for rapid production of cheap hybrid models that is used to calibrate wind tunnels and to measure aerodynamic coefficient. The surface finish roughness being an important parameter in testing of aerodynamic properties of fabricated wind tunnel models, they found that, with FDM of ABS-M30, acceptable dimensional accuracy and surface roughness can be achieved by setting the layer thickness to 0.127 mm which was the minimum feasible value at that time. They concluded that the wind tunnel models fabricated using AM methods can be used in subsonic and transonic wind tunnel testing for aerodynamic data base development (Daneshmand et al. 2013: 432).

Addanki, Medha, Venkatesh & Deepesh 2012 applied chemical treatments using Dimethylketone (Acetone) and Methylethylketone (MEK) to improve the surface finish of ABS P400 parts obtained through FDM. The concentration, the temperature of the chemical solutions, the initial roughness and the time for which the part is treated are the four variables that were taken into consideration. By using Design of Experiments (DOF) and Analysis of Variance (ANOVA) methods, they optimised the chemical treatment. With a maximum curing time varying from 2 to 4 hours, a drastic improvement of surface finishes, comparatively equal to the level of the surface finish of plastic moulded parts was found. The above post processing technique was recommended to be marked as it was economically acceptable.

Kuo & Su 2013 found a simple and economical method to improve the surface quality of a wax injection tool fabricated from ABS through the FDM process. Using an appropriate vibratory filling mechanism, a mixture of a hardener and composite of aluminium powder (70%) and epoxy liquid resin (30%) was used as filling material, to fill the parabolic surface profile of FDM fabricated part as illustrated in Figure 4.14.

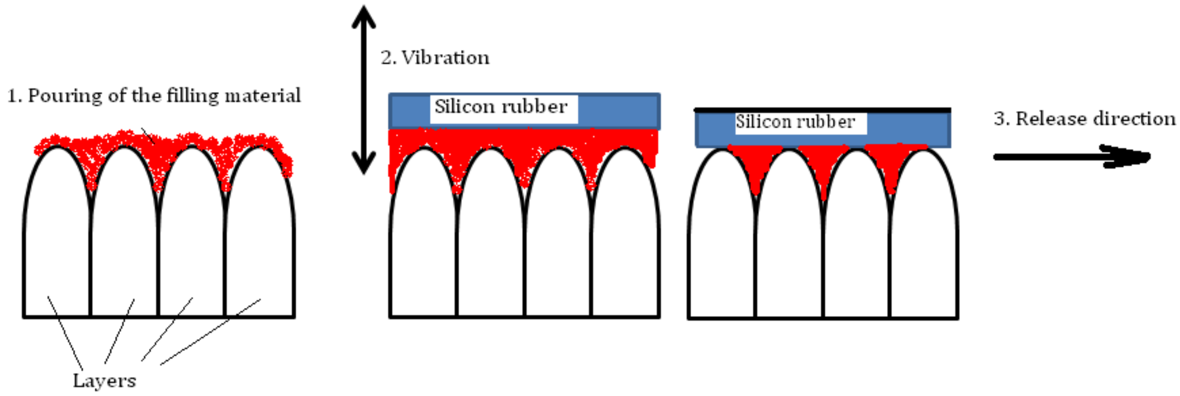

Figure 4.12: Improvement of surface finish by filling process of epoxy-based composite

The surface roughness of the wax pattern was reduced from 1710 to 276 µm R_a, thus achieving 83.85% of improvement (Kuo & Su 2013: 468).

Recently, Stratasys Inc. commercialized a semi-automatic process named the Finishing Touch™ Smoothing Station to improve the roughness of FDM parts to a surface finish closer to that of injection-moulded parts. It is reported that with a layer thickness of 0.254 mm, the surface finish of parts produced with a Fortus 3D Production System can be improved from 600 µm R_a to (40-60) µm R_a, thus improving surface roughness by up to 10 or 15 times (Stratasys, Inc. 2013). For small and medium enterprises, the high price of the smoothing system may be the main drawback to use this technology. Available findings in literature on surface finish improvement of plastic parts manufactured through AM are summarized in Table 4.2.

Table 4.2: Summary of improvement of surface finish

Year	Material and AM process	Used technique for improvement of surface finish	Obtained surface finish R_a (µm)
1998	SLA	Adaptive algorithm followed by abrasive flow machining	1.27
2000		CNC machining with a ball end mill cutter	4-6
2003	FDM of ABS	Hot Cutter Machining	Improvement from 100 to 0.5 (in depth)
2009	SLS of Duraform (PA12)	Vibratory grinding (Tumbling) in ceramic medias	2
	FDM of ABS	Chemical treatment: immersion in a bath of Acetone (90%) and water (10%) for 5 min.	Improvements from (17.2-11.8) to (4.6-2.2) for top surfaces and from (18.8-16.2) to (8.7 5.8) for side surfaces
2012	FDM of ABS-M30	Electroplating with Chromium coating	Improvement from 16 to 0.832.
	FDM of ABS P400	Chemical treatments: with Acetone and Methylethylketone (MEK) for a period from 2 to 4h	Improvement of surface finish to the level of the surface finish of plastic moulded parts
2013	FDM of ABS	Filling of the parabolic surface profile with Aluminium-epoxy resin liquid composite	Improvement of surface quality from 1710 to 276
	FDM of ABS P400, ABS-M30, ABS-M30i, ABSplus-P430 and ABSi	Smoothing station fluid with compressed air before burnishing or sand blasting	Improvement from 600 to (40-60)

4.4 Conclusion

Literature has shown that the surface finish of AM parts can be predicted through mathematical models. Layer thickness and build orientation are the most significant parameters that influence the roughness of AM surfaces. There exist discrepancies between analytical predicted and practical experimental measured results with differences varying with the level of accuracy of the mathematical models. These models may not consider process parameters such as air gap, raster angle, bead (road) width, particle size, laser power, scanning speed, model temperature, etc. The "in-process" techniques such as adaptive slicing algorithms or the powder blowing away with a pressurised air, to improve the surface roughness of additive manufactured parts is sometimes also not taken into consideration. For the FDM process in particular, the adjustment of process parameters such as layer thickness, raster angle, air gap and speed of deposition can contribute to a better surface finish and dimensional accuracy and reduce the cost of post processing works (Bakar, Alkahari & Boejang 2010: 972, Singh & Kumar 2014: 53). From the literature survey, in terms of plastics, only electroplating with a Chromium coating, hot cutter machining, abrasive flow machining and chemical treatment with immersion in acetone and Methylethylketone solutions, have been investigated by other researchers as a post processing techniques for improvement of the surface finish of ABS parts manufactured through FDM. Their investigations were not extended to the effect of the treatments on the roughness of different surface inclination angles. With exception of the work done by Schmid et al. where the surface finish of Duraform PA 12 was improved through tumbling techniques, there are no other findings on improvement of surface finish of nylon and Alumide® parts manufactured through LS process. As there is no single method to improve surface finish, and each method has its advantages and limitations (Singh & Kumar ibid.: 52), there is a need of conducting a comparative study among different post processing techniques for the AM processes and materials that are considered in this study.

CHAPTER 5: POST PROCESSING TECHNIQUES AND DIMENSIONAL ACCURACY OF SMALL PLASTIC PARTS MANUFACTURED THROUGH ADDITIVE MANUFACTURING

5.1 Description of the test piece geometry

The investigation of six post processing techniques for improvement of the surface finish of small plastic parts manufactured through AM and the influence of these techniques on the dimensional accuracy of the parts was carried out on custom designed prismatic test pieces illustrated in Figure 5.1. SolidWorks software was used to design the CAD model.

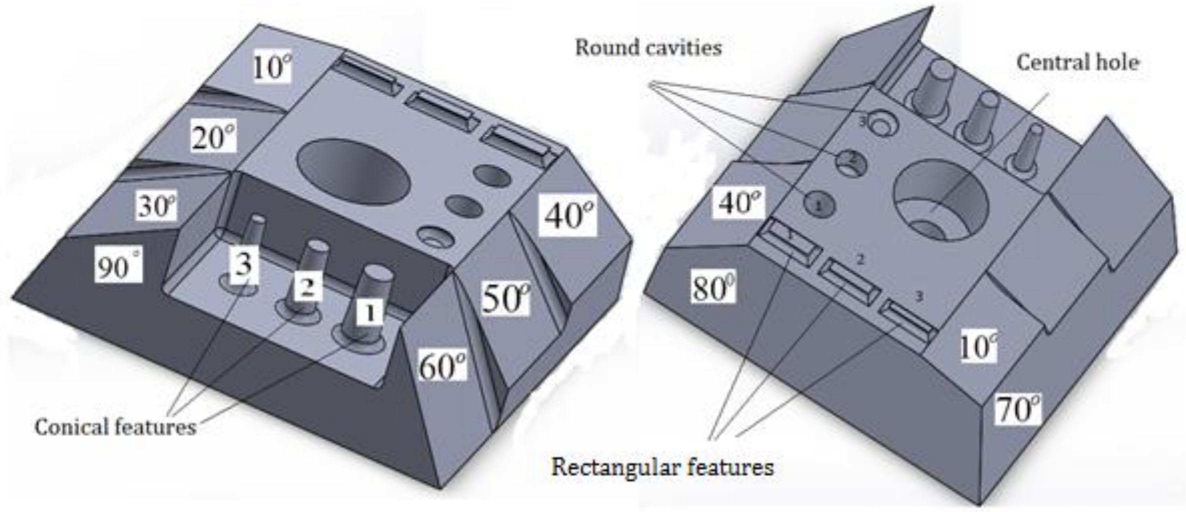

Figure 5.1: The CAD model of the test pieces

The test piece design has a base size of 60 x 60 mm^2 with a height of 19.20 mm. For one of the post-processing techniques namely CNC machining, oversized test pieces with a base size of 60.72 x 60.72 mm^2, and with heights of 19.56 mm were manufactured to allow for the removal of material during the machining process. The test piece design has different planar surfaces with inclination angles varying from 0° (horizontal) to 90° (vertical) with an increment of 10°. This is to show the variation of the stair-step effect with different inclination angles and to investigate the effect of the different post-processing processes on this. The following features were also included in the test piece design:

- Three truncated conical features with a height of 10 mm and with different diameters. The purpose is to investigate if thin features will deflect or break off during tumbling process.
- Three protruding rectangular features with a height of 1.2 mm, but with different dimensions This is to examine the result of tumbling on small protruding features which are likely to be damaged or removed by the process.
- Three round cavities (blind holes) of a diameter of 4.8 mm but of different depths. This is to determine if a process such as spraying will fill/partially fill cavities.
- From the top view, a central hole of diameter 14.69 mm and depth of 10.30 mm, concentrically connected from the bottom side to another hole of 6.60 mm diameter for the clamping of the test piece in the case of CNC machining, touch probe scanning or surface roughness measurement.
- All corners on the top surface of the test piece design were filleted to a radius of 1 mm. The reason for this is because the stylus of the touch probe scanner used to measure geometrical accuracy of the test pieces has a diameter of 2 mm. If the corners were left to be square, the scanner would not be able to measure this and it will show as deviations from the CAD design.

Table 5.1 summarizes the dimensions of the provided small features of the test piece.

Table 5.1: Dimensions of small features of the test piece

<table>
<tr><th>Features</th><th>Height h (mm)</th><th>Bottom and top diameter D x d (mm)</th><th>Bottom rectangle L x w (mm)</th><th>Top rectangle L x w (mm)</th><th>Diameter (mm)</th></tr>
<tr><td>Truncated cone 1</td><td rowspan="3">10</td><td>6.90 x 3.95
(7.50 x 4.55)</td><td>NA</td><td>NA</td><td>NA</td></tr>
<tr><td>Truncated cone 2</td><td>5.90 x 2.95
(6.50 x 3.55)</td><td>NA</td><td>NA</td><td>NA</td></tr>
<tr><td>Truncated cone 3</td><td>4.90 x 1.95
(5.50 x 2.55)</td><td>NA</td><td>NA</td><td>NA</td></tr>
<tr><td>Rectangular protrusion 1</td><td rowspan="3">1.2</td><td>NA</td><td>9.20 x 4.40
(9.20 x 5.12)</td><td>7.20 x 2.40
(7.20 x 3.12)</td><td>NA</td></tr>
<tr><td>Rectangular protrusion 2</td><td>NA</td><td>9.20 x 3.80
(9.20 x 4.52)</td><td>7.20 x 1.80
(7.20 x 2.52)</td><td>NA</td></tr>
<tr><td>Rectangular protrusion 3</td><td>NA</td><td>9.04 x 3.20
(9.20 x 3.92)</td><td>7.20 x 1.20
(7.20 x 1.92)</td><td>NA</td></tr>
<tr><td>Round cavity 1</td><td>8</td><td>NA</td><td>NA</td><td>NA</td><td rowspan="3">4.8
(4.08)</td></tr>
<tr><td>Round cavity 2</td><td>4.8</td><td>NA</td><td>NA</td><td>NA</td></tr>
<tr><td>Round cavity 3</td><td>1.2</td><td>NA</td><td>NA</td><td>NA</td></tr>
</table>

The dimensions for the features of the oversized test piece where they differ from the dimensions of the features of the standard test piece are shown in brackets.

The SolidWorks file was converted into STL format, the design was sliced using Magics RP Tools from Materialise and the sliced file was sent to the LS and FDM processes for manufacturing of the physical test pieces. Taking into consideration the degradation of the powder when it is repeatedly used and its possible negative impact on the surface finish of the test pieces manufactured through the LS process, the powders that were used in manufacturing the nylon and Alumide® test pieces were checked to be within an acceptable mass flow rate. To compensate for the shrinkage of the test pieces, correct scaling was done before the manufacture of the test pieces. Table 5.2 shows the process parameters of LS of nylon PA 2200 and Alumide®.

Table 5.2: Process parameters for LS of nylon PA2200 and Alumide® test pieces

Process parameters	**Nylon PA2200**	**Alumide®**
Average grain size (μm)	56	60
Average melting point (°C)	172-180	172-180
Laser power (W)	48	48
Scanning speed (mm/s)	4500	4500
Part bed temperature (°C)	177.5	179
Layer thickness (μm)	150	150
Part build orientation (°)	0	0
LS Machine	EOS P385	EOS P385
Build rate (mm/hour)	20	20
Mass flow rate (g/10 min)	30	30
Scaling factor in x, y and z-directions	1.0229; 1.030 and 1.018	1.0229; 1.030 and 1.018

The ABS test pieces were manufactured through the FDM process according to the process parameters listed in Table 5.3.

Table 5.3: Process parameters for FDM of ABS test pieces

Material	ABS P400 (white)
Layer thickness	0.254 mm
Raster width	0.5 mm
Part build orientation	0°
STL scale	1.0
FDM Machine	Dimension SST 1200
Model interior	Solid-Normal
Support fill	Sparse

5.2 Description of the post processing techniques and touch probe scanning process

The additive manufactured test pieces were post processed through tumbling, shot peening, hand finishing, CNC machining, spray painting and chemical treatment by dissolving the surfaces. The touch probe scanning technique was used for the qualitative and quantitative assessments for the dimensional accuracy of the post processed test pieces as compared to the dimensions of the "as built" test piece.

The sharing of activities in execution of the six post processing techniques is summarized in Table 5.4.

Table 5.4: Sharing of activities for execution of post processing techniques

Post processing techniques	**Nylon**	**Alumide®**	**ABS**	**Place of execution**
	Number of post processed test pieces			
Tumbling	4	4	4	CUT,CRPM
Shot peening	4	4	4	CUT, CRPM
CNC machining	1	1	1	CUT, PDTS
Hand finishing	4	4	4	De Montfort University (UK)
Spray painting	4	4	4	De Montfort University (UK)
Chemical treatments	1	1	3	De Montfort University (UK)
Subtotal	18	18	20	
Total	56			

5.2.1 Tumbling

Tumbling is a mechanical surface finish process whereby parts are tumbled with an abrasive media in a container. The tumbling causes the parts to rub against the media and each other and in the process rounds corners, removes burrs and to smooth rough surfaces. This is a relatively low cost process and the only labour involved is the loading and unloading of the tumbler's container or barrel. It is mainly applicable for small objects that do not have protrusions that are easily broken off. Tumbling of thermoplastics can be done wet as well as dry.

The nylon, Alumide® and ABS test pieces were tumbled in a Rösler Vibratory finishing machine type R220EC as shown in Figure 5.2, with a rotation speed of 1500 rpm. The tumbling media used was Rösler ceramic chips of type RSG 06/06S mixed with RMB/D1 15/18S. Rösler L161/025 liquid solution was used with the ceramic chips as lubricating medium.

Figure 5.2: Tumbling process

Table 5.5 shows the time for which the nylon, Alumide® and ABS test pieces were tumbled.

Table 5.5: Tumbling periods for nylon, Alumide® and ABS test pieces

Tumbling period (hours)		
Nylon	Alumide®	ABS
1.5	1.5	1
3	3	2
4.5	4.5	3
6	6	4

5.2.2 Shot peening

Shot peening is a cold mechanical surface treatment mainly aimed at enhancing the fatigue strength of metal components by creating residual compressive stresses on the surface and at the same time, improving the surface finish of the component. In the process, particles such as steel, ceramic or glass beads are accelerated by compressed air to impact the work material and produce many dents on the surface and the affected layer below the surface.

The effect of shot peening was investigated for improving the surface finish of the nylon, Alumide® and ABS test pieces. A MICRO 750S PEENMATIC shot peening cabinet was used for this purpose. The unit has a blasting nozzle with a diameter of 7 mm and 0.5 mm diameter stainless steels balls were accelerated under a pressure of 5 Bar, to impact the surfaces of the test pieces.

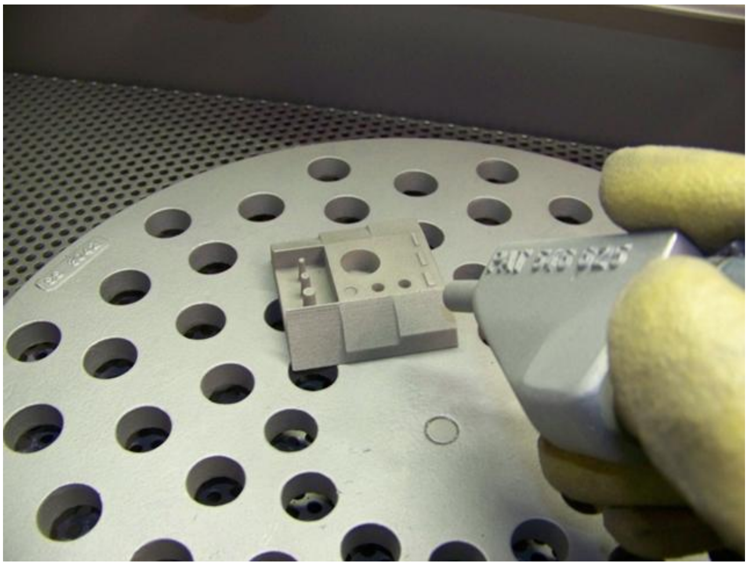

Figure 5.3: Shot peening process

Table 5.6 shows the time period for which nylon, Alumide® and ABS test pieces were shot peened.

Table 5.6: Shot peening period for nylon, Alumide® and ABS pieces

Shot peening period (min.)		
Nylon	Alumide®	ABS
2	1	2
4	2	4
6	3	6
8	4	8

5.2.3 Hand finishing

Layers of MS epoxy primer were applied with an airbrush on the surfaces of the nylon, Alumide® and ABS test pieces. Each layer was followed by sanding with sanding paper that was performed by hand. Sanding paper of grades P60, P180, P320 and P400 were used, starting with the coarsest grid and finishing with the smoothest. Figure 5.4 illustrates the hand finishing of a nylon test piece where a sanding process is performed after an application of a layer of MS epoxy primer.

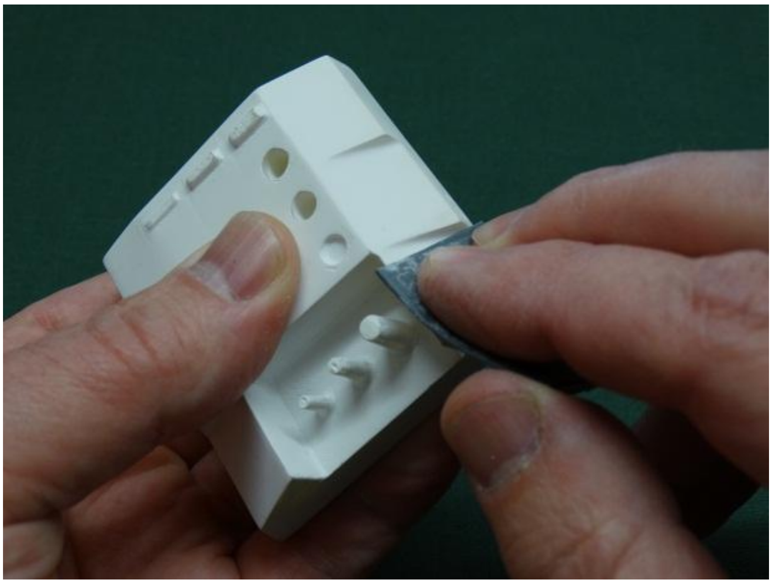

Figure 5.4: Hand finishing process

Table 5.7 shows the duration of the different processes used in the hand finishing technique for improvement of the surface finish of the test pieces.

Table 5.7: Duration of different hand finishing process used on nylon, Alumide® and ABS test pieces

Processes	**Names and designations of the test pieces**			
	Nylon 1 (HFN1) Alumide® 1 (HFA1) ABS1 (HFABS1)	Nylon 2 (HFN2) Alumide® 2 (HFA2) ABS2 (HFABS2)	Nylon 3 (HFN3) Alumide® 3 (HFA3) ABS3 (HFABS3)	Nylon 4 (HFN4) Alumide® 4 (HFA4) ABS4 (HFABS4)
	Duration of the process (min)			
Sand	45	90	45	90
Sand +Prime	45	90	45	90
Sand+Prime+Sand	45	90	45	90
Sand+Prime+ Sand+Prime			25	25
Sand+Prime+ Sand+Prime+Sand			25	25
Total time	2 h 15 min	4 h 30 min	3 h 5 min	5 h 20 min

5.2.4 Spray painting

To investigate what surface improvement can be achieved through only applying paint to the surfaces of the test pieces, paint was applied using an airbrush. Figure 5.5 shows the spray painting technique performed on Alumide® test piece.

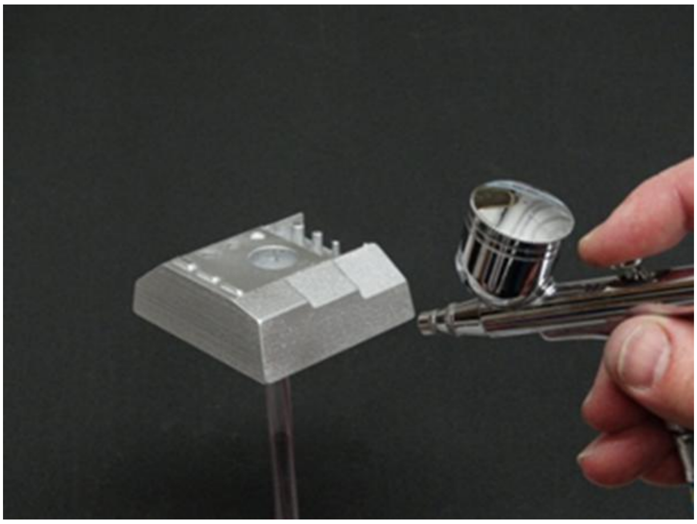

Figure 5.5: Spray painting process

Table 5.8 indicates the number of layers of undercoat that was applied to the different test pieces. All test pieces were finally covered with a coat of silver paint to more clearly show the stair-step effect on the different surfaces.

Table 5.8: Spray painting process

Steps	**Names and designations of test pieces**
Step 1: One coat of primer	Nylon 1 (SPN1) Alumide® 1 (SPA1) ABS1 (SPABS)
Step 2: One coat of silver paint	
Step 1: Two coats of primer	Nylon 2 (SPN2) Alumide® 2 (SPA2) ABS2 (SPABS2)
Step 2: One coat of silver paint	
Step 1: Three coats of primer	Nylon 3 (SPN3) Alumide® 3 (SPA3) ABS3 (SPABS3)
Step 2: One coat of silver paint	
Step 1: Four coats of primer	Nylon 4 (SPN4) Alumide® 4 (SPA4) ABS4 (SPABS4)
Step 2: One coat of silver paint	

5.2.5 CNC machining

CNC machining of the nylon, Alumide® and ABS test pieces that were manufactured oversized was performed on a DAHLIH MCV-720 three axis milling machine as shown in Figure 5.6.

Figure 5.6: DAHLIH MCV-720 CNC milling machine

Figure 5.7 shows the used cutting techniques on different surfaces of the test pieces

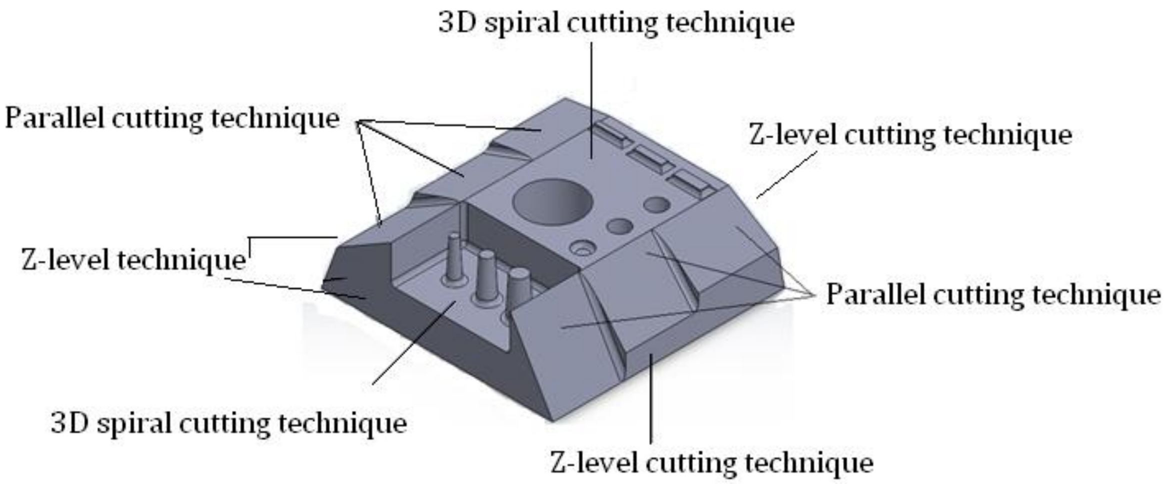

Figure 5.7: Used cutting techniques for CNC machining of the test pieces

Table 5.9 summarizes the used cutting parameters for CNC machining.

Table 5.9: Cutting parameters for CNC machining

Cutting parameter	**Value**
Cutting tool	3 mm diameter ball cutter
Rotation speed of the spindle (rpm)	4000
Feed rate (mm/min)	600
Step-over (mm)	0.2
Cutting depth (mm)	0.3

5.2.6 Chemical treatments

The chemical treatments consisted of immersion of the nylon, Alumide® and ABS test pieces into acetone, resorcinol as well as formic and nitric acids at room temperature. In addition to room temperature treatments, the ABS test pieces were immersed into a heated bath of acetone at 50°C and into acetone vapour at 110°C. The dissolving effect of the acids on the surfaces of the test pieces was observed. Table 5.10 summarizes the chemical treatment processes.

Table 5.10: Chemical treatment processes

<table>
<tr><th></th><th colspan="2">Nylon</th><th colspan="2">Alumide®</th><th colspan="3">ABS</th></tr>
<tr><td rowspan="2">Chemical treatment</td><td colspan="7">Immersion into</td></tr>
<tr><td>Formic acid</td><td>Resorcinol acid</td><td>Nitric acid</td><td>Resorcinol acid</td><td colspan="3">Acetone</td></tr>
<tr><td>Period</td><td>48 h</td><td>3 h</td><td>48 h</td><td>3 h</td><td>1 min</td><td>1 min</td><td>20 min</td></tr>
<tr><td>Temperature</td><td colspan="5">Room temperature</td><td>50°C</td><td>110°C</td></tr>
<tr><td colspan="5">Designation of the test pieces</td><td>CT-ABS1</td><td>CT-ABS2</td><td>CT-ABS3</td></tr>
</table>

Figure 5.8 shows effects of acetone on the surface of nylon and Alumide® test pieces.

Figure 5.8: Effects of acetone on the surfaces of nylon and Alumide® test pieces

It was observed that acetone did not dissolve the surfaces of nylon nor the surfaces of Alumide® test pieces.

Figure 5.9 shows the effects of resorcinol and formic acids on the surfaces of nylon test pieces.

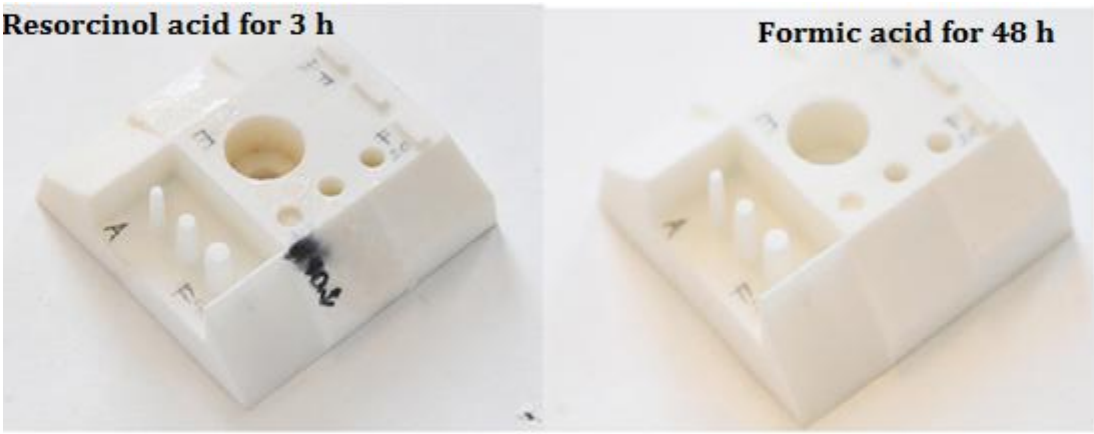

Figure 5.9: Effects of resorcinol and formic acids on surfaces of nylon test pieces

It was observed that neither resorcinol nor formic acid had dissolved the surfaces of nylon test pieces.

Figure 5.10 shows the effects of resorcinol and nitric acids on the surfaces of Alumide® test pieces.

Resorcinol acid for 3 h

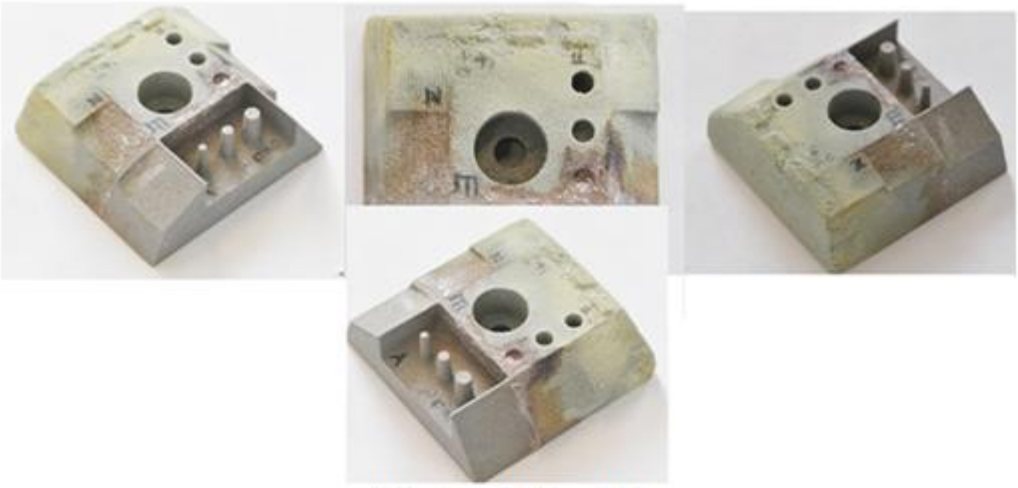

Nitric acid for 48 h

Figure 5.10: Effects of resorcinol and nitric acids on surfaces of Alumide® test pieces

In a similar manner as for nylon test pieces, it was observed that neither resorcinol acid nor nitric acid did not dissolve the surfaces of Alumide® test pieces.

Figure 5.11 shows the effects of acetone on the surfaces of the ABS test pieces.

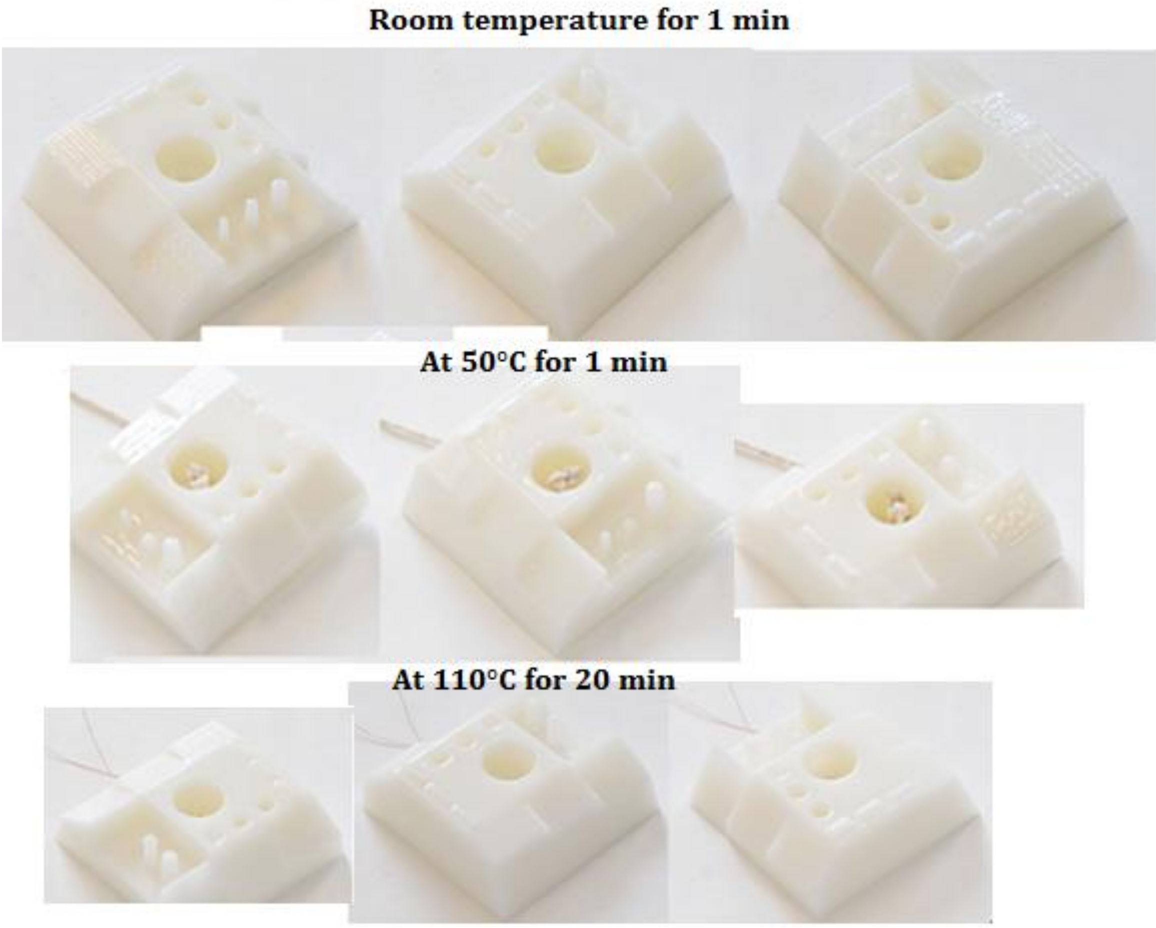

Figure 5.11: Effects of acetone on surfaces of ABS test pieces

It was observed that for the above three cases, acetone dissolve the surfaces of ABS pieces

5.2.7 Touch probe scanning

A Renishaw® Cyclone RG24 Coordinate Measuring Machine (CMM) or also known as a touch probe scanner was used to investigate the effect of the six post processing techniques on the dimensional accuracy of the additive manufactured test pieces. An "as built" nylon, Alumide® and ABS test piece was scanned followed by one test piece from each post processing technique. In each case the test piece to which the heaviest post processing was applied was scanned to clearly show the effect of the technique on the geometrical accuracy. It was not possible to scan each test piece before and after each post processing technique because of cost time and constraints. It was assumed that since the test pieces were manufactured in the same batches on the same AM machine that their dimensions are the same. The touch probe scanning machine has a ruby ball stylus of 2 mm diameter and a scanning rate up to 140 points per second with a resolution of 0.1 mm. The "as built" and post processed test pieces, were touch probe scanned and the results recorded as a point cloud and then converted to STL file with Trace scan 24A software. The STL file is processed by Geomagic Qualify software where the dimensions of the post processed test pieces are compared to the dimensions of the "as built" test pieces and the deviation ranges were recorded. For each scanned sample, with a nominal deviation range of ±0.1 mm, the 3D scanning technology of Geomagic Qualify software generates a colour map with the corresponding deviation ranges and a preliminary statistical report. Figure 5.12a shows the setup of a test piece on the touch probe scanner while Figure 5.12b shows a typical image of a scanned "as built" test piece along with the deviation range colour chart.

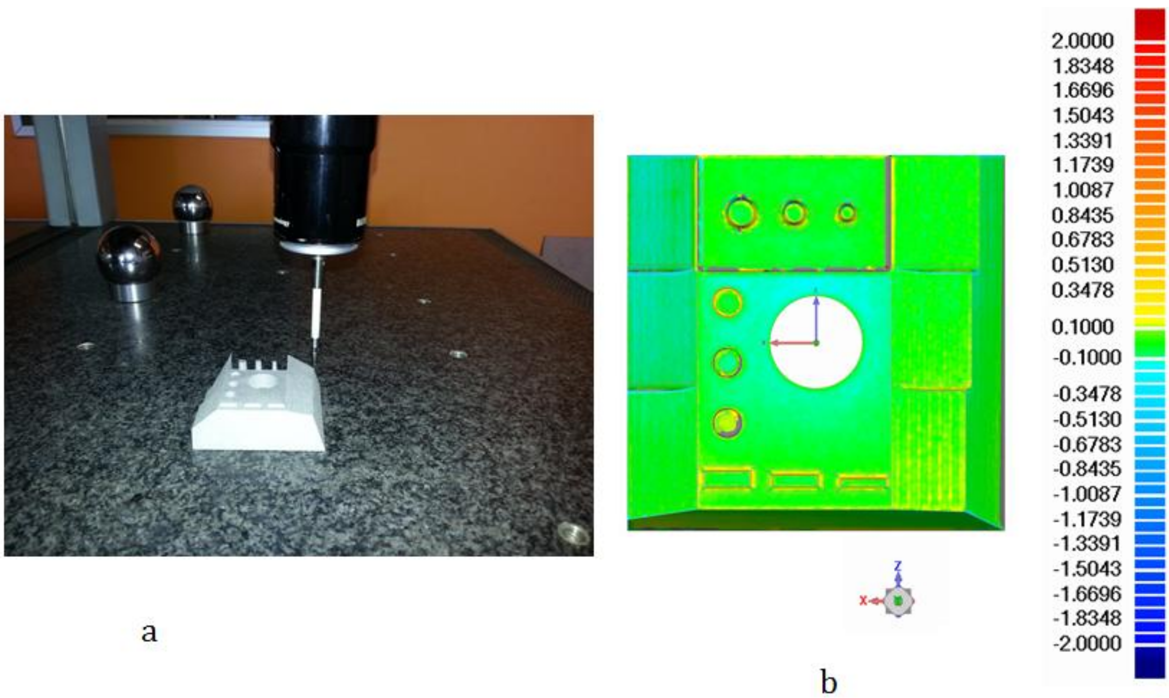

Figure 5.12: Setup on touch probe scanner (a) and example of colour chart of deviation ranges of "as built" test piece from CAD design (b)

5.3 Analysis of dimensional accuracy

5.3.1 Visual inspection of touch probe scan results

A visual inspection of the chemically treated nylon and Alumide® test pieces showed that neither acetone, formic acid nor resorcinol acid dissolved the surfaces of the test pieces; hence only a chemically treated ABS test piece was touch probe scanned.

Geomagic Qualify® which is professional engineering software for quality control of dimensional accuracy of manufactured parts was used to produce images for analysis of dimensional accuracy of the test pieces. The visual inspection of images generated by Geomagic Qualify® software were analysed with the use of Adobe® Photoshop® CS2 software in order to highlight areas of specific colour along with the corresponding deviation range according to the colour map.

Table 5.11 provides a summary of touch probe scanned post processed test pieces.

Table 5.11: Summary of touch probe scanned post processed test pieces

Post processing technique	Nylon	Alumide®	ABS
	Period of operation/specification of the process		
Tumbling	6 h	6 h	4 h
Shot peening	8 min	4 min	8 min
Hand finishing	9 sanding steps and 6 steps of priming	9 sanding steps and 6 steps of priming	9 sanding steps and 6 steps of priming
Spray painting	4 coats of primer and one spray coat of silver paint	4 coats of primer and one spray coat of silver paint	4 coats of primer and one spray coat of silver paint
CNC machining	As specified by the cutting parameters		
Chemical treatment			Immersion into acetone bath at room temperature for a period of 1 min

The results of the visual inspection of the images produced by touch probe scanning process of post processed test pieces are summarized in Appendices 4, 5 and 6.

5.3.2 Test of homogeneity between "as built" and post processing techniques

For each touch probe scanned test piece, Geomagic Qualify® software provides preliminary statistical data on the deviation range distribution in the form of a table and histogram chart. In addition to this, there is a need of having a quantitative comparative measure to assess the extent to which the proportions of deviation ranges for "as built" and for any post processing technique are the same. For this purpose, the Chi-square test for a Null Hypothesis (H_o) is used, with a probability of rejecting H_0 when H_0 is true (also known as the Significance level) α =0.002.

Null Hypothesis (H_0): The proportions of deviation ranges are the same as one compares "as built" to anyone of the post processing techniques.

The Chi-square test or the goodness of fit test, denoted by χ^2 is a statistic measurement that reflects the magnitude of discrepancies between the observed and the expected cell counts. When the differences are significant, the value of χ^2 tends to be large, suggesting that the Null Hypothesis H_0-of no difference between the proportions of deviation ranges for "as built" compared to any post processing technique should be rejected. On the other hand a small value of χ^2 will occur when the observed and expected cell are similar, implying that the Null Hypothesis H_0- is true and should not be rejected.

A conclusion is reached by comparing the calculated P-value to the Significance level α for the test. The P-value is computed as the probability of observing a value of Chi - square χ^2 at least as large as the observed value when the Null Hypothesis H_0 is true; or in other words, the P-value is the smallest value of α for which H_0 can be rejected.

The preliminary statistical deviation ranges were classified in 24 categories. Applying the CHSQ.TEST function available in Microsoft Excel spread sheet, the P-value for each post processing technique was computed and the results are presented in Appendices 1, 2 and 3.

5.3.3 Test for the difference in population proportions

To establish which deviation range proportion (row) is significantly larger or smaller compared to the proportion of "as built" versus any post processing technique's proportion (columns), it is needed to test for the differences in population (treatment) proportions for each individual deviation range to both "as built" and tumbling for example. For each deviation range, the test statistic Z-observed (Z_{obs}) calculated from the observed proportions will be compared to the value of the Inverse Normal Distribution, denoted $z_{\alpha/2}$, associated with the level of Significance $\alpha/2$.

For any individual deviation range, for example taking into consideration the tumbling post processing technique,

Let π_1-the true proportion of "as built" test piece and

π_2-the true proportion of tumbled test piece

The Null Hypothesis H_0: There is no difference in the true proportions of "as built" test piece versus tumbled test piece ($\pi_1 = \pi_2$).

The test statistic Z_{obs}, for each deviation range (row) is determined as follows:

$$Z_{obs} = \frac{p_1 - p_2}{\sqrt{p(1-p)\left(\frac{1}{n_1} + \frac{1}{n_2}\right)}} \tag{5.1}$$

p is the overall proportion of points for the considered deviation range;

$$p = \frac{x_1 + x_2}{n_1 + n_2} \tag{5.2}$$

x_1-the number of touch probe scanned points in the considered deviation range for "as built" test piece;

x_2-the number of touch probe scanned points in the considered deviation range for tumbled test piece;

n_1-the total number of touch probe scanned points for the "as built" test piece;

n_2-the total number of touch probe scanned points for tumbled test piece;

$p_1 = \frac{x_1}{n_1}$-the proportion of points for "as built" test piece and

$p_2 = \frac{x_2}{n_2}$-The proportion of points for tumbled test piece.

The Null Hypothesis is rejected if $Z_{obs} < -z_{\alpha/2}$ or $Z_{obs} > z_{\alpha/2}$

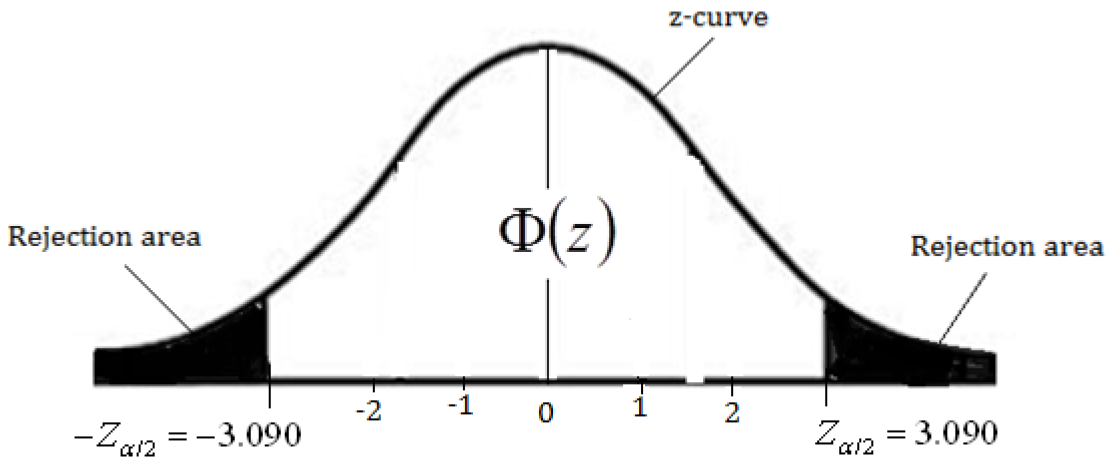

Figure 5.13: Standard normal z-curve

For a level of significance α=0.002, the cumulative area is given for the smallest and the greatest values $-Z_{\alpha/2} = -3.090$ and $Z_{\alpha/2} = 3.090$ respectively.

The detailed computations of Chi-square test (P-value) and the test statistic Z-observed (Z_{obs}) for each deviation range are presented in Appendices 1, 2 and 3. Tables 5.12-5.14 present the summaries of deviation ranges of rejection or non-rejection of the Null Hypothesis for nylon, Alumide® and ABS test pieces.

Table 5.12: Summary of Chi square and Z-statistic tests for nylon test pieces

	Deviation ranges		Post processing techniques				
	>=Min.	<Max.	Tumbling	Shot peening	Hand finishing	Spray painting	CNC machining
1	-2.000	-0.926	Rejected	Rejected	Rejected	Not rejected	Not rejected
2	-0.926	-0.844	Not rejected	Rejected	Not rejected	Not rejected	Not rejected
3	-0.844	-0.761	Not rejected	Rejected	Rejected	Not rejected	Not rejected
4	-0.761	-0.678	Rejected	Rejected	Rejected	Not rejected	Rejected
5	-0.678	-0.596	Rejected	Rejected	Rejected	Not rejected	Rejected
6	-0.596	-0.513	Rejected	Rejected	Rejected	Not rejected	Rejected
7	-0.513	-0.430	Rejected	Rejected	Rejected	Not rejected	Rejected
8	-0.430	-0.348	Rejected	Rejected	Rejected	Rejected	Rejected
9	-0.348	-0.265	Rejected	Rejected	Rejected	Rejected	Rejected
10	-0.265	-0.183	Rejected	Rejected	Rejected	Rejected	Rejected
11	-0.183	-0.100	Rejected	Rejected	Rejected	Rejected	Rejected
12	-0.100	0.100	Rejected	Rejected	Rejected	Rejected	Rejected
13	0.100	0.183	Rejected	Rejected	Rejected	Rejected	Rejected
14	0.183	0.265	Rejected	Rejected	Rejected	Rejected	Rejected
15	0.265	0.348	Rejected	Rejected	Rejected	Rejected	Rejected
16	0.348	0.430	Rejected	Rejected	Rejected	Rejected	Rejected
17	0.430	0.513	Rejected	Rejected	Rejected	Rejected	Rejected
18	0.513	0.596	Rejected	Rejected	Rejected	Rejected	Rejected
19	0.596	0.678	Rejected	Rejected	Rejected	Rejected	Rejected
20	0.678	0.761	Rejected	Rejected	Rejected	Rejected	Rejected
21	0.761	0.844	Rejected	Rejected	Rejected	Rejected	Rejected
22	0.844	0.926	Rejected	Rejected	Rejected	Rejected	Rejected
23	0.926	1.009	Not rejected	Not rejected	Not rejected	Rejected	Rejected
24	1.009	2.000	Rejected	Rejected	Not rejected	Rejected	Rejected
P-value			0	0	0	0	0

Table 5.13: Summary of Chi-square and Z-statistic tests for Alumide® test pieces

	Deviation ranges		Post processing techniques				
			Tumbling	Shot peening	Hand finishing	Spray painting	CNC machining
	>=Min.	<Max.					
1	-2.000	-0.926	Rejected	Rejected	Not rejected	Not rejected	Not rejected
2	-0.926	-0.844	Not rejected	Not rejected	Not rejected	Not rejected	Not rejected
3	-0.844	-0.761	Not rejected	Not rejected	Not rejected	Not rejected	Not rejected
4	-0.761	-0.678	Rejected	Not rejected	Not rejected	Rejected	Rejected
5	-0.678	-0.596	Rejected	Rejected	Rejected	Rejected	Rejected
6	-0.596	-0.513	Rejected	Rejected	Rejected	Rejected	Rejected
7	-0.513	-0.430	Rejected	Rejected	Rejected	Not rejected	Rejected
8	-0.430	-0.348	Rejected	Rejected	Rejected	Rejected	Rejected
9	-0.348	-0.265	Rejected	Rejected	Rejected	Rejected	Rejected
10	-0.265	-0.183	Rejected	Rejected	Rejected	Rejected	Rejected
11	-0.183	-0.100	Rejected	Rejected	Rejected	Rejected	Rejected
12	-0.100	0.100	Rejected	Rejected	Rejected	Rejected	Rejected
13	0.100	0.183	Rejected	Rejected	Rejected	Rejected	Rejected
14	0.183	0.265	Rejected	Rejected	Rejected	Rejected	Rejected
15	0.265	0.348	Rejected	Rejected	Rejected	Rejected	Rejected
16	0.348	0.430	Rejected	Rejected	Rejected	Rejected	Rejected
17	0.430	0.513	Rejected	Rejected	Rejected	Rejected	Rejected
18	0.513	0.596	Rejected	Rejected	Rejected	Rejected	Rejected
19	0.596	0.678	Rejected	Rejected	Rejected	Rejected	Rejected
20	0.678	0.761	Rejected	Rejected	Rejected	Rejected	Rejected
21	0.761	0.844	Rejected	Rejected	Rejected	Rejected	Rejected
22	0.844	0.926	Rejected	Rejected	Rejected	Rejected	Rejected
23	0.926	1.009	Rejected	Rejected	Not rejected	Rejected	Rejected
24	1.009	2.000	Rejected	Rejected	Not rejected	Rejected	Rejected
P-value			0	0	0	0	0

Table 5.14: Summary of Chi-square and Z-statistic tests for ABS test pieces

	Deviation ranges		Post processing techniques					
	>=Min.	<Max.	Tumbling	Shot peening	Hand finishing	Spray painting	CNC machining	Chemical treatment
1	-2.000	-0.926	Rejected	Rejected	Not rejected	Not rejected	Rejected	Rejected
2	-0.926	-0.844	Rejected	Not rejected	Rejected	Not rejected	Not rejected	Not rejected
3	-0.844	-0.761	Rejected	Rejected	Rejected	Not rejected	Not rejected	Not rejected
4	-0.761	-0.678	Rejected	Rejected	Rejected	Not rejected	Rejected	Not rejected
5	-0.678	-0.596	Rejected	Rejected	Rejected	Rejected	Rejected	Rejected
6	-0.596	-0.513	Rejected	Rejected	Rejected	Not rejected	Rejected	Rejected
7	-0.513	-0.430	Rejected	Rejected	Rejected	Rejected	Rejected	Rejected
8	-0.430	-0.348	Rejected	Rejected	Rejected	Not rejected	Rejected	Rejected
9	-0.348	-0.265	Rejected	Rejected	Rejected	Rejected	Rejected	Rejected
10	-0.265	-0.183	Rejected	Rejected	Rejected	Rejected	Rejected	Rejected
11	-0.183	-0.100	Rejected	Rejected	Rejected	Rejected	Rejected	Rejected
12	-0.100	0.100	Rejected	Rejected	Rejected	Rejected	Rejected	Rejected
13	0.100	0.183	Rejected	Rejected	Rejected	Rejected	Rejected	Rejected
14	0.183	0.265	Rejected	Rejected	Rejected	Rejected	Rejected	Rejected
15	0.265	0.348	Rejected	Rejected	Rejected	Rejected	Rejected	Rejected
16	0.348	0.430	Rejected	Rejected	Rejected	Rejected	Rejected	Rejected
17	0.430	0.513	Rejected	Rejected	Rejected	Rejected	Rejected	Rejected
18	0.513	0.596	Not rejected	Rejected	Rejected	Rejected	Rejected	Rejected
19	0.596	0.678	Not rejected	Rejected	Rejected	Rejected	Rejected	Not rejected
20	0.678	0.761	Not rejected	Rejected	Rejected	Rejected	Rejected	Rejected
21	0.761	0.844	Rejected	Rejected	Rejected	Rejected	Rejected	Rejected
22	0.844	0.926	Rejected	Rejected	Rejected	Rejected	Rejected	Rejected
23	0.926	1.009	Rejected	Rejected	Not rejected	Rejected	Rejected	Rejected
24	1.009	2.000	Not rejected	Rejected	Not rejected	Not rejected	Rejected	Rejected
P-value			0	0	0	0	0	0

5.3.4 Observations and conclusion on Chi-square and Z-tests

The computation of the Chi-square test for "as built" compared to tumbling, shot peening, hand finishing, spray painting and CNC machining post processing techniques gives a P-value=0 for each of the post processing technique for the nylon, Alumide® and ABS test pieces (Appendices 1, 2 and 3). The Chi-square test is performed to establish whether there is a significant difference between the true proportions when one considers all deviation ranges for the two techniques combined. Since the P-value is less than the Significance level for the test (α=0.002), the Null Hypothesis H_0 is rejected for all post processing techniques. This indicates that there are significant differences in the proportions of all the deviation ranges (rows) as one compares "as built" test pieces to tumbled, shot peened, hand finished, spray painted, chemical treated or CNC machined test pieces (columns).

However, the Z- test for differences in population proportions indicates that there exist a number of deviation ranges where the Null Hypothesis H_0 is not rejected i.e there is no difference in proportions of the number of points for both "as built" and a post processing technique. Table 5.15 highlights the deviation ranges for which H_0 is true, along with the percentage of number of observed points.

Table 5.15 : The deviation ranges with no difference in population proportions

	Nylon				**Alumide®**				**ABS**			
	Deviation ranges (mm)		p1 x 100	p2 x 100	Deviation ranges (mm)		p1 x 100	p2 x 100	Deviation ranges (mm)		p1 x 100	p2 x 100
Tumbling	-0.926	-0.844	0	0	-0.926	-0.844	0	0	0.513	0.596	0.1	0
	-0.844	-0.761	0	0	-0.844	-0.761	0	0	0.596	0.678	0.1	0
	0.926	1.009	0	0					0.678	0.761	0.1	0
	1.009	2	0	0					1.009	2.000	0.1	0.1

	Nylon				Alumide®				ABS			
	Deviation ranges (mm)		p1 x 100	p2 x 100	Deviation ranges (mm)		p1 x 100	p2 x 100	Deviation ranges (mm)		p1 x 100	p2 x 100
Shot peening	0.926	1.009	0	0	-0.926	-0.844	0	0	-0.926	-0.844	0	0
					-0.844	-0.761	0	0				
					-0.678	-0.596	0	0				
Hand finishing	-0.926	-0.844	0	0	-2.000	-0.926	0	0	-2.000	-0.926	0	0
	0.926	1.009	0	0	-0.926	-0.844	0	0				
	1.009	2.000	0	0	-0.844	-0.761	0	0				
					-0.761	-0.678	0	0				
Spray painting	-2.000	-0.926	0	0	-2.000	-0.926			-2.000	-0.926	0	0
	-0.926	-0.844	0	0	-0.926	-0.844			-0.926	-0.844	0	0
	-0.844	-0.761	0	0	-0.844	-0.761			-0.844	-0.761	0	0
	-0.761	-0.678	0	0					-0.761	-0.678	0	0
	-0.678	-0.596	0	0					-0.596	-0.513	0	0
	-0.596	-0.513	0	0					-0.430	-0.348	0.1	0.1
	-0.513	-0.430	0	0					1.009	2.000	0.1	0.1
CNC machining	-2.000	-0.926	0	0	-2.000	-0.926	0	0	-0.926	-0.844	0	0
	-0.926	-0.844	0	0	-0.926	-0.844	0	0	-0.844	-0.761	0	0
	-0.844	-0.761	0	0	-0.844	-0.761	0	0				
Chemical treatment									-2.000	-0.926	0	0
									-0.926	-0.844	0	0
									-0.844	-0.761	0	0

For "as built" and all post processing techniques, it is observed that the population proportions are the same in extreme positive or negative deviation ranges where a very small number of points (0 or 0.1%) is found to fall into such deviation ranges. This indicates that the Z- test confirms that, for nylon, Alumide® and ABS test pieces, there exist strong evidences to conclude that the proportions in deviation ranges are not the same when one compares the "as built" versus tumbling, shot peening, hand finishing, spray painting, CNC machining or chemical treatment.

5.3.5 Analysis and discussion of touch probe scan results

In this analysis and discussion, the qualitative appreciations shown in Table 5.16 were used in the assessment of the level of dimensional accuracy in terms of the percentage of the total number of touch probe scanned points of the post processed test piece, qualified to be within ± 0.1 mm deviation range from the geometry of the "as built" test piece.

Table 5.16: Qualitative appreciations of dimensional accuracy of post processing techniques

Percentage of number of points within ± 0.1 mm deviation range	Qualitative appreciation
Equal or greater to 90%	Excellent
Equal or greater to 80% and less than 90%	Very good
Equal or greater to 70% and less than 80%	Good
Equal or greater to 60% and less than 70%	Satisfactory
Less than 60%	Poor

A. Nylon

i. Tumbling

The visual inspection of the touch probe scanned tumbled nylon test piece for a period of 6 h shows that 90% of the touch probe scanned horizontal surfaces and surfaces inclined from 10° to 90° are in ± 0.1 mm deviation range (Figure 5.14a). This is in agreement with statistical results where the tumbling process for a period of 6 h performed on nylon test piece produced very good dimensional accuracy with 88.3% of the total number of touch probe scanned points being in ± 0.1 mm deviation range from the geometry of the "as built" test piece (Figure 5.15). It is observed that the surfaces of the small protrusions, round cavities and conical features occupy 7.3% of the total number of touch probe scanned points and are covered by (-0.183 to -0.1) mm deviation range. The transition areas and sharp corners which represent 2.6% are worn away to give a deviation range (-2 to 0.183) mm with 2.1% being in (-0.348 to -0.183) mm. A negligible proportion representing 1.8% of points is found to be in the positive deviation range (0.1 to 0.430) mm (Appendix 1A). This may be attributed to touch probe scanning error as tumbling is a removal process, only negative deviation ranges should be expected. It can be concluded that within ± 0.1 mm deviation range from the geometry of the "as built" test piece, despite the rounding of sharp corners, the tumbling technique applied to nylon for a period of 6 h produced very good dimensional accuracy.

ii. Shot peening

The visual inspection estimated that almost 95% of touch probe scanned shot peened horizontal surfaces of nylon test piece for a period of 8 min, are within a ±0.1 mm deviation range (Figure 5.14b). The overall statistical results confirmed that the shot peening of nylon test piece for a period of 8 min exhibited very good dimensional accuracy where a rate of 82.6 % of the total number of touch probe scanned points on the surfaces of the shot peened test piece was found to be in a ±0.1 mm deviation range from the geometry of the "as built" test piece (Figure 5.15). It is observed that for the surfaces at inclination angle varying from 10° to 30°, 90% of points fall within the dimensional accuracy within ±0.1 mm deviation range. Some areas are characterized by ±0.1 mm with a tendency to the lower limit. As the inclination angle increases from 40° to 60°, the proportion of the surface covered by the ±0.1 mm deviation range decreases with the increased of inclination angle. The transition areas between surfaces and sharp corners are covered by (-0.678 to -0.100) mm negative deviation range. This is in agreement with Appendix 1B, where 11.7% of the points are in (-0.761 to -0.1) mm negative deviation range with 6.3% in (-0.183 to -0.1) mm. The proportion decreases, to give advantage of the positive deviation range, with the increase of the inclination angle. On the lower part of 50° and 60° inclination angles, in non-uniform manner, positive deviation ranges (0.1 to 0.513) mm are observed. This is confirmed by the statistics of the Appendix 1B and Figure 5.15, where 5.6 % of the scanned points are in the positive deviation range with 4.7% in (0.1 to 0.183) mm deviation range. This may be attributed to the error generated by the scanning process, being known that the touch probe scanner becomes less accurate by approaching vertical inclinations.

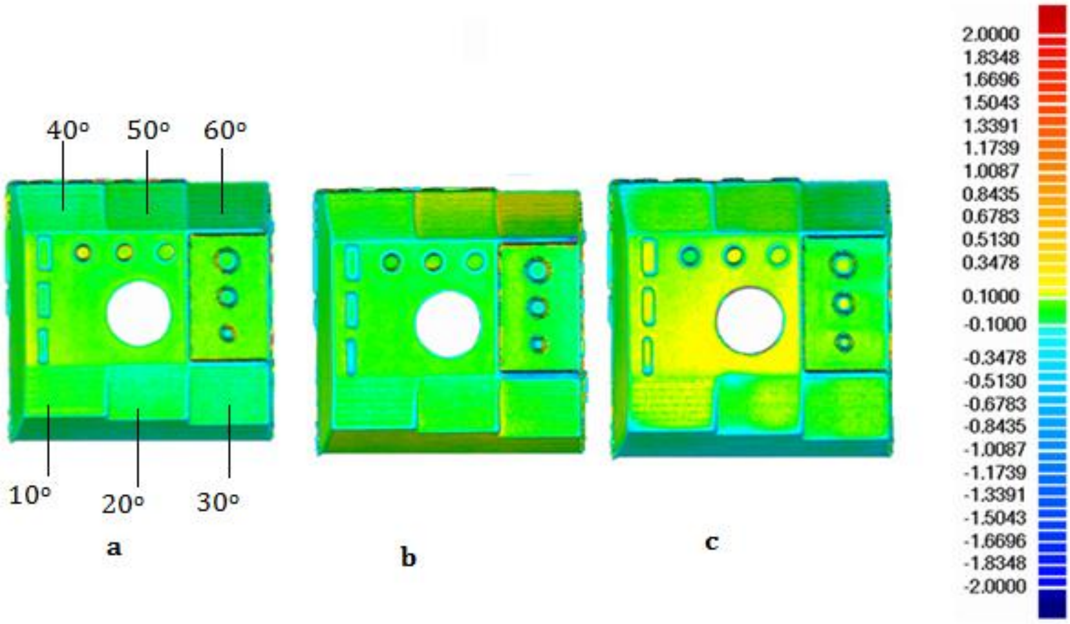

Figure 5.14: Touch probe scanned of tumbled (a), shot peened (b) and hand finished (c) nylon test pieces

iii. Hand finishing

The visual inspection of the touch probe scanned hand finished nylon test piece shows that, on the main horizontal surfaces as well as over the horizontal surfaces of small features, a combination of deviation ranges (-0.183 to -0.1) mm with 10.5% and (0.1 to 0.183) mm with 19.8% dominates the surfaces. The deviation range on transition areas between surfaces, tend to the negative side (-0.678 to -0.100) mm (Figure 5.14c). Statistical results (Figure 5.15 and Appendix 1C) confirmed that a satisfactory dimensional accuracy with 63.5% of the total number of touch probe scanned points within ±0.1 mm deviation range was achieved by the hand finishing technique (9 sanding steps + 6 priming steps) performed on nylon test piece for a period of 5 h 20 min. The MS epoxy priming process which adds material and the sanding process which takes away the material in a non-uniform manner can explain the presence of both positive and negative deviation ranges across an individual surface. In general the hand finishing technique is not consistent in distribution of the deviation ranges over the different surfaces, neither over an individual surface. It can be concluded that within

±0.1 mm deviation range from the geometry of the "as built" nylon test piece, the hand finishing technique performed for a period of 5 h 20 min produced satisfactory dimensional accuracy.

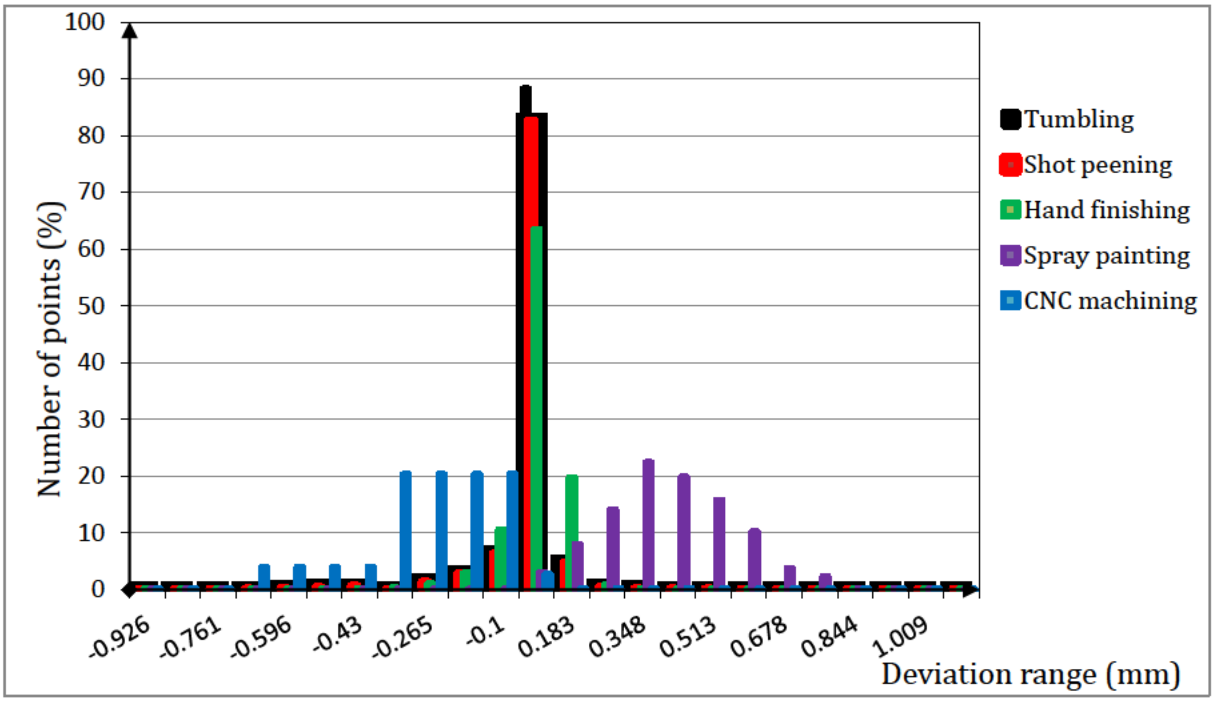

Figure 5.15: Comparison of dimensional deviations of post processing techniques for nylon test pieces from the "as built" nylon test piece

iv. Spray painting

Statistical results (Appendix 1D and Figure 5.15) show that for spray painting performed on nylon test piece with four undercoats with MS epoxy primer, followed by one layer of silver paint, (0.1 to 0.513) mm positive deviation ranges are produced with a relatively smooth variation in percentage of number of points. Only 3% of the total number of touch probe scanned points fall within the ±0.1 mm deviation range. Visual inspection shows that this proportion represents the transition areas between surfaces. This is attributed to the fact that the paint draws away from the edges of the flat surfaces because of surface tension when the paint is still wet. A good distribution of positive deviation ranges (0.1 to 0.513) mm can be observed.

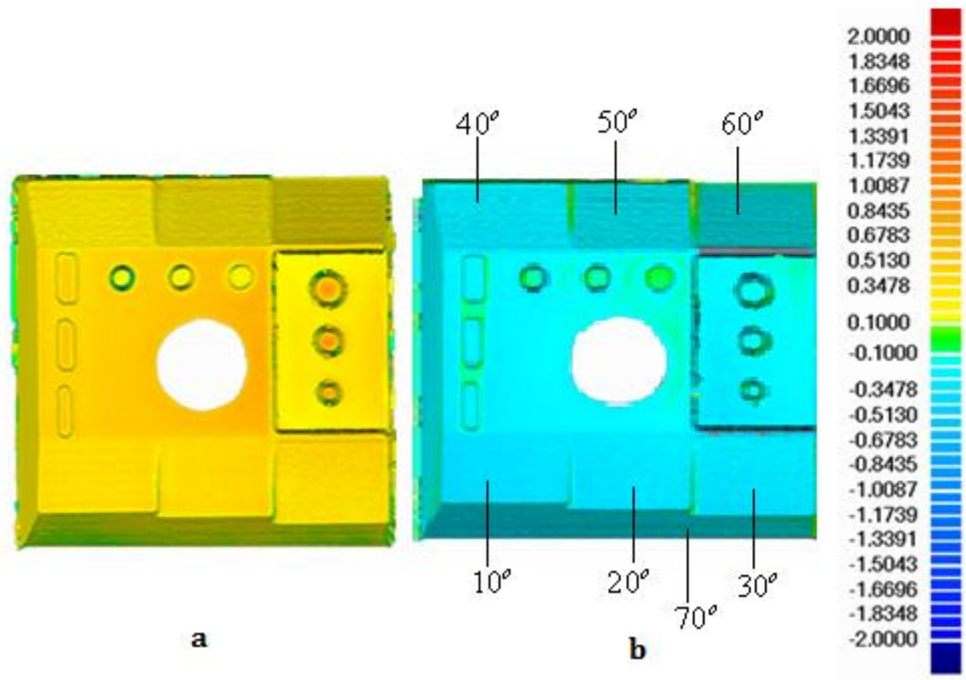

Figure 5.16: Touch probe scanned spray painted (a) and CNC machined (b) nylon test pieces

Figure 5.16a illustrates that spray painting is consistent in producing a relatively uniform distribution of positive deviation ranges across individual surfaces as well as across the entire test piece. It can be concluded that within the ±0.1 mm deviation range from the geometry of the "as built" nylon test piece, the spray painting technique produced very poor dimensional accuracy.

v. CNC machining

In a similar manner to spray painting, for CNC machining only 2.6% of points measured fell within the ±0.1 mm deviation range. Visual inspection shows that this proportion represents the transition areas between surfaces, the areas between protrusions and the bottom surfaces of the round cavities where the cutting tool could not have access due to the complexity of the test piece (Figure 5.13b). While the spray painting shows more or less a smooth variation of positive deviation ranges, the CNC machining shows a wide negative deviation range (-0.348 to -0.183) mm occupying 81.2% of points distributed equally over the range, appearing on horizontal surfaces and surfaces inclined from 10° to 40°, followed by a similar phenomenon observed in (-0.761 to -0.430) mm deviation ranges, dropping to a coverage of 15.6% of the total number of touch probe scanned points (Figure 5.15 and Appendix 1E). Figure 5.13b shows that these deviation ranges are observed on the surfaces with 50°, 60° and 70° inclination angles. It can be realized that with a complex test piece with different inclination angles and small features, CNC machining has limitation in maintaining consistency of dimensional accuracy for a wide range of inclination angles due to limitation in machine- tool settings. The wide deviation in accuracy can be attributed to incorrect setup of the test piece on the CNC machine emphasising the importance of correct set up and calibration of the machine.

B. Alumide®

i. Tumbling

The visual inspection of the touch probe scanned tumbled Alumide® test piece for a period of 6 h showed a high predominance of scanned points falling within the ±0.1 mm deviation range. An excellent uniformly distributed combination of points with (-0.5130 to -0.1) mm and (0.1 to 0.5130) mm deviation ranges characterized the horizontal and inclined surfaces. The presence of (0.1 to 0.5130) mm positive deviation range covering 3.3% (Appendix 2A) which is not expected as tumbling is a removal process, may be a result of scanning error.

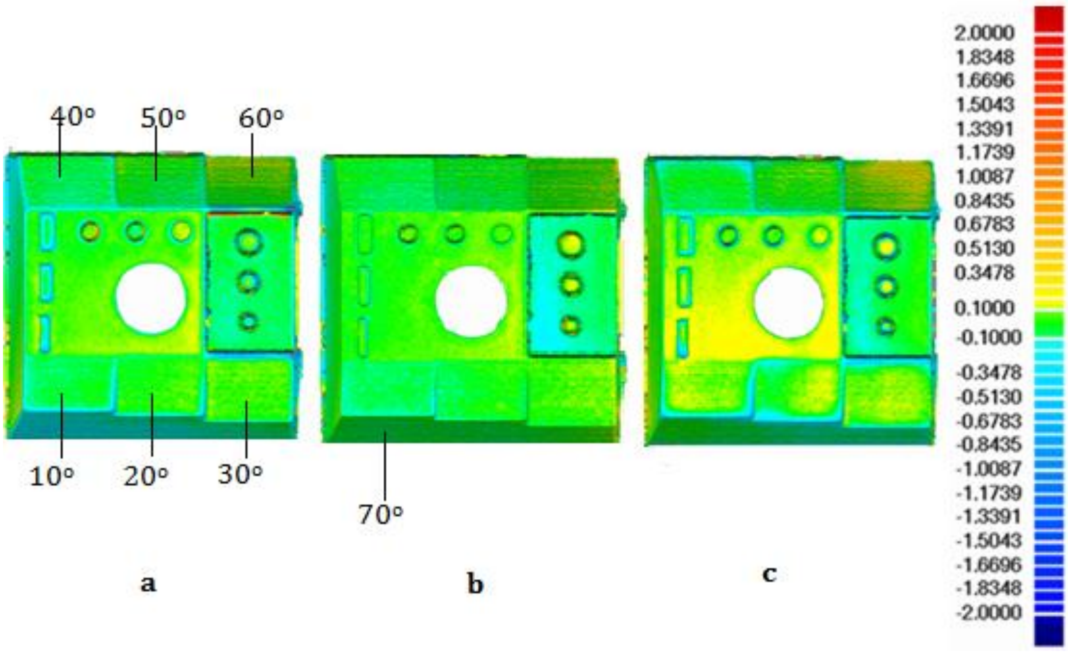

Figure 5.17: Touch probe scanned tumbled (a), shot peened (b) and hand finished (c) Alumide® test pieces

Figure 5.17a and Appendix.5 show that the transition areas between surfaces and sharp corners are worn away. This effect is very pronounced on small protrusions with a proportion of 16 % of points where (-0.5130 to -0.1) mm negative deviation ranges are observed.

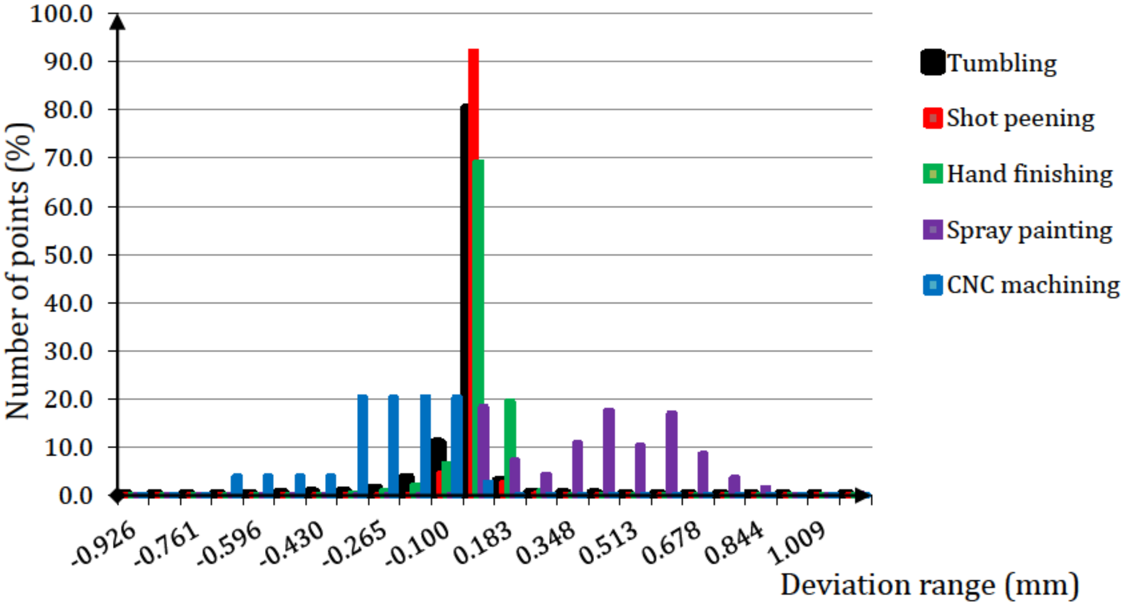

Figure 5.18: Comparison of dimensional deviations of post processing techniques for Alumide® test pieces from the "as built" Alumide® test piece

The statistical results (Figure 5.18 and Appendix 2A) confirm that 80.1% of the total number of touch probe scanned points on the surface of the tumbled Alumide® test piece fall within within ±0.1 mm deviation range from the geometry of the "as built" test piece. It can be concluded that within a ±0.1 mm deviation range, despite the rounding of the sharp corners and heavy wearing of small protrusions, the tumbling technique performed on Alumide® test piece for a period of 6 h produced very good dimensional accuracy.

ii. Shot peening

The shot peening of Alumide® test piece (Figure 5.17b), conducted for a period of 4 min, produced an excellent predominance of ±0.1 mm deviation range in a uniformly distributed combination with (0.1 to 0.5130) mm deviation ranges. The degree of predominance of ±0.1 mm deviation range increases with the increase of inclination angle from 0 to 70°.

It is observed that the lower horizontal surface was dominated up to 80% by (-0.5130 - 0.1) mm negative deviation range, which may probably be caused by a high concentration of blasting shots which caused more compressive effect in this area since the test piece was manually shot peened in a confined space. Transition areas and sharp corners are partially kept within ±0.1 mm deviation ranges but transition areas on the surface inclined at 10° showed (-0.182 to -0.1) mm deviation ranges. In general, visual inspection showed that the shot peening post processing technique exhibited an excellent consistency in distribution of ±0.1 mm deviation ranges. Figure 5.18 and Appendix 2B provide statistical results confirming that an excellent proportion of 92.1% of the total touch probe scanned points is within the ±0.1 mm deviation range from the geometry of the “as built “Alumide® test piece.

iii. Hand finishing

A hand finishing technique consisting of nine sanding steps and six priming steps were applied to the Alumide® test piece for a period of 5 h 20 min. A visual inspection of the touch probe scanned hand finished Alumide® test piece (Figure 5.17c and Appendix 5) showed a relatively wide (0.1 to 0.5130) mm positive deviation range characterized by 50% of the upper horizontal surface. The other half is characterized by a uniformly distributed combination of ±0.1 mm and (0.1 to 0.5130) mm deviation ranges. The right side of the lower horizontal surface is characterized by a deviation range of ±0.1 mm while the left side is dominated by a uniformly distributed combination of ±0.1 mm and (-0.3478 to -0.1) mm deviation range. Over the surfaces at 10°, 20°, 30° and 60° inclination angles, the hand finishing process produces a wide non-uniform distributed deviation range (-0.1 to 0.513) mm over each individual surface; whereas a uniform distributed deviation range of ±0.1 mm is covering the faces inclined at 40° and 50°. The transition areas and sharp corners are locally worn away to produce wide deviation ranges (-0.5130 to -0.1) mm. In general, the hand finishing is characterized by a non-uniform distribution of deviation ranges across surfaces with different inclination angles as well as over individual surfaces. Statistical results (Figure 5.18 and Appendix 2C) indicate that satisfactory dimensional accuracy with a proportion of 69.2% of the total number of the touch probe scanned points of the hand finished Alumide® test piece falling within the ±0.1 mm deviation range from the geometry of the "as built" Alumide® test piece was achieved. Therefore, it can be concluded that the hand finishing technique was characterized by a lack of consistency in distribution of deviation ranges across individual surfaces of test pieces. However across all the surfaces of the entire test pieces, satisfactory dimensional accuracy within ±0.1 mm deviation range as compared to the geometry of the "as built"Alumide® test piece could be obtained.

iv. Spray painting

The Alumide® test piece was spray painted with four undercoats of MS epoxy primer, followed by one layer of silver paint. Visual inspection of the touch probe scanned Alumide® spray painted test piece (Figure 5.19a and Appendix 5) shows that the edges of round cavities, small portions of transition areas between surfaces, a part of the face inclined at 70° and some separate localised negligible areas, are within ±0.1 mm deviation range. These are the areas where due to surface tension; the paint draws away from the edges of flat surfaces when it is still wet. Figure 5.19a illustrates that the spray painting displays uniformly distributed positive deviation ranges namely (0.1 to 0.8436) mm, (0.5130 to 1.1730) mm and (0.5783 to 1.5143) mm, which cover different specific areas.

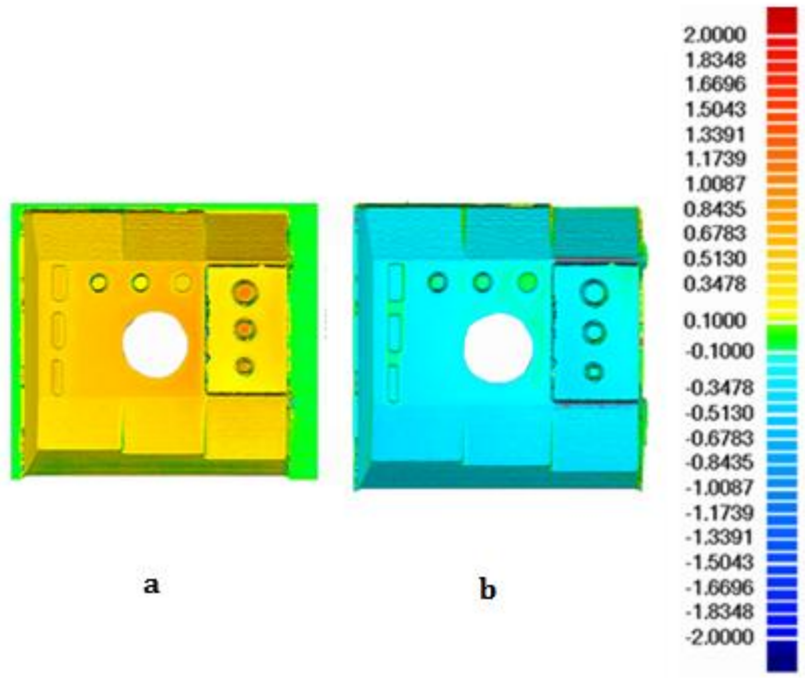

Figure 5.19: Touch probe scanned spray painted (a) and CNC machined (b) Alumide® test pieces

Statistical results (Figure 5.18 and Appendix 2D) indicate that only 18.3% of the total number of touch probe scanned points on the surfaces of spray painted Alumide® test piece, fall within the ±0.1 mm deviation range compared to the geometry of the "as built" test piece. The remaining portion of points is more or less uniformly distributed through a wide positive deviation range varying from 0.1 to 0.844 mm. It can be concluded that the spray painting technique produced an excellent consistency in positive deviation ranges across all surfaces of Alumide® test piece. However, within ±0.1 mm deviation range from the geometry of the "as built" test piece, the significant positive deviation ranges led to tangible changes of the dimensions of the "as built" test piece, thus producing very poor dimensional accuracy.

v. CNC machining

The visual inspection of touch probe scanned CNC machined Alumide® test pieces (Figure 5.19b) shows that the trend observed with CNC machining for nylon test piece is in a similar manner repeated for Alumide®. Two distinct negative deviation ranges (-0.761 to -0.430) mm and (-0.430 to -0.183) mm occur for CNC machining of Alumide® test piece. Only 2.6% of the total touch probe scanned points satisfied the ±0.1 mm deviation range (Figure 5.18 and Appendix 2E). It can be still concluded that the error in setup and calibration of the CNC machine was the cause of the negative deviation ranges which led to an unexpected detrimental effect on the dimensional accuracy of the "as built" test piece.

C. ABS

i. Tumbling

The visual inspection of touch probe scanned tumbled ABS test piece shows that the tumbling technique applied on ABS test piece for a period of 4 h, exhibited an excellent conservation of the ±0.1 mm deviation range, uniformly distributed on wide horizontal surfaces and on all surfaces with inclination from 10° to 70° (Figure 5.20a and Appendix 6). The transition areas are worn away to fall within a deviation range of (-0.513 to -0.1) mm. The surfaces of small protrusions are extremely worn away to reach (-1.339 to -0.843) mm deviation ranges, while the conical features are broken off (Figure6.35).

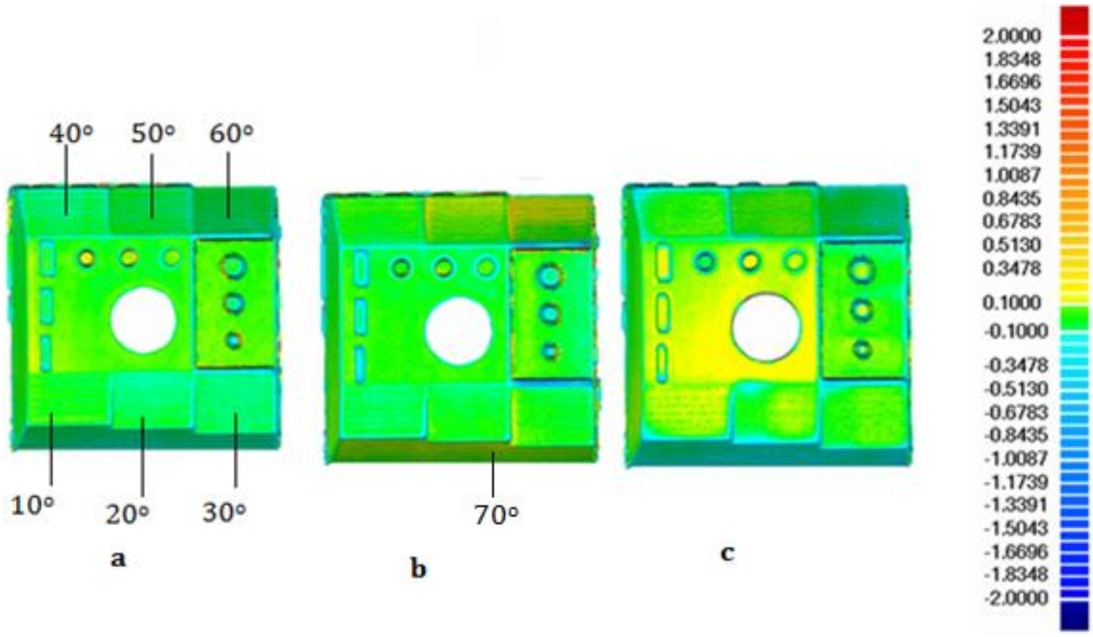

Figure 5.20: Touch probe scanned tumbled (a), shot peened (b) and hand finished (c) ABS test pieces

The tumbling process works well with wide plane surfaces and may also be used to round sharp corners. Though tumbling is a material removal process, (0.1 to 0.183) mm positive deviations from the “as built” ABS test piece occupy 6.6% of the total number of touch probe scanned points on the horizontal surface. When the physical test piece is checked, it is observed that when the tumbling process is prolonged beyond 3 h, the external layers of the ABS test piece start delaminating from the core test piece but are not yet removed, thus showing a positive deviation range when that area is touch probe scanned.

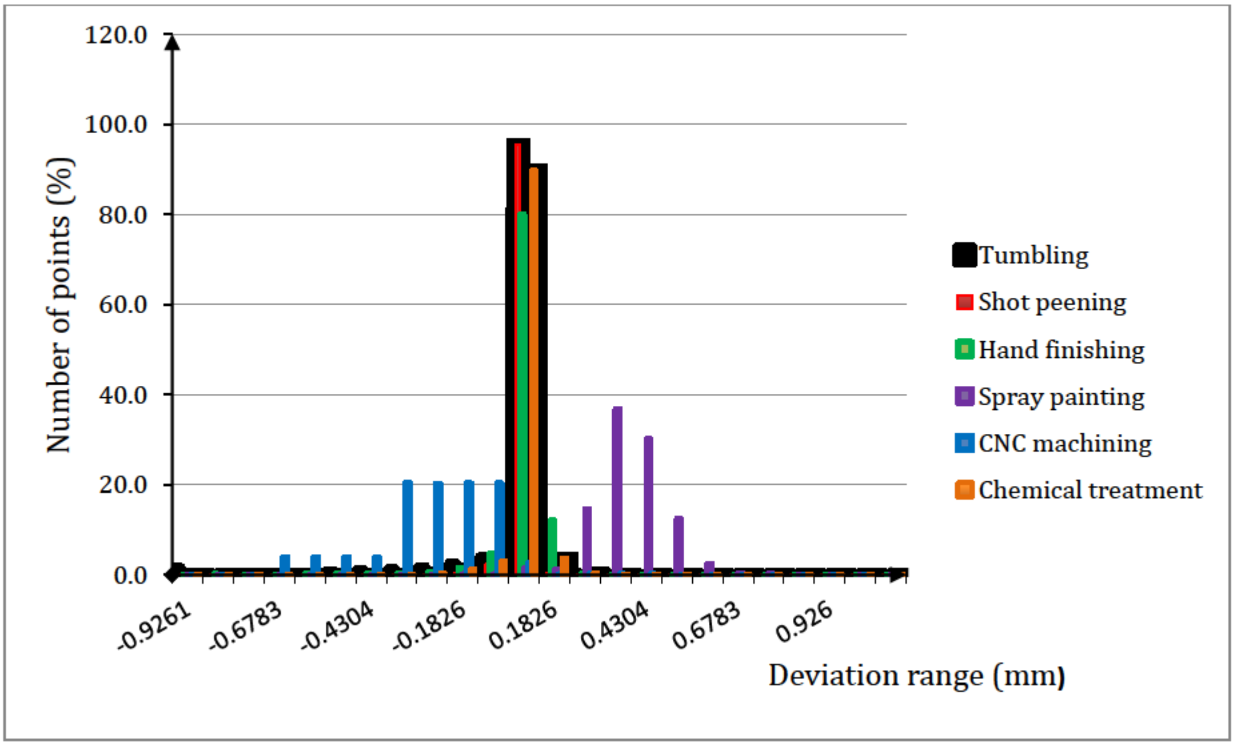

Figure 5.21: Comparison of dimensional deviations of post processing techniques for ABS test pieces from the "as built" ABS test piece

Statistical results (Figure 5.21 and Appendix 3A) confirm that 81% of the total number of touch probe scanned points is within ±0.1 mm deviation range. It can be concluded that within a ±0.1 mm deviation range from the geometry of the "as built" test piece, despite the rounding of sharp corners, heavy wearing of small protrusions and breaking away of components with relatively long protrusions such as the conical features, the tumbling technique applied to ABS test piece for a period of 4 h produced very good dimensional accuracy.

ii. Shot peening

The visual inspection of the touch probe scanned shot peened ABS test piece for a period of 8 min shows that the shot peening technique removes the high points or hills which result from the stair step effect of the FDM process. The appearance of the removed hills decreases with the increase of inclination angle from 10° to 40°. The predominance of the ±0.1 mm deviation range is decreased as inclination angle increase from 50° to 70° and positive deviation ranges appear (Figure 5.20b). This unexpected behaviour may be attributed to, the inaccuracy of the touch probe scanning machine when approaching the vertical direction. Producing a negative deviation range (-0.348 to -0.1) mm, the shot peening technique affects the protrusions in different ways: it is observed that the shots compressed heavily the surface of protrusion 1 while protrusions 2 and 3 were less compressed. As the process is manually conducted the intensity of the shots which depends on the shooting angle, determines the amount by which a particular surface is compressed. It is also observed that the delamination of external layers of the surfaces, especially for 10°, 20°, and 30°, surface angles occurs to produce (-0.678 to -0.1) mm deviation range covering the zones of delamination (Appendix 6B). Statistical results (Figure 5.21 and Appendix 3B) confirm that within a ±0.1 mm deviation range from the geometry of the "as built" ABS test piece, the highest coverage of 95.6% of the total number of touch probe scanned points, was recorded with the shot peening of ABS test piece for a period of 8 min. It can be concluded that despite the removal of the sharp corners of the small protrusions and the delamination of surfaces where the stair step effect is more pronounced, within ±0.1 mm the deviation range from the geometry of the "as built" ABS test piece, the shot peening technique applied on ABS test piece for a period of 8 min, produced excellent dimensional accuracy.

iii. Hand finishing

The hand finishing technique consisting of nine sanding steps and 6 priming steps for a period of 5 h 20 min was performed on the ABS test piece. The visual inspection of the touch probe scanned hand finished ABS test piece shows that the priming adds material in the valleys and the sanding removes materials from the hills. The adding and removing of material is not consistent across the surfaces of the test pieces with a significant variation across individual observed surfaces. This is more pronounced on the surfaces inclined at 10° and 60°. A non-uniform distribution with a wide deviation range of (-0.1 to 0.513) mm is achieved on relatively wide horizontal surfaces. For small features, a wide deviation range of ±0.348 mm is observed (Figure 5.20c and Appendix 6). Statistical results (Figure 5.21 and Appendix 3C) indicate that within a ±0.1 mm deviation range from the geometry of the "as built" ABS test piece a rate of 79.9% of the total number of the touch probe scanned points was achieved. It can be concluded that though the hand finishing technique applied on ABS test piece is generally characterized by the lack of consistency in distribution of deviation range, a good dimensional accuracy could be achieved in the ±0.1 mm deviation range from the geometry of the “as built” ABS test piece.

iv. Spray painting

Figure 5.22a shows that, in a similar manner to nylon and Alumide®, the spray painting of ABS test piece with four undercoats of MS epoxy primer, followed by one layer of silver paint, produced a uniform distribution of positive deviation ranges. Almost 99% of points are covered and uniformly distributed within the (0.1 to 0.596) mm deviation range across all surfaces of the test piece. However, the statistical results (Figure 5.21 and Appendix 3D) indicate that only a very small proportion of 1.3% of the total number of touch probe scanned points on the surfaces of the spray painted ABS test piece satisfies the ±0.1 mm deviation range from the geometry of “as built” ABS test piece. This rate appears at the transition areas of round cavities, small protrusions, conical features and small portion on one of the faces at 90° where the primer and the silver paint were drawn away because of the fluid surface tension when they were still wet.

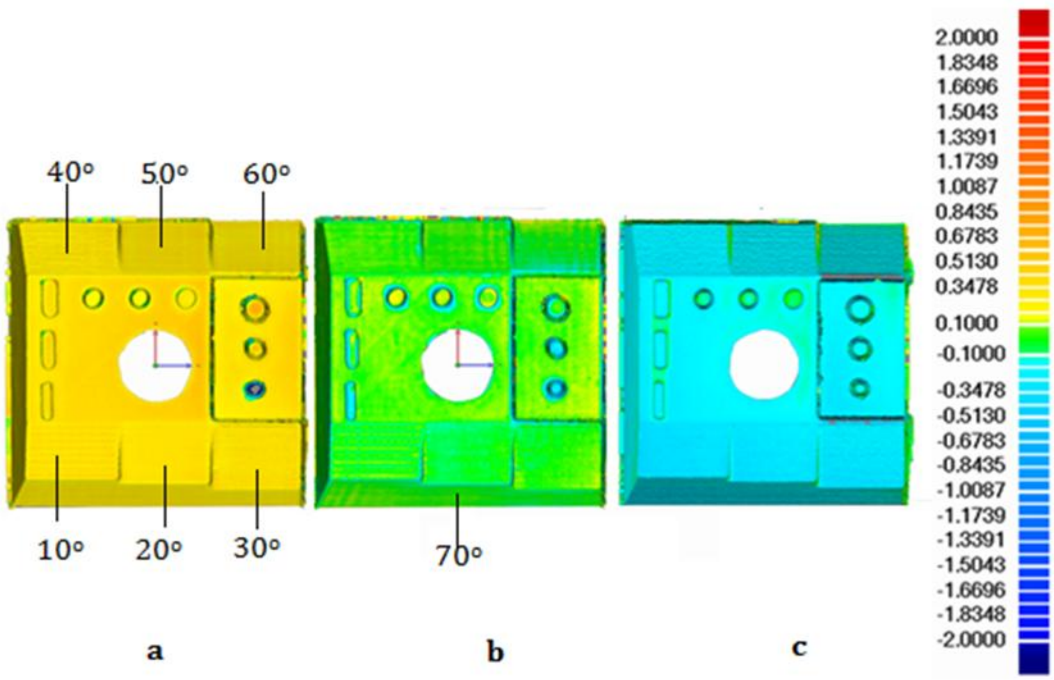

Figure 5.22: Touch probe scanned spray painted (a), chemical treated (b) and CNC machined (c) ABS test pieces

It can be concluded that in a similar manner to nylon and Alumide® test pieces, the spray painting technique applied to ABS test piece produced an excellent consistency in distribution of positive deviation ranges from the “as built” ABS test piece, thus leading to a significant negative effect on the dimensional accuracy of the “as built” test piece.

v. Chemical treatment

A chemical treatment consisting of immersion of ABS test piece (CT-ABS1) in a bath of acetone at room temperature for a period of 60 s was performed. The visual inspection of the touch probe scanned chemically treated ABS test piece showed a uniformly distributed combination of ±0.1 mm and (0.1 to 0.183) mm deviation ranges with a high predominance of the former to cover the horizontal surfaces. Surfaces at inclination angles from 10° to 70° are practically 100% covered by the ±0.1 mm deviation range (Figure 5.22b and Appendix 6). A negative deviation ranges (-0.596 to -0.1) mm is observed on the surfaces of small protrusions, edges of round cavities and conical features. In addition to the dissolving effect on the surfaces of ABS test piece by acetone, during the immersion process, shrinkage of the ABS test piece might have occurred. This is in agreement with the research conducted by Galantucci, Lavecchia & Percoco 2009 where it was concluded that a similar treatment of ABS part with acetone showed shrinkage of the part by 1%. Statistical results (Figure 5.21 and Appendix 3E) indicate that 5.1% of touch probe scanned points is within the (-0.596 to -0.1) mm deviation range where 4.3 % is covered by the (-0.265 to -0.1) mm deviation range. It is obvious that these are the negative ranges observed at small protrusions, edges of round cavities and conical features. It is also confirmed that within the ±0.1 mm deviation range from the geometry of the “as built” ABS test piece, a proportion of 89.8% of the total number of touch probe scanned points on the surface of ABS test piece was achieved. It can be concluded that chemical treatment which consisted of immersion of ABS test piece in a bath of acetone at room temperature for a period of 60 s was able to dissolve the stair steps on inclined surfaces and at the same time, to produce very good dimensional accuracy of the ABS test piece.

vi. CNC machining

During the visual inspection, the trend observed with CNC machining of nylon and Alumide® test pieces is in a similar manner repeated for ABS test piece (Figure 5.22c).

Statistical results indicate that only 2.6% of the total touch probe scanned points after CNC machining satisfied the ±0.1 mm deviation range from the geometry of the "as built" ABS test piece. Two distinct negative deviation ranges: (-0.430 to -0.1) mm with 81.2% coverage and (-0.761 to -0.430) mm with 15.6% coverage dominate the ABS, CNC machined test piece (Figure 5.21 and Appendix 3F). As it was stipulated earlier, these unexpected results might be caused by incorrect set up and calibration of the CNC machine rather than the ability of the CNC machining process to produce accurate dimensions.

5.3.6 General conclusion

Statistically, it was shown that there exists a significant difference between deviation range proportions as one compares the "as built" to any one of the six considered post processing techniques.

Within the ±0.1 mm deviation range from the "as built" test piece, with a good uniform distribution of ±0.1 mm deviation ranges across the relatively wide surfaces of the test piece, the tumbling technique applied to nylon, Alumide® and ABS test pieces produced very good dimensional accuracy. 88.3%, 80.1% and 81% of the total number of touch probe scanned points on the surface of the test pieces were achieved for the nylon, Alumide® and ABS test pieces respectively. For all three materials, the tumbling technique was characterized by the rounding of sharp corners, wearing away of small protrusions, and the breaking off of the conical features. For ABS test pieces, delamination of external layers occurred when the tumbling process was prolonged beyond a period of 3 h.

From the geometry of the "as built" test pieces for all three materials, the shot peening technique produced a very good uniform distribution of ±0.1 mm deviation range across relatively wide surfaces, leading to very good dimensional accuracy for nylon test piece where 82.6% of the total number of points fall into the ±0.1 mm deviation range. Excellent dimensional accuracy rates were obtained for Alumide® and ABS test pieces at 92.1% and 95.6% respectively. Shot peening is generally characterized by the wearing away of small protrusions and sharp corners and a possible concentration of shots into confine area such as corners as the process is manually conducted. For ABS test pieces, the shot peening delaminates the external layers of relatively wide surfaces. This is more pronounced on 10°, 20° and 30° surface inclination angles where the stair step effect is more evidenced.

With a generalized lack of consistency in a uniform distribution of deviation ranges even across individual surfaces, within the ±0.1 mm deviation range from the "as built" test pieces, hand finishing produced satisfactory dimensional accuracy for nylon and Alumide® with 63.5% and 69.2% of the total number of touch probe scanned points on the surfaces of the nylon and Alumide® test pieces respectively. For the ABS test piece despite the lack of consistency in a uniform distribution of the ±0.1 mm deviation range, it can be stated that very good dimensional accuracy was achieved as the rate of points falling within the ±0.1 mm deviation range was raised to 80%.

Spray painting was generally dominated by consistent and uniform distribution of significant positive deviation ranges across almost the entire test piece for all the three materials because of a build-up of paint on the surfaces, thus leading to poor dimensional accuracy.

CNC machining showed a trend of producing negative deviation ranges closed to the targeted ±0.1 mm deviation range from the "as built" test piece. These unexpected results indicate that excess material has been removed from the surfaces of the test pieces. The repeated error for the all three CNC machined test pieces may be caused by improper setup or calibration during the setting of the cutting parameters of the machine in the vertical direction (Z-axis).

The chemical treatment consisting of dissolving the surfaces of ABS test piece by acetone for a period of 60 s at room temperature was found to produce, over all relatively wide surfaces, an excellent uniform distribution of ±0.1 mm deviation range from the "as built" test piece. Despite the presence of (-0.183 to -0.1) mm negative deviation range at the region of small protrusions, round cavities, sharp edges and top surfaces of the conical features, an excellent dimensional accuracy with a proportion of 90% of the total number of touch probe scanned points on the surfaces of the ABS test piece was attained.

The following part of this study is to be focussed on the quantitative assessment of the surface finish improvement by the six post processing techniques applied on the nylon, Alumide® and ABS test pieces obtained through AM.

CHAPTER 6: MEASUREMENTS OF SURFACE ROUGHNESS

No in depth study has yet been performed on surface finish improvement of nylon, Alumide® and ABS parts manufactured through LS and FDM processes. This research work will focus on a comparative study of six post processing techniques namely tumbling, shot peening, CNC machining, spray painting, chemical treatment with acetone; and hand finish through sanding for improvement of surface finish of small plastic test pieces obtained from said materials and processes.

6.1 Description of measuring instrument and measurement setup

6.1.1 Surface roughness measuring tester

Surface roughness measurements were performed using a Mitutoyo SURFTEST SJ-210 Surface Roughness Measuring Tester (SRMT). The SURFTEST SJ-210 is a portable surface roughness measuring instrument, which traces the surfaces of parts, calculates their surface roughness based on roughness standards and displays the results on a Liquid Crystal Display (LCD) screen (Mitutoyo Corporation 2009). The table 6.1 shows the main specifications of the apparatus.

Table 6.1: Specifications of the Surface Roughness Measuring Tester

<table>
<tr><th>Parameter</th><th colspan="2">Specification</th></tr>
<tr><td>Compatible roughness measurement standards</td><td colspan="2">JIS-B-0601-2001, JIS-B-0601-1994, JIS-B-0601-1982, VDA, ISO-1997 and ANSI</td></tr>
<tr><td>Surface finish measurement range (μm)</td><td colspan="2">-200 to +160</td></tr>
<tr><td>Default roughness measurement parameters</td><td colspan="2">R_a, R_z and R_q</td></tr>
<tr><td>Cut-off value or sampling length, λ_c (mm)</td><td colspan="2">0.08, 0.25, 0.8 and 2.5</td></tr>
<tr><td>Number of sampling length, N</td><td colspan="2">1, 2, 3, 4 and 5</td></tr>
<tr><td>Evaluation length range $\ell_n = \lambda_c \times N$ (mm)</td><td colspan="2">0.30 to 16</td></tr>
<tr><td>Measurement traversal speed (mm/s)</td><td colspan="2">0.25, 0.5 and 0.75</td></tr>
<tr><td>Return traversal speed (mm/s)</td><td colspan="2">1</td></tr>
<tr><td>Stylus material</td><td colspan="2">Diamond</td></tr>
<tr><td>Tip radius (μm)</td><td colspan="2">5</td></tr>
<tr><td>Measuring force (mN)</td><td colspan="2">4</td></tr>
<tr><td>Weight (kg)</td><td colspan="2">0.5</td></tr>
<tr><td rowspan="3">Power supply</td><td rowspan="2">AC adapter</td><td>Rating: 9 V, 1.3 A</td></tr>
<tr><td>Supply voltage:100 V</td></tr>
<tr><td colspan="2">Built-in battery: Ni-H battery</td></tr>
</table>

The figure 6.1 shows the main units of the SRMT during the calibration process.

Figure 6.1: Main units of the surface roughness measurement tester SJ-210

6.1.2 Development of the supporting jig for SRMT

The same test pieces as described in previous chapters were used for determining the effect of post-processing on the surface roughness of the pieces. The test pieces have surfaces with inclination angles varying from 0° to 90° from the horizontal direction. In order to take accurate measurements of the roughness of the different surfaces, each surface must be positioned such that it is parallel to the axis of movement of the detector of the SRMT. This will enable the stylus to be in a proper contact with the measured surface while the stylus is scratching across the surface. For this purpose, a supporting jig for the test pieces was designed and constructed. Figure 6.2 shows the main features of the developed supporting jig.

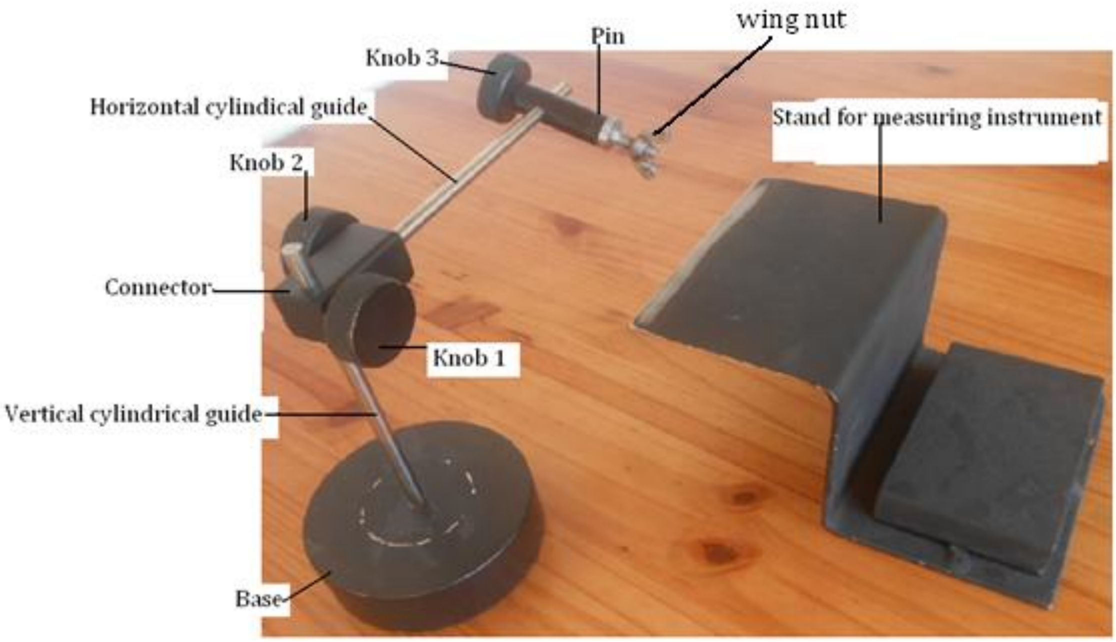

Figure 6.2: Supporting jig for test pieces

A vertical cylindrical guide is rigidly attached to a heavy disk which serves as a base for the jig. A horizontal cylindrical guide is mounted perpendicularly to the vertical guide through a connector which allows the horizontal guide to slide and rotate on the vertical guide. The sliding and rotating motions between the two guides can be locked through knob 1 while rotation of the horizontal guide can be locked through knob 2. The assembly of the connector, knobs and the horizontal guide is able to slide along the vertical guide when knob 1 is loosened and to rotate in the horizontal plane. The test piece is mounted on a pin with a threaded protrusion on one end which fits the central hole of the test piece. This arrangement allows the test piece to rotate on the pin and it can be locked in place through a wing nut. The pin slides and rotates on the horizontal guide and it can be locked in position through knob 3. A heavy stand is provided to support the detector of the SRMT.

6.1.3 Surface finish measurement setup

When the test piece is fitted onto the jig, it can be positioned such that a particular surface for measurement will be parallel to the horizontal plane. Figure 6.3 illustrates the clamping system of the test piece (a) and the setup for the measurement of the surface roughness of the test piece on the surface inclined at an angle of 60° (b).

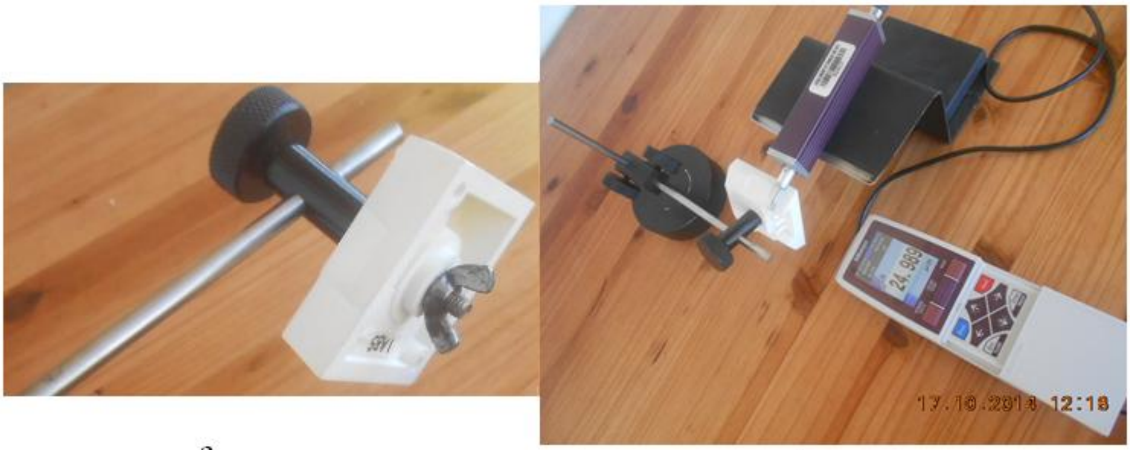

a b

Figure 6.3: Clamping of the test piece (a); Setup of surface roughness measurement (b)

After the calibration process and the setting of the desired measurement conditions such as the cut-off length λc, the number of sampling N, the parameter for surface roughness, the roughness measurement standard and the traversal measuring speed, the detector unit is positioned on the stand. The display unit and the detector unit are connected through a connecting cable. The test piece is positioned little bit lower than the detector in order to enable the surface into consideration to be brought smoothly into contact with the stylus. After the stylus is in contact with the surface into consideration, the START/STOP button which is on the control board of the display unit is pressed. The stylus starts to traverse the surface while an image in a wave form which shows the movement of the stylus into valleys and hills of irregularities of the surface is displayed on the LCD screen. When the set traversal length of the stylus is finished, the stylus with the detector returns back to the origin position and the result of measurement is digitally displayed on the LCD screen. Table 6.2 shows the used measuring parameters and conditions to obtain the results of the measurements of the surface roughness.

Table 6.2: Measurement parameter and conditions

Measuring parameters/conditions	**Specifications**
Measurement Standards	ISO-1997
Roughness measurement parameter	R_a
Cut-off value or sampling length, λ_c (mm)	2.5
Number of sampling length, N	2, 3, 4 and 5
Evaluation length range $\ell_n = \lambda_c \times N$ (mm)	5 to 12.5
Measurement traversal speed (mm/s)	0.5

For each measured surface, three surface roughness measurements were taken at different places: left, middle and right sides of the surface. The arithmetic average was calculated and considered as the roughness measure on that particular surface.

$$R_{a_{average}} = \frac{Ra_{LS} + Ra_{MS} + Ra_{RS}}{3} \tag{6.1}$$

$R_{a_{average}}$ -Arithmetic average of surface finish;

$R_{a_{LS}}$ -The measured surface finish at the left side;

$R_{a_{MS}}$ -The measured surface finish at the middle side;

$R_{a_{RS}}$ - The measured surface finish at the right side.

Figure 6.4 shows the approximate zones on the surfaces of the test piece where the surface roughness measurements were taken.

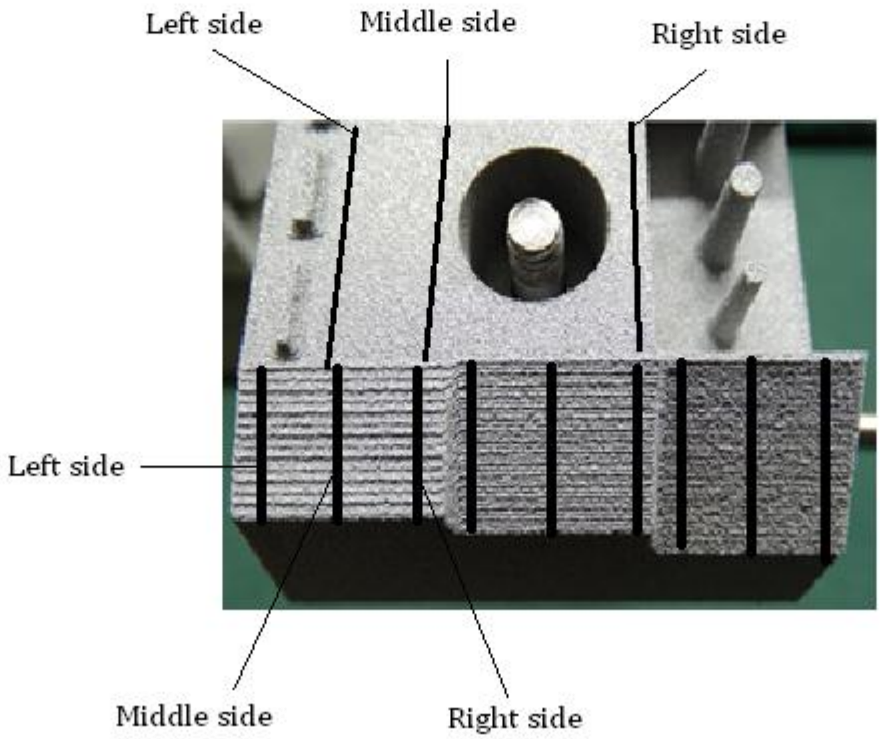

Figure 6.4: Approximate zones of surface roughness measurements

As the visual inspection (Figures 5.8, 5.9 & 5.10) showed that neither acetone, formic acid, or resorcinol acid dissolve the surface of nylon or Alumide® test pieces, the surface roughness of chemically treated nylon and Alumide® test pieces were not measured. As acetone showed a dissolving effect on the surface of ABS test pieces, the surface roughness of ABS chemically treated test pieces with acetone was measured.

6.2 Measurements of surface roughness for nylon test pieces

6.2.1 Results of measurements of surface roughness for nylon test pieces

The surface roughness of "as built", tumbled, shot peened, hand finished, spray painted and CNC machined nylon test pieces were measured.

A. Tumbling

The results of the surface roughness measurements for tumbled nylon test pieces are shown in Table 6.3 and Figure 6.5.

Table 6.3: Average surface finish for tumbled nylon test pieces

Inclination angle ɵ (°)	As built	Tumbling period 1h 30 min	3h 00	4h 30 min	6h 00	% Improvement of surface roughness at 6h 00
	Surface roughness, Ra (μm)					
0	12.371	6.084	3.121	2.915	2.353	81.0
10	42.505	16.802	16.076	13.930	9.206	78.3
20	47.565	19.841	21.566	15.198	13.264	72.1
30	40.335	17.067	14.306	9.988	6.577	83.7
40	29.736	13.835	15.081	10.538	5.706	80.8
50	26.550	12.084	13.708	9.935	6.033	77.3
60	23.623	11.014	10.107	8.262	4.610	80.5
70	25.213	8.025	8.266	9.222	5.864	76.7
80	18.201	6.560	6.941	7.770	5.617	69.1
90	18.368	9.633	8.396	6.570	5.327	71.0
Standard deviation	11.588	4.719	5.377	3.498	2.929	

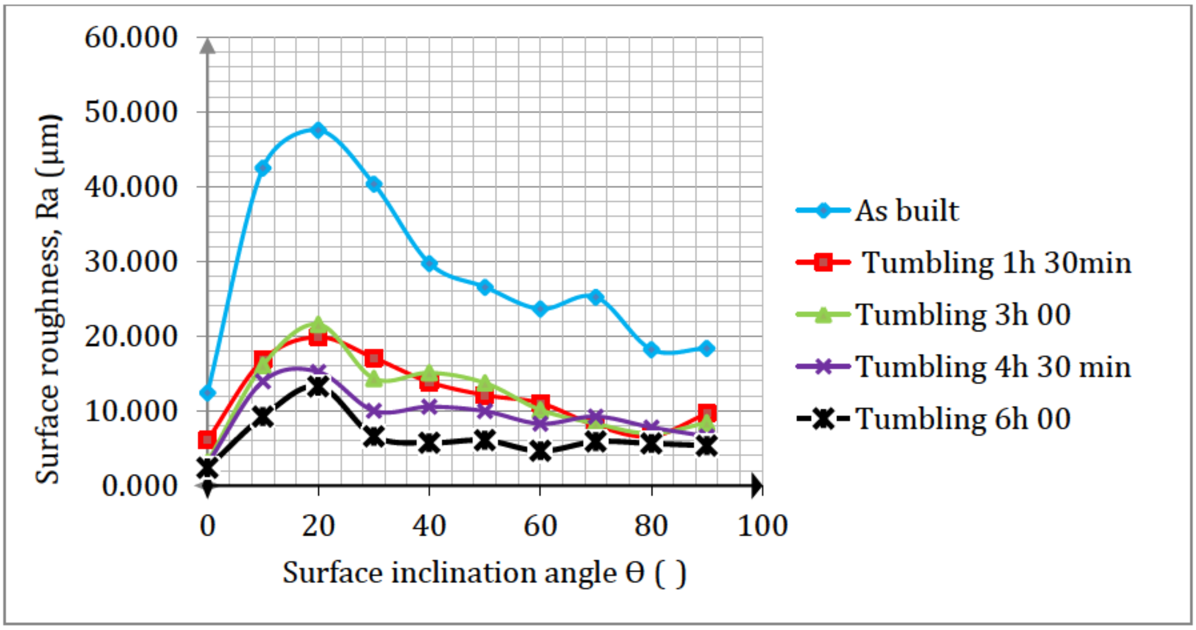

Figure 6.5: Surface inclination angle versus surface roughness for tumbled nylon test pieces

B. Shot peening

The results of the surface roughness measurements for shot peened nylon test pieces are shown in Table 6.4 and Figure 6.6.

Table 6.4: Average surface roughness for shot peened nylon test pieces

Surface inclination angle θ(°)		Shot peening period				% improvement of surface roughness at 8 min
	As built	2 min	4 min	6 min	8 min	
	Surface finish, Ra (μm)					
0	12.371	3.736	4.083	3.755	3.701	70.1
10	42.505	13.731	7.278	7.569	4.477	89.5
20	47.565	10.779	6.757	6.326	6.104	87.2
30	40.335	11.649	6.419	5.375	6.051	85.0
40	29.736	8.899	6.024	6.015	5.905	80.1
50	26.550	6.034	5.877	5.573	4.626	82.6
60	23.623	6.793	5.865	5.049	5.030	78.7
70	25.213	6.621	6.002	5.091	5.430	78.5
80	18.201	6.141	5.693	5.536	5.114	71.9
90	18.368	6.041	5.460	4.899	5.367	70.8
Standard deviation	11.588	3.116	0.846	1.001	0.764	

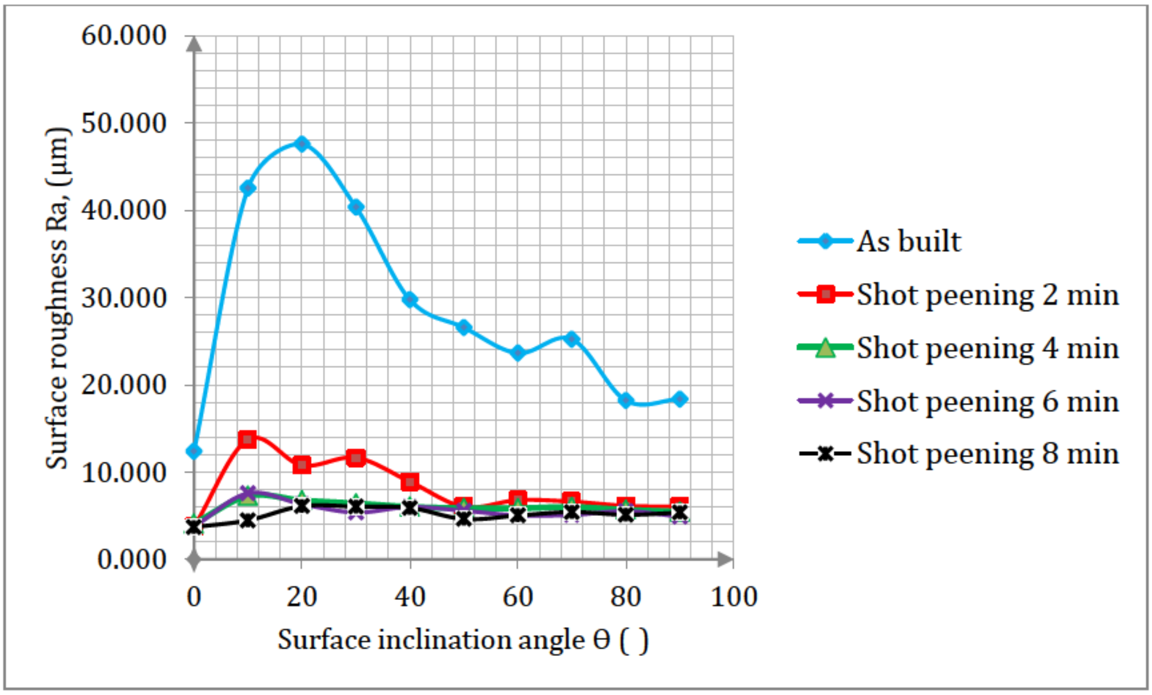

Figure 6.6: Surface inclination angle versus surface roughness for shot peened nylon test pieces

C. Hand finishing

The results of the surface roughness measurements for hand finishing for nylon test pieces are shown in Table 6.5 and Figure 6.7. The designations of the test pieces are according to Table 5.7.

Table 6.5: Average surface roughness for hand finished nylon test pieces

Surface inclination angle Θ (°)	As built	HFN1	HFN2	HFN3	HFN4	% improvement of surface roughness for HFN4 test piece
	Surface finish, Ra (μm)					
0	12.371	4.155	3.061	1.760	1.712	86.2
10	42.505	6.135	2.985	1.845	1.511	96.4
20	47.565	14.715	4.275	1.657	1.125	97.6
30	40.335	13.099	5.138	1.454	1.371	96.6
40	29.736	8.841	5.961	1.176	1.189	96.0
50	26.550	11.318	7.196	1.097	0.952	96.4
60	23.623	9.506	7.716	2.149	1.166	95.1
70	25.213	11.294	5.925	2.014	1.528	93.9
80	18.201	9.173	8.809	2.632	0.980	94.6
90	18.368	11.859	8.640	3.879	1.601	91.3
Standard deviation	11.588	3.1636	2.126	0.8119	0.2676	

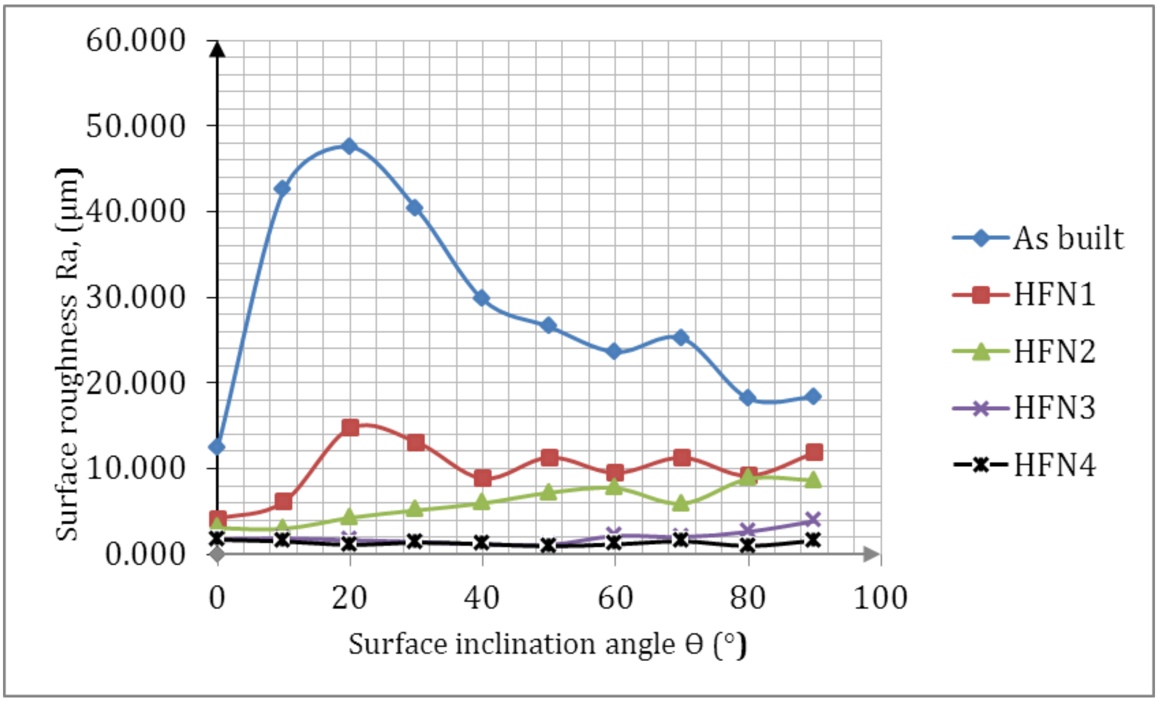

Figure 6.7: Surface inclination angle versus surface roughness for hand finished nylon test pieces

D. Spray painting

The results of the surface roughness measurements for spray painted nylon test pieces are shown in Table 6.6 and Figure 6.8. The designations of the test pieces are according to Table 5.8.

Table 6.6: Average surface roughness for spray painted nylon test pieces

Surface inclination angle Ɵ (°)	As built	SPN1	SPN2	SPN3	SPN4	% improvement of surface roughness
	Surface finish, Ra (μm)					
0	12.371	3.153	2.498	1.689	1.257	89.8
10	42.505	21.827	11.419	10.394	8.145	80.8
20	47.565	14.986	7.916	4.850	3.777	92.1
30	40.335	11.670	8.190	3.582	3.960	90.2
40	29.736	9.622	7.809	6.838	4.166	86.0
50	26.550	10.012	6.552	4.223	3.952	85.1
60	23.623	7.199	7.162	4.635	4.748	79.9
70	25.213	8.432	6.148	3.247	4.829	80.8
80	18.201	10.382	6.651	4.013	2.364	87.0
90	18.368	9.682	6.420	3.730	3.846	79.1
Standard deviation	11.588	4.947	2.212	2.383	1.783	

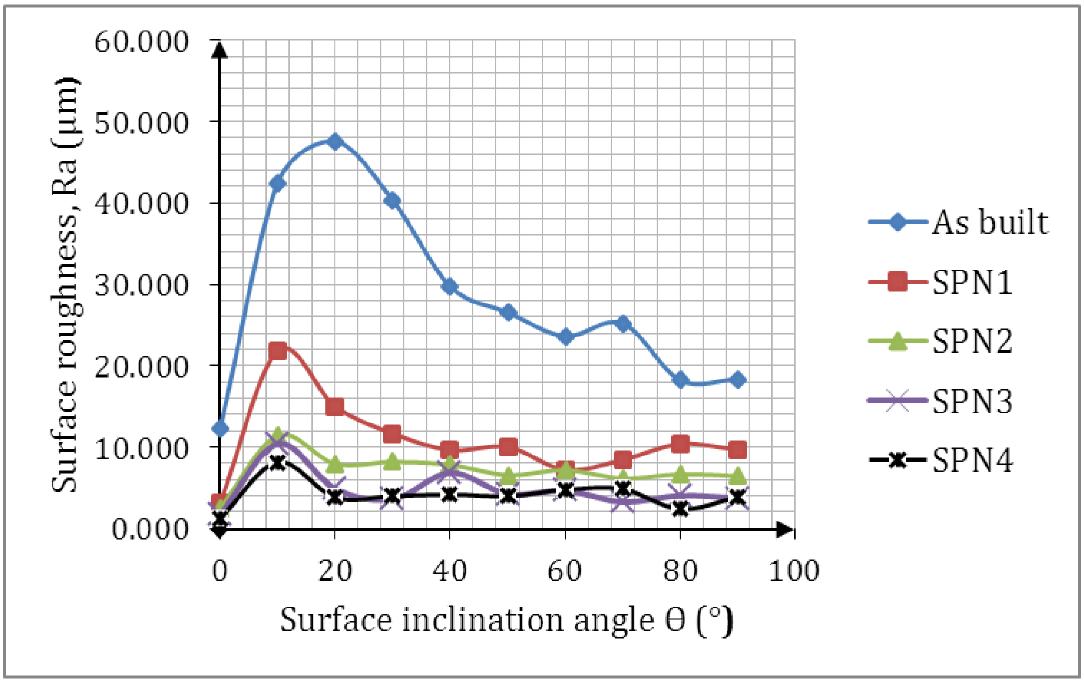

Figure 6.8: Surface inclination angle versus surface finish for spray painted nylon test pieces

E. CNC machining

The results of the surface roughness measurements for CNC machined nylon test pieces are shown in Table 6.7 and Figure 6.9.

Table 6.7: Average surface roughness for CNC machined nylon test piece

Surface inclination angle θ (°)	As built	CNC machining	% improvement of surface finish
	Surface finish Ra, (μm)		
0	12.371	12.733	-2.9
10	42.505	9.937	76.6
20	47.565	15.479	67.5
30	40.335	5.735	85.8
40	29.736	3.802	87.2
50	26.550	3.741	85.9
60	23.623	5.570	76.4
70	25.213	1.433	94.3
80	18.201	2.854	84.3
90	18.368	3.024	83.5
Standard deviation	11.588	4.698	

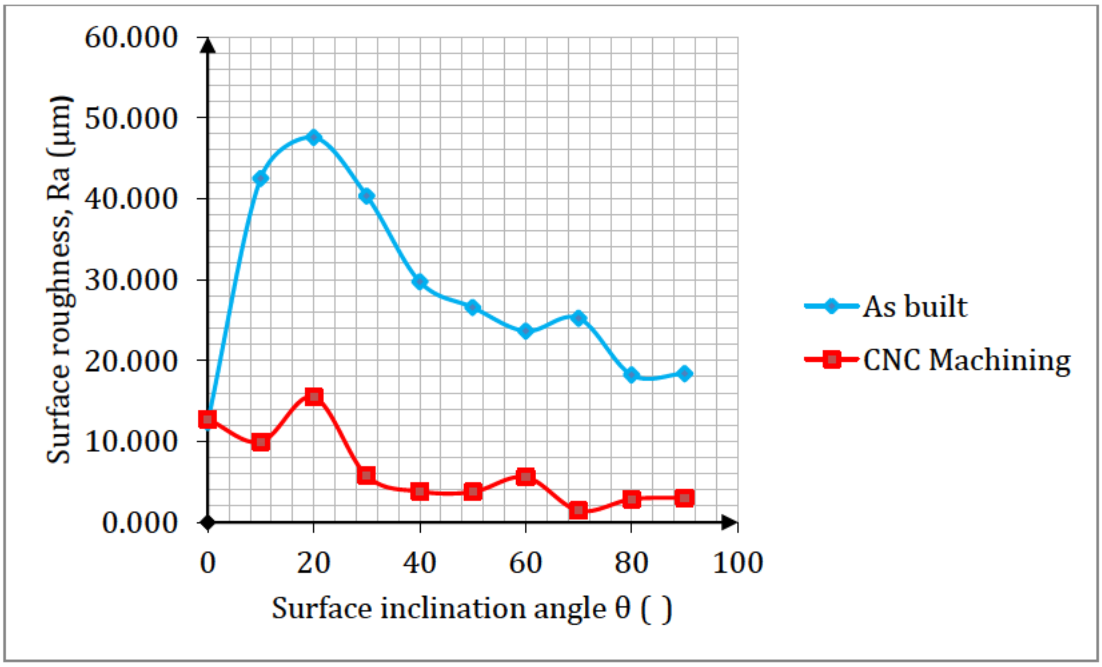

Figure 6.9: Surface inclination angle versus surface roughness for CNC machined nylon test piece

6.2.2 Observations and analysis of the results

A preliminary comparison of effectiveness of the post processing techniques can be performed by rating the percentage of improvement of the surface roughness (starting by the highest percentage) on a particular surface and analyzing the degree of repeatability of the rating through all the surfaces. The following abbreviations are used:

T-Tumbling, SPe-Shot peening, HF-Hand Finishing, SP-Spray Painting, CT-Chemical Treatment and CNC-CNC Machining. From Tables 6.3 to 6.7, the case of nylon test pieces is presented in Table 6.8.

Table 6.8: Rating of post processing techniques for nylon test pieces

Surface inclination angle θ (°)	Tumbling	Shot peening	Hand finishing	Spray painting	CNC machinin g	Rating of post processing techniques
	% improvement of surface roughness					
0	81.0	70.1	86.2	89.8	-2.9	SP,HF,T,SPe,CNC
10	78.3	89.5	96.4	80.8	76.6	HF,SPe,SP,T,CNC
20	72.1	87.2	97.6	92.1	67.5	HF,SP,SPe,T,CNC
30	83.7	85.0	96.6	90.2	85.8	HF,SP,CNC,SPe,T
40	80.8	80.1	96.0	86.0	87.2	HF,CNC,SP,T,SPe
50	77.3	82.6	96.4	85.1	85.9	HF,CNC,SP,SPe,T
60	80.5	78.7	95.1	79.9	76.4	HF,T,SP,SPe,CNC
70	76.7	78.5	93.9	80.8	94.3	CNC,HF,SP,SPe,T
80	69.1	71.9	94.6	87.0	84.3	HF,SP,CNC,SPe,T
90	71.0	70.8	91.3	79.1	83.5	HF,CNC,SP,T,SPe
Standard deviation	2.929	0.764	0.268	1.783	4.698	

From Table 6.8, the following observations can be highlighted:

A. Hand finishing

The hand finishing process with the lowest standard deviation occupies the first position on eight surfaces (from 10° to 60°, 80° and 90°), and the second position on the other two remaining surfaces (0 and 70°). The lowest percentage of improvement of surface finish is 86.2% on 0° surface angle while the highest being 97.6% on 20° surface angle. From Figure 6.7, a progressive improvement of surface finish across all surfaces is observed from "as built" to HFN1, from HFN1 to HFN2, from HFN2 to HFN3 and from HFN3 to HFN4 test pieces. In Figure 6.10, it can be observed that for HFN4 test piece, the surface finish across the surface inclination angle is almost constant. This is reflected by the small standard deviation of surface finish on the entire piece, which equals 0.268.

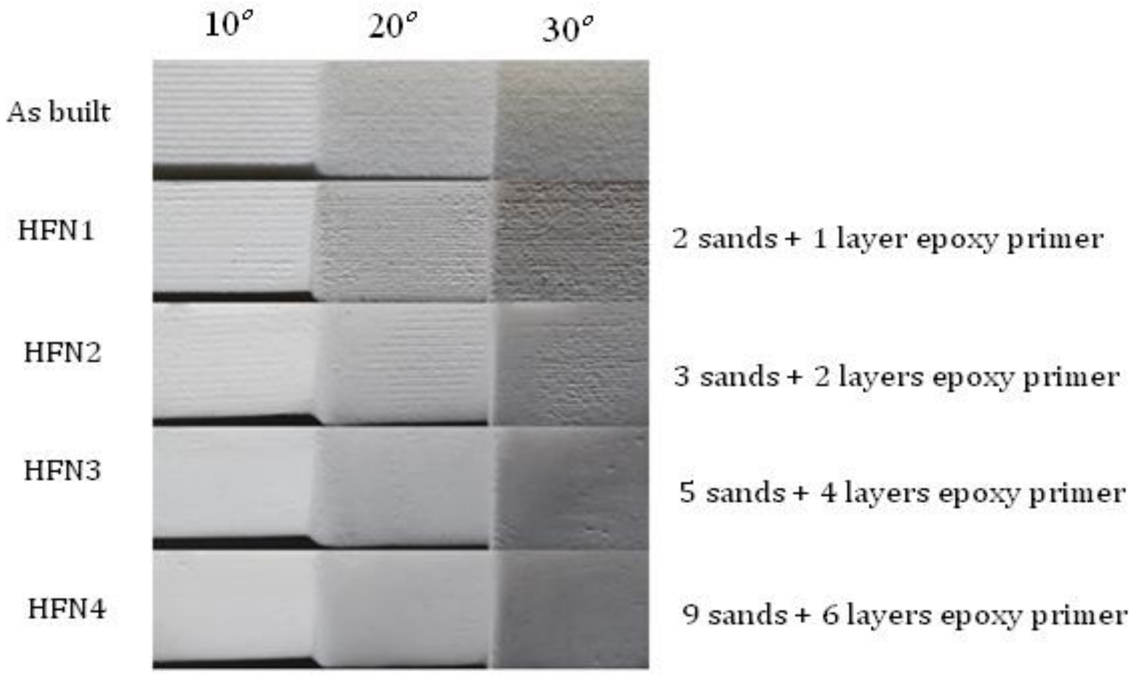

Figure 6.10: Improvement of surface finish of nylon test pieces by sanding and epoxy priming

It can be concluded that with a satisfactory dimensional accuracy of 63.5 % of points falling within the ±0.1 mm deviation range from the "as built" nylon test piece, the hand finishing technique performed for a period of 5h 20 min on HFN4 test piece, improved the surface finish from (12.371-47.565) to (1.712-1.125) μm Ra which is equivalent to an improvement of roughness between 86.2 and 97.6% on the surfaces.

B. Spray painting

Despite the poor dimensional accuracy with only 3% of points within ±0.1 mm deviation range from the "as built" nylon test piece, the spray painting technique improved the surface finish up to (1.257-3.777) μm Ra, thus producing an improvement of surface finish between 79.1 and 92.2%. The standard deviation which is equal to 1.783 indicates that the produced surface finish does not show big differences from one surface to another; and this can be seen from Table 6.8 where the spray painting in terms of percentage improvement of surface finish across the surfaces, occupies from first to the third position. In Figure 6.8, it can be seen that across all surfaces, the surface finish improves progressively with the application additional primer coats. This can be observed in Figure 6.11 which illustrates the progressive improvement of surface finish on 10°, 20° and 30° inclination angles.

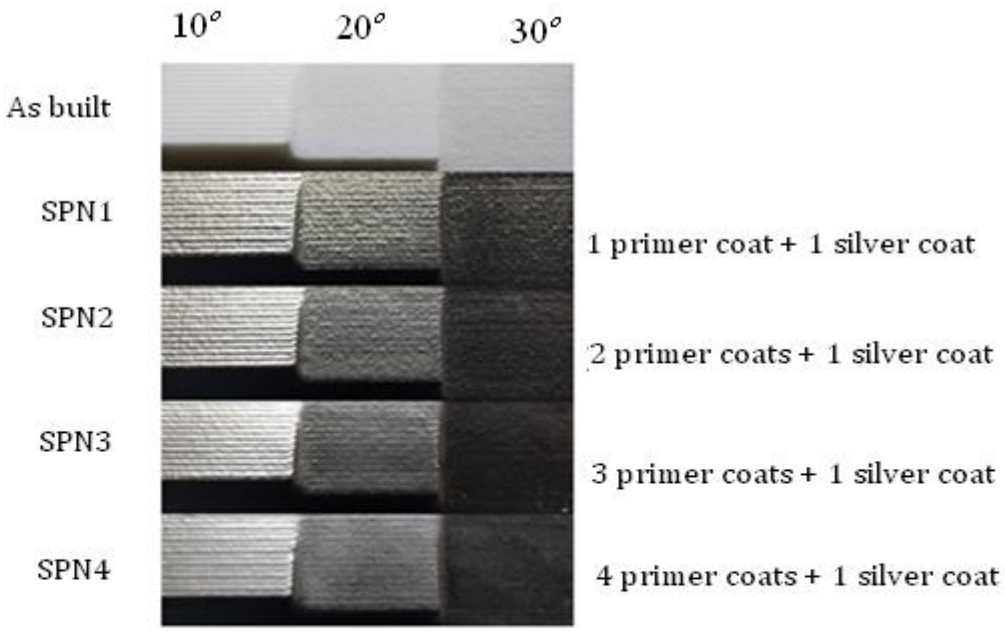

Figure 6.11: Improvement of surface finish of nylon test pieces by spray painting technique

An optimal surface finish is achieved in the case of SPN4 test piece where it can be observed that for 20 to 60° surface inclination angle, the surface finish is stabilized and remains practically at a constant value of 4.166 μm Ra, with exception of the surface finish of 2.364 μm R_a measured at 80° surface inclination angle.

C. Shot peening

With an excellent dimensional accuracy where 82.6 % of the total number of scanned points fall into the ±0.1 mm deviation range from the geometry of the "as built" nylon test piece, the shot peening technique applied to nylon test piece for a period of 8 min produced a very good improvement of surface finish varying from 70.1 to 89.5% with a small standard deviation of 0.764 which indicates that the shot peening of nylon test pieces produce surfaces with roughness which are not widely dispersed across the surface inclination angles. This can be observed from Figure 6.6 where the shot peening technique performed for 6 min and 8 min produce on 20° to 90° surface angles, a surface finish which oscillate around 6 µm R_a. However the percentage of improvement of surface finish is a bit lower when compared to hand finishing or spray painting techniques, this can be observed from Table 6.8, where the shot peening technique appears mostly in the third, fourth and fifth positions. Figure 6.12a shows the surface finish improvement on 10°, 20° and 30° surface inclination angles for shot peened nylon test pieces.

D. Tumbling

With very good dimensional accuracy with 88.3% of the total number of touch probe scanned points falling within the ± 0.1 mm deviation range from the "as built" nylon test piece, the tumbling technique applied to nylon test pieces for a period of 6 h produced 69.1 to 83.7% of improvement of surface finish with a standard deviation of 2.929. This can be observed on Figure 6.5 where the technique when applied for a period of 6 h, the surface finish on 30°to 90° surface angles is practically kept to a constant value of 6 µm R_a. From Table 6.8, the tumbling technique dominates fourth and a fifth positions, which indicates that the surface finish improvement is reduced across the surfaces when a comparison is made against the cases of hand finishing, spray painting or shot peening. It should be noticed that the improvement of surface finish through the tumbling technique is not totally progressive. At some stage, the surface finish may be improved, and later be increased. It can be observed that the tumbling applied for a period of 3 h increased the surface finish obtained compared to a tumbling period of 1 h 30 min. This can be explained by the fact that with the tumbling technique being a material removal process, there exists a transition period where fine burrs are created on the surfaces of the test pieces which are later removed by the tumbling process. This state is characterized by a poor surface finish. Figure 6.12b illustrates surface finish improvement on 10°, 20° and 30° surface angles through tumbling of nylon test pieces.

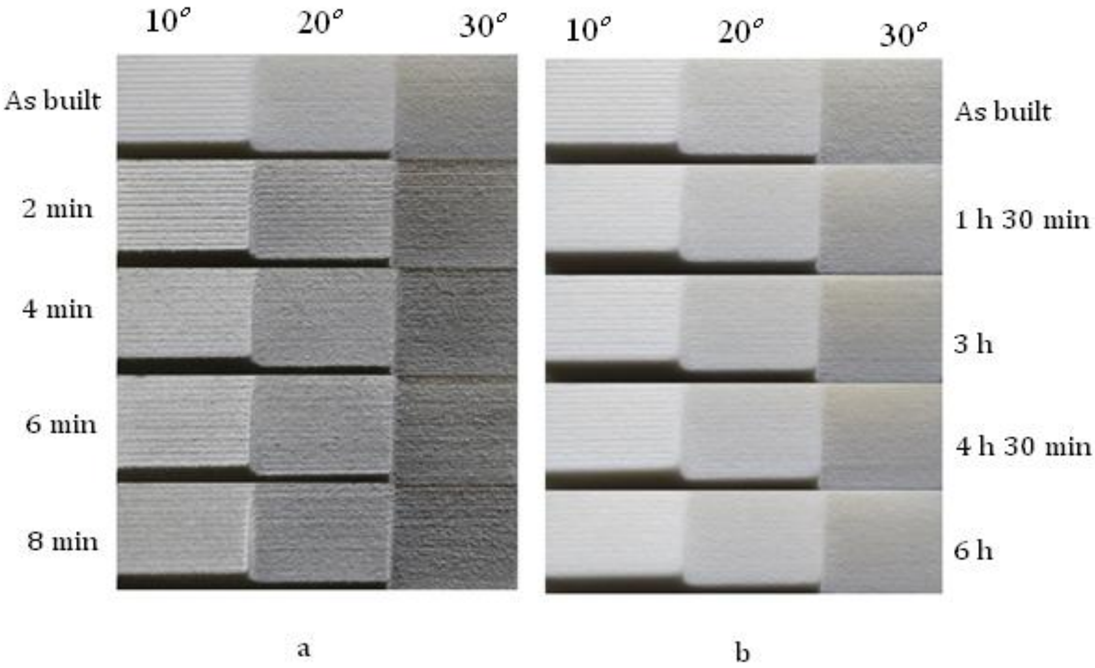

Figure 6.12: Improvement of surface finish of nylon test pieces through shot peening (a) and tumbling (b)

E. CNC machining

With poor dimensional accuracy with only 2.6% of the total number of touch probe scanned points falling in the ± 0.1 mm deviation range from the "as built" nylon test piece, the CNC machining technique could exhibit a negative effect on improvement of surface finish where on the horizontal surface, the surface roughness increased by 2.9%. The highest standard deviation of 4.698 indicates that the surface finish produced by CNC machining is widely dispersed across surfaces. From Table 6.8, it can be see that CNC machining occupies from first to fifth positions, second and fifth positions being dominant. This behavior indicates that the level of improvement of surface finish across the surfaces is reduced compared to hand finishing or spray painting. Compared to the shot peening and tumbling techniques, CNC machining exhibited a low percentage of surface finish improvement on 10° and 20° where the stair step effect is more pronounced; whereas at 30° surface angle, the level of improvement of the three techniques is approximately the same and equal to 85%. From 40° to 90° surface angles, the improvement of surface finish produced by CNC machining increases compared to shot peening or tumbling. Figure 6.9 shows that the CNC machined surface finish, following the trend of the surface finish of "as built" test piece which keeps changing across surfaces. This behavior can be explained by the fact that the cutting parameters were kept identical for all surface inclination angles and the inherited surface finish from the "as built" test piece influenced the final surface finish of CNC machined test piece.

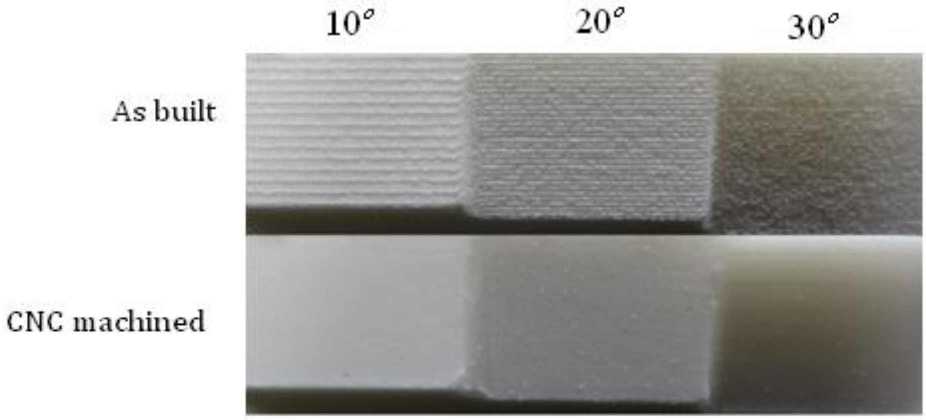

Figure 6.13: Improvement of surface finish of nylon test piece through CNC machining

Figure 6.13 illustrates the surface finish improvement produced through CNC machining on 10°, 20° and 30° surface inclination angles of the nylon test piece.

6.2.3 Conclusions

1. All five considered post processing techniques have improved the surface finish of the nylon test pieces produced though the LS process.
2. Despite the low dimensional accuracy produced by the hand finishing and spray painting techniques, in terms of improvement of surface finish of small nylon test pieces manufactured through the LS process, these two techniques are preferable. This is followed by shot peening, then tumbling and finally CNC machining. However for surface angles equal or greater to 30°, CNC machining produced higher percentage of improvement of surface finish comparatively to shot peening or tumbling techniques.
3. With exception of spray painting and CNC machining where the sharp corners, small protrusions do not wear off, the other three investigated post processing techniques, at different levels, come out with the negative deviations ranges at the specific areas such as sharp corners, transitions edges between relatively wide surfaces and small

protrusions. Despite the above mentioned dimensional accuracy defects on these specific areas of the test pieces, the shot peening and tumbling techniques provide the optimal solution for improvement of surface finish of small LS nylon test pieces with the least negative effects on the dimensional accuracy of the test pieces. Within the ±0.1 mm deviation range from the "as built" nylon test piece, shot peening technique produced very good dimensional accuracy of 82.6 % and an improvement of surface finish varying between 70.1 to 89.5% with a standard deviation of 0.764. Very good dimensional accuracy of 88.3% and an improvement of surface finish varying from 69.1 to 83.7% with a standard deviation of 2.929 were achieved through the tumbling process of nylon test pieces manufactured through LS process.

6.3 Measurements of surface roughness for Alumide® test pieces

6.3.1 Results of measurements of surface roughness for Alumide® test pieces

The surface roughness of "as built", tumbled, shot peened, hand finished, spray painted and CNC machined Alumide® test pieces were measured.

A. Tumbling

The results of the surface roughness measurements for tumbling of Alumide® test pieces are shown in Table 6.9 and Figure 6.14.

Table 6.9: Average surface roughness for tumbling of Alumide® test pieces

Surface inclination angle Θ (°)	As built	Tumbling period 1 h 30 min	3 h	4 h 30 min	6 h	% improvement of surface finish for 6 h
	Surface finish, Ra (µm)					
0	14.921	8.239	6.098	5.141	3.801	74.5
10	32.725	19.749	17.196	15.695	8.283	74.7
20	37.643	19.340	13.008	8.075	8.191	78.2
30	32.975	16.335	11.780	9.147	6.474	80.4
40	34.268	11.677	9.119	8.840	6.191	81.9
50	34.016	15.044	9.043	8.192	6.907	79.7
60	31.511	10.895	9.063	7.189	6.066	80.7
70	22.181	10.761	7.558	6.439	6.302	71.6
80	19.115	10.461	7.859	7.170	5.529	71.1
90	18.716	10.955	7.393	6.494	6.620	64.6
Standard deviation	8.148	4.005	3.313	2.885	1.279	

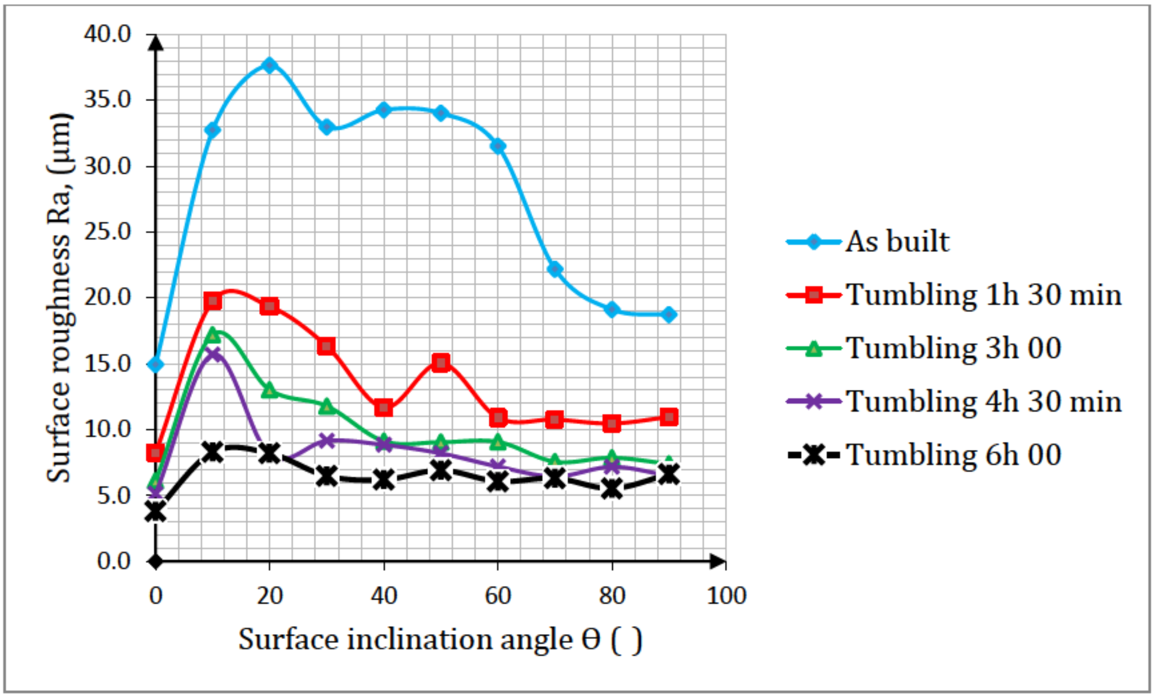

Figure 6.14: Surface inclination angle versus surface roughness for tumbled Alumide® test pieces

B. Shot peening

The results of the surface roughness measurements for shot peening of Alumide® test pieces are shown in Table 6.10 and Figure 6.15.

Table 6.10: Average surface roughness for shot peening of Alumide® test pieces

Surface inclination angle ϴ (°)	As built	Shot peening period				% improvement of surface finish	
		1 min	2 min	3 min	4 min	3 min	4 min
	Surface finish, Ra (µm)						
0	14.921	10.699	8.703	7.782	9.046	47.8	39.4
10	32.725	17.325	16.323	16.247	12.693	50.4	61.2
20	37.643	12.388	13.702	10.885	12.256	71.1	67.4
30	32.975	12.968	14.629	11.258	13.282	65.9	59.7
40	34.268	17.449	12.944	10.932	10.968	68.1	68.0
50	34.016	16.499	10.309	10.605	13.131	68.8	61.4
60	31.511	13.690	11.307	10.733	12.381	65.9	60.7
70	22.181	13.788	12.144	9.618	11.703	56.6	47.2
80	19.115	12.688	12.081	9.408	10.455	50.8	45.3
90	18.716	10.564	11.747	9.657	11.110	48.4	40.6
Standard deviation	8.148	2.518	2.165	2.202	1.324		

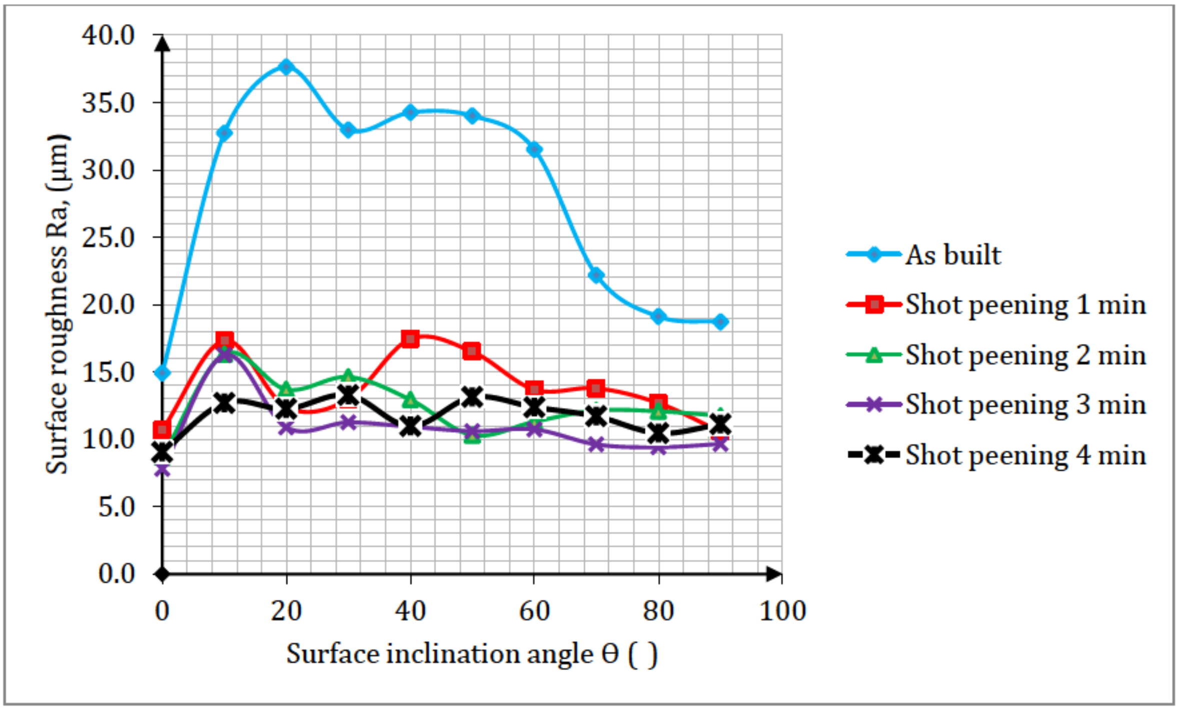

Figure 6.15: Surface inclination angle versus surface roughness for shot peened Alumide® test pieces

C. Hand finishing

The results of the surface roughness measurements for hand finishing of Alumide® test pieces are shown in Table 6.11 and Figure 6.16. The designations of the test pieces are according to Table 5.7.

Table 6.11: Average surface roughness for hand finishing of Alumide® test pieces

Surface inclination angle θ (°)	As built	HFA1	HFA2	HFA3	HFA4	% improvement of surface finish for HFA4
	Surface roughness, Ra (µm)					
0	14.921	4.368	4.070	1.953	1.839	87.7
10	32.725	5.030	5.014	1.797	1.740	94.7
20	37.643	7.293	7.453	2.379	1.534	95.9
30	32.975	10.131	7.266	2.782	1.438	95.6
40	34.268	7.396	5.600	1.637	1.601	95.3
50	34.016	8.245	5.847	1.537	1.370	96.0
60	31.511	8.227	5.827	2.143	1.376	95.6
70	22.181	7.401	10.256	4.105	2.174	90.2
80	19.115	7.788	6.263	2.757	1.388	92.7
90	18.716	8.503	7.782	3.731	1.927	89.7
Standard deviation	8.1483	1.6675	1.7348	0.8718	0.2741	

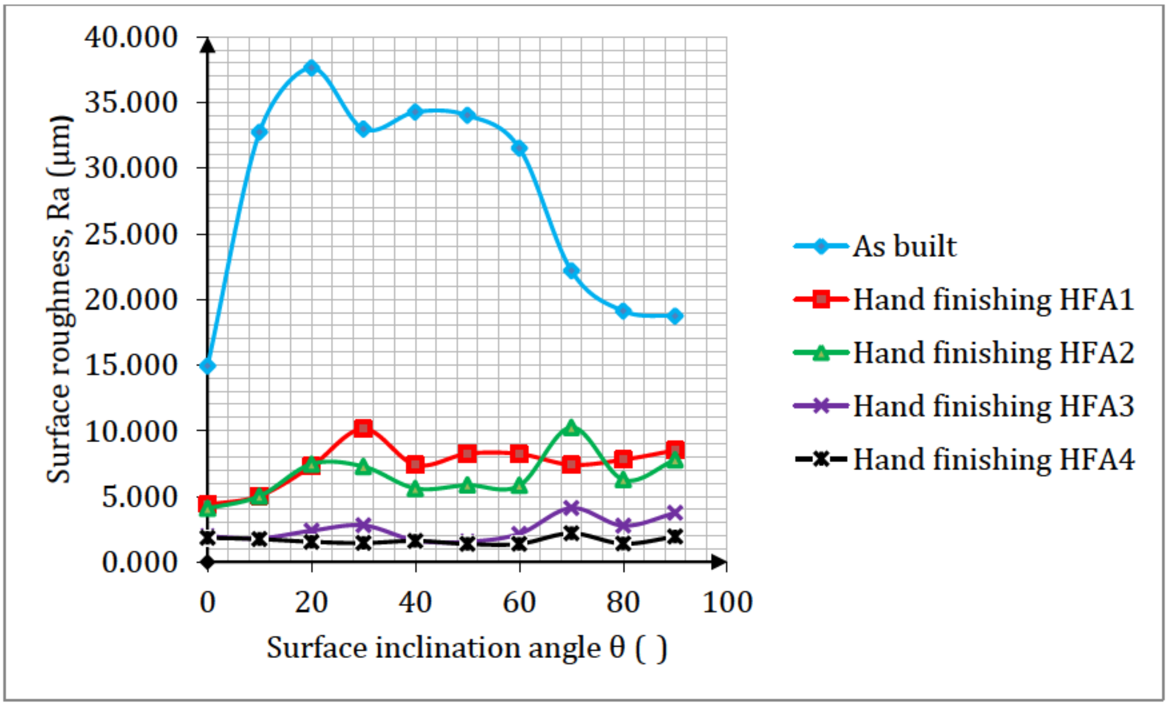

Figure 6.16: Surface inclination angle versus surface roughness for hand finished Alumide® test pieces

D. Spray painting

The results of the surface roughness measurements for spray painting of Alumide® test pieces are shown in Table 6.12 and Figure 6.17. The designations of the test pieces are according to Table 5.8.

Table 6.12: Average surface roughness for spray painting of Alumide® test pieces

Surface inclination angle θ (°)	Designation of the test pieces					% improvement of surface finish for SPA4
	As built	SPA1	SPA2	SPA3	SPA4	
	Surface finish, Ra (µm)					
0	14.921	4.680	3.862	2.683	1.711	88.5
10	32.725	25.041	10.755	11.656	6.803	79.2
20	37.643	17.688	6.902	5.376	2.897	92.3
30	32.975	12.285	5.868	3.852	3.703	88.8
40	34.268	10.480	6.370	4.534	3.447	89.9
50	34.016	9.672	5.673	4.287	2.656	92.2
60	31.511	13.272	5.430	3.941	2.952	90.6
70	22.181	8.922	6.855	3.690	3.650	83.5
80	19.115	8.512	4.275	3.418	2.948	84.6
90	18.716	7.848	5.807	4.786	3.574	80.9
Standard deviation	8.148	5.812	1.886	2.515	1.326	

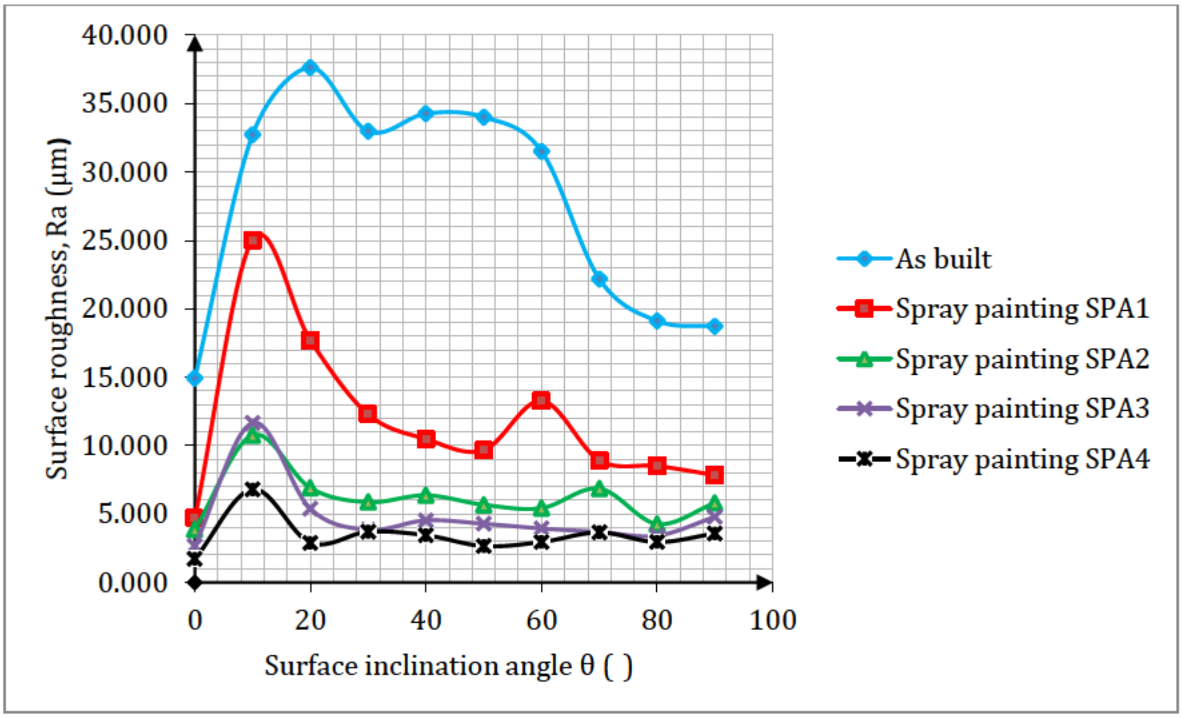

Figure 6.17: Surface inclination angle versus surface roughness for spray painted Alumide® test pieces

E. CNC machining

The results of the surface roughness measurements for CNC machining of Alumide® parts are shown in Table 6.13 and Figure 6.18.

Table 6.13: Average surface roughness for CNC machining of Alumide® test piece

Surface inclination angle θ (°)	As built	CNC machining	% improvement of surface finish
	Surface roughness, Ra (μm)		
0	14.921	5.522	63.0
10	32.725	7.239	77.9
20	37.643	11.628	69.1
30	32.975	4.554	86.2
40	34.268	5.260	84.7
50	34.016	4.933	85.5
60	31.511	3.717	88.2
70	22.181	2.399	89.2
80	19.115	2.709	85.8
90	18.716	3.471	81.5
Standard deviation	8.148	2.693	

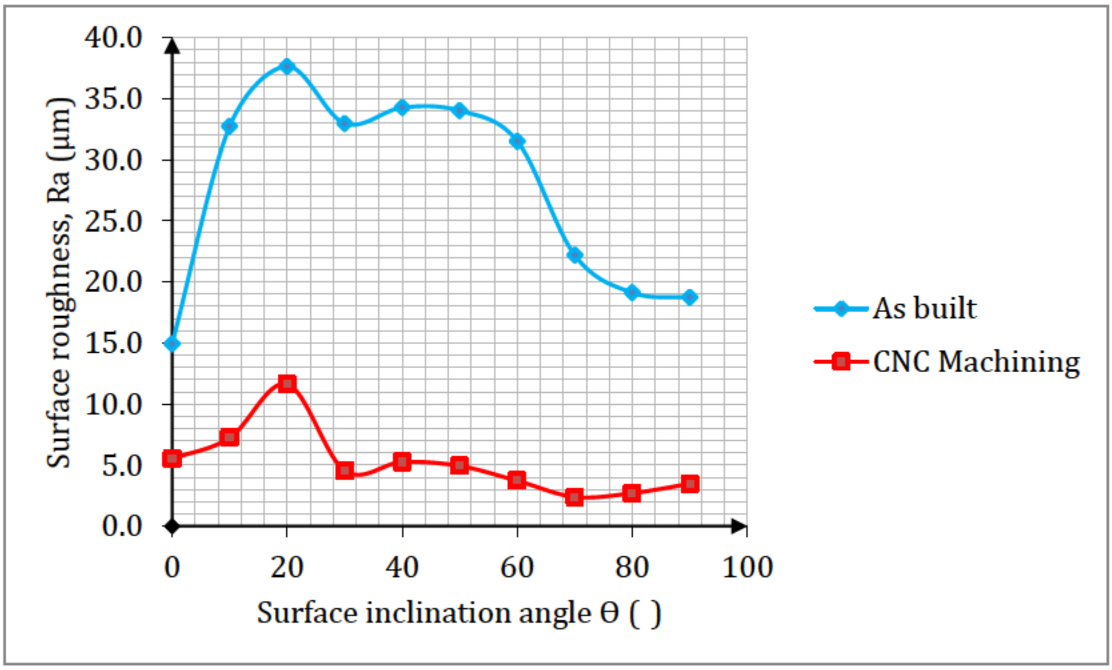

Figure 6.18: Surface inclination angle versus surface roughness for CNC machined Alumide® test piece

6.3.2 Observations and analysis of the results

The rating of the percentage of improvement of the surface finish of the five post processing techniques across the surface inclination angles on the Alumide® test pieces is presented in Table 6.14.

Table 6.14: Rating of improvement of surface finish for Alumide® test pieces

Surface inclination angle θ (°)	Tumbling	Shot peening 3 min	Hand finishing	Spray painting	CNC machining	Rating of post processing techniques
	% improvement of surface roughness					
0	74.5	47.8	87.7	88.5	63.0	SP,HF,T,CNC,SPe
10	74.7	50.4	94.7	79.2	77.9	HF,SP,CNC,T,SPe
20	78.2	71.1	95.9	92.3	69.1	HF,SP,T,SPe,CNC
30	80.4	65.9	95.6	88.8	86.2	HF,SP,CNC,T,SPe
40	81.9	68.1	95.3	89.9	84.7	HF,SP,CNC,T,SPe
50	79.7	68.8	96.0	92.2	85.5	HF,SP,CNC,T,SPe
60	80.7	65.9	95.6	90.6	88.2	HF,SP,CNC,T,SPe
70	71.6	56.6	90.2	83.5	89.2	HF,CNC,SP,T,SPe
80	71.1	50.8	92.7	84.6	85.8	HF,CNC,SP,T,SPe
90	64.6	48.4	89.7	80.9	81.5	HF,CNC,SP,T,SPe
Standard deviation	1.279	2.202	0.274	1.326	2.693	

A. Hand finishing

With a dimensional accuracy of 65.5% within a ±0.1 mm deviation range, the hand finishing technique occupies the first positions with an improvement of surface finish ranging from 87.7 to 96% with a small standard deviation of 0.274. From Figure 6.16, with exception of a negligible portion appearing on the 70° surface inclination angle where the surface finish of HFA1 test piece is less than the surface finish of the HFA2 test piece, it can be observed that the surface roughness of the test pieces decreases progressively with the further application of sanding and priming. Finally, the surface finish across all surfaces on the HFA4 test piece could be stabilized at a value of more or less 2 µm R_a. Figure 6.19 illustrates the progressive improvement of surface roughness on 10°, 20° and 30° surface inclination angles of hand finished Alumide® test pieces.

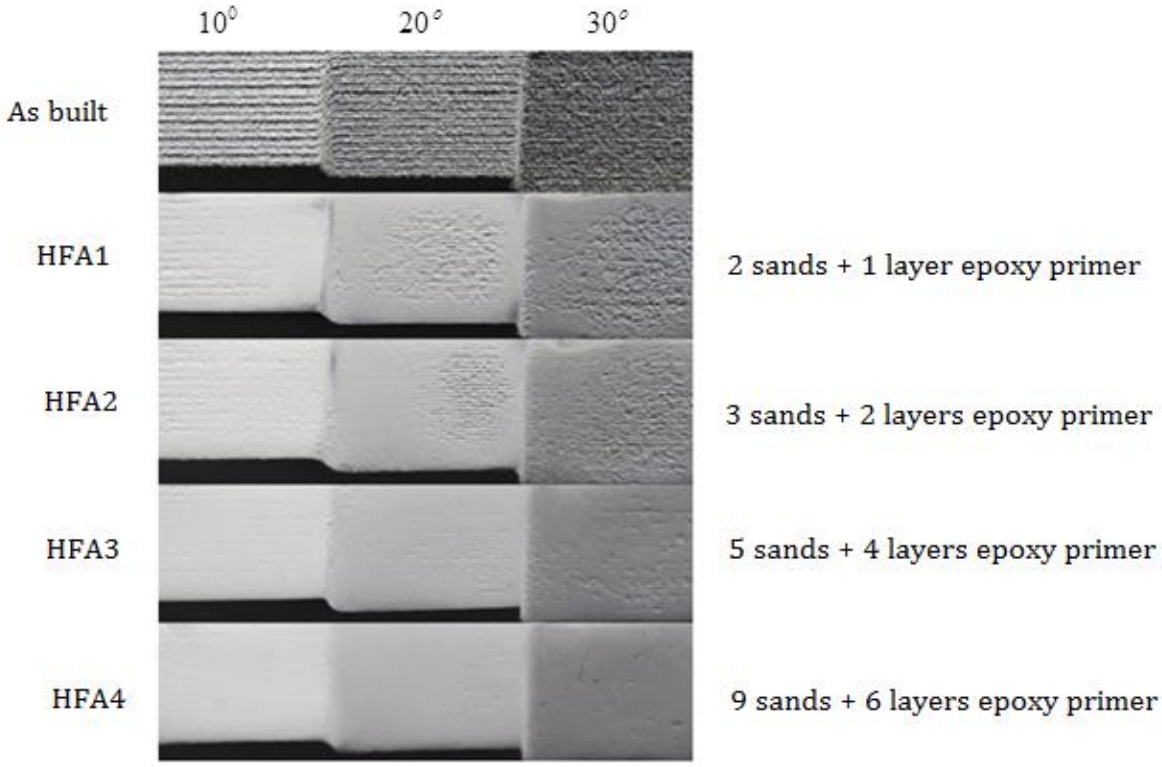

Figure 6.19: Surface finish improvement of Alumide® test pieces by hand finishing

It can be observed that the surface roughness for hand finishing with 9 sanding steps and application of 6 layers of MS epoxy primer performed on HFA4 test piece produced a uniform surface roughness across the 10°, 20° and 30° surface inclination angles. A similar trend is observed on the other surfaces of the test piece.

B. Spray painting

With a dimensional accuracy of 18% within a ±0.1 mm deviation range, 79.2 to 92.3% improvement of surface roughness with a relatively small standard deviation of 1.326 was achieved by the spray painting technique applied to the SPA4-Alumide® test piece. From Table 6.14, it can be realized that with an advantage of being at the first position for the horizontal surface, 60% of second positions and 30% of third positions are occupied by the spray painting technique. Figure 6.17 shows that the surface finish is improved progressively across all surface inclination angles with the increase of the number of applied undercoats.

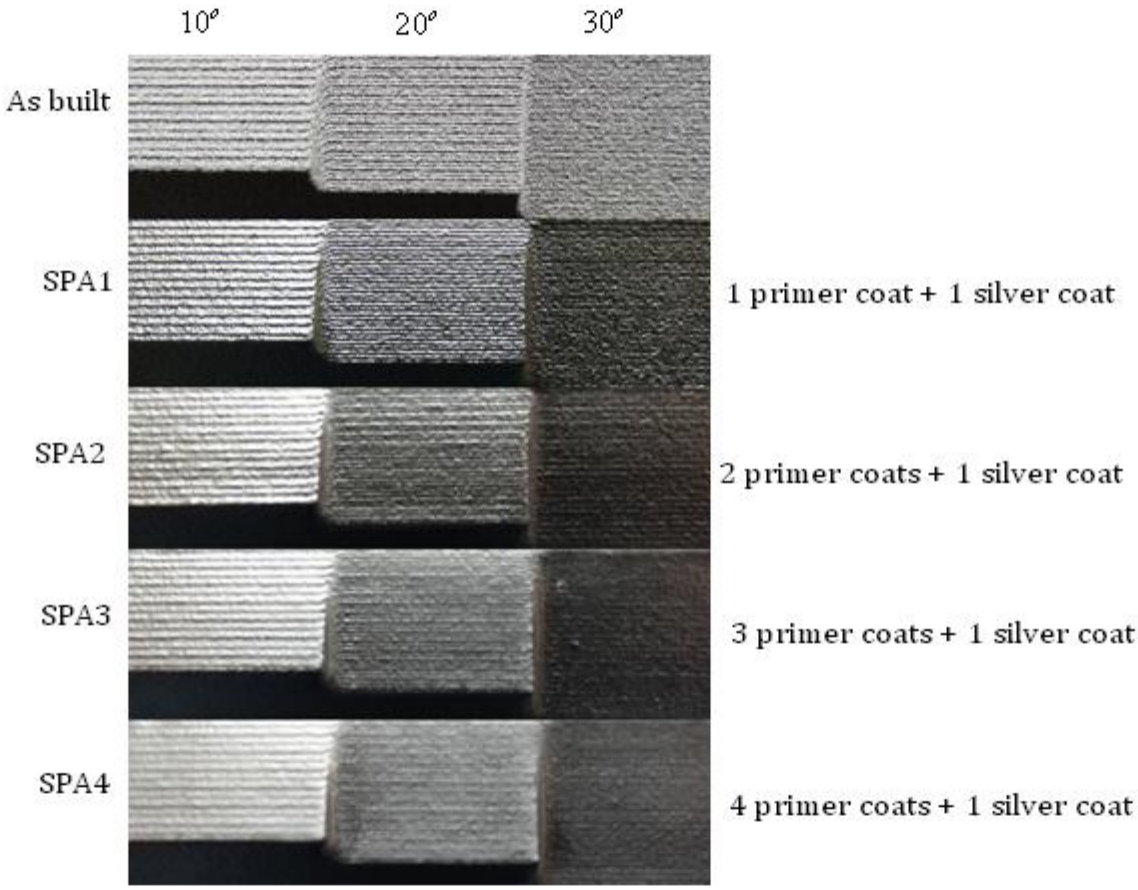

Figure 6.20: Surface finish improvement of Alumide® test pieces by spray painted

The application of four undercoats followed by silver painting leads to the stabilization of surface finish around 3 μm R_a for the 20° to 90° surface angle range.

C. CNC machining

For CNC machining of Alumide® test piece, only 2.6% of the total touch probe scanned points satisfied the ±0.1 mm deviation from the geometry of the "as built" test piece. This unexpected behavior of CNC machining as compared to other post processing techniques may be attributed to the setup of the test piece on the machine or to the machine calibration. From Table 6.14, CNC machining occupies dominantly fifth and third position, thus making this technique to be classified on the third position for improvement of surface finish of Alumide® test piece. With a standard deviation of 2.693, CNC machining improved the surface finish from 14.921 to 5.522 µm R_a on the horizontal surface; and from 22.181 to 2.399 µm R_a on the surface inclined at 70°, thus producing 63 to 89.2 % of improvement of surface finish across all surfaces of the test piece. The horizontal surface with the roughest initial surface finish, and surfaces at 10° and 20°, where the stair-step effect is more pronounced experienced low improvement of surface finish. By keeping the same cutting parameters (cutting depth, step-over and feed rate) in order to have the same range of dimensional accuracy, the surface finish of surfaces at 10° and 20° improved but did not attain the surface finish of 5.522 µm R_a measured on the horizontal surface. Figure 6.18 also shows that the trend of variation of the surface roughness across the surface inclination angles for "as built" test piece is in a similar manner followed for the CNC machined test piece. This implies that the stabilization of the surface finish across all the surface inclination angles through CNC machining is only possible if each surface inclination angle is assigned its own cutting parameters, thus keeping changing the setup of the machine, which leads to excessive machining time and costs.

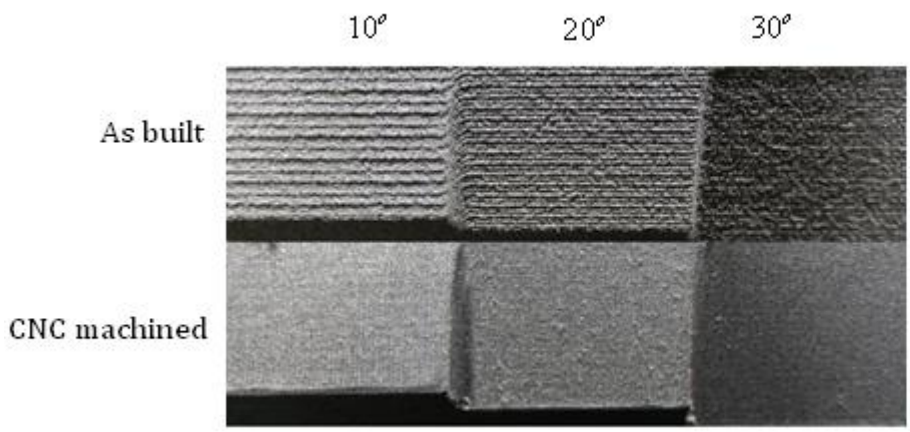

Figure 6.21: Improvement of surface finish of Alumide® test piece by CNC machining

For the other surfaces, the surface finish is reduced considerably to attain 80.5 to 89.2% of improvement with a standard deviation of 1.1 indicating relative small differences of surface finish across these surfaces (Table 6.13).

D. Tumbling

With 80.1 % of dimensional accuracy within the ±0.1 mm deviation range, tumbling of Alumide® performed for a period of 6 h exhibited a good improvement of surface roughness ranging from 64.6 to 81.9% with a small standard deviation of 1.279. Though the surface roughness values obtained through the tumbling technique are higher than the values obtained by CNC machining, the low standard deviation is an advantage for the tumbling technique when a uniform surface finish across the entire part is desired. From Figure 6.14, there is a progressive improvement of surface finish with the increase of tumbling period. For the test piece subjected to a tumbling process for a period of 6 h, the surface finish on 30° to 90° surface angles varies slightly and practically, it can be assumed to be fixed at an average value of 6.3 μm R_a with a standard deviation of 0.44.

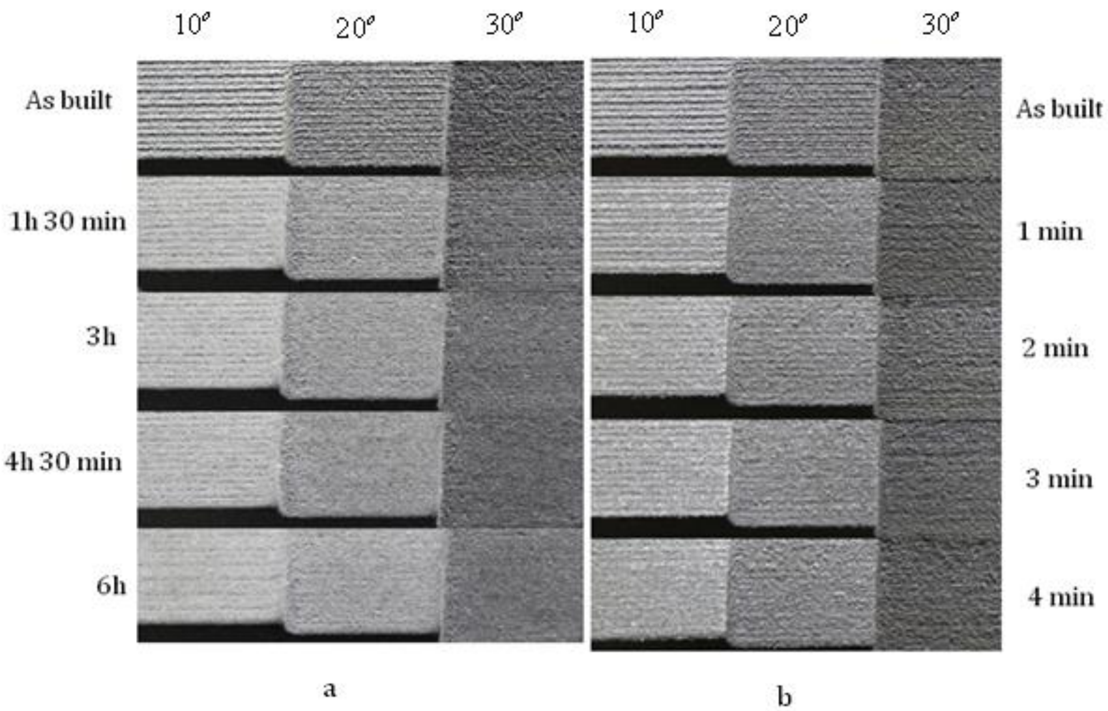

Figure 6.22: Surface finish improvement for Alumide® test pieces by Tumbling (a) and by shot peening (b)

Figure 6.22a shows a progressive improvement of the surface roughness on 10°, 20° and 30° surface inclination angles of the tumbled Alumide® test pieces. A similar behavior is observed on other surfaces of the test pieces.

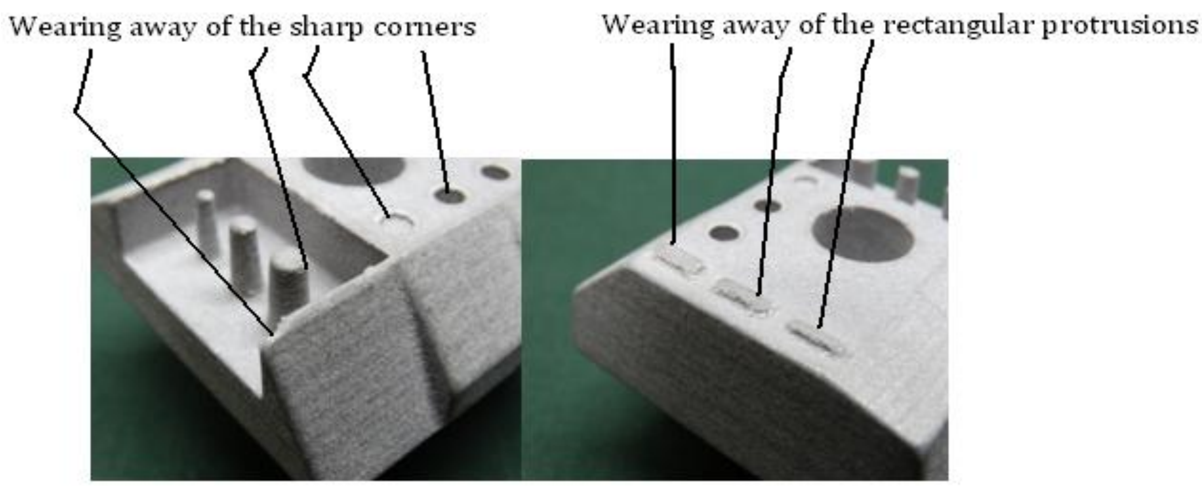

Figure 6.23: Effect of tumbling process on sharp corners and small protrusions

However, the sharp corners and protrusions are badly worn away during the tumbling process of the test pieces, thus locally affecting negatively the dimensional accuracy of the test pieces. Figure 6.23 shows the effect of tumbling technique for a period of 6 h on the sharp corners and protrusions of Alumide® test piece.

E. Shot peening

The shot peening produced a dimensional accuracy of 92.1% within ±0.1 mm deviation range. From Table 6.14, the shot peening technique performed for a period of 3 min takes the fifth (last) positions with 47.8 to 71.1% of improvement of surface finish with a standard deviation of 2.202. Table 6.10 supported by Figure 6.15 show that the increase of the period for shot peening of Alumide® test piece from 3 to 4 min worsened the surface finish for 20° to 90° surface angles. It can also be observed that the improvement of the surface finish through increase of shot peening period does not produce necessarily a progressive decrease of surface irregularities across the entire test piece (Figure 6.22b). However the shot peening for a period of 3 min produced a relatively constant surface roughness value which can be averaged to 10.4 μm R_a with a standard deviation of 0.713 for 20° to 90° surface angles. This is an advantage where a uniform surface roughness is desired for the entire part.

6.3.3 Conclusions

1. All five considered post processing techniques have improved the surface finish of the Alumide® test pieces produced though the LS process.
2. Likewise for nylon test pieces, despite of the low dimensional accuracy produced by the hand finishing and spray painting techniques, in terms of improvement of surface finish of small Alumide® test pieces manufactured through LS process, the last two techniques are most preferable, followed by CNC machining, tumbling and finally shot peening.
3. Within a ±0.1 mm deviation range from the geometry of 'as built" test piece, despite the negative effect on the dimensional accuracy on sharp corners and protrusions of the test pieces, the tumbling and shot peening techniques provide the optimal solution for improvement of surface finish of small LS Alumide® test pieces. The tumbling technique will be useful for parts without sharp corners or protrusions. The tumbling technique produced dimensional accuracy of 80.1% and an improvement of surface finish from 64.6 to 81.9%, with a standard deviation of 1.279. A dimensional accuracy of 92.1% and an improvement of surface finish varying from 47.8 to 71.1% with a standard deviation of 2.929 were achieved through the shot peening process. In the range of 30° to 90° surface angles, a uniform surface finish of 6.3 µm and 10.4 µm R_a can be achieved through tumbling and shot peening respectively.

6.4 Measurements of surface roughness for ABS test pieces

6.4.1 Results of measurements of surface roughness for ABS test pieces

A. Tumbling

The results of the surface roughness measurements for tumbling of ABS test pieces are shown in Table 6.15 and Figure 6.24.

Table 6.15: Average surface roughness for tumbling of ABS test pieces

Surface inclination angle ϴ (°)	As built	Tumbling period				% improvement of surface finish for 4 h
		1 h	2 h	3 h	4 h	
0	18.613	15.868	13.272	13.462	11.684	37.2
10	52.569	45.294	42.931	39.818	38.566	26.6
20	66.326	57.260	32.229	46.925	47.597	28.2
30	43.602	34.007	31.886	32.987	29.679	31.9
40	35.541	32.326	22.876	24.106	20.988	40.9
50	29.612	28.350	21.981	21.068	18.518	37.5
60	26.271	26.589	18.672	19.015	14.795	43.7
70	23.249	24.377	16.373	15.540	11.426	50.9
80	22.421	17.372	14.884	15.934	13.465	39.9
90	20.966	17.311	13.265	12.022	10.658	49.2
Standard deviation	15.704	13.185	9.889	11.931	12.792	

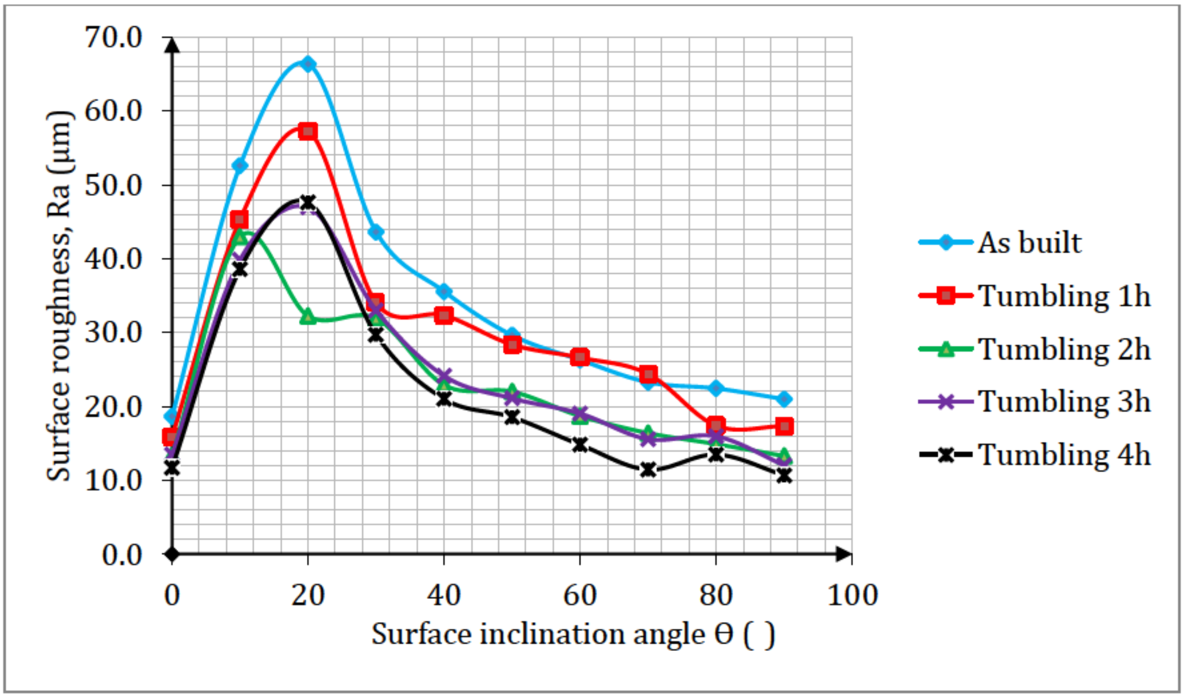

Figure 6.24: Surface inclination angle versus surface roughness for tumbled ABS test pieces

B. Shot peened

The results of the surface roughness measurements for shot peening of ABS test pieces are shown in Table 6.16 and Figure 6.25.

Table 6.16: Average surface roughness for shot peening of ABS test pieces

Surface inclination angle Θ (°)	As built	Shot peening period				% improvement of surface finish for 8 min
		2 min	4 min	6 min	8 min	
		Surface finish, Ra (µm)				
0	18.613	14.695	12.455	10.917	8.249	55.7
10	52.569	34.443	31.059	31.878	26.717	49.2
20	66.326	34.726	27.342	23.636	20.074	69.7
30	43.602	15.882	9.525	8.844	11.244	74.2
40	35.541	10.662	7.393	7.501	8.243	76.8
50	29.612	8.412	8.067	7.026	7.388	75.0
60	26.271	7.597	6.633	7.676	10.183	61.2
70	23.249	7.518	8.416	8.741	7.213	69.0
80	22.421	12.315	11.570	11.062	7.480	66.6
90	20.966	8.406	9.643	6.816	6.850	67.3
Standard deviation	15.704	10.486	8.6563	8.4462	6.6744	

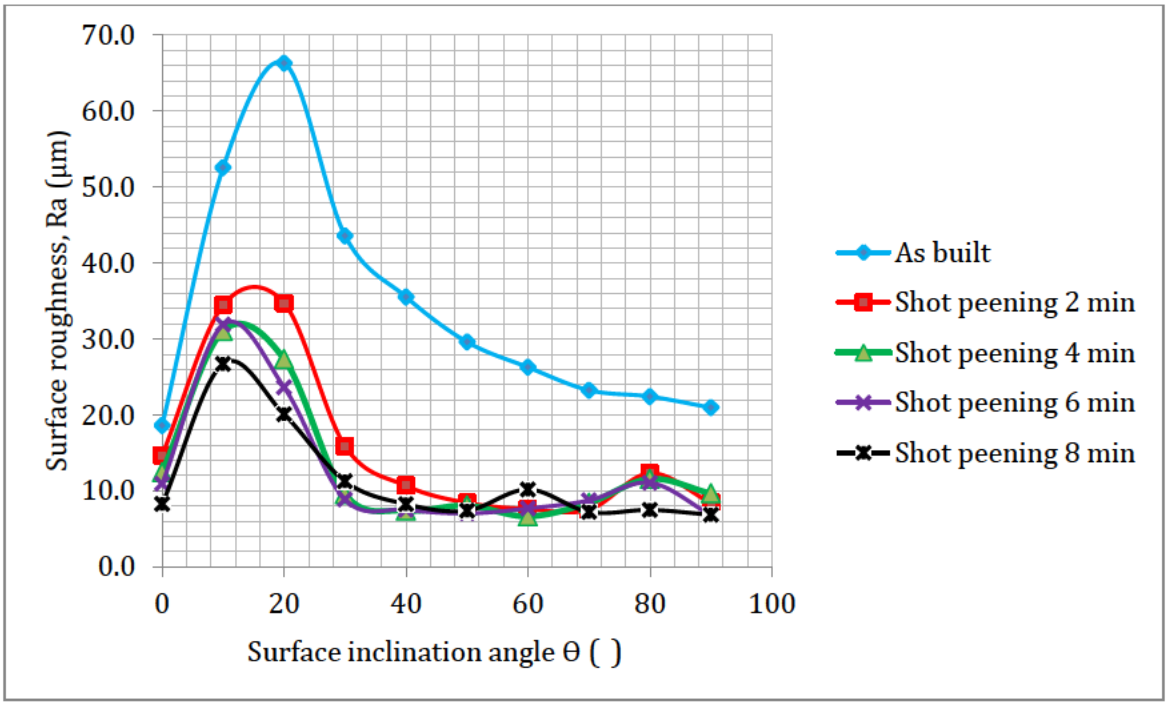

Figure 6.25: Surface inclination angle versus surface roughness for shot peened ABS test pieces

C. Hand finishing

The results of the surface roughness measurements for hand finishing of ABS test pieces are shown in Table 6.17 and Figure 6.25. The designations of the test pieces are according to Table 5.7.

Table 6.17: Average surface roughness for hand finish of ABS test pieces

Surface inclination angle θ (°)	As built	Hand finished test pieces				% improvement of surface finish for HFABS4
		HFABS1	HFABS2	HFABS3	HFABS4	
	Surface finish, Ra (µm)					
0	18.613	1.095	1.303	1.196	0.852	95.4
10	52.569	1.390	1.480	1.911	1.435	97.3
20	66.326	1.081	1.141	1.212	1.155	98.3
30	43.602	0.803	1.260	1.156	1.014	97.7
40	35.541	0.987	0.864	1.190	0.925	97.4
50	29.612	1.053	0.972	1.322	0.942	96.8
60	26.271	1.178	1.267	1.716	0.856	96.7
70	23.249	1.194	1.570	1.264	1.154	95.0
80	22.421	1.353	4.418	3.004	1.330	94.1
90	20.966	1.701	1.743	1.858	1.160	94.5
Standard deviation	15.704	0.249	1.024	0.579	0.199	

The figure 6.26 shows the variation of the surface roughness with the inclination angle.

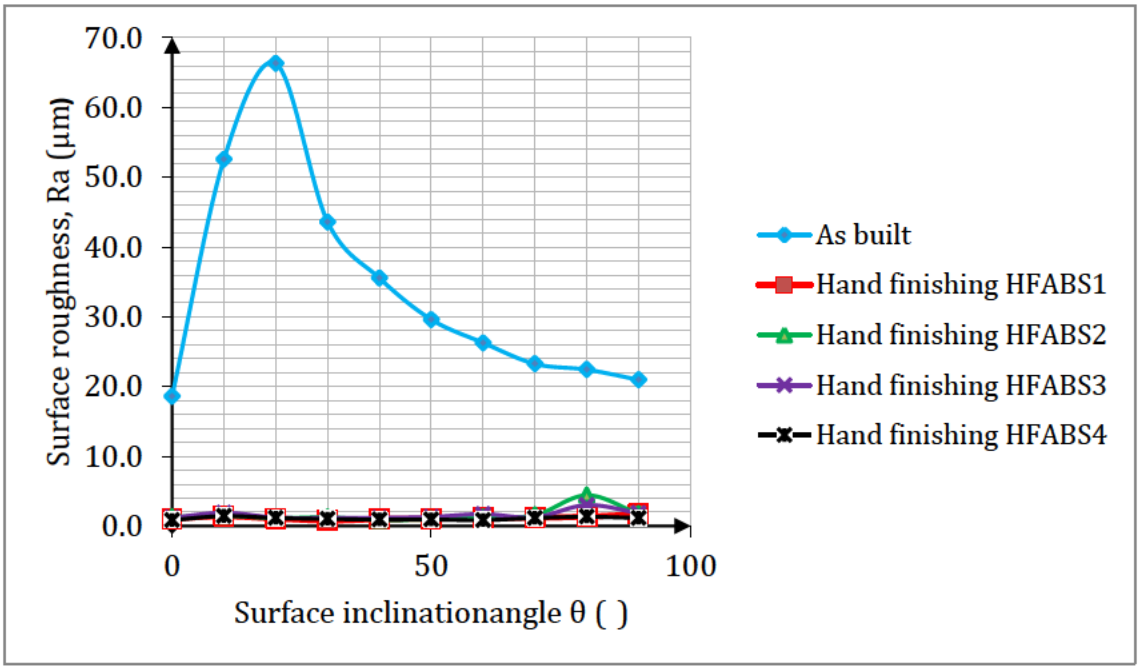

Figure 6.26: Surface inclination angle versus surface roughness for hand finished ABS test pieces.

D. Spray painting

The results of the surface roughness measurements for spray painting of ABS test pieces are shown in Table 6.18 and Figure 6.27. The designations of the test pieces are according to Table 5.8.

Table 6.18: Average surface roughness for spray painting of ABS test pieces

Surface inclination angle θ (°)	As built	Spray painted test pieces				% improvement of surface finish for SPABS4
		SPABS1	SPABS2	SPABS3	SPABS4	
	Surface finish, Ra (µm)					
0	18.613	2.830	3.780	1.471	1.369	92.6
10	52.569	30.029	35.994	13.587	8.873	83.1
20	66.326	17.318	14.295	5.281	3.910	94.1
30	43.602	6.525	4.853	2.175	2.064	95.3
40	35.541	3.996	3.176	2.459	1.800	94.9
50	29.612	3.113	2.602	1.884	1.408	95.2
60	26.271	4.789	3.480	2.602	1.734	93.4
70	23.249	3.184	3.124	2.782	1.948	91.6
80	22.421	3.459	2.492	2.200	1.786	92.0
90	20.966	4.111	3.588	2.997	2.800	86.6
Standard deviation	15.704	8.8829	10.524	3.608	2.2737	

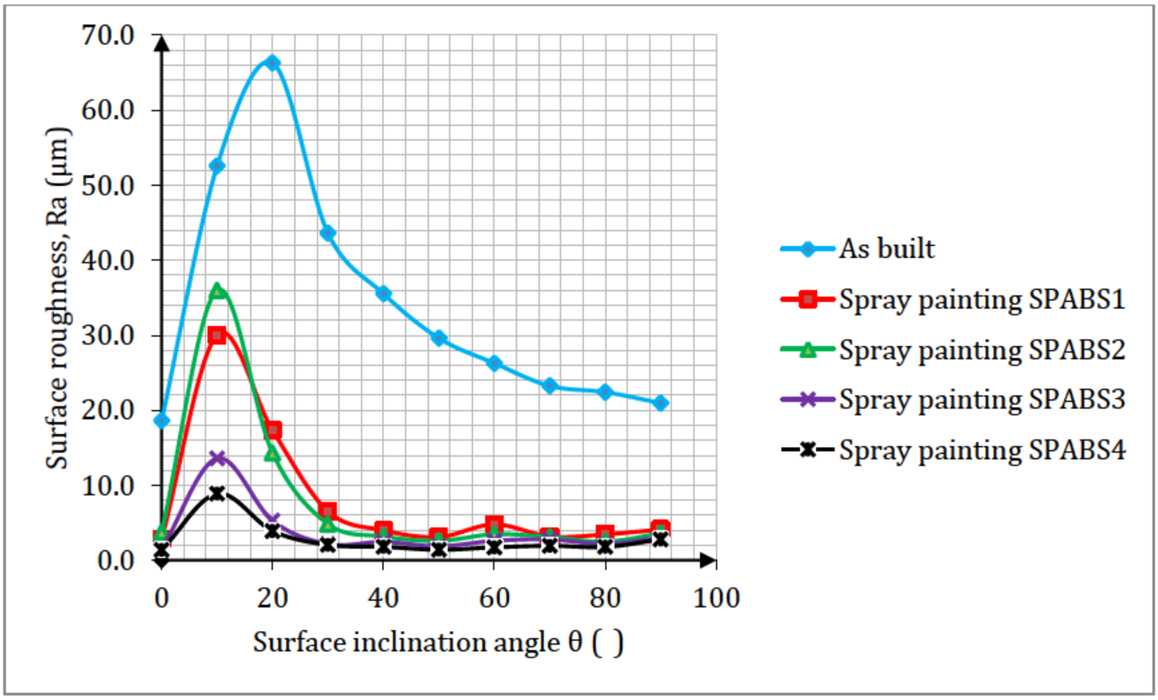

Figure 6.27: Surface inclination angle versus surface roughness for spray-painted ABS test pieces

E. Chemical treatments

The results of the surface roughness measurements for chemical treatment of ABS test pieces are shown in Table 6.19 and Figure 6.28. The designation of the test pieces are according to Table 5.9.

Table 6.19: Average surface finish for chemical treatments of ABS test pieces with acetone

Surface inclination angle θ (°)	As built	Chemical treatment			% improvement of surface finish		
		CT1	CT2	CT3			
	Surface finish, Ra (µm)				CT1	CT2	CT3
0	18.613	2.692	2.681	2.002	85.5	85.6	89.2
10	52.569	17.688	4.708	3.978	66.4	91.0	92.4
20	66.326	4.870	4.575	4.423	92.7	93.1	93.3
30	43.602	4.712	4.612	5.181	89.2	89.4	88.1
40	35.541	4.505	2.955	7.038	87.3	91.7	80.2
50	29.612	3.470	3.601	4.560	88.3	87.8	84.6
60	26.271	2.709	3.280	2.988	89.7	87.5	88.6
70	23.249	3.033	2.945	1.431	87.0	87.3	93.8
80	22.421	2.831	2.451	2.173	87.4	89.1	90.3
90	20.966	4.193	2.866	4.753	80.0	86.3	77.3
Standard deviation	15.704	4.5146	0.8612	2.297			

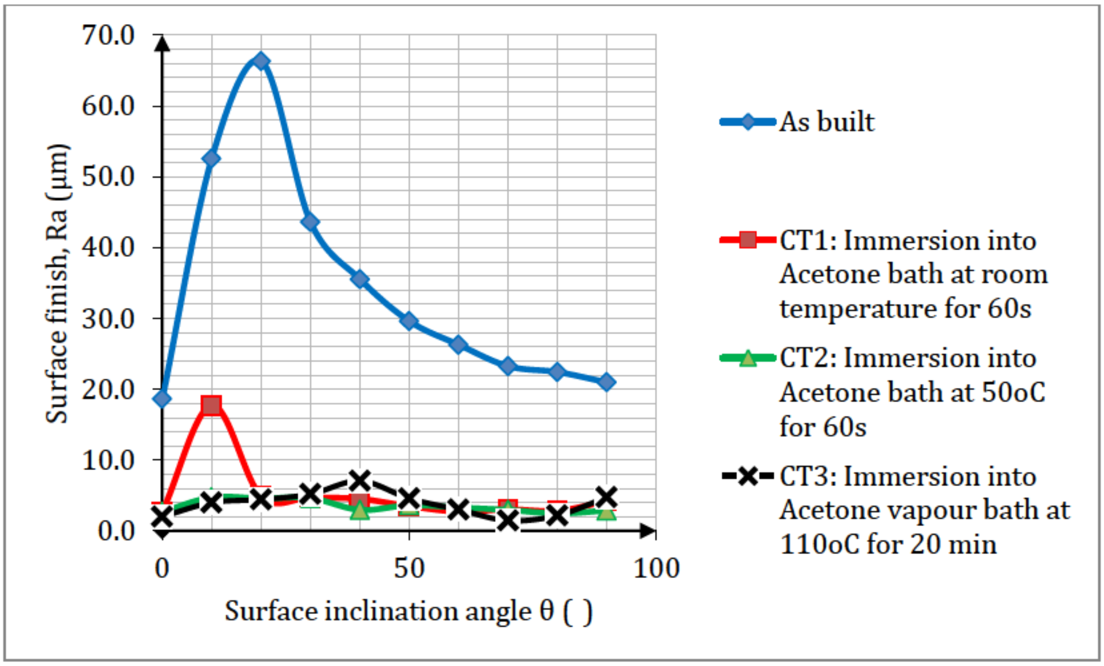

Figure 6.28: Surface inclination angle versus surface roughness for chemically treated ABS test pieces with acetone acid

F. CNC machining

The results of the surface roughness measurements for CNC machining of ABS test piece are shown in Table 6.20 and Figure 6.29.

Table 6.20: Average surface finish for CNC Machining of ABS test piece

Surface inclination angle θ (°)	As built	CNC machining	% improvement of surface finish
0	18.613	4.647	75.0
10	52.569	4.181	92.0
20	66.326	4.682	92.9
30	43.602	3.072	93.0
40	35.541	6.104	82.8
50	29.612	3.989	86.5
60	26.271	5.755	78.1
70	23.249	4.823	79.3
80	22.421	2.144	90.4
90	20.966	5.601	73.3
Standard deviation	15.704	1.223	

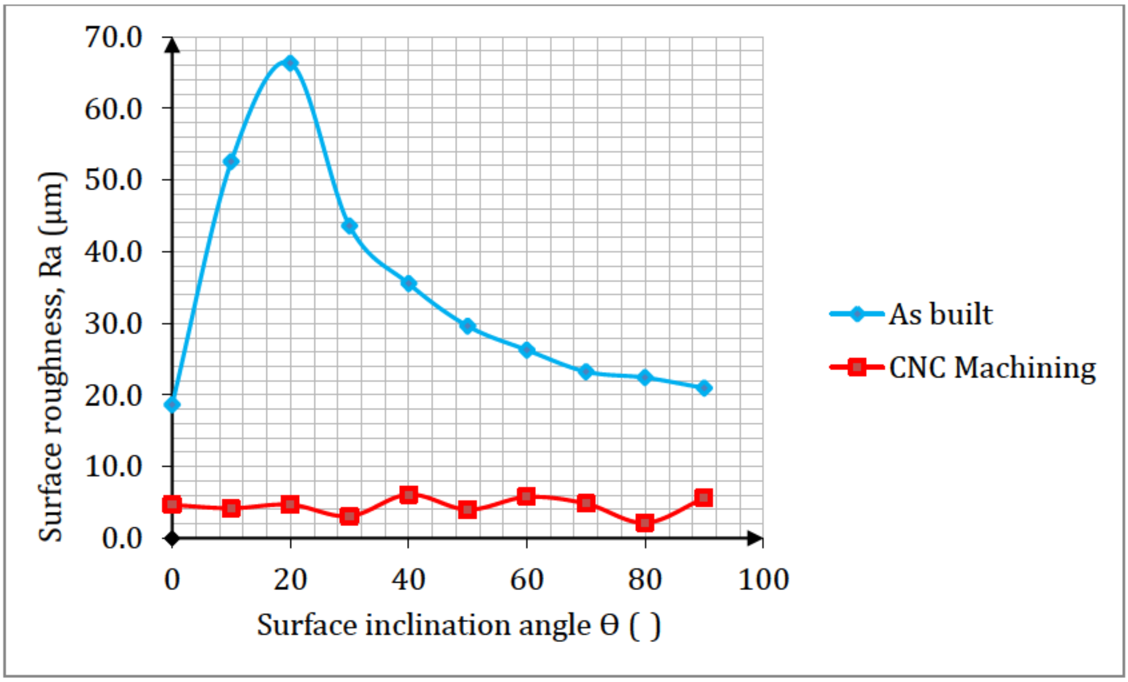

Figure 6.29: Surface inclination angle versus surface roughness for CNC machined ABS test piece

6.4.2 Observations and analysis of the results

In addition to the five post processing techniques for which the surface roughness of nylon and Alumide® test pieces were measured, the surface roughness of ABS test pieces subjected to chemical treatments was also measured. The following additional abbreviations are used in Table 6.21.

CT1-Chemical Treatment of CT-ABS1 test piece: immersion into acetone bath for a period of 60 s at room temperature;

CT2-Chemical Treatment of CT-ABS2 test piece: immersion into acetone bath heated at 50°C for a period of 60 s;

CT3-Chemical Treatment of CT-ABS3 test piece: immersions into acetone vapour bath for a period of 20 min at 110°C.

The rating of the percentage of improvement of the surface finish of the six post processing techniques across the surface inclination angles on the ABS test pieces is presented in Table 6.21.

Table 6.21: Rating of improvement of surface finish for ABS test pieces

Surface inclination angle θ (°)	Tumbling	Shot peening	Hand finishing	Spray painting	Chemical treatment			CNC machining	Rating of improvement of post processing techniques
					CT1	CT2	CT3		
	% improvement of surface finish								
0	37.2	55.7	95.4	92.6	85.5	85.6	89.2	75.0	HF,SP,CT3,CT2,CT1,CNC, SPe,T
10	26.6	49.2	97.3	83.1	66.4	91.0	92.4	92.0	HF,CT3,CNC,CT2,SP,CT1, SPe,T
20	28.2	69.7	98.3	94.1	92.7	93.1	93.3	92.9	HF,SP,CT3,CT2,CNC,CT1, SPe,T
30	31.9	74.2	97.7	95.3	89.2	89.4	88.1	93.0	HF,SP,CNC,CT2,CT1,CT3, SPe,T
40	40.9	76.8	97.4	94.9	87.3	91.7	80.2	82.8	HF,SP,CT2,CT1,CNC,CT3, SPe,T
50	37.5	75.0	96.8	95.2	88.3	87.8	84.6	86.5	HF,SP,CT1,CT2,CNC,CT3, SPe,T
60	43.7	61.2	96.7	93.4	89.7	87.5	88.6	78.1	HF,SP,CT1,CT3,CT2,CNC, SPe,T
70	50.9	69.0	95.0	91.6	87.0	87.3	93.8	79.3	HF,SP,CT3,CT2,CT1,CNC, SPe,T
80	39.9	66.6	94.1	92.0	87.4	89.1	90.3	90.4	HF,SP,CT3,CNC,CT2,CT1, SPe,T
90	49.2	67.3	94.5	86.6	80.0	86.3	77.3	73.3	HF,SP,CT2,CT1,CT3,CNC, SPe,T
Stand. Dev.	12.79	6.674	0.199	2.274	4.515	0.861	2.297	1.223	

A. Hand finishing

With 79.9% of dimensional accuracy, the hand finishing technique occupies first positions across all surfaces of the test pieces. With a standard deviation of 0.199, an improvement of surface finish ranging from 94.1 to 98.3% was achieved with application of 9 sanding steps and 6 layers of epoxy primer. The small standard deviation indicates that there exist negligible differences between the values of surface finish across all surfaces. This can be observed on Figure 6.26 where the surface finish across all surface angles for all hand finished test pieces can be practically equated to an average value of 1.082 μm R_a. Figure 6.26 also indicates that even with two sanding steps and one layer epoxy primer, an excellent surface finish can be achieved. The above discussed hand finishing technique provides an appropriate solution where the sanding is able to reduce considerably the large step widths.

Figure 6.30 illustrates the improvement of the surface finish of ABS test pieces through the hand finishing process on 10°, 20° and 30° surface inclination angles.

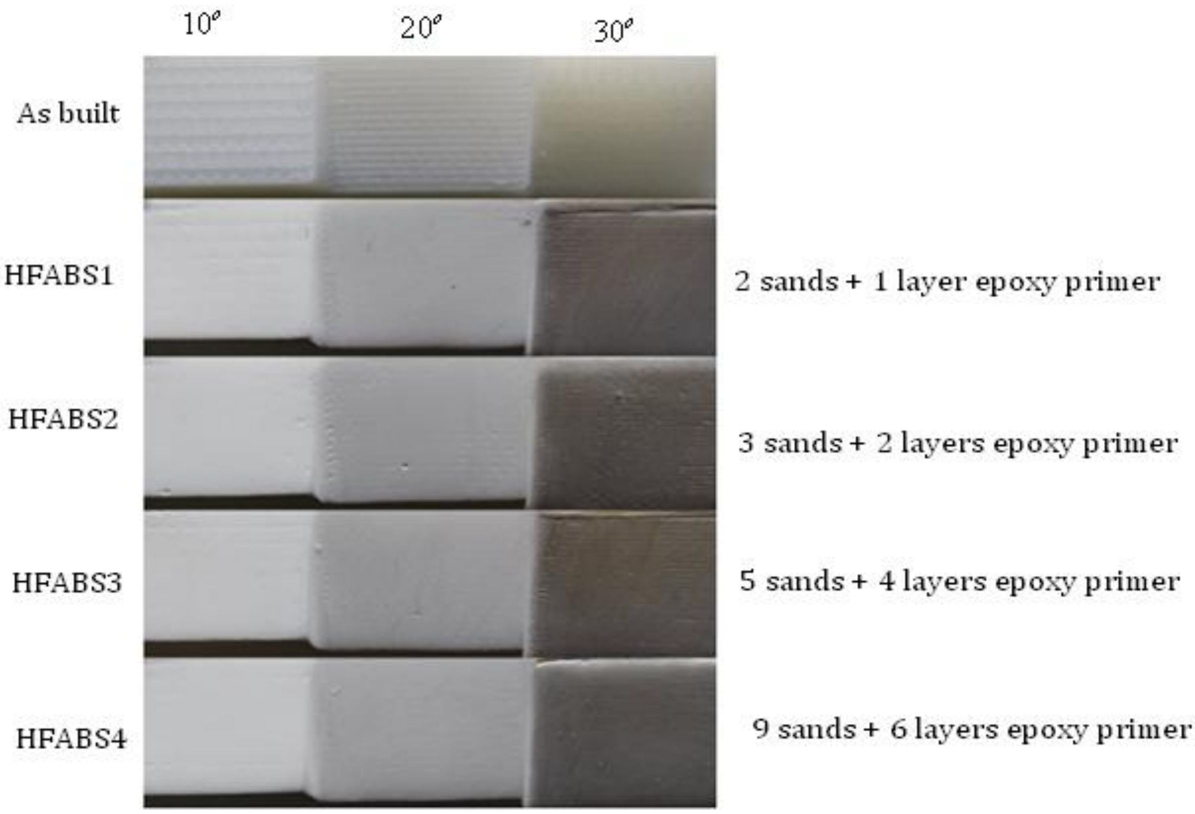

Figure 6.30: Hand finished ABS test pieces.

A quick improvement of surface roughness through the hand finishing technique is also observed on horizontal surfaces and on surfaces with inclination angles from 40° to 90°.

B. Spray painting

Despite the poor dimensional accuracy where only 1.3% of the total number of touch probe scanned points is with the ±0.1 mm deviation range from the geometry of the "as built" ABS test piece, the spray painting technique performed on ABS test pieces, with four undercoats (priming) followed by one layer of silver paint exhibited 83.1 to 95.3% improvement of surface finish with a standard deviation of 2.274. Table 6.21 shows that 90% of second position is occupied by the spray painting technique. Figure 6.27 shows that the surface roughness improves progressively with the increase of the number of undercoats. It can be realized that in the range of 30° to 90° surface angles, the surface finish of SPABS4 is practically stabilized to an average value of 2 μm R_a, which is an advantage for a uniform surface finish across the above surface angle range. Figure 6.31 shows the surface finish of 10°, 20° and 30° surface inclination angles of spray painted ABS test pieces.

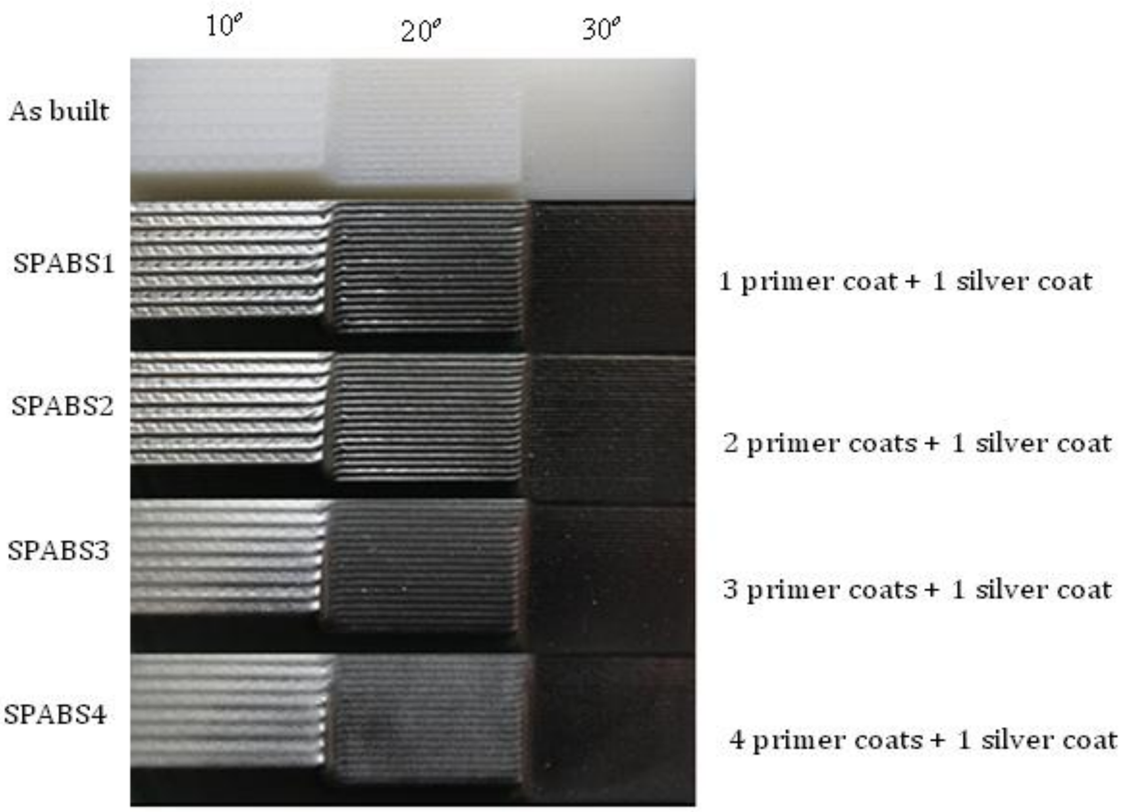

Figure 6.31: Spray painted ABS test pieces

It can be noted that the lowest improvement of surface finish is observed at 10°and 20° surface angles where the stair-step effect is more pronounced or a surface with the largest step widths. The uniform undercoating and painting across the entire test piece does not provide enough coverage to eliminate the stair steps.

C. Chemical treatment

The ranking of chemical treatments CT1, CT2 and CT3 of ABS test pieces can be clarified by Table 6.22 derived from Table 6.21.

Table 6.22: Comparison of chemical treatments

Positions	CT1	CT2	CT3
	Frequency of appearance		
1	0	0	0
2	0	0	1
3	2	2	4
4	2	6	1
5	3	2	1
6	3	0	2
7	0	0	1
8	0	0	0
Decision	Third	Second	First

Among the three considered chemical treatments, immersion of ABS test piece into acetone vapour bath for a period of 20 min at 110°C showed the best performance by dissolving the stair steps at 10° surface inclination angle, thus improving the surface finish by 92.4%, an improvement which is a little bit higher than 91% achieved by the immersion of ABS test piece into an acetone bath heated to 50°C for a period of 60 s. The frequency of four times for CT3 at the third position while the other techniques have a frequency of two times also strengthens the selection of CT3 to be the most preferable chemical treatment to achieve smoother surfaces. However if attention is paid to the differences of percentages of improvement of surface finish for 0°, 20°, 30°, 50°, 60°, 70° and 80° surface angles, it can be realized that the differences of percentages for CT1, CT2 and CT3 are not significant. This argument is in agreement with Figure 6.28 where in the above mentioned angle range, the curves of SABS1, SABS2 and SABS3 almost overlap, with exception of 10° surface angle where the immersion into acetone bath at room temperature for a period of 60 s did not succeed to scale down the surface finish to an average value of 4.343 μm Ra, thus producing improvement of surface finish ranging from 66.4 to 92.7% with 89.8% dimensional accuracy within the ±0.1 mm deviation range from the geometry of the "as built" ABS test piece. It can be concluded that the immersion of ABS test pieces into an acetone bath at 50°C for a period of 60 s produces an almost equal effect in improvement of the surface finish to the immersion of ABS test piece into an acetone vapour bath at 110°C for a period of 20 min.

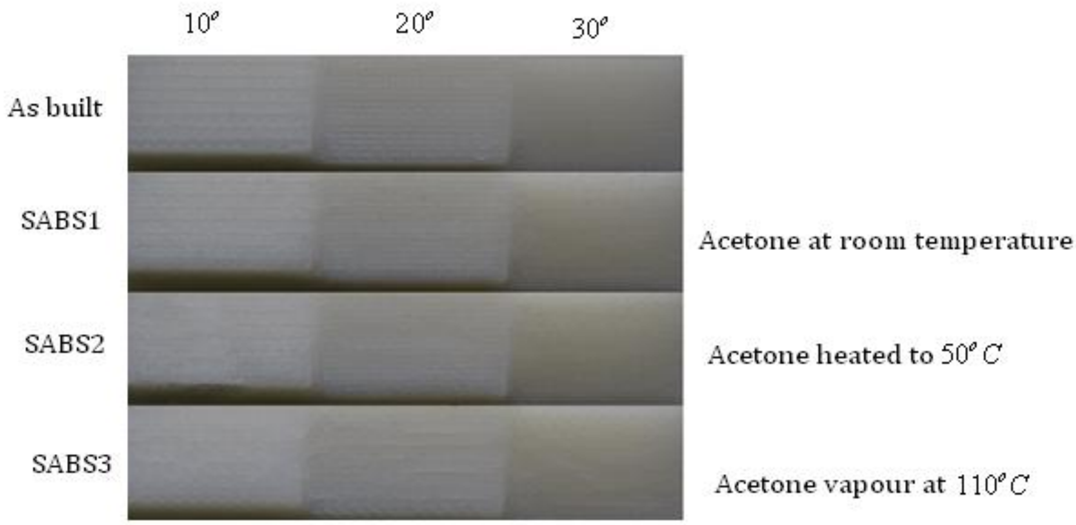

Figure 6.32: Chemically treated ABS test pieces

If a uniform surface finish across the entire test piece is required, the first preference will be given to immersion in an acetone bath at 50°C for a period of 60 s with a standard deviation of 0.861. This offers the advantage of a shorter period to perform the process, less risk in not having to heat the acetone which is highly flammable as well as less energy consumed. In Figure 6.32, with exception of the high surface roughness of 17.688 μm R_a on 10° surface angle of CT-ABS1 test piece, it can be observed that immersion of ABS test pieces in acetone baths, for different periods produce almost equal surface roughness improvement on 10°, 20° and 30° and this trend is also observed on other surfaces of the test pieces.

D. CNC machining

Despite the poor dimensional accuracy of 2.6% within ±0.1 mm produced by CNC machining of ABS test piece, 73.3 to 93% of improvement of surface finish was achieved with a relatively small standard deviation of 1.223.

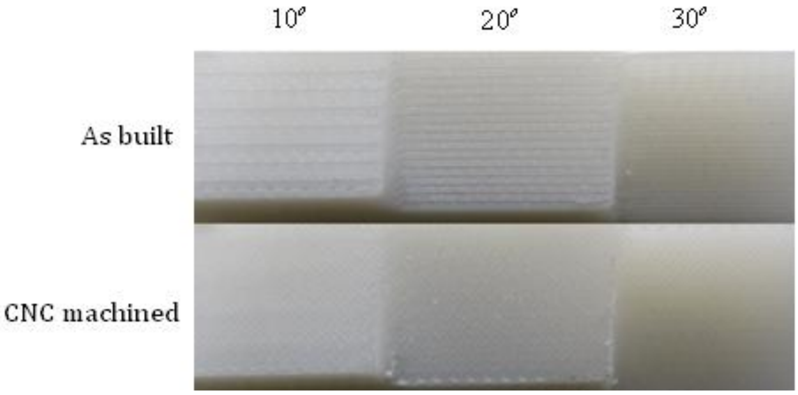

Figure 6.33: CNC machined ABS test piece

In a similar manner to nylon and Alumide® CNC machined test pieces, a harmonization of surface finish across all the surface inclination angles requires the variation of the cutting parameters, which will lead to extra machining time and costs.

E. Shot peening

With 95.6% of dimensional accuracy within the ±0.1 mm deviation range, the shot peening of ABS test pieces performed for a period of 8 min, depending on the surface angle, showed poor to good improvement of surface finish ranging from 49.2 to 76.8%. For all surface inclination angles, Table 6.21 shows that the shot peening occupies seventh position, which clearly indicates that hand finishing, spray painting, chemical treatments with acetone and CNC machining perform better where the improvement of surface finish of ABS test pieces is concerned. From Figure 6.25, it can be realized that when the shot peening period is gradually increased from 2 to 6 min with increment of 2 min, there is a progressive improvement of surface finish for the entire range of surface angles. When the period is increased up to 8 min, there is an increase of surface finish for 30° to 60° surface angles, this being very pronounced on the surfaces inclined at 30° and 60°. For the 70° to 90° range, a progressive improvement of surface finish with increase of shot peening period is again observed. Figure 6.34 clearly shows that the middle area of the 10°, 20° and 30° surface angles as well as edges and thin walls of the piece are damaged by the shot peening process. At the same time, the measurements of surface roughness on these damaged surfaces indicate that the surface finish is reduced. This can be explained by the following:

- The stair-step effect is more pronounced on these surfaces and the observed damages are in the range of the same magnitude as the amount of hills compressed by the shots contributing for improvement of surface finish;
- The used measurement result value is the average of left, middle and right side measurements. The left and right side measurements contribute in scaling down the measured surface finish and reduce the effect of the high surface finish value measured at the middle of the surface.

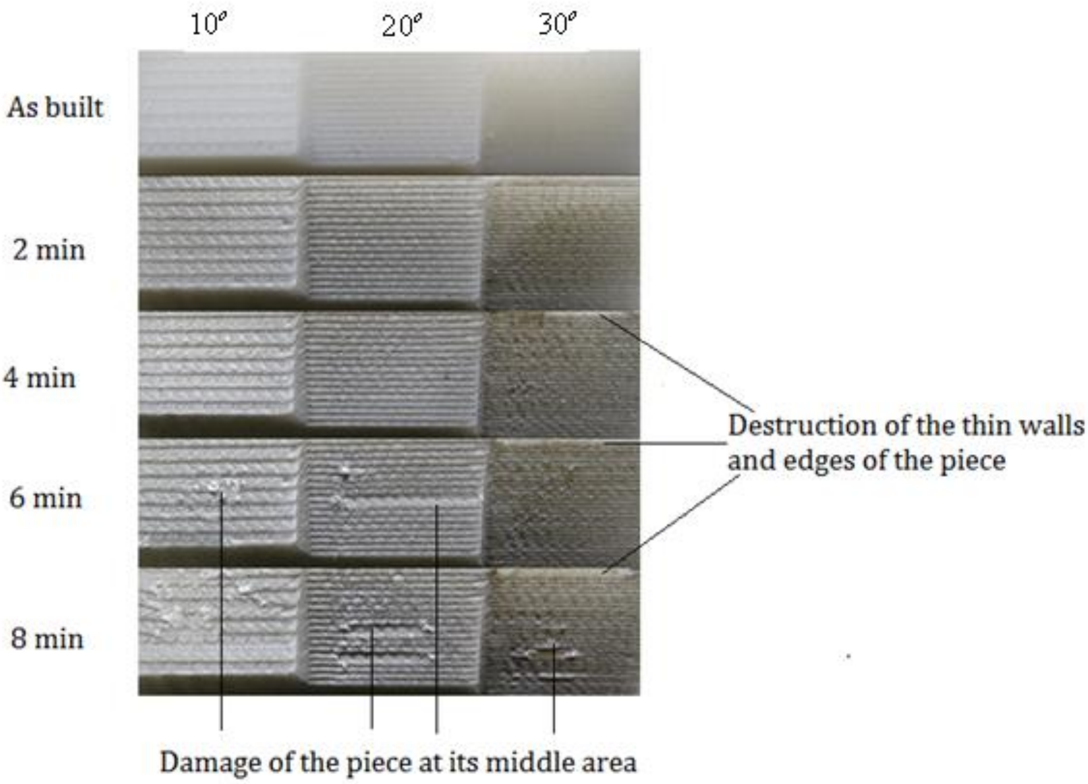

Figure 6.34: Problems associated with the shot peening of ABS test pieces

The highest improvement is achieved at the 10°, 20° and 30° surface angles. A standard deviation of 6.674 indicates that there exists a high level of variation of surface finish across the entire test piece, which is a disadvantage when a uniform surface finish is required. It can be concluded that despite excellent dimensional accuracy exhibited by shot peening of ABS test pieces fabricated through FDM process, the shot peening prolonged beyond a period of 4 min leads to a damage of surface, thus does not improve the surface finish of the test piece. Since the shot peening was performed by hand, the results can be variable: where the shot blasting is for example concentrated may cause the damage to the surface in less time than specified here.

F. Tumbling

The tumbling technique was the last process applied to improve the surface finish of ABS test pieces. When the process was performed for a period of one hour, the following signs of the weakness of ABS material under tumbling process were observed:

- ABS material in the form of fibers are detached from edges and thin walls;
- Conical features are broken and removed from the test pieces.

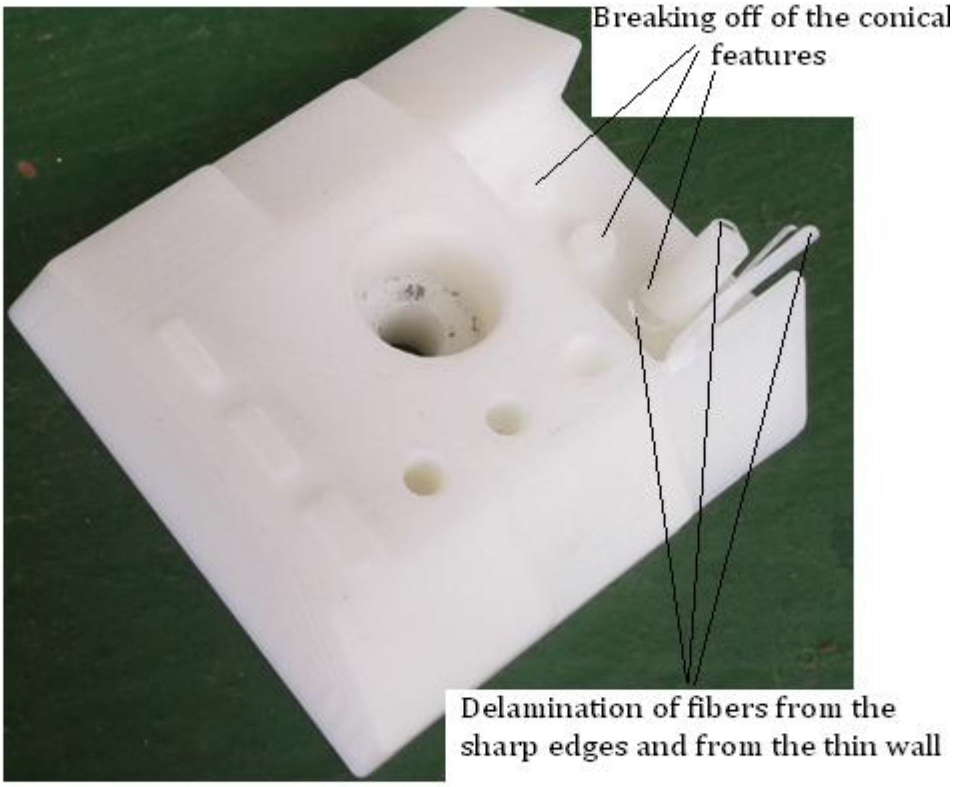

Figure 6.35: Problems associated with tumbling of ABS test piece for a period of one hour

Taking into consideration the above weaknesses, the tumbling process was performed for 1 h, 2 h, 3 h and 4 h periods.

Within the ±0.1 mm deviation range, the tumbling technique applied to ABS test piece for a period of 4 hours produced a very good dimensional accuracy of 81%. Poor to satisfactory improvement of surface finish varying from 26.6 to 50.9% with a standard deviation of 12.792 was observed, thus putting the tumbling technique applied to ABS test pieces in the last positions in Table 6.21. Figure 6.24 shows that the process of improvement of the surface finish with increase of the tumbling time is not progressive on 10° and 20° surface inclination angles where the stair-step effect is more obvious. For the remaining range of surface angles, it can be practically considered that the improvement takes place with the increase of the tumbling period. It can be also be realized that up to a period of four hours of tumbling, the curve of improvement of surface finish still follows the trend of the surface finish of the "as built" test piece and does not show any stabilization of surface finish across the surface inclination angles. This behavior is a disadvantage when a uniform surface finish is required through tumbling of additive manufactured parts with various surface inclination angles.

6.4.3 Conclusions

1. All eight considered post processing techniques have improved the surface finish of the ABS test pieces produced though the FDM process.
2. Likewise for nylon and Alumide® test pieces, despite of the low dimensional accuracy produced by the hand finishing and spray painting techniques, in terms of improvement of surface finish of small ABS test pieces obtained through the FDM process, the two techniques are the first preference, followed by chemical treatments by immersion into acetone, CNC machining, shot peening and finally tumbling.
3. Though tumbling and shot peening may slightly improve the surface finish of ABS test pieces, the shot peening period should be limited to two minutes whereas the tumbling is not recommended at all. The two techniques cause serious damage to ABS test pieces by delamination of the material on edges, thin walls and from surfaces where the stair-step effect is more pronounced.
4. All three chemical treatments of ABS test pieces through immersion into acetone baths proved that chemical treatment is an optimal technique to improve the surface finish of ABS test pieces obtained through the FDM process without negatively influencing the dimensional accuracy of the test pieces. With an excellent dimensional accuracy of 89.8% within the ±0.1 mm deviation range from the geometry of the "as built" test piece, immersion of ABS test piece into acetone bath at room temperature for a period of 60 s produced the highest improvement of surface finish ranging from 85.6 to 92.7%. Therefore it is recommended that this technique shall be applied to FDM ABS parts for improvement of surface finish. The care should

be taken on thin features which might be partially or completely dissolved, thus producing a negative effect on the dimensional accuracy of the part.

5. CNC machining is capable of improving the surface finish in the range of 73.3 to 93%. However, for small parts with geometrical complexities, there exists a high risk of impacting negatively the dimensional accuracy especially in Z-direction. As the setting of CNC machining process involves high skilled people, the unitary production cost will be prohibitively high if the comparison is made to chemical treatment where a relatively big number of pieces can be immersed into the same acetone bath.

CHAPTER 7: GENERAL CONCLUSIONS, RECOMMENDATIONS AND FUTURE WORK

7.1 General conclusions

Six post processing techniques for improvement of surface finish of small plastic test pieces from nylon and Alumide® material manufactured through the LS process; and from ABS material obtained through the FDM process were investigated. Tumbling, shot peening, hand finishing, spray painting and CNC machining techniques were applied to nylon, Alumide® and ABS test pieces. The chemical treatment technique by immersion of test pieces into acetone baths was only investigated for ABS test pieces as there was no effect when this technique was applied to nylon or to Alumide® test pieces. Statistical methods through Chi-square test and test for difference in population proportions were applied. It was found that there exist significant differences between dimension deviation range proportions as one compares the "as built" to any one of the six considered post processing techniques.

Within the ±0.1 mm deviation range from the geometry of the "as built" test piece, for all three investigated materials, the hand finishing technique exhibited the highest percentage of improvement of surface finish of the test pieces. However the hand finishing technique was always characterized by a long period of processing time extending to 5 h 20 min to finish a single test piece; and finally characterized by a lack of consistency for a uniform distribution of deviation ranges across individual surface as wells as across the entire test piece.

With a low dimensional accuracy, the spray painting was generally characterized by a uniform distribution of positive deviation ranges and improvement of surface finish in the range of 79 to 92% for nylon and Alumide®; and 83 to 95% for ABS test pieces. The building up of the paint on all surfaces and the filling of small cavities by the paint are the major disadvantages of the spray painting technique. The hand finishing and spray painting techniques are recommended to be applied to additive manufactured parts for form purposes as the two techniques provide an excellent aesthetic appearance to the parts.

It was found that though the tumbling technique produced a good improvement of surface finish for nylon and Alumide® test pieces, the techniques affected negatively the dimensional accuracy of the small protrusions and the sharp corners of nylon and

Alumide® test pieces where a heavy wearing off of the material at these specific areas was observed. A similar trend is also observed with the shot peening of nylon test piece for a period of 8 min. Shot peening of nylon test piece for a period of 8 min produced 70.1 to 89% of surface finish improvement with 82.6% of dimensional accuracy, while the tumbling technique for a period of 6 h produced 69.1 to 83.7% of surface improvement with 88.3% of dimensional accuracy. Though the differences are not significant, these statistics indicate that on one hand, shot peening for nylon is preferable if a single small part is to be processed. On the other hand, if many parts without sharp angles or small protrusions are to be processed, the tumbling technique will be the optimal solution. Tumbling of Alumide® test piece for a period of 6 h produced 64.6 to 81.9% of surface finish improvement with 80.1% dimensional accuracy, while shot peening for a period of 8 min generated 47.8 to 71.1% of surface improvement with 92.1% of dimensional accuracy. With significant differences in percentages of surface finish improvement and dimensional accuracy, it can be realized that tumbling, with less dimensional accuracy, produced better surface finish improvement compared to shot peening with less surface finish improvement but with high dimensional accuracy. Taking into consideration of the possibility of tumbling a big number of small parts in one batch, the tumbling of small Alumide® parts offers more advantages than the shot peening. For LS nylon and Alumide® parts without small protrusions or sharp corners, tumbling and shot peening can be the optimal solutions to improve the surface finish of the parts, without influencing negatively the dimensional accuracy of the parts.

While tumbling and shot peening can be applied to laser sintered nylon and Alumide® parts, with a care taken to small protrusions and sharp corners, the two post processing techniques should not be applied to ABS parts manufactured through the FDM process for improvement of surface finish. With the tumbling technique small protrusions are broken off and delamination takes place on sharp corners Shot peening damages surfaces of ABS parts manufactured through the FDM process by delamination of the external layers of the surfaces.

The chemical treatment applied to ABS test pieces was found to be an optimal solution to dissolve the stair-steps, thus improving the surface finish up to 93% with a dimensional accuracy of 90%. The technique can be applied to FDM of ABS parts for form, fit and functional purposes.

CNC machining produced surface finish improvement in the range of 67.5 to 94.3% with a standard deviation of 4.968 for nylon, 63 to 89.2% with a standard deviation of 2.693 for Alumide®, and 73.3 to 93% with a standard deviation of 1.223 for ABS test piece. These statistics indicate that with identical setup of cutting parameters, the surface finish improvements differ from one material to another with significant difference in standard deviations. This implies that for a uniform distribution of surface finish across all the surface inclination angles, each surface inclination angle must be assigned its own cutting parameters. This would have increased the overall production time, thus leading to extra machining cost for a single test piece. In addition to that, although CNC machining improved the surface finish of the small plastic test pieces, it was realized that an error in machine-tool setting in Z-direction led to negative dimension deviation ranges which was repeated for all three CNC machined test pieces. Accurate calibration of the CNC machine and set-up of the parts is critical since good dimensional accuracy should be possible through CNC machining.

7.2 Recommendations

In regards to improvement of the surface finish of additive manufactured parts from nylon, Alumide® and ABS materials, the following recommendations are made:

i. Tumbling and shot peening techniques can be applied to LS nylon and Alumide® parts to improve their surface finish without significant detrimental effects on the dimensional accuracy of the parts. However a care must be taken on eventual small protrusions and sharp corners where the material is heavily worn off. The two techniques are not recommended for improvement of surface finish of FDM ABS parts as the breaking off of relatively long entities and small protrusions; and a tangible delamination of layers from the surface of the parts take place.
ii. For additive manufactured parts for form purpose where only a good aesthetic appearance is required, hand finishing and spray painting can be performed on LS nylon and Alumide®; and on FDM of ABS parts to improve their surface finish. A special attention must be paid on small cavities where accumulation of paint in the case of spray painting, and the lack of accessibility for hand finishing can lead to excessive dimension inaccuracy.
iii. Immersion of FDM ABS parts into acetone bath is highly recommended for improvement of the surface finish without significant detrimental effects on the

dimensional accuracy of the ABS parts. However this technique should not be used on LS nylon or Alumide® parts as the acetone does not dissolve the surfaces of parts fabricated in nylon or Alumide® materials.

iv. CNC machining can be applied to LS nylon and Alumide®; and to FDM ABS parts to improve the surface finish. In order to achieve a desired dimensional accuracy, a correct calibration of the machine and a precise setting of cutting parameters in vertical direction must be ensured. However for parts with complex geometries, this technique is not recommended as the production time and cost will be prohibitively high.

7.3 Future work

The preliminary statistical data obtained from the touch probe scanning technique were generalized to the entire test piece and not specific to an individual surface inclination angle. Future works should concentrate on acquisition of the dimensional deviation ranges based on each individual inclined surface in order to establish any correlation between the dimensional accuracy and the surface finish of each post processing technique.

To establish the degree of repeatability of results, for the end-used functional shot peened and tumbled nylon and Alumide® parts, future research should focus on shot peening and tumbling process parameters that influence the surface finish and dimensional accuracy of the parts. The effect of post processing techniques on mechanical properties of tumbled and shot peened nylon and Alumide®; and chemically treated ABS parts is also a major concern for future study.

Stainless steel, maraging steel and Ti6Al4V powders are widely used for DMLS technology to manufacture biomedical, automotive and aerospace engineering parts. In practice, the surface finish of parts obtained by the DMLS process is improved before the parts are used for any specific application. The investigation on improvement of surface finish through shot peening and tumbling techniques shall be extended to DMLS of stainless steel, maraging steel and Ti6Al4V materials.

Based on the results of this study, future works shall elaborate procedures and methodologies to enable the service bureaus that manufacture prototypes to apply the findings of this investigation to real world projects and products.

LIST OF REFERENCES

1. Addanki, S.R., Medha, A.D., Venkatesh, J.V.L. & Deepesh, O., 2012, Investigation of post processing techniques to reduce the surface roughness of fused deposition modelled parts*, International Journal of Mechanical Engineering and Technology (IJMET)* 3(3), 531-544.
2. Anitha, R., Arunachalam, S. & Radhakrishnan, P., 2001, Critical parameters influencing the quality of prototypes in fused deposition modelling, *Journal of Material Processing Technology* 118, 385-388.
3. Anoop, K.S., Ohdar, R.K. & Mahapatra S.S., 2009, Improving dimensional accuracy of Fused Deposition Modelling part using Taguchi method, *Material and Design* 30, 4243-4252.
4. Anoop, K.S., Vedansh, C., Saurav, D. & Siba, S.M., 2011, Optimization of process parameters in Fused Deposition Modeling using weighted principal component analysis, *Journal of Advanced Manufacturing Systems* 10(2), 241-259.
5. ASM International, 1988, *Engineering Plastics, Engineered Materials handbook*, Materials Park, vol. 2.
6. Bacchewar, P.B., Singhal, S.K., et al., 2007, Statistical modelling and optimization of surface roughness in selective laser sintering process, Proceedings of Institutions of *Mechanical Engineers*, Part B: journal of Manufacture 221(1), 35-52.
7. Bakar, N.S.A., Alkahari, M.R. & Boejang, H., 2010, Analysis of fused deposition modelling performance, *Journal of Zhejiang University-SCIENCE A (Applied Physics Engineering)* 11(12), 972-977.
8. Behnam, N., 2011, Surface roughness estimation for FDM systems, Master thesis, Dept of Applied Science in the program of Mechanical Engineering, Ryerson University, Toronto, Ontario, Canada.
9. Campbell, R.I., Martorelli, M. & Lee, H.S., 2002, Surface roughness visualization for rapid prototyping models, *Computer Aided Design* 34(10), 717-725.
10. Caulfield, B., McHugh, P.E. & Lohfeld, S., 2007, Dependence of mechanical properties of polyamide components on build parameters in SLS process*, Journal of Materials Processing Technology* 182(1), 477-488.

11. Chen, D. & Cheng, F., 1999, Integration of product and process development using rapid prototyping and workcell technologies, *Journal of Industrial Technologies* 16(1).
12. Chen, Y. & Lu, J., 2013, RP part surface quality versus build orientation: when layer are getting thinner, *International Journal of Advanced Manufacturing Technology* 67(1-4), 377-385.
13. Chua, C.K., Leong K.F. & Lim C.S., 2010, *Rapid Prototyping: Principles and Applications*, 3rd edn, World Scientific Publishing Co. Pte.Ltd, Singapore.
14. Combrinck, J., Booysen, G.J., Van der Walt, J.G. & De Beer D.J., 2012, Limited run production using of Alumide® tooling for the plastic injection moulding process, *South Africa Journal of Industrial Engineering* 23 (2), 131-146.
15. Daekeon, A., Hochan, K. & Seokhee, L., 2008, Surface roughness prediction using measured data and interpolation in layered manufacturing, *Journal of Material Processing Technology* 209(2) 664-671.
16. Daekeon, A., Jin-Hwe, K., Soonman, K., Jungil, S. & Seokhee, L., 2009, Representation of surface roughness in fused deposition modelling, *Journal of Materials processing Technology* 209, 5593-5600.
17. Daneshmand, S. & Aghanajafi, C., 2012, Description and modelling of additive manufacturing technology for aerodynamic coefficient measurement, *Journal of mechanical Engineering* 58(2), 125-133.
18. Daneshmand, S., Aghanajafi, C. & Shahverdi, H., 2013, Investigation of rapid manufacturing technology effect on aerodynamics properties, *Tehnicki Vjesnik* 20(3), 425-433.
19. De Beer, D., Booysen, G., Barnard, L. and Truscott, M., 2005, Rapid tooling in support of accelerated new product development, *Assembly Automation* 25(4), 306-308.
20. De Beer, D.J. & Booysen, G.J., 2005, Rapid tooling using Alumide®, in Virtual modelling and rapid manufacturing-Bartolo (eds.), *Proceedings of the 2nd International Conference on Advanced Research and Rapid Prototyping,* Leiria, Portugal, 28 September -1 October, 2005, pp. 387-394.
21. De Beer, D.J., Becker, L., Van del Walt, P., Mauchline, D., Campbell, R.I. & Dean, L.T., 2012, Additive manufacturing of alumide jewellery, *Proceedings of 13th Annual RAPDASA Conference, Pretoria, South Africa*, 11 pp.

22. Douglas, S.T. & Stanley, W.G., 2014, Costs and cost effectiveness of additive manufacturing, *NIST Special publication* 1176, 1-77.

23. EOS GmbH-Electro-Optical Systems, 2014, *Alumide PA12-MD(Al*), retrieved from www.materialdatacenter.com. [Accessed 21 July 2014].

24. Equbal, A., Sood, A.K., Toppo, V., Ohdar, R.K. and Mahapatra, S.S., 2010, Prediction analysis of sliding wear performance fused deposition modelling –processed ABS plastic parts, *Proceedings of Institution of Mechanical Engineers, Part J: Journal of Engineering tribology* 224, 1261-1271.

25. Galantucci, L.M., Lavecchia, F. & Percoco, G., 2009, Experimental study aiming to enhance the surface finish of fused deposition modelled parts, *CIRP Annals-manufacturing Technology* 58(1) 189-192.

26. Giovanni, S., Liang H., Richard M. E & Kenneth E., 2013, Surface roughness analysis, modelling and prediction in selective laser melting, *Journal of Materials Processing Technology* 213(4), 589-597.

27. Goodridge, R.D., Tuck, C.J. & Hague, R.J.M., 2012, Laser Sintering of polyamides and other polymers, *Progress in Materials Science* 57(2), 229-267.

28. Gornet , T.J., Davis, K.R., Starr, T.L. and Mulloy, K.M. [n.d.], Characterization of Selective Laser Sintering™ materials to determine process stability. [s.l.].

29. Iliescu, M., Tabeshfar, K., Ighigeanu, A. & Dobrescu, G., 2009, Importance of rapid prototyping to product design, *U.P.B Sci.Bull*, Series D 71(2), 117-124.

30. Kamrani, A.K. & Nasr, E.A (eds), 2006, *Rapid prototyping: Theory and practice*. Springer. Houston, TX, USA.

31. Kaufui, V.W. & Aldo, F., 2012, A review of Additive Manufacturing. ISRB *Mechanical Engineering* 2012, 1-10.

32. Koike, M., Greer, P., Owen, K., Lilly, G., Murr, L.E., Gaytan, S.M., Martinez, E. & Okabe, T., 2011. Evaluation of Titanium alloys fabricated using Rapid Prototyping technologies-Electron Beam Melting and Laser Beam Melting, *Materials* 4(10), 1776-1792.

33. Kruth, J.P., Levy, G., Schinder, R., Craeghs, T. & Yasa, E., 2008, Consolidation of polymers by Selective laser Sintering. [s.l.].

34. Kulkarni, P. & Dutta, D., 2000, On integration of layered manufacturing and material removal process, *International Journal of Mechanical Engineering* 122(1), 100-108.

35. Kumar, S., 2003. Selective laser Sintering: A Qualitative and Objective Approach. *JOM,* 43-47.

36. Kuo, C.C. & Su, S.J., 2013, A simple method for improving surface quality of rapid prototype, *Indian Journal of Engineering Sciences* 20, 465-470.

37. Lamikiz, A., Sanchez, J.A.,Lopez de Lacalle & Arana, J.L., 2007, Laser polishing of parts built up by selective laser sintering. *International Journal of Machine Tools & Manufacture* 47(12-13), 2040-2050.

38. Liron, N., 2005, An investigation of performance of low cost rapid prototyping machines, MSc. thesis, Dept. of Engineering & Technology, University of Montfort.

39. Marcincinova, L.N. & Kuric, I., 2012, Basic and Advanced Materials for Fused Deposition Modelling Rapid Prototyping Technology, *Manufacturing and Industry Engineering* 11(1), 24-27.

40. Matthew, F., Sunjay, B.J. & Richard, A.W., 2003, Rapid prototyping and integrated product/process development tool-an overview of issues and economics, *Journal of Chinese Institute of Industrial Engineers* 20(3), 240-246.

41. Mireles, J., Adame, A., Espalin, D., Medina, F., Winker, R., Hoppe, T., Zinniel, B. & Wicker, R., Reviewed August 17th 2011, Analysis of sealing methods for FDM fabricated parts, *Couri Symposium*, 185-196.

42. Mitutoyo Corporation, 2009, *Surface roughness measuring tester SJ-210, User's manual.*

43. Mohammadjafari, M., Shamsuddin, A., Siti, ZMD. & Zayandenroodi, H., 2011, The importance of project management in small-and medium-sized enterprises (SMEs) for the development of new products through E-collaboration, *African Journal of Business Management* 5(30), 11844-11855.

44. Mousah, A.A., 2011, Effects of filler content and coupling agents on mechanical and geometrical accuracy of selective laser sintered parts in glass bead-filled polyamide 12 composites, PhD thesis, Manufacturing Centre- School of Engineering, Cardiff University, UK.

45. Nancharaiah, T., Ranga, R. & Ramachandra, V.R, 2010, An experimental investigation on surface quality and dimensional accuracy of FDM components, *International Journal of Emerging Technologies* 1(2), 106-111.

46. Nexant Inc., 2009. Nylon 6 and Nylon 6/6: Report Abstract. Available from: http://www.chemsystems.com/PERP Program-Nylon 6 and Nylon 6/6. [Accessed 8th August 2013].
47. Novakova, L.M. & Novak, M., 2012, Testing of materials for rapid prototyping Fused Deposition Modelling technology, *World Academy of Science, Engineering and Technology* 70, 410-414.
48. Ocloo, C.E., Akaba, S., Worwui-Brown, D.K., 2014, Globalization and Competitiveness: challenges of Small and Medium Enterprises (SMEs) in Accra, Ghana, *International Journal of Business and Social Science* 5(4), 287-296.
49. Pandey, P.M., Reddy, N.V. & Dhande, S.G., 2003, Real time adaptive slicing for fused deposition modelling, *International Journal of Machine Tools & Manufacture* 43(1) 61-71.
50. Pandey, P.M., Reddy, N.V., & Dhande, S.G., 2003, Improvement of surface finish by staircase machining in fused deposition modelling, *Journal of Material Processing Technology* 132(1-3), 323-331.
51. Paul, B.K. & Baskaran, S., 1996, Issues in fabricating manufacturing tooling using powder-based additive freeform fabrication, *Journal of materials Processing Technology* 61(1-2), 168-172.
52. Pham, D.T., Dotchev, K.D. & Yusoff, W.A.Y., 2008, Deterioration of polyamide powder properties in laser sintering process, *Journal of Mechanical Engineering Science* 222, 2163-2176).
53. Philips Plastics Corporation, 2009, Choosing the right rapid prototype source for your product development program, Hudson, Wiscosin, USA.
54. Raghunath, N. and Pandey, M.P., 2007, Improving accuracy through shrinkage modelling by using Tagushi method in Selective laser Sintering, *International Journal of Machine Tools & Manufacture* 47, 985-995.
55. Reeves, P.E. & Cobb, R.C. [n.d.], Reducing the surface deviation of stereolithography using alternative build strategy, [s.l].
56. Schmid, M., Simon, C. & Levy, G.N., 2009, Finishing of SLS-parts for rapid manufacturing (RM)-a comprehensive approach, *INSPIRE*, 1-10.
57. Shrivastava, V., Parida, S.K. & Pandey, P.M., 2010, Surface roughness studies in Selective Laser Sintering of Glass Filled Polyamide, *Proceedings of 36th International MATADOR Conference*, Manchester 2010.

58. Singh, G.B. & Kumar, P., 2014, Methods to improve surface finish of parts produced by Fused Deposition Modelling, *Manufacturing Science and Technology* 2(3), 51-55.
59. Singh, S., Sachdeva, A. & Sharma, V.S., 2012, Investigation on dimensional accuracy/ Mechanical properties of part produced by Selective laser Sintering, *International Journal of Applied Science and Engineering* 10(1) 59-68.
60. Stratasys, Inc. 2013, Fortus finishing touch™ Smoothing Station. Available from: http://www.stratasys.com/3D Printers/Fortus finishing touch smoothing station. [Accessed 20th February 2014].
61. Tanay, V.D., Prashant, M.K., Gaurav, C.N. & Vishal, N.B., 2013, Multi objective optimization of built orientation for rapid prototyping of connecting rod, *International Journal of scientific research and management* 1(1), 13-18.
62. Urednik, 2013, Alumide®-Polyamide carbon fiber-reinforced, retrieved from www.3dimpuls.com [Accessed 21 July 2014].
63. Vasudevarao, B., Prakash, D.N and Handerson, M., [n.d.], Sensitivity of Rapid Prototyping surface finish to process parameter variation.
64. Vijay, P., Danaiah P. & Rajesh, K.V.D., 2011, Critical parameters affecting Rapid Prototyping surface finish, *Journal of Mechanical Engineering and Automation* 1(1), 17-20.
65. William, R.E. & Melton, V.L., 1998, Abrasive flow finishing of stereo-lithography prototypes, *Rapid Prototyping Journal* 4(2), 56-67.
66. Wohlers, T. & Gornet, T., 2011, History of additive manufacturing, Wohlers Report 2011, State of the Industry, WOHLERS ASSOCIATES, INC.
67. Yasa, E. & Kruth, J., 2011, Application of Laser re-melting on Selective laser Melting parts, *Advances in Production Engineering and Management* 6(4) 259-270.
68. Zarringhalam, H., Hopkinson N., Kamperman N.F. & de Vlieger J.J., 2006, Effect of processing on microstructure and properties of SLS Nylon 12, *Material Science and Engineering*, 172-180.
69. Ziemian, C., Sharma, M. & Ziemian, S., 2012, Anisotropic Mechanical properties of ABS parts fabricated by Fused Deposit Modelling, *Mechanical Engineering, Dr. Murat Gokcek (Ed.), In Tech,* 159-180.

APPENDIX 1: COMPUTATION OF THE CHI-SQUARE TEST- χ^2 AND Z_{obs} FOR NYLON TEST PIECES

A. Tumbling

	Deviation ranges (mm)		Observed number of points		Expected number of points		Chi-square test (P-value)	% of observed number of points		Z_{obs}	Conclusion
	>=Min.	<Max.	As built- x_1	Tumbling -x_2	As built	Tumbling		As built p_1 x 100	Tumbling p_2 x 100		
1	-2.000	-0.926	33	342	183	192	0	0.0	0.1	-15.548	Rejected
2	-0.926	-0.844	6	56	30	32		0.0	0.0	-2.514	Not Rejected
3	-0.844	-0.761	10	48	28	30		0.0	0.0	-1.899	Not Rejected
4	-0.761	-0.678	21	103	61	63		0.0	0.0	-4.099	Rejected
5	-0.678	-0.596	38	165	99	104		0.0	0.0	-6.336	Rejected
6	-0.596	-0.513	57	202	127	132		0.0	0.1	-7.204	Rejected
7	-0.513	-0.430	97	200	145	152		0.0	0.1	-4.992	Rejected
8	-0.430	-0.348	227	464	338	353		0.1	0.1	-11.478	Rejected
9	-0.348	-0.265	741	1277	987	1031		0.2	0.4	-25.452	Rejected
10	-0.265	-0.183	1873	5971	3838	4006		0.6	1.7	-203.018	Rejected
11	-0.183	-0.100	24408	25290	24315	25383		7.4	7.3	9.611	Rejected
12	-0.100	0.100	288851	306026	291046	303831		87.1	88.3	-226.865	Rejected
13	0.100	0.183	7629	4902	6131	6400		2.3	1.4	154.806	Rejected
14	0.183	0.265	2408	550	1447	1511		0.7	0.2	99.280	Rejected
15	0.265	0.348	1605	258	911	952		0.5	0.1	71.663	Rejected

	Deviation ranges (mm)		Observed number of points		Expected number of points		Chi-square test (P-value)	% of observed number of points		Z_{obs}	Conclusion
	>=Min.	<Max.	As built- x_1	Tumbling -x_2	As built	Tumbling					
16	0.348	0.430	1173	209	676	706	0	0.4	0.1	51.340	Rejected
17	0.430	0.513	715	69	384	400		0.2	0.0	34.247	Rejected
18	0.513	0.596	525	60	286	299		0.2	0.0	24.674	Rejected
19	0.596	0.678	472	61	261	272		0.1	0.0	21.827	Rejected
20	0.678	0.761	367	53	205	215		0.1	0.0	16.689	Rejected
21	0.761	0.844	260	24	139	145		0.1	0.0	12.509	Rejected
22	0.844	0.926	189	10	97	102		0.1	0.0	9.469	Rejected
23	0.926	1.009	49	5	26	28		0.0	0.0	2.333	Not Rejected
24	1.009	2.000	67	51	58	60		0.0	0.0	0.958	Not Rejected
	Subtotal		**n_1=331821**	**n_2=346396**							
	Grand Total		**n= 678217**								

B. Shot peening

	Deviation ranges (mm)		Observed number of points		Expected number of points		Chi-square test (P-value)	% of observed number of points		Z_{obs}	Conclusion
	>=Min.	<Max.	As built- x_1	Shot peening-x_2	As built	Shot peening		As built p_1 x 100	Shot peening p_2 x 100		
1	-2.000	-0.926	33	87	57	63	0	0.0	0.0	-4.418	Rejected
2	-0.926	-0.844	6	53	28	31		0.0	0.0	-4.041	Rejected
3	-0.844	-0.761	10	118	61	67		0.0	0.0	-9.319	Rejected
4	-0.761	-0.678	21	390	196	215		0.0	0.1	-31.953	Rejected
5	-0.678	-0.596	38	885	440	483		0.0	0.2	-73.433	Rejected
6	-0.596	-0.513	57	1360	675	742		0.0	0.4	-112.980	Rejected
7	-0.513	-0.430	97	2166	1078	1185		0.0	0.6	-179.343	Rejected
8	-0.430	-0.348	227	203	205	225		0.1	0.1	4.048	Rejected
9	-0.348	-0.265	741	4804	2642	2903		0.2	1.3	-347.437	Rejected
10	-0.265	-0.183	1873	10083	5696	6260		0.6	2.8	-698.818	Rejected
11	-0.183	-0.100	24408	22895	22536	24767		7.4	6.3	342.235	Rejected
12	-0.100	0.100	288851	301298	281155	308994		87.1	82.6	1406.869	Rejected
13	0.100	0.183	7629	17026	11746	12909		2.3	4.7	-752.553	Rejected
14	0.183	0.265	2408	1422	1825	2005		0.7	0.4	106.631	Rejected
15	0.265	0.348	1605	430	969	1066		0.5	0.1	116.165	Rejected
16	0.348	0.430	1173	367	734	806		0.4	0.1	80.306	Rejected

	Deviation ranges (mm)		Observed number of points		Expected number of points		Chi-square test (P-value	% of observed number of points		Z_{obs}	Conclusion
	>=Min.	<Max.	As built- x_1	Shot peening-x_2	As built	Shot peening		As built p_1 x 100	Shot peening p_2 x 100		
17	0.430	0.513	715	361	513	563	0	0.2	0.1	36.994	Rejected
18	0.513	0.596	525	311	398	438		0.2	0.1	23.163	Rejected
19	0.596	0.678	472	179	310	341		0.1	0.0	29.586	Rejected
20	0.678	0.761	367	105	225	247		0.1	0.0	25.981	Rejected
21	0.761	0.844	260	66	155	171		0.1	0.0	19.137	Rejected
22	0.844	0.926	189	23	101	111		0.1	0.0	16.086	Rejected
23	0.926	1.009	49	19	32	36		0.0	0.0	3.035	Not Rejected
24	1.009	2.000	67	27	45	49		0.0	0.0	4.061	Rejected
	Subtotal		**n_1=331821**	**n_2=364678**							
	Grand Total		**n=696499**								

C. Hand finishing

	Deviation ranges (mm)		Observed number of points		Expected number of points		Chi-square test (P-value)	% of observed number of points		Z_{obs}	Conclusion
	>=Min.	<Max.	As built- x_1	Hand finishing-x_2	As built	Hand finishing		As built p_1 x 100	Hand finishing p_2 x 100		
1	-2.000	-0.926	33	824	57	63	0	0.0	0.2	-26.619	Rejected
2	-0.926	-0.844	6	93	28	31		0.0	0.0	-2.925	Not Rejected
3	-0.844	-0.761	10	135	61	67		0.0	0.0	-4.202	Rejected
4	-0.761	-0.678	21	152	196	215		0.0	0.0	-4.393	Rejected
5	-0.678	-0.596	38	314	440	483		0.0	0.1	-9.262	Rejected
6	-0.596	-0.513	57	355	675	742		0.0	0.1	-9.985	Rejected
7	-0.513	-0.430	97	421	1078	1185		0.0	0.1	-10.821	Rejected
8	-0.430	-0.348	227	1007	205	225		0.1	0.3	-26.058	Rejected
9	-0.348	-0.265	741	3345	2642	2903		0.2	1.0	-87.010	Rejected
10	-0.265	-0.183	1873	9881	5696	6260		0.6	2.9	-267.977	Rejected
11	-0.183	-0.100	24408	35952	22536	24767		7.4	10.5	-364.978	Rejected
12	-0.100	0.100	288851	217002	281155	308994		87.1	63.5	2704.609	Rejected
13	0.100	0.183	7629	67510	11746	12909		2.3	19.8	-2010.102	Rejected
14	0.183	0.265	2408	3106	1825	2005		0.7	0.9	-21.152	Rejected

	Deviation ranges (mm)		Observed number of points		Expected number of points		Chi-square test (P-value)	% of observed number of points		Z_{obs}	Conclusion
	>=Min.	<Max.	As built- x_1	Hand finishing-x_2	As built	Hand finishing		As built p_1 x 100	Hand finishing p_2 x 100		
15	0.265	0.348	1605	929	969	1066	0	0.5	0.3	24.354	Rejected
16	0.348	0.430	1173	102	734	806		0.4	0.0	37.238	Rejected
17	0.430	0.513	715	60	513	563		0.2	0.0	22.772	Rejected
18	0.513	0.596	525	56	398	438		0.2	0.0	16.318	Rejected
19	0.596	0.678	472	68	310	341		0.1	0.0	14.076	Rejected
20	0.678	0.761	367	96	225	247		0.1	0.0	9.491	Rejected
21	0.761	0.844	260	29	155	171		0.1	0.0	8.039	Rejected
22	0.844	0.926	189	17	101	111		0.1	0.0	5.981	Rejected
23	0.926	1.009	49	28	32	36		0.0	0.0	0.756	Not Rejected
24	1.009	2.000	67	14	45	49		0.0	0.0	1.852	Not Rejected
	Subtotal		n_1=331821	n_2=341496							
	Grand Total		n=673317								

D. Spray painting

	Deviation ranges (mm)		Observed number of points		Expected number of points		Chi-square test (P-value)	% of observed number of points		Z_{obs}	Conclusion
	>=Min.	<Max.	As built- x_1	Spray pianting- x_2	As built	Spray painting		As built p_1 x 100	Spray painting p_2 x 100		
1	-2.000	-0.926	33	52	40	45	0	0.0	0.0	-1.553	Not Rejected
2	-0.926	-0.844	6	16	10	12		0.0	0.0	-0.954	Not Rejected
3	-0.844	-0.761	10	19	14	15		0.0	0.0	-0.803	Not Rejected
4	-0.761	-0.678	21	18	18	21		0.0	0.0	0.560	Not Rejected
5	-0.678	-0.596	38	24	29	33		0.0	0.0	1.894	Not Rejected
6	-0.596	-0.513	57	74	62	69		0.0	0.0	-1.059	Not Rejected
7	-0.513	-0.430	97	100	93	104		0.0	0.0	0.859	Not Rejected
8	-0.430	-0.348	227	93	151	169		0.1	0.0	16.482	Rejected
9	-0.348	-0.265	741	144	418	467		0.2	0.0	70.179	Rejected
10	-0.265	-0.183	1873	257	1006	1124		0.6	0.1	188.367	Rejected
11	-0.183	-0.100	24408	490	11760	13138		7.4	0.1	2748.123	Rejected
12	-0.100	0.100	288851	11236	141739	158348		87.1	3.0	31964.05 3	Rejected
13	0.100	0.183	7629	29320	17452	19497		2.3	7.9	-2134.299	Rejected
14	0.183	0.265	2408	51931	25666	28673		0.7	14.0	-5053.355	Rejected
15	0.265	0.348	1605	82876	39903	44578		0.5	22.4	-8321.161	Rejected

	Deviation ranges (mm)		Observed number of points		Expected number of points		Chi-square test (P-value	% of observed number of points		Z_{obs}	Conclusion
	>=Min.	<Max.	As built- x_1	Spray pianting- x_2	As built	Spray painting		As built p_1 x 100	Spray painting p_2 x 100		
16	0.348	0.430	1173	73618	35326	39465	0	0.4	19.9	-7420.585	Rejected
17	0.430	0.513	715	58470	27955	31230		0.2	15.8	-5918.527	Rejected
18	0.513	0.596	525	37814	18108	20231		0.2	10.2	-3820.482	Rejected
19	0.596	0.678	472	13646	6668	7450		0.1	3.7	-1346.310	Rejected
20	0.678	0.761	367	8541	4207	4701		0.1	2.3	-834.446	Rejected
21	0.761	0.844	260	709	458	511		0.1	0.2	-42.952	Rejected
22	0.844	0.926	189	535	342	382		0.1	0.1	-33.235	Rejected
23	0.926	1.009	49	321	175	195		0.0	0.1	-27.325	Rejected
24	1.009	2.000	67	401	221	247		0.0	0.1	-33.471	Rejected
	Subtotal		**n_1=331821**	**n_2=370705**							
	Grand Total		**n=702526**								

E. CNC machining

	Deviation ranges (mm)		Observed number of points		Expected number of points		Chi-square test (P-value)	% of observed number of points		Z_{obs}	Conclusion
	>=Min.	<Max.	As built- x_1	CNC machining- x_2	As built	CNC machining		As built p_1 x 100	CNC machining p_2 x 100		
1	-2.000	-0.926	33	48	40	41		0.0	0.0	-1.602	Not Rejected
2	-0.926	-0.844	6	10	8	8		0.0	0.0	-0.432	Not Rejected
3	-0.844	-0.761	10	20	15	15		0.0	0.0	-1.087	Not Rejected
4	-0.761	-0.678	21	13118	6522	6617		0.0	3.9	-1444.896	Rejected
5	-0.678	-0.596	38	13117	6530	6625		0.0	3.9	-1442.883	Rejected
6	-0.596	-0.513	57	13116	6539	6634		0.0	3.9	-1440.646	Rejected
7	-0.513	-0.430	97	13123	6563	6657		0.0	3.9	-1436.942	Rejected
8	-0.430	-0.348	227	68306	34021	34512		0.1	20.3	-7510.470	Rejected
9	-0.348	-0.265	741	68207	34227	34721	0	0.2	20.3	-7442.023	Rejected
10	-0.265	-0.183	1873	68300	34835	35338		0.6	20.3	-7325.594	Rejected
11	-0.183	-0.100	24408	68414	46079	46743		7.4	20.3	-4816.140	Rejected
12	-0.100	0.100	288851	8750	147735	149866		87.1	2.6	31361.749	Rejected
13	0.100	0.183	7629	458	4015	4072		2.3	0.1	803.279	Rejected
14	0.183	0.265	2408	458	1423	1443		0.7	0.1	218.965	Rejected
15	0.265	0.348	1605	458	1024	1039		0.5	0.1	129.096	Rejected
16	0.348	0.430	1173	458	810	821		0.4	0.1	80.749	Rejected

	Deviation ranges (mm)		Observed number of points		Expected number of points		Chi-square test (P-value	% of observed number of points		Z_{obs}	Conclusion
	>=Min.	<Max.	As built- x_1	CNC machining- x_2	As built	CNC machining		As built p_1 x 100	CNC machining p_2 x 100		
17	0.430	0.513	715	44	377	382	0	0.2	0.0	75.166	Rejected
18	0.513	0.596	525	43	282	286		0.2	0.0	54.012	Rejected
19	0.596	0.678	472	42	255	259		0.1	0.0	48.191	Rejected
20	0.678	0.761	367	45	205	207		0.1	0.0	36.109	Rejected
21	0.761	0.844	260	15	137	138		0.1	0.0	27.443	Rejected
22	0.844	0.926	189	17	102	104		0.1	0.0	19.277	Rejected
23	0.926	1.009	49	16	32	33		0.0	0.0	3.719	Rejected
24	1.009	2.000	67	23	45	45		0.0	0.0	4.961	Rejected
	Subtotal		**n_1=331821**	**n_2=336606**							
	Grand Total		**n=668427**								

APPENDIX 2: COMPUTATION OF THE CHI-SQUARE TEST- χ^2 AND Z_{obs} FOR ALUMIDE® TEST PIECES

A. Tumbling

	Deviation ranges (mm)		Observed number of points		Expected number of points		Chi-square test (P-value)	% of observed number of points		Z_{obs}	Conclusion
	>=Min.	<Max.	As built- x_1	Tumbling -x_2	As built	Tumbling		As built p_1 x 100	Tumbling p_2 x100		
1	-2.000	-0.926	55	124	89	90	0	0.0	0.0	-5.102	Rejected
2	-0.926	-0.844	17	50	33	34		0.0	0.0	-2.446	Not Rejected
3	-0.844	-0.761	22	52	37	37		0.0	0.0	-2.220	Not Rejected
4	-0.761	-0.678	35	92	63	64		0.0	0.0	-4.222	Rejected
5	-0.678	-0.596	39	321	179	181		0.0	0.1	-20.969	Rejected
6	-0.596	-0.513	79	913	494	498		0.0	0.2	-62.037	Rejected
7	-0.513	-0.430	111	1456	780	787		0.0	0.4	-100.057	Rejected
8	-0.430	-0.348	231	1931	1077	1085		0.1	0.5	-126.410	Rejected
9	-0.348	-0.265	792	4073	2422	2443		0.2	1.1	-243.758	Rejected
10	-0.265	-0.183	9571	12323	10902	10992		2.6	3.4	-198.935	Rejected
11	-0.183	-0.100	53204	38997	45909	46292		14.6	10.6	1090.600	Rejected
12	-0.100	0.100	238576	294007	265187	267396		65.5	80.1	-3978.563	Rejected
13	0.100	0.183	24669	10019	17272	17416		6.8	2.7	1105.888	Rejected

	Deviation ranges (mm)		Observed number of points		Expected number of points		Chi-square test (P-value)	% of observed number of points		Z_{obs}	Conclusion
	>=Min.	<Max.	As built- x_1	Tumbling -x_2	As built	Tumbling		As built p_1 x 100	Tumbling p_2 x100		
14	0.183	0.265	22824	908	11817	11915	0	6.3	0.2	1645.650	Rejected
15	0.265	0.348	8298	596	4429	4465		2.3	0.2	578.507	Rejected
16	0.348	0.430	2132	402	1262	1272		0.6	0.1	130.109	Rejected
17	0.430	0.513	626	233	428	431		0.2	0.1	29.644	Rejected
18	0.513	0.596	453	160	305	308		0.1	0.0	22.093	Rejected
19	0.596	0.678	249	113	180	182		0.1	0.0	10.279	Rejected
20	0.678	0.761	266	80	172	174		0.1	0.0	14.011	Rejected
21	0.761	0.844	283	58	170	171		0.1	0.0	16.925	Rejected
22	0.844	0.926	330	25	177	178		0.1	0.0	22.910	Rejected
23	0.926	1.009	396	21	208	209		0.1	0.0	28.162	Rejected
24	1.009	2.000	703	38	369	372		0.2	0.0	49.941	Rejected
	Subtotal		**n_1=363961**	**n_2=366992**							
	Grand Total		**n= 730953**								

B. Shot peening

	Deviation ranges (mm)		Observed number of points		Expected number of points		Chi-square test (P-value)	% of observed number of points		Z_{obs}	Conclusion
	>=Min.	<Max.	As built- x_1	Shot peening- x_2	As built	Shot peening		As built p1 X 100	Shot peening p2 X 100		
1	-2.000	-0.926	55	17	36	36	0	0.0	0.0	4.405	Rejected
2	-0.926	-0.844	17	3	10	10		0.0	0.0	1.630	Not Rejected
3	-0.844	-0.761	22	6	14	14		0.0	0.0	1.857	Not Rejected
4	-0.761	-0.678	35	8	22	21		0.0	0.0	3.138	Rejected
5	-0.678	-0.596	39	13	26	26		0.0	0.0	3.011	Not Rejected
6	-0.596	-0.513	79	51	66	64		0.0	0.0	3.167	Rejected
7	-0.513	-0.430	111	45	79	77		0.0	0.0	7.619	Rejected
8	-0.430	-0.348	231	92	163	160		0.1	0.0	16.051	Rejected
9	-0.348	-0.265	792	368	585	575		0.2	0.1	48.782	Rejected
10	-0.265	-0.183	9571	651	5156	5066		2.6	0.2	1040.825	Rejected
11	-0.183	-0.100	53204	16465	35138	34531		14.6	4.6	4258.552	Rejected
12	-0.100	0.100	238576	329328	286427	281477		65.5	92.1	-11279.493	Rejected
13	0.100	0.183	24669	9561	17264	16966		6.8	2.7	1745.492	Rejected
14	0.183	0.265	22824	732	11881	11675		6.3	0.2	2579.600	Rejected
15	0.265	0.348	8298	150	4261	4187		2.3	0.0	951.658	Rejected

	Deviation ranges (mm)		Observed number of points		Expected number of points		Chi-square test (P-value)	% of observed number of points		Z_{obs}	Conclusion
	>=Min.	<Max.	As built- x_1	Shot peening- x_2	As built	Shot peening		As built p1 X 100	Shot peening p2 X 100		
16	0.348	0.430	2132	39	1095	1076	0	0.6	0.0	244.454	Rejected
17	0.430	0.513	626	20	326	320		0.2	0.0	70.761	Rejected
18	0.513	0.596	453	24	241	236		0.1	0.0	50.073	Rejected
19	0.596	0.678	249	20	136	133		0.1	0.0	26.714	Rejected
20	0.678	0.761	266	13	141	138		0.1	0.0	29.532	Rejected
21	0.761	0.844	283	9	147	145		0.1	0.0	31.994	Rejected
22	0.844	0.926	330	6	169	167		0.1	0.0	37.842	Rejected
23	0.926	1.009	396	8	204	200		0.1	0.0	45.315	Rejected
24	1.009	2.000	703	43	376	370		0.2	0.0	77.022	Rejected
	Subtotal		**n_1=363961**	**n_2=357672**							
	Grand Total n=721633										

C. Hand finishing

	Deviation ranges (mm)		Observed number of points		Expected number of points		Chi-square test (P-value)	% of observed number of points		Z_{obs}	Conclusion
	>=Min.	<Max.	As built- x_1	Hand finishing-x_2	As built	Hand finishing		As built p_1 x 100	Hand finishing p_2 x 100		
1	-2.000	-0.926	55	55	56	54	0	0.0	0.0	-0.216	Not Rejected
2	-0.926	-0.844	17	26	22	21		0.0	0.0	-0.943	Not Rejected
3	-0.844	-0.761	22	45	34	33		0.0	0.0	-2.325	Not Rejected
4	-0.761	-0.678	35	53	45	43		0.0	0.0	-1.889	Not Rejected
5	-0.678	-0.596	39	71	56	54		0.0	0.0	-3.268	Rejected
6	-0.596	-0.513	79	193	139	133		0.0	0.1	-11.407	Rejected
7	-0.513	-0.430	111	470	296	285		0.0	0.1	-35.380	Rejected
8	-0.430	-0.348	231	1350	807	774		0.1	0.4	-109.827	Rejected
9	-0.348	-0.265	792	3201	2038	1955		0.2	0.9	-237.595	Rejected
10	-0.265	-0.183	9571	7537	8730	8378		2.6	2.2	160.403	Rejected
11	-0.183	-0.100	53204	22951	38861	37294		14.6	6.6	2735.832	Rejected
12	-0.100	0.100	238576	241622	245041	235157		65.5	69.2	-1233.264	Rejected
13	0.100	0.183	24669	67798	47185	45282		6.8	19.4	-4294.915	Rejected
14	0.183	0.265	22824	3194	13277	12741		6.3	0.9	1821.108	Rejected
15	0.265	0.348	8298	286	4380	4204		2.3	0.1	747.282	Rejected

	Deviation ranges (mm)		Observed number of points		Expected number of points		Chi-square test (P-value)	% of observed number of points		Z_{obs}	Conclusion
	>=Min.	<Max.	As built- x_1	Hand finishing-x_2	As built	Hand finishing		As built p_1 x 100	Hand finishing p_2 x 100		
16	0.348	0.430	2132	142	1160	1114	0	0.6	0.0	185.329	Rejected
17	0.430	0.513	626	44	342	328		0.2	0.0	54.192	Rejected
18	0.513	0.596	453	27	245	235		0.1	0.0	39.687	Rejected
19	0.596	0.678	249	64	160	153		0.1	0.0	17.030	Rejected
20	0.678	0.761	266	61	167	160		0.1	0.0	18.910	Rejected
21	0.761	0.844	283	33	161	155		0.1	0.0	23.223	Rejected
22	0.844	0.926	330	12	175	167		0.1	0.0	29.657	Rejected
23	0.926	1.009	396	10	207	199		0.1	0.0	36.017	Rejected
24	1.009	2.000	703	34	376	361		0.2	0.0	62.358	Rejected
	Subtotal		**n_1=363961**	**n_2=349279**							
	Grand Total		**n=713240**								

D. CNC machining

	Deviation ranges (mm)		Observed number of points		Expected number of points		Chi-square test (P-value)	% of observed number of points		Z_{obs}	Conclusion
	>=Min.	<Max.	As built- x_1	CNC machining- x_2	As built	CNC machining		As built p_1 x 100	CNC machining p_2 x 100		
1	-2.000	-0.926	55	48	54	49	0	0.0	0.0	0.294	Not Rejected
2	-0.926	-0.844	17	10	14	13		0.0	0.0	0.586	Not Rejected
3	-0.844	-0.761	22	20	22	20		0.0	0.0	0.036	Not Rejected
4	-0.761	-0.678	35	13118	6833	6320		0.0	3.9	-1340.832	Rejected
5	-0.678	-0.596	39	13117	6835	6321		0.0	3.9	-1340.351	Rejected
6	-0.596	-0.513	79	13116	6855	6340		0.0	3.9	-1336.458	Rejected
7	-0.513	-0.430	111	13123	6875	6359		0.0	3.9	-1334.143	Rejected
8	-0.430	-0.348	231	68306	35607	32930		0.1	20.3	-6977.152	Rejected
9	-0.348	-0.265	792	68207	35847	33152		0.2	20.3	-6913.845	Rejected
10	-0.265	-0.183	9571	68300	40456	37415		2.6	20.3	-6091.435	Rejected
11	-0.183	-0.100	53204	68414	63183	58435		14.6	20.3	-1968.246	Rejected
12	-0.100	0.100	238576	8750	128492	118834		65.5	2.6	21712.017	Rejected
13	0.100	0.183	24669	458	13054	12073		6.8	0.1	2290.822	Rejected
14	0.183	0.265	22824	458	12096	11186		6.3	0.1	2115.981	Rejected
15	0.265	0.348	8298	458	4549	4207		2.3	0.1	739.428	Rejected
16	0.348	0.430	2132	458	1346	1244		0.6	0.1	155.109	Rejected

	Deviation ranges (mm)		Observed number of points		Expected number of points		Chi-square test (P-value)	% of observed number of points		Z_{obs}	Conclusion
	>=Min.	<Max.	As built- x_1	CNC machining- x_2	As built	CNC machining		As built p_1 x 100	CNC machining p_2 x 100		
17	0.430	0.513	626	44	348	322	0	0.2	0.0	54.814	Rejected
18	0.513	0.596	453	43	258	238		0.1	0.0	38.522	Rejected
19	0.596	0.678	249	42	151	140		0.1	0.0	19.293	Rejected
20	0.678	0.761	266	45	162	149		0.1	0.0	20.596	Rejected
21	0.761	0.844	283	15	155	143		0.1	0.0	25.281	Rejected
22	0.844	0.926	330	17	180	167		0.1	0.0	29.530	Rejected
23	0.926	1.009	396	16	214	198		0.1	0.0	35.887	Rejected
24	1.009	2.000	703	23	377	349		0.2	0.0	64.263	Rejected
	Subtotal		**n_1=363961**	**n_2=336606**							
	Grand Total		**n=700567**								

E. Spray painting

	Deviation ranges (mm)		Observed number of points		Expected number of points		Chi-square test (P-value)	% of observed number of points		Z_{obs}	Conclusion
	>=Min.	<Max.	As built- x_1	Spray painting-x_2	As built	Spray painting		As built p1 x 100	Spray painting p2 x 100		
1	-2.000	-0.926	55	30	43	42	0	0.0	0.0	2.660	Not Rejected
2	-0.926	-0.844	17	12	15	14		0.0	0.0	0.525	Not Rejected
3	-0.844	-0.761	22	8	15	15		0.0	0.0	1.500	Not Rejected
4	-0.761	-0.678	35	6	21	20		0.0	0.0	3.121	Rejected
5	-0.678	-0.596	39	8	24	23		0.0	0.0	3.334	Rejected
6	-0.596	-0.513	79	18	49	48		0.0	0.0	6.558	Rejected
7	-0.513	-0.430	111	41	76	76		0.0	0.0	7.500	Rejected
8	-0.430	-0.348	231	73	153	151		0.1	0.0	16.953	Rejected
9	-0.348	-0.265	792	109	453	448		0.2	0.0	73.538	Rejected
10	-0.265	-0.183	9571	198	4912	4857		2.6	0.1	1010.762	Rejected
11	-0.183	-0.100	53204	667	27087	26784		14.6	0.2	5666.006	Rejected
12	-0.100	0.100	238576	65808	153048	151336		65.5	18.3	18555.070	Rejected
13	0.100	0.183	24669	26169	25562	25276		6.8	7.3	-193.717	Rejected
14	0.183	0.265	22824	15109	19073	18860		6.3	4.2	813.736	Rejected
15	0.265	0.348	8298	38842	23703	23437		2.3	10.8	-3341.960	Rejected
16	0.348	0.430	2132	63505	33003	32634		0.6	17.6	-6697.365	Rejected

	Deviation ranges (mm)		Observed number of points		Expected number of points		Chi-square test (P-value)	% of observed number of points		Z_{obs}	Conclusion
	>=Min.	<Max.	As built- x_1	Spray painting-x_2	As built	Spray painting		As built p1 x 100	Spray painting p2 x 100		
17	0.430	0.513	626	36835	18836	18625	0	0.2	10.2	-3950.558	Rejected
18	0.513	0.596	453	61163	30981	30635		0.1	17.0	-6622.995	Rejected
19	0.596	0.678	249	30615	15519	15345		0.1	8.5	-3312.725	Rejected
20	0.678	0.761	266	12932	6636	6562		0.1	3.6	-1381.973	Rejected
21	0.761	0.844	283	5639	2978	2944		0.1	1.6	-584.595	Rejected
22	0.844	0.926	330	521	428	423		0.1	0.1	-21.237	Rejected
23	0.926	1.009	396	477	439	434		0.1	0.1	-9.319	Rejected
24	1.009	2.000	703	1106	910	899		0.2	0.3	-44.818	Rejected
	Subtotal		**n_1=363961**	**n_2=359891**							
	Grand Total		**n=723852**								

APPENDIX 3: COMPUTATION OF THE CHI-SQUARE TEST- χ^2 AND Z_{obs} FOR ABS TEST PIECES

A. Tumbling

	Deviation ranges (mm)		Observed number of points		Expected number of points		Chi-square test (P-value)	% of observed number of points		Z_{obs}	Conclusion
	>=Min.	<Max.	As built- x_1	Tumbling - x_2	As built	Tumbling		As built p_1 x 100	Tumbling p_2 x 100		
1	-2.000	-0.926	87	4798	2373	2512	0	0.0	1.3	-65.666	Rejected
2	-0.926	-0.844	17	819	406	430		0.0	0.2	-11.177	Rejected
3	-0.844	-0.761	13	700	346	367		0.0	0.2	-9.576	Rejected
4	-0.761	-0.678	21	742	371	392		0.0	0.2	-10.044	Rejected
5	-0.678	-0.596	20	959	476	503		0.0	0.3	-13.086	Rejected
6	-0.596	-0.513	55	1773	888	940		0.0	0.5	-23.928	Rejected
7	-0.513	-0.430	115	2923	1476	1562		0.0	0.8	-39.089	Rejected
8	-0.430	-0.348	236	3351	1742	1845		0.1	0.9	-43.274	Rejected
9	-0.348	-0.265	692	5242	2882	3052		0.2	1.5	-62.924	Rejected
10	-0.265	-0.183	3604	7928	5602	5930		1.1	2.2	-57.384	Rejected
11	-0.183	-0.100	50069	13057	30663	32463		14.8	3.6	557.503	Rejected
12	-0.100	0.100	266246	290385	270376	286255		78.6	81.0	-118.635	Rejected
13	0.100	0.183	9509	23816	16187	17138		2.8	6.6	-191.848	Rejected
14	0.183	0.265	2970	537	1703	1804		0.9	0.1	36.384	Rejected
15	0.265	0.348	1443	181	789	835		0.4	0.1	18.793	Rejected

	Deviation ranges (mm)		Observed number of points		Expected number of points		Chi-square test (P-value)	% of observed number of points		Z_{obs}	Conclusion
	>=Min.	<Max.	As built- x_1	Tumbling -x_2	As built	Tumbling		As built p_1 x 100	Tumbling p_2 x 100		
16	0.348	0.430	856	171	499	528	0	0.3	0.0	10.260	Rejected
17	0.430	0.513	540	136	328	348		0.2	0.0	6.080	Rejected
18	0.513	0.596	260	121	185	196		0.1	0.0	2.153	Not Rejected
19	0.596	0.678	267	130	193	204		0.1	0.0	2.131	Not Rejected
20	0.678	0.761	272	127	194	205		0.1	0.0	2.246	Not Rejected
21	0.761	0.844	320	107	207	220		0.1	0.0	3.234	Rejected
22	0.844	0.926	342	82	206	218		0.1	0.0	3.908	Rejected
23	0.926	1.009	373	76	218	231		0.1	0.0	4.450	Rejected
24	1.009	2.000	364	422	382	404		0.1	0.1	-0.511	Not Rejected
	Subtotal		**n_1=338691**	**n_2=358583**							
	Grand Total		**n= 697274**								

B. Shot peening

	Deviation ranges		Observed number of points		Expected number of points		Chi-square test (P-value)	% of observed number of points		Z_{obs}	Conclusion
	>=Min.	<Max.	As built- x_1	Shot peening- x_2	As built	Shot peening		As built p_1 x 100	Shot peening p_2 x 100		
1	-2.000	-0.926	87	33	59	61	0	0.0	0.0	5.033	Rejected
2	-0.926	-0.844	17	35	26	26		0.0	0.0	-1.599	Not Rejected
3	-0.844	-0.761	13	407	208	212		0.0	0.1	-35.611	Rejected
4	-0.761	-0.678	21	432	224	229		0.0	0.1	-37.135	Rejected
5	-0.678	-0.596	20	305	161	164		0.0	0.1	-25.741	Rejected
6	-0.596	-0.513	55	359	205	209		0.0	0.1	-27.399	Rejected
7	-0.513	-0.430	115	356	233	238		0.0	0.1	-21.598	Rejected
8	-0.430	-0.348	236	415	322	329		0.1	0.1	-15.783	Rejected
9	-0.348	-0.265	692	588	634	646		0.2	0.2	10.595	Rejected
10	-0.265	-0.183	3604	1321	2439	2486		1.1	0.4	212.669	Rejected
11	-0.183	-0.100	50069	8107	28814	29362		14.8	2.3	3881.101	Rejected
12	-0.100	0.100	266246	329930	295282	300894		78.6	95.6	-5301.846	Rejected
13	0.100	0.183	9509	1691	5547	5653		2.8	0.5	723.404	Rejected
14	0.183	0.265	2970	522	1730	1762		0.9	0.2	226.502	Rejected
15	0.265	0.348	1443	193	810	826		0.4	0.1	115.530	Rejected
16	0.348	0.430	856	70	459	467		0.3	0.0	72.557	Rejected

	Deviation ranges		Observed number of points		Expected number of points		Chi-square test (P-value)	% of observed number of points		Z_{obs}	Conclusion
	>=Min.	<Max.	As built- x_1	Shot peening- x_2	As built	Shot peening		As built p_1 x 100	Shot peening p_2 x 100		
17	0.430	0.513	540	77	306	311	0	0.2	0.0	42.802	Rejected
18	0.513	0.596	260	58	158	160		0.1	0.0	18.716	Rejected
19	0.596	0.678	267	83	173	177		0.1	0.0	17.100	Rejected
20	0.678	0.761	272	40	155	157		0.1	0.0	21.450	Rejected
21	0.761	0.844	320	8	162	166		0.1	0.0	28.767	Rejected
22	0.844	0.926	342	14	176	180		0.1	0.0	30.252	Rejected
23	0.926	1.009	373	12	191	194		0.1	0.0	33.290	Rejected
24	1.009	2.000	364	73	216	221		0.1	0.0	26.944	Rejected
	Subtotal		**n_1=338691**	**n_2=345129**							
	Grand Total		**n=683820**								

C. Hand finishing

	Deviation ranges (mm)		Observed number of points		Expected number of points		Chi-square test (P-value)	% of observed number of points		Z_{obs}	Conclusion
	>=Min.	<Max.	As built- x_1	Hand finishing-x_2	As built	Hand finishing		As built p_1 x 100	Hand finishing p_2 x 100		
1	-2.000	-0.926	87	117	101	103	0	0.0	0.0	-2.018	Not Rejected
2	-0.926	-0.844	17	334	174	177		0.0	0.1	-22.056	Rejected
3	-0.844	-0.761	13	79	46	46		0.0	0.0	-4.584	Rejected
4	-0.761	-0.678	21	129	75	75		0.0	0.0	-7.502	Rejected
5	-0.678	-0.596	20	617	317	320		0.0	0.2	-41.547	Rejected
6	-0.596	-0.513	55	581	316	320		0.0	0.2	-36.575	Rejected
7	-0.513	-0.430	115	605	358	362		0.0	0.2	-34.020	Rejected
8	-0.430	-0.348	236	808	519	525		0.1	0.2	-39.631	Rejected
9	-0.348	-0.265	692	1795	1236	1251		0.2	0.5	-76.229	Rejected
10	-0.265	-0.183	3604	5401	4476	4529		1.1	1.6	-122.180	Rejected
11	-0.183	-0.100	50069	15936	32811	33194		14.8	4.7	2416.982	Rejected
12	-0.100	0.100	266246	273704	268410	271540		78.6	79.9	-303.047	Rejected
13	0.100	0.183	9509	41446	25330	25625		2.8	12.1	-2215.723	Rejected
14	0.183	0.265	2970	360	1655	1675		0.9	0.1	184.119	Rejected
15	0.265	0.348	1443	95	765	773		0.4	0.0	95.019	Rejected
16	0.348	0.430	856	55	453	458		0.3	0.0	56.460	Rejected

	Deviation ranges (mm)		Observed number of points		Expected number of points		Chi-square test (P-value	% of observed number of points		Z_{obs}	Conclusion
	>=Min.	<Max.	As built- x_1	Hand finishing-x_2	As built	Hand finishing		As built p_1 x 100	Hand finishing p_2 x 100		
17	0.430	0.513	540	66	301	305	0	0.2	0.0	33.438	Rejected
18	0.513	0.596	260	174	216	218		0.1	0.1	6.198	Rejected
19	0.596	0.678	267	116	190	193		0.1	0.0	10.729	Rejected
20	0.678	0.761	272	109	189	192		0.1	0.0	11.569	Rejected
21	0.761	0.844	320	52	185	187		0.1	0.0	18.918	Rejected
22	0.844	0.926	342	8	174	176		0.1	0.0	23.531	Rejected
23	0.926	1.009	373	9	190	192		0.1	0.0	25.644	Rejected
24	1.009	2.000	364	45	203	206		0.1	0.0	22.504	Rejected
	Subtotal		**n_1=338691**	**n_2=342641**							
	Grand Total		**n=681332**								

D. Spray painting

	Deviation ranges (mm)		Observed number of points		Expected number of points		Chi-square test (P-value)	% of observed number of points		Z_{obs}	Conclusion
	>=Min.	<Max.	As built- x_1	Spray painting-x_2	As built	Spray painting		As built p_1 x 100	Spray painting p_2 x 100		
1	-2.000	-0.926	87	125	104	108	0	0.0	0.0	-2.301	Not Rejected
2	-0.926	-0.844	17	27	22	22		0.0	0.0	-0.623	Not Rejected
3	-0.844	-0.761	13	36	24	25		0.0	0.0	-1.509	Not Rejected
4	-0.761	-0.678	21	56	38	39		0.0	0.0	-2.292	Not Rejected
5	-0.678	-0.596	20	71	45	46		0.0	0.0	-3.371	Rejected
6	-0.596	-0.513	55	103	77	81		0.0	0.0	-3.067	Not Rejected
7	-0.513	-0.430	115	179	144	150		0.0	0.1	-3.968	Rejected
8	-0.430	-0.348	236	230	228	238		0.1	0.1	1.093	Not Rejected
9	-0.348	-0.265	692	318	494	516		0.2	0.1	27.172	Rejected
10	-0.265	-0.183	3604	378	1949	2033		1.1	0.1	227.465	Rejected
11	-0.183	-0.100	50069	412	24704	25777		14.8	0.1	3485.518	Rejected
12	-0.100	0.100	266246	4628	132556	138318		78.6	1.3	18370.640	Rejected
13	0.100	0.183	9509	3776	6501	6784		2.8	1.1	413.307	Rejected
14	0.183	0.265	2970	51219	26518	27671		0.9	14.5	-3235.827	Rejected

	Deviation ranges (mm)		Observed number of points		Expected number of points		Chi-square test (P-value)	% of observed number of points		Z_{obs}	Conclusion
	>=Min.	<Max.	As built- x_1	Spray painting-x_2	As built	Spray painting		As built p_1 x 100	Spray painting p_2 x 100		
15	0.265	0.348	1443	129768	64210	67001	0	0.4	36.7	-8625.005	Rejected
16	0.348	0.430	856	106541	52556	54841		0.3	30.1	-7104.293	Rejected
17	0.430	0.513	540	43610	21605	22545		0.2	12.3	-2894.667	Rejected
18	0.513	0.596	260	8806	4437	4629		0.1	2.5	-573.916	Rejected
19	0.596	0.678	267	1337	785	819		0.1	0.4	-71.172	Rejected
20	0.678	0.761	272	828	538	562		0.1	0.2	-36.593	Rejected
21	0.761	0.844	320	263	285	298		0.1	0.1	4.768	Rejected
22	0.844	0.926	342	149	240	251		0.1	0.0	13.978	Rejected
23	0.926	1.009	373	136	249	260		0.1	0.0	17.027	Rejected
24	1.009	2.000	364	415	381	398		0.1	0.1	-2.366	Not Rejected
	Subtotal		**n_1=338691**	**n_2=353411**							
	Grand Total		**n=692102**								

E. Chemical treatment

	Deviation ranges (mm)		Observed number of points		Expected number of points		Chi-square test (P-value)	% of observed number of points		Z_{obs}	Conclusion
	>=Min.	<Max.	As built- x_1	Chemical treatment-x_2	As built	Chemical treatment		As built p_1 x 100	Chemical treatment p_2 x 100		
1	-2.000	-0.926	87	29	57	59	0	0.0	0.0	5.352	Rejected
2	-0.926	-0.844	17	23	20	20		0.0	0.0	-0.569	Not Rejected
3	-0.844	-0.761	13	44	28	29		0.0	0.0	-2.895	Not Rejected
4	-0.761	-0.678	21	50	35	36		0.0	0.0	-2.713	Not Rejected
5	-0.678	-0.596	20	67	43	44		0.0	0.0	-4.389	Rejected
6	-0.596	-0.513	55	178	115	118		0.0	0.1	-11.488	Rejected
7	-0.513	-0.430	115	305	208	212		0.0	0.1	-17.763	Rejected
8	-0.430	-0.348	236	639	434	441		0.1	0.2	-37.672	Rejected
9	-0.348	-0.265	692	1793	1231	1254		0.2	0.5	-102.947	Rejected
10	-0.265	-0.183	3604	4517	4023	4098		1.1	1.3	-87.106	Rejected
11	-0.183	-0.100	50069	10328	29922	30475		14.8	3.0	3672.878	Rejected
12	-0.100	0.100	266246	309618	285300	290564		78.6	89.8	-4192.452	Rejected
13	0.100	0.183	9509	13039	11171	11377		2.8	3.8	-334.246	Rejected

	Deviation ranges (mm)		**Observed number of points**		**Expected number of points**		**Chi-square test (P-value**	**% of observed number of points**			
	>=Min.	**<Max.**	**As built- x_1**	**Chemical treatment-x_2**	**As built**	**Chemical treatment**					
14	0.183	0.265	2970	1269	2100	2139		0.9	0.4	156.733	Rejected
15	0.265	0.348	1443	634	1029	1048		0.4	0.2	74.525	Rejected
16	0.348	0.430	856	409	627	638		0.3	0.1	41.144	Rejected
17	0.430	0.513	540	336	434	442		0.2	0.1	18.691	Rejected
18	0.513	0.596	260	321	288	293		0.1	0.1	-5.831	Rejected
19	0.596	0.678	267	280	271	276	0	0.1	0.1	-1.364	Not Rejected
20	0.678	0.761	272	194	231	235		0.1	0.1	7.109	Rejected
21	0.761	0.844	320	140	228	232		0.1	0.0	16.582	Rejected
22	0.844	0.926	342	121	229	234		0.1	0.0	20.388	Rejected
23	0.926	1.009	373	197	282	288		0.1	0.1	16.179	Rejected
24	1.009	2.000	364	409	383	390		0.1	0.1	-4.400	Rejected
	Subtotal		**n_1=338691**	**n_2=344940**							
	Grand Total		**n=683631**								

F. CNC machining

	Deviation ranges (mm)		Observed number of points		Expected number of points		Chi-square test (P-value)	% of observed number of points		Z_{obs}	Conclusion
	>=Min.	<Max.	As built- x_1	CNC machining-x_2	As built	CNC machining		As built p_1 x 100	CNC machining p_2 x 100		
1	-2.000	-0.926	87	48	68	67	0	0.0	0.0	3.321	Rejected
2	-0.926	-0.844	17	10	14	13		0.0	0.0	0.595	Not Rejected
3	-0.844	-0.761	13	20	17	16		0.0	0.0	-0.611	Not Rejected
4	-0.761	-0.678	21	13118	6590	6549		0.0	3.9	-1130.820	Rejected
5	-0.678	-0.596	20	13117	6589	6548		0.0	3.9	-1130.820	Rejected
6	-0.596	-0.513	55	13116	6606	6565		0.0	3.9	-1127.730	Rejected
7	-0.513	-0.430	115	13123	6639	6599		0.0	3.9	-1123.186	Rejected
8	-0.430	-0.348	236	68306	34377	34165		0.1	20.3	-5877.362	Rejected
9	-0.348	-0.265	692	68207	34556	34343		0.2	20.3	-5829.685	Rejected
10	-0.265	-0.183	3604	68300	36063	35841		1.1	20.3	-5587.838	Rejected
11	-0.183	-0.100	50069	68414	59424	59059		14.8	20.3	-1610.540	Rejected
12	-0.100	0.100	266246	8750	137922	137074		78.6	2.6	22090.965	Rejected
13	0.100	0.183	9509	458	4999	4968		2.8	0.1	776.419	Rejected

	Deviation ranges (mm)		Observed number of points		Expected number of points		Chi-square test (P-value)	% of observed number of points		Z_{obs}	Conclusion
	>=Min.	<Max.	As built- x_1	CNC machining-x_2	As built	CNC machining		As built p_1 x 100	CNC machining p_2 x 100		
14	0.183	0.265	2970	458	1719	1709	0	0.9	0.1	215.310	Rejected
15	0.265	0.348	1443	458	953	948		0.4	0.1	84.279	Rejected
16	0.348	0.430	856	458	659	655		0.3	0.1	33.909	Rejected
17	0.430	0.513	540	44	293	291		0.2	0.0	42.538	Rejected
18	0.513	0.596	260	43	152	151		0.1	0.0	18.598	Rejected
19	0.596	0.678	267	42	155	154		0.1	0.0	19.285	Rejected
20	0.678	0.761	272	45	159	158		0.1	0.0	19.455	Rejected
21	0.761	0.844	320	15	168	167		0.1	0.0	26.164	Rejected
22	0.844	0.926	342	17	180	179		0.1	0.0	27.879	Rejected
23	0.926	1.009	373	20	197	196		0.1	0.0	30.280	Rejected
24	1.009	2.000	364	23	194	193		0.1	0.0	29.249	Rejected
	Subtotal		**n_1=338691**	**n_2=336610**							
	Grand Total		**n=675301**								

APPENDIX 4: VISUAL INSPECTION OF THE DIMENSIONAL ACCURACY FOR NYLON TEST PIECES

A. Horizontal surfaces, rectangular protrusions, round cavities and conical features

Process	Horizontal surfaces	Small protrusions	Top holes	Conical features	Touch probe scan picture	Conclusion
Tumbling	±0.1 mm deviation ranges dominate the upper horizontal surface up to 70%. The remaining 30% is covered by a uniformly distributed combination of ±0.1 mm and (0.1 to 0.348) mm. The transition areas are in the (-0.348 to -0.1) mm deviation ranges. The lower horizontal surface is almost up to 100% dominated by the ±0.1 mm deviation range.	(-0.678 to -0.100) mm deviation range cover the transition areas while ±0.1 mm cover the top surfaces of the protrusions.	Non-uniformly distributed combination of ±0.1 mm and (0.1 to 0.678) mm with predominance of ±0.1 mm is observed. The transition areas are dominated by (-0.513 to -0.1) mm	Non-uniformly distributed combination of ±0.1 mm and (-0.513 to -0.1) mm with predominance of ±0.1 mm is observed. The transition areas are dominated by (-0.513 to -0.1) mm	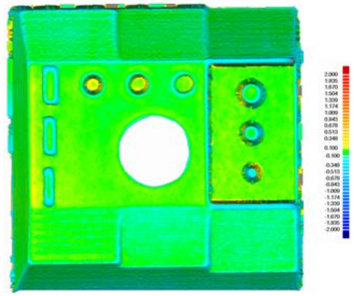	The tumbling technique keeps to ±0.1 mm deviation ranges up to 90%. The transition areas or the sharp corners are worn out to be in a deviation range of (-0.513 to -0.1) mm. A small percentage of the dimensions are in the deviation range of (0.1 to 0.348) mm, this may be as a result of defects in scanning process since the scanner is less accurate approaching vertical direction.

Process	Horizontal surfaces	Small protrusions	Top holes	Conical features	Touch probe scan picture	Conclusion
Shot peening	±0.1 mm deviation ranges cover 100% of the upper and lower surfaces.	(-0.6783 to -0.100) mm cover the surfaces of the features up to 70%, the remaining 30% is covered by ±0.1 mm.	±0.1 mm deviation ranges cover the horizontal surfaces. (-0.6783 to -0.100) mm deviation range characterizes the transition areas.	The top surfaces of the two biggest conical features are characterized by ±0.1 mm and (-0.6783 to -0.100) mm deviation ranges, the former at the centre and the latter extending towards the circumference of the cone. The smallest feature is covered by (-0.6783 to -0.100) mm deviation ranges.	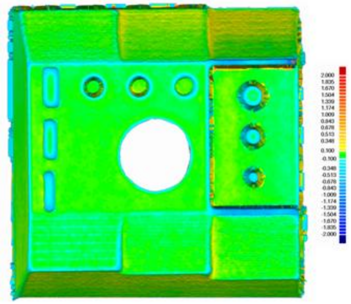	The shot peening technique produces 100% coverage of ±0.1 mm on the horizontal surfaces. The shots compress the edges of transition areas of small protrusions and conical features to yield (-0.6783 to -0.100) mm deviation ranges.
Hand finishing	The upper horizontal surface is dominated by (0.1 to 0.513) mm up to 80%. The area closer to peripheries has a mixture of (0.1 to 0.513) mm and ±0.1 mm. The lower surface up to 98% is covered with ±0.1 mm deviation ranges.	The transition surfaces between the horizontal and protrusions are dominated by (-0.678 to -0.1) mm deviation ranges and the tops of the protrusions are covered (0.1 to 0.513) mm deviation ranges.	The contours of the 3 holes contain small presence of (-0.678 to -0.1) mm deviation ranges, while the top surface areas are characterized by non-uniform combination of ±0.1 mm, and uniform mixture of ±0.1 mm and (0.1 to 0.513) mm	The contours of the three conical features are covered by (-0.513 to -0.1) mm deviation ranges, while the top surface are of different deviation ranges: (0.1 to 0.513) mm, mixture (0.1 to 0.513) mm of and ±0.1 mm.	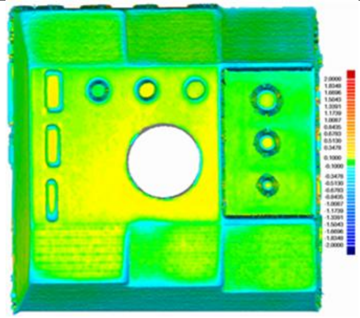	The hand finishing deviation range is uniform over the main horizontal surfaces as well as well as over the horizontal surfaces of small features, leading to a deviation range of (-0.1 to +0.2) mm covering 95%. However the deviation range on transition areas between surfaces, tend to negative side (-0.6783 to -0.1000) mm. The sanding effect can explain this phenomenon. The hand finishing technique is not consistent in distribution of the deviation range over the surface.

Process	Horizontal surfaces	Small protrusions	Top holes	Conical features	Touch probe scan picture	Conclusion
Spray-painting	The upper surface is dominated up to 98% by (+0.513 to 1.009) mm deviation range. The lower surface is dominated by (0.1 to 0.513) mm up to 90 % and 10 % being covered by (0.3478 to 0.844) mm	The transition surface between the horizontal and protrusions as well as the top are dominated by (0.3478 to 0.844) mm deviation ranges	The contours of the three round cavities contain small amount of ±0.1 mm, while the top surfaces are dominated by (0.1 to 0.348) mm.	The contours of the three conical features contain a small coverage of ± 0.1 mm while the top surfaces are dominated by (0.678 to 1.174) mm deviation ranges	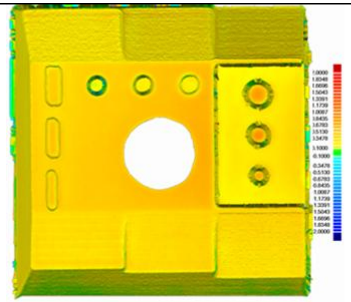	The spray painting technique is more uniform and consistent compared to the hand finishing technique. However higher deviation ranges of (0.678 to 1.174) mm are registered.
CNC machining	A uniformly distributed (-0.5130 to -0.1) mm deviation ranges cover the surface up to 80%. A uniformly distributed combination of ±0.1 mm and (-0.5130 to -0.1) deviation ranges occupy 20% of the surfaces	Almost 100% of the surface is within a deviation range of (-0.513 to -0.1) mm. The transition areas are in ±0.1 mm deviation range.	The bottom surface of the round cavities are in ±0.1 mm	100% of the top surface and 60% of the lateral surfaces are in (-0.5130 to -0.1) mm deviation ranges whereas 40% of the lateral surfaces is in ±0.1 mm deviation range.	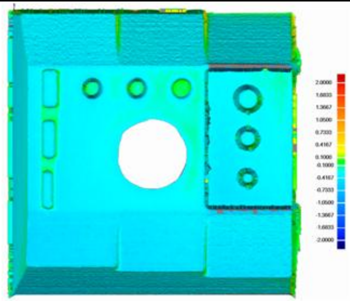	The deviation range of (-0.513 to -0.1) mm dominates the CNC machined part. The trend to negative range is explained by the fact that it strongly possible that there was an error in setting up of the cutting parameters and in calibration of the machine in vertical direction. The cutting tool has limited access to small transition areas which remains in deviation range of ±0.1 mm.

B. Surfaces inclined at 10°, 20°, 30° and 70°

Process	Inclination angle of the surface from the horizontal				Touch probe scan picture	Conclusion
	10°	20°	30°	70°		
Tumbling	This surface is dominated by ±0.1 mm deviation range up to 100%, with a tendency to the upper limit. The transition areas (sharp corners) are characterized by a deviation range of (-0.678 to -0.1) mm.	The surface is dominated by ±0.1 mm up to 100%, with a tendency to the lower limit. The transition areas (sharp corner) are characterized by a deviation range of (-0.678 to -0.1) mm.	The surface is dominated by ±0.1 mm up to 100%, with a tendency to the lower limit. The transition areas (sharp corners) are characterized by a deviation range of (-0.678 to -0.1) mm.	A small amount of (-0.513 to -0.348) mm deviation ranges up to 10% appear on the surface, the remaining part, probably being covered by ±0.1 mm deviation ranges.	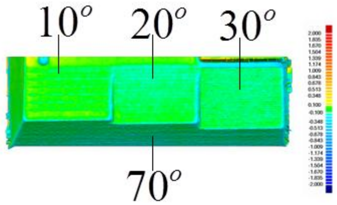	The tumbling technique keeps ±0.1 mm deviation ranges up to 90%. The transition areas or the sharp corners are worn out to be in deviation range of (-0.678 to -0.1) mm.
Shot peening	The surface is dominated by ±0.1 mm, almost up to 100%. The transition areas are characterized by a deviation range of (-0.678 to -0.1) mm.	80% of the surface is dominated by ±0.1 mm and 20% is a uniformly distributed mixture of (-0.348 to -0.1) mm and ±0.1 mm, the latter being more pronounced. The sharp corners are characterized by a deviation range of (-0.678 to -0.1) mm.	The surface is dominated almost up to 90% by ±0.1 mm deviation ranges, the remaining being covered by (0.1 to 0.348) mm pronounced near the transition to the 20° surface angle.	A uniformly distributed combination of ±0.1 mm and (0.1 to 0.513) mm occupies the surface.	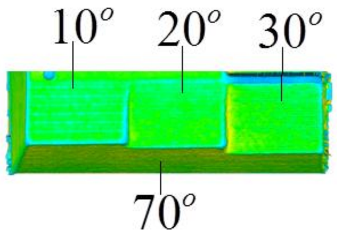	The shot peening process dimension accuracy is kept dominated by the deviation range of ±0.1 mm up to 90%. Some areas have are characterized by ±0.1 mm with a tendency to the lower limit. The transition areas are worn out to be in deviation range of (-0.678 to -0.1) mm.

	Inclination angle of the surface from the horizontal				**Touch probe scan picture**	**Conclusion**
	10°	**20°**	**30°**	**70°**		
Hand finishing	A non-uniformly distributed combination of ±0.1) mm and (0.1 to 0.513) mm deviation ranges, with a predominance of the latter up to 70% characterizes the surface. (-0.513 to -0.1) mm deviation ranges cover the transitions areas.	±0.1 mm deviation ranges dominates a separate area up to 50%, while (0.1 to 0.513 mm) deviation ranges dominate another separate area up to 30%. (-0.513 to -0.1) mm appears up to 20% at the transition edges	Uniformly distributed ±0.1 mm deviation ranges dominate up to 90 %. The remaining 10% constituting the transition areas being covered by. (-0.513 to -0.1) mm.	Not hand finished.	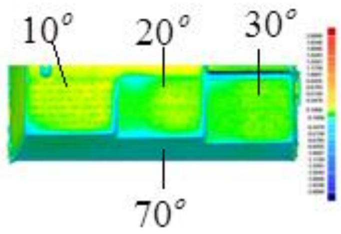	The hand finishing process is not consistent in deviation ranges distribution over the surfaces of the part. The inconsistence can also be observed on one separate surface, where a big contrast is observed over the 20° surface inclination angle. The transition edge areas are worn away during the sanding and negative deviation range of (-0.513 to -0.1) mm are produced.
Spray-painting	(0.1 to 0.844) mm deviation ranges cover the surface almost up to 100%. Non- significant transition areas are covered by ±0.1 mm deviation ranges.	(0.1 to 0.844) mm deviation ranges cover the surface almost up to 100%. Non-significant transition areas are covered by ±0.1 mm deviation ranges.	(0.1 to 0.844) mm deviation ranges cover the surface almost up to 100%. Non-significant transition areas are covered by ±0.1 mm deviation ranges.	The mixture of ±0.1 mm and (0.1 to 0.844) mm) deviation ranges cover the surface.	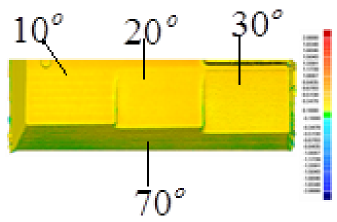	The spray painting raises the deviation range up to 0.844 mm, but maintaining the consistency of the deviation range distribution. The effect of manually performed operation is observed on 70° surface inclination angle where an unevenly distributed paint leads to lack of consistency in deviation range. Non-significant transition areas are not sprayed painted.
CNC Machining	A uniformly distributed (-0.5130 to -0.1) mm deviation ranges cover the surface up to 99%. The deviation range ±0.1 mm appear slightly at transition areas	A uniformly distributed (-0.5130 to -0.1) mm deviation range cover the surface up to 99%. The deviation range ±0.1 mm appear slightly at transition areas	A uniformly distributed (-0.5130 to -0.1) mm deviation ranges cover the surface up to 99%. The deviation range ±0.1 mm appear slightly at transition areas	A uniformly distributed (-0.7333 to -1.050) deviation ranges cover the surface up to 100%.	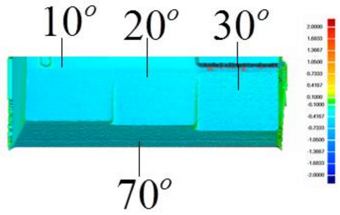	The deviation range of (-0.513 to -0.1) mm dominates the CNC machined part. The trend to negative range is explained by the fact that it strongly possible that there was an error in setting up of the cutting parameters and in calibration of the machine in the vertical direction. The cutting tool has a limited access to small transition areas which remains in a deviation range of ±0.1 mm.

C. Surfaces inclined at 40°, 50° and 60°

Process	**Inclination angle of the surface from the horizontal**			**Touch Probe scan picture**	**Conclusion**
	40°	**50°**	**60°**		
Tumbling	The surface is covered a non-uniformly distributed combination of ±0.1 mm with a tendency to the upper limit and ±0.1 mm with a tendency to the lower limit. The transition areas are covered by (-0.513 to 0.1) mm.	±0.1 mm deviation ranges dominates the surface up to 95%. The transition areas are covered by (-0.513 to 0.1) mm	±0.1 mm deviation ranges dominates the surface up to 95%. The transition areas are covered by (-0.513 to 0.1) mm.	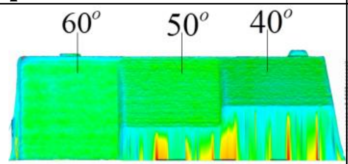	The tumbling technique keeps the deviation ranges in the proximity of ±0.1 mm. The transition area are worn out to produce (-0.513 to -0.1) mm deviation ranges.
Shot peening	±0.1 mm deviation ranges cover the surface almost up to 100%.	80% of the surface is covered by ±0.1 mm deviation ranges. This consists of the big upper part of the surface and small separate zones of the lower part. The remaining 20% of the surface is covered by a uniformly distributed combination of ±0.1 mm and (0.1 to 0.513) mm deviation ranges. The upper transition edge is under (-0.678 to -0.1) mm with a high tendency to the lower limit.	45% of the surface (the upper part) is covered by ±0.1 mm deviation ranges. 55% of the surface (the lower part and the right transition edge) is covered by a non-uniformly combination of ±0.1 mm and (0.1 to 0.513) mm with a predominance of the latter.	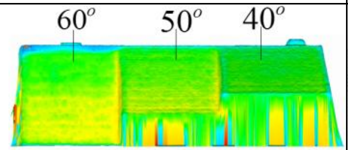	With the shot peening technique, the proportion of the surface covered by ±0.1 mm deviation ranges varies with the inclination angle. The proportion decreases with the increase of the inclination angle. On the lower part of 50° and 60° inclination angles, positive deviation range (0.1 to 0.513) mm characterizes the areas. This unexpected observation may be attributed to scanning error since shot peening is an abrasive process and cannot add material. On the sharp corners, the shots remove the material to produce (-0.678 to -0.1) mm deviation ranges. In general up to 75% of the surfaces are in ±0.1 mm deviation ranges.

Process	Inclination angle of the surface from the horizontal			Touch Probe scan picture	Conclusion
	40°				
Hand finishing	Up to 100%, the surface is dominated by ±0.1 mm, uniformly distributed over the surface. The transition areas and corners are covered by (-0.678 to -0.1) mm deviation ranges with a tendency to the lower limit.	Up to 100%, the surface is dominated by ±0.1 mm, uniformly distributed over the surface. The transition areas and corners are covered by (-0.678 to -0.1) mm deviation ranges with a tendency to the lower limit.	A non-uniformly distributed combination of (-0.678 to -0.1) mm and ±0.1 mm deviation ranges cover the surface. The latter being predominant up to 80%. The transition areas and corners are covered by (-0.678 to -0.1) mm deviation ranges with a tendency to the lower limit.	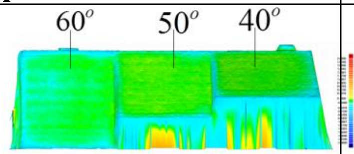	Up to 90% the deviation ranges ±0.1 mm cover the surfaces. The hand finishing technique has kept excellently ±0.1 mm the deviation ranges over the surfaces. The transition areas are worn out to give (-0.678 to -0.1) mm deviation ranges with a tendency to the lower limit.
Spray painting	A uniformly distributed combination of (0.1 to 0.513) mm and (0.513 to 678) mm with a proportion of 45% and 55% respectively.	A uniformly distributed combination of (0.1 to 0.513) mm and (0.513 to 678) mm with a proportion of 55% and 45% respectively.	Almost 100% of the surface is covered by (0.1 to 0.513) mm deviation ranges.	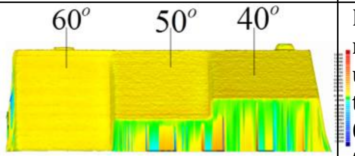	For angles 40° and 50°, the deviation range (0.1 to 0.678) mm maintains a uniform consistent distribution. For 60°, the deviation range becomes (0.1 to 0.513) mm. The increase of the flow of the paint with the increase of the inclination angle can explain the difference in deviation ranges on the faces of 40°, 50° and 60°.
CNC Machining	A uniformly distributed (-0.5130 to -0.1) mm deviation ranges cover the surface up to 99%. The deviation range ±0.1 mm appear slightly at transition areas	A uniformly distributed (-0.513 to -0.1) mm deviation ranges cover the surface up to 99%. The deviation range ±0.1 mm appears slightly at sharp corners.	A uniformly distributed (-0.513 to -0.1) mm deviation range cover the surface up to 99%. A deviation range of ±0.1 mm appear slightly at transition areas	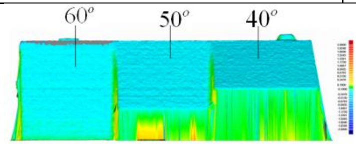	A deviation range of (-0.761 to -0.430) mm dominates the surfaces inclined at 50° and 60° of the CNC machined part. The trend to negative range is explained by the fact that it is strongly possible that there was an error in setting up of the cutting parameters and in calibration of the machine in vertical direction. The cutting tool has a limited access to small transition areas which remains in a deviation range of ±0.1 mm.

APPENDIX 5: VISUAL INSPECTION OF THE DIMENSIONAL ACCURACY FOR ALUMIDE® TEST PIECES

A. Horizontal surfaces, rectangular protrusions, round cavities and conical features

Process	Horizontal surfaces	Small protrusions	Round cavities	Conical features	Touch probe scan picture	Conclusion
Tumbling	The upper horizontal surface is characterized by uniformly distributed combination of ±0.1 mm and (0.1 to 0.513) mm deviation ranges which cover 90%, the remaining 10% being covered by pure (0.1 to 0.513) mm deviation ranges. The deviation ranges (-0.513 to -0.1) mm dominate the transition areas. The lower horizontal surface is characterized by a uniformly distributed combination of ±0.1 mm and (-0.5130 to -0.1) mm.	A non-uniformly distributed deviation ranges of ±0.1 mm and (-0.513 to -0.1) mm cover the horizontal surfaces. Deviation ranges (-0.5130 to -0.1) mm dominate the transition areas.	The deviation ranges ±0.513 mm covers the horizontal surfaces. The deviation range of (-0.513 to -0.1) mm dominate the transition areas	The deviation ranges ±0.513 mm covers the horizontal surfaces. The deviation range of (-0.5130 to -0.1) mm dominate the transition areas	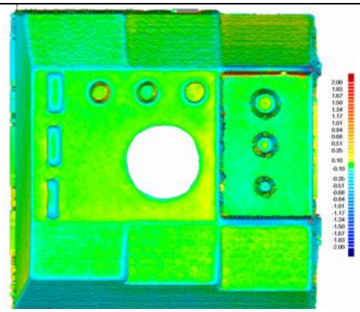	Uniformly distributed combination of deviation ranges ±0.1 mm with (-0.513 to -0.1) mm and (0.1 to 0.513) mm characterizes the horizontal surfaces. The transition areas are dominated by (-0.530 to -0.1) mm deviation ranges. Tumbling process keeps the majority of the surface in deviation ranges of ±0.1 mm. The effect of tumbling is clearly demonstrated at the transition areas and surfaces of small protrusions where negative deviation ranges of (-0.513 to -0.1) mm are observed.

Process	Horizontal surfaces	Small protrusions	Round cavities	Conical features	Touch probe scan picture	Conclusion
Shot peening	A uniform distributed combination of deviation range of ±0.1 mm and (0.1 to 0.5130) mm characterizes the upper surface. The deviation ranges of (-0.513 to -0.1) mm and ±0.1 mm dominate the lower surface up to 80%, the remaining 20% being dominated by a deviation range of ±0 1mm.	A uniform distributed combination of deviation ranges of ±0.1 mm and (0.1 to 0.513) mm with a predominance of ±0.1 mm characterizes the surface. The deviation ranges of (-0.5130 to -0.1) mm characterize some transition areas.	A uniform distributed combination of deviation range of ±0.1 mm and (0.1 to 0.513) mm characterizes the upper surface. The deviation ranges of (-0.5130 to -0.1) mm characterize locally the transition areas.	Uniform distributed combination of deviation range of ±0.1 mm and (0.1 to 0.513) mm with a predominance of (0.1 to 0.513) mm characterizes the upper surface. The periphery areas are characterized by combination of deviation ranges of ±0.1 mm and (0.1 to 0.513) mm	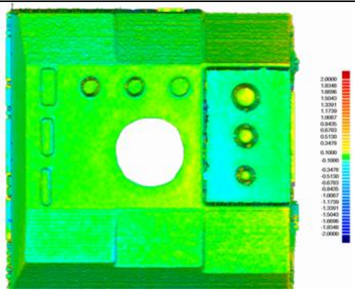	The combination of deviation ranges ±0.1 mm and (0.1 to 0.513) mm, with a predominance of ±0.1 mm is dominant up to 95% on upper horizontal surface, protrusions and conical top surfaces. The deviation ranges of (-0.5130to -0.1) mm dominates also up to 80% the lower horizontal surface. The shot peening process exhibits an excellent uniform distribution of the deviation ranges over the surface. The sharp corners of transition areas are partially removed. With a resolution of 0.1 mm, the shot peening process maintains up to 80% the dimensions in the deviation range of ±0.1 mm.
Hand finishing	The deviation ranges of (0.1 to 0.513) mm characterize 50% of the upper surface, the other half is characterized by a uniformly distributed combination of ±0.1 mm and (0.1 to 0.513) mm. The right side of the lower surface is characterized by a deviation range of ±0.1 mm while the left side is dominated by a uniformly distributed combination of ±0.1 mm and (-0.3478 to -0.1) mm.	The deviation ranges ±0.1 mm dominate the horizontal surface of protrusion 3, a non -uniformly distributed combination of ±0.1 mm and (0.1 to 0.513) mm characterize protrusion 2 and 3. The corners are dominated by (-0.6783 to 0.1) mm.	±0.1 mm deviation ranges characterize the horizontal surface of two holes while a non-uniformly distributed combination of ±0.1 mm and (0.1 to 0.513) mm dominate the bottom surface of third round cavity. The transition areas are characterized by (-0.513 to -0.1) mm deviation ranges.	The deviation ranges of (0.1 to 0.513 are pronounced on the top surfaces. The bottom transition areas are characterized by deviation ranges of (-0.5130 to 0.1) mm.	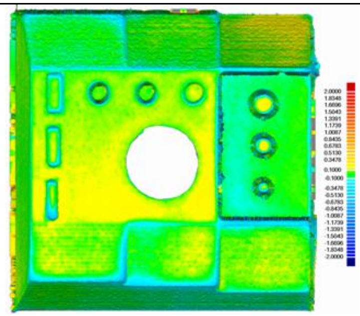	The hand finishing is characterized by a locally uniformly distributed deviation ranges of (-0.5130 to -0.1) mm, ±0.1 mm and (0.1 to 0.513) mm. Over the entire surface the hand finishing does not keep the consistency of the deviation ranges. The sharp corners of transition areas are partially removed, in a non-continuous manner.

Process	Horizontal surfaces	Small protrusions	Round cavities	Conical features	Touch probe scan picture	Conclusion
Spray-painting	Uniformly distributed deviation ranges of (0.5130 to 1.173) mm cover the entire upper surface. The lower surface being characterized by deviation ranges of (0.1 to 0.847) mm.	Uniformly distributed deviation ranges of (0.513 to 1.173) cover the features	The surfaces are characterized by deviation ranges of (0.1 to 0.847) mm. The transitions areas show in non- continuous manner ±0.1 mm deviation ranges.	(0.578 to 1.514) mm) deviation ranges are observed. The transitions areas show in non-continuous manner ±0.1 mm deviation ranges.	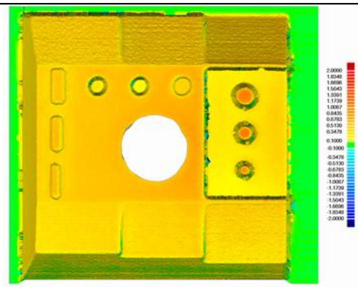	The spray painting displays uniformly distributed deviation ranges of (0.1 to 0.844) mm, (0.513 to 1.173) mm and (0.578 to 1.514) mm, covering different specific areas. Rounded transition areas, some separate negligible areas are not covered well in paint. The spray painting produces significant changes in dimensions of the test piece but being consistent from one area to another.
CNC machining	A uniformly distributed (-0.513 to -0.1) mm deviation ranges cover the surface up to 80%. A uniformly distributed combination of ±0.1 mm and (-0.5130 to -0.1) mm deviation ranges occupy 20% of the surfaces	Almost 100% of the surface is within a deviation range of (-0.513 to -0.1) mm. The transition areas are in ±0.1 mm deviation range.	The bottom surfaces of the round cavities are in ±0.1 mm	100% of the top surface and 60% of the lateral surfaces are in (-0.513 to -0.1) mm deviation ranges whereas 40% of the lateral surfaces is in ±0.1 mm deviation range.	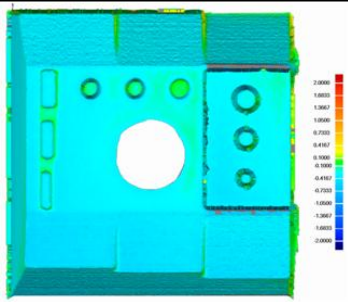	The deviation range of (-0.513 to -0.1) mm dominates the CNC machined test piece. The trend to negative range is explained by the fact that it is strongly possible that there was an error in setting up of the cutting parameters and in calibration of the machine in the vertical direction. The cutting tool has a limited access to small transition areas which remains in deviation range of ±0.1 mm.

B. Surfaces inclined at 10°, 20°, 30° and 70°

Process	Inclination angle of the surface from the horizontal				Touch probe scan picture	Conclusion
	10°	20°	30°	70°		
Tumbling	±0.1 mm deviation ranges cover up to 98% of the surface. The remaining 2% and the transition areas are covered by the deviation range of (-0.5130 to -0.1) mm	±0.1 mm deviation ranges cover up to 100% the surface. The transition areas are covered by the deviation range of (-0.513 to -0.1) mm.	±0.1 mm deviation ranges cover up to 100% the surface. The transition areas are covered by the deviation range of (-0.513 to -0.1) mm.	A uniformly distributed combination of (-0.513 to -0.1) and ±0.1 mm deviation ranges cover the surface.	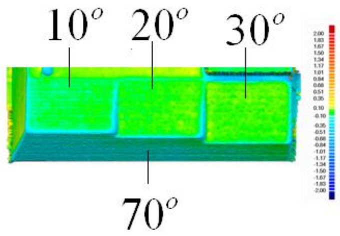	The tumbling process has conserved ±0.1 mm deviation ranges up to practically 100% of surfaces at 10°, 20°, and 30°. The deviation ranges of (-0.513 to -0.1) mm are observed on the surface at 70° meaning that the tumbling process succeeded to reduce the deviation range to approach ±0.1 mm. The transition areas are worn out to be in the deviation range of (-0.513 to -0.1) mm.
Shot peening	±0.1 mm deviation ranges cover up to 80%, the remaining 20% being covered by a uniformly distributed combination of ±0.1 mm and (-0.513 to -0.1) mm with a predominance of ±0.1 mm deviation ranges. The transition areas are in (-0.513 to -0.1) mm deviation ranges.	±0.1 mm deviation ranges cover up to 95%, the remaining 5% being covered by (-0.513 to -0.1) mm, appearing as separate spots near the surface at 10° and transition areas.	±0.1 mm deviation ranges cover up to 95%, the remaining 5% being covered by (0.1 to 0.513) mm, appearing as separate spots at the extreme right end of the surface.	A uniformly distributed combination of (-0.513 to -0.1) mm and ±0.1 mm with a predominance of the latter characterizes 100% the surface.	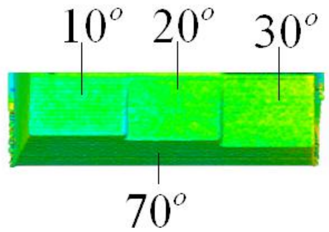	The shot peening process conserves ±0.1 mm deviation range up to 98% of the surfaces, including some of the transition areas. As the process is manual, some transition areas are worn out to give (-0.513 to -0.1) mm deviation ranges. The presence of positive deviation range of (0.1 to 0.513) mm on 20° and 30° surface inclination angles may be attributed to slight delamination resulting in burrs on the surfaces.

Process	Inclination angle of the surface from the horizontal				Touch probe scan picture	Conclusion
	10°	20°	30°	70°		
Hand finishing	A non -uniformly distributed combination of ±0.1 mm and (0.1 to 0.513) mm deviation range cover the surface. (-0.513 to -0.1) mm deviation range characterize the transition areas	A non-uniformly distributed combination of ±0.1 mm and (0.1 to 0.513) mm deviation range cover the surface. (-0.513 to -0.1) mm deviation range characterize the transition areas	A non -uniformly distributed combination of ±0.1 mm and (0.1 to 0.513) deviation range cover the surface. (-0.513 to -0.1) mm deviation range characterize the transition areas.	A uniformly distributed combination of (-0.513 to -0.1) mm and ±0.1 mm with a predominance of the latter characterizes 100% of the surface.	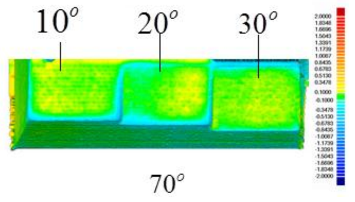	Over the surfaces at 10°, 20° and 30°, the hand finishing process produces a wide non- uniformly distributed deviation range (-0.1 to 0.513) mm over the surfaces. The transition areas are worn out and deviation ranges (-0.513 to -0.1) mm are observed. Uniformly distributed deviation ranges of (-0.513 to 0.1) mm are observed at the 70°surface. The hand finishing process is not consistent in distribution of deviation ranges.
Spray painting	Uniformly distributed deviation ranges of (0.1 to 0.844) mm, are observed and cover 100% of the surface. ±0.1 mm deviation ranges appear at transition areas.	Uniformly distributed deviation ranges of (0.1 to 0.844) mm, are observed and cover 100% of the surface. ±0.1 mm deviation ranges appear at transition areas.	Uniformly distributed deviation ranges of (0.1 to 0.844) mm, are observed and cover 100% of the surface. ±0.1 mm deviation ranges appear at transition areas.	Uniformly distributed deviation ranges of (0.1 to 0.844) mm, are observed and cover 100% of the surface. ±0.1 mm deviation ranges appear at transition areas.	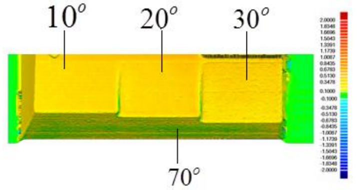	The spray painting exhibits wide (0.1 to 0.844) mm and excellently consistent deviation ranges. Because of surface tension the paint draws away from the transition areas resulting in a thin coverage within the ±0.1 mm deviation range.
CNC Machining	A uniformly distributed (-0.513 to -0.1) mm deviation ranges cover the surface up to 99%. A deviation range of ±0.1 mm appears at transition areas.	A uniformly distributed (-0.513 to -0.1) mm deviation ranges cover the surface up to 99%. A deviation range of ±0.1 mm appears at transition areas.	A uniformly distributed (-0.513 to -0.1) mm deviation ranges cover the surface up to 99%. A deviation range of ±0.1 mm appears at transition areas.	A uniformly distributed (-0.733 to -1.050) mm deviation ranges cover the surface up to 100%.	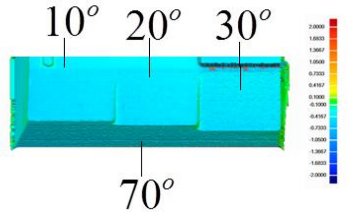	The deviation range of (-0.513 to -0.1) mm dominates the CNC machined test piece. The trend to negative range is explained by the fact that it strongly possible that there was an error in setting up of the cutting parameters and in calibration of the machine in vertical direction. The cutting tool has a limited access to small transition areas which remains in a deviation range of ±0.1 mm.

C. Surfaces inclined at 40°, 50° and 60°

Process	Inclination angle of the surface from the horizontal			Touch probe scan picture	Conclusion
	40°	50°	60°		
Tumbling	±0.1 mm deviation ranges cover up to 95% the surface. The remaining 5% is covered by (-0.348 to -0.1) mm deviation ranges which appear as separate spots in different places. The transition areas are in (-0.678 to -0.1) mm deviation ranges.	±0.1 mm deviation ranges cover almost 100% the surface. The transition areas are in (-0.678 to -0.1) mm deviation ranges.	±0.1 mm deviation ranges cover the upper part of the surface which approximately represents 50% of the entire surface. The remaining 50% are covered by a non-uniformly distributed combination of ±0.1 mm and (0.1 to 0.513) mm. The transition areas are in the (-0.678 to -0.1) mm deviation ranges.	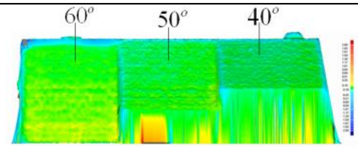	The tumbling process has conserved ±0.1 mm deviation ranges up to practically 100% of surfaces at 40°, 50° and the half of the surface at 60°. The positive deviation range observed at the lower part of the surface at 60°, probably is a touch probe scanning error. In general, the tumbling process exhibits a very good conservation of the deviation range at the level of ±0.1 mm.
Shot peening	±0.1 deviation ranges cover up to 95% of the surface, including the transition areas. The remaining 5% is covered by (-0.348 to -0.mm) deviation ranges which appear as separate spots in different places.	±0.1 mm deviation ranges cover almost 100% of the surface, including the transition areas.	±0.1 mm deviation ranges cover the upper part of the surface which approximately represents 90% of the entire surface. The remaining 10%, near the left side of the surface are covered by a non-uniformly distributed combination of ±0.1 mm and (0.1 to 0.513) mm, with a predominance of (0.1 to 0.513) mm.	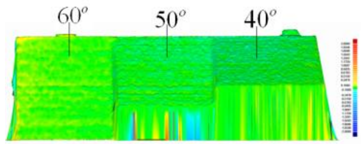	The shot peening process has conserved ±0.1 mm deviation ranges up to practically 100% of surfaces at 40°, 50° and up to 90% of the surface at 60°. The positive deviation range observed at the left end of the part on the surface at 60° is probably a result of scanning fault. The transition areas are kept in deviation ranges of ±.1 mm, with exception of the left edge. In general, the shot peening process exhibits an excellent conservation of the deviation ranges at the level of ±0.1 mm.

Process	Inclination angle of the surface from the horizontal			Touch probe scan picture	Conclusion
	40°	50°	60°		
Hand finishing	±0.1 mm deviation ranges cover almost 100% of the surface. Transition areas are in (-0.678 to -0.1) mm deviation ranges.	±0.1 mm deviation ranges cover almost 100% of the surface. Transition areas are in (-0.678 to -0.1) mm deviation ranges.	Three non-uniformly distributed deviation ranges are observed: ±0.1 mm, a combination of ±0.1 mm and (0.1 -0.513) mm and (0.1 -0.513) mm. Transition areas are in (-0.678 to -0.1) mm deviation ranges.	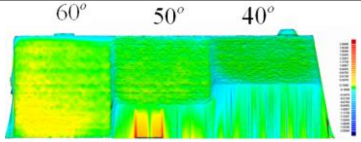	The hand finishing technique displays a very good conservation of the deviation range on surfaces at 40° and 50°. This trend is not conserved when working on a surface at 60°, which the smoothest surface among the three surfaces. In general the hand finishing displayer a good conservation of deviation range at the level of ±0.1 mm, with exclusion of small areas where the sanding operation did not succeed to remove the excess material.
Spray painting	(0.1 to 0.844) mm deviation ranges, uniformly distributed are obtained and cover 100% of the surface. ±0.1 mm deviation ranges appear at transition areas.	(0.1 to 0.844) mm deviation ranges, uniformly distributed are obtained and cover 100% the surface. ±0.1mm deviation ranges appear at transition areas.	(0.1 to 0.844) mm deviation ranges, uniformly distributed are obtained and cover 100% the surface. ±0.1 mm deviation ranges appear at transition areas	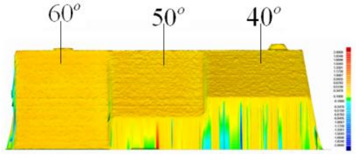	The spray painting exhibits wide (0.1 to 0.844) mm deviation range in a uniform consistent manner through surfaces. Because of surface tension the paint draws away from the transition areas resulting in a thin coverage within the ±0.1 mm deviation range.
CNC machining	A uniformly distributed (-0.513 to -0.1) mm deviation ranges cover the surface up to 99%. A deviation range of ±0.1 mm appears at transition areas.	A uniformly distributed (-0.513 to -0.1) mm deviation ranges cover the surface up to 99%. A deviation range of ±0.1 mm appears at transition areas.	A uniformly distributed (-0.513 to -0.1) mm deviation ranges cover the surface up to 99%. A deviation range of ±0.1 mm appears at transition areas.	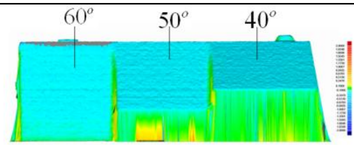	A deviation range of (-0.513 to -0.1 mm) dominates the CNC machined part. The trend to negative range is explained by the fact that it strongly possible that there was an error in setting up of the cutting parameters and in calibration of the machine in vertical direction. The cutting tool has a limited access to small transition areas which remains in deviation range of ±0.1 mm.

APPENDIX 6: VISUAL INSPECTION OF THE DIMENSIONAL ACCURACY FOR ABS TEST PIECES

A. Horizontal surfaces, rectangular protrusions, round cavities and conical features

Process	Horizontal surfaces	Small protrusions	Round cavities	Conical features	Touch probe scan picture	Conclusion
Tumbling	±0.1 mm deviation ranges covers 100% of the upper and lower surface. The transition areas are in the (-0.513 to -0.100) mm deviation range.	Deviation ranges of ±0.1 mm, (-0.513 to -0.1) mm, (-0.843 to -0.1) mm and (-1.339 to -0.843) mm are observed.	±0.1 mm deviation ranges covers 100% of the surface. The transition areas are in the (-0.513 to -0.1) mm deviation range.	The conical features are out of the specified extreme ranges.	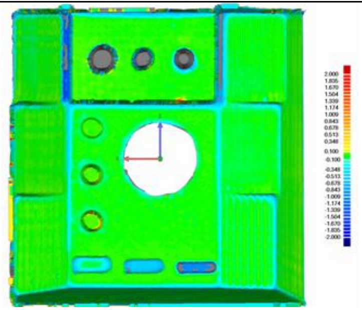	The tumbling exhibits an excellent conservation of ±0.1 mm deviation ranges on horizontal surfaces. The transition areas are worn away to be in deviation range of (-0.513 to -0.1) mm. The small protrusions are extremely worn away to reach (-1.339 to -0.843) mm deviation ranges. The conical features are broken off. The tumbling process works excellently with horizontal surfaces but it rounds the sharp corners.
Shot peening	±0.1 mm deviation ranges covers 100% of the upper and lower surface. Some zones of the transition areas are in (-0.513 to -0.1) mm deviation ranges.	Two protrusions are dominated by ±0.1 mm deviation ranges up to 90% with the remaining 10% near the transition areas covered by (-0.513 to -0.1) mm deviation ranges.	±0.1 mm deviation ranges covers almost up to 100% of the bottom surface of the round cavities.	Deviation ranges (0.1 to 0.513) mm, ±0.1 mm, (-0.513 to -0.1 mm), (-0.843 to -0.1) mm and (-1.339 to -0.843) mm are observed.	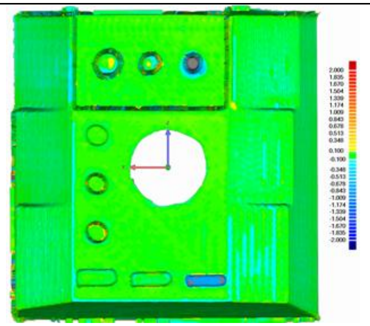	The shot peening technique keeps ±0.1 mm deviation ranges on the horizontal surfaces. The shot peening technique affects the protrusions in different ways: as the process is conducted manually, on some areas the shots compress the material; this is observed on one protrusion and regions of transition areas. The smallest conical feature is broken off while the other two are also partially broken off.

Process	Horizontal surfaces	Small protrusions	Round cavities	Conical features	Touch probe scan picture	Conclusion
Hand finishing	A non-uniformly distributed combination of ±0.1 mm and (0.1 to 0.513) mm deviation ranges, with a predominance of the latter, covers the upper and lower surfaces. The deviation ranges (-0.513 to -0.1) mm are observed on some regions of transition areas.	A non-uniformly distributed combination of (-0.513 to -0.1) mm, ±0.1 mm and (0.1 to 0.513) mm deviation ranges, with a predominance of the latter, covers the surface of two protrusions. The other protrusion are characterized by deviation ranges of (-1.009 to -0.513) mm.	A uniformly distributed combination of ±0.1 mm and (0.1 to 0.513) mm characterizes the bottom surfaces of the round cavities. The transition area being under (-0.513 to -0.1) mm deviation ranges.	A noticeable contrast among the three conical features: From (-0.513 to -1.174) mm to (-0.1 to 0.513) mm, and out of range.	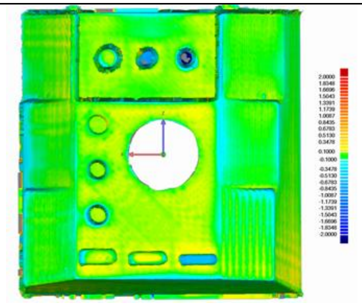	The hand finishing is satisfactory consistent on big horizontal surfaces in keeping a wide deviation range (-0.1 to 0.513) mm. For small conical features, the consistence is reduced and the difference is significant. The smallest conical feature is broken off while the middle feature is extremely damaged to the point to be broken away. The transition areas are worn away by the sanding process. The hand finishing is not consistent in keeping uniform distribution of deviation ranges across individual surfaces and small features. In particular, ±0.1 mm deviation ranges is poorly covered.
Spray-painting	A uniformly distributed combination of (0.1 to 0.513) mm and (0.513 to 1.009) mm deviation ranges is observed on both upper and low horizontal surfaces.	A uniformly distributed (0.1 to 0.513) mm deviation range is observed. The deviation ranges ±0.1 mm appear at corners in the form of small spots.	A uniformly distributed (0.1 to 0.513) mm deviation range is observed. The deviation ranges ±0.1 mm appear at transition areas.	A non-uniformly distributed combination of (0.1 to 0.513) mm and (0.513 to 1.009) mm deviation ranges is observed on the top surfaces. The deviation ranges ±0.1 mm appear at the base of the features.	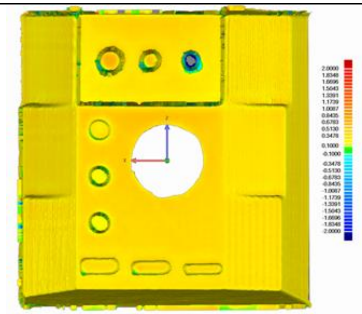	The spray painting technique displays a good consistence in deviation ranges. Some transition areas and separate miniscule areas in the form of small spots are not spray-painted. This may be caused by the flow of the paints from these areas due to fluid surface tension when the paint is still wet.

Process	Horizontal surfaces	Small protrusions	Round cavities	Conical features	Touch probe scan picture	Conclusion
Chemical treatment	A uniformly distributed combination of ±0.1 mm and (0.1 to 0.513) mm deviation ranges cover the both upper and lower horizontal surfaces. One transition area is characterized by (-0.513 to -0.1) mm deviation ranges.	(-0.5130 to -0.1) mm deviation ranges cover the sharp corners and the horizontal surface of the protrusion 3. ±0.1 mm characterize the top surface of the protrusion 2 and a combination of ±0.1 mm and (0.1-0.5130) mm characterizes the protrusion 1.	±0.1 mm, (0.1 to 0.530) mm and their combination in different proportions are observed. (-0.513 to 0.1) mm cover the transition areas.	(-0.513 to -0.1) mm and ±0.1 mm cover the top areas of the conical features.	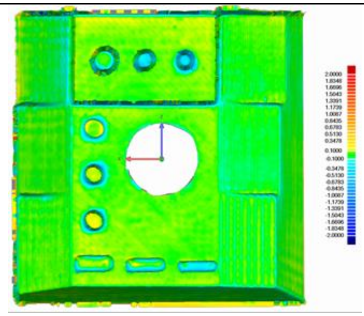	The chemical treatment was able to remove materials from the transition areas by keeping the deviation range of the horizontal surfaces in (-0.1 to 0.513) mm with a predominance of ±0.1 mm). The small elements such as protrusions and the conical features are dissolved into acetone at room temperature for a period of 60 s.
CNC machining	A uniformly distributed (-0.513 to -0.1) mm deviation ranges cover the surface up to 80%. A uniformly distributed combination of ±0.1 mm and (-0.513 to -0.1) mm deviation ranges occupy 20% of the surfaces	Almost 100% of the surface is within a deviation range of (-0.513 to -0.1) mm. The transition areas are in ±0.1 mm deviation range.	The bottom surface of the round cavities are in ±0.1 mm	100% of the top surface and 60% of the lateral surfaces are in (-0.513 to -0.1 mm) deviation ranges whereas 40% of the lateral surfaces is in ±0.1 mm deviation range.	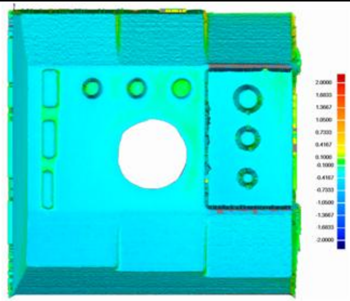	The deviation range of (-0.513 to -0.1 mm) dominates the CNC machined test piece. The trend to negative range is explained by the fact that it strongly possible that there was an error in setting up of the cutting parameters and in calibration of the machine in vertical direction. The cutting tool has a limited access to small transition areas which remains in deviation range of ±0.1 mm.

B. Surfaces inclined at 10°, 20°, 30° and 70°

Process	Inclination angle of the surface from the horizontal				Touch probe scan picture	Conclusion
	10°	20°	30°	70°		
Tumbling	±0.1 mm deviation ranges covers 100% of the upper and lower surface. The transition areas are in (-0.348 to -0.1) mm deviation ranges.	±0.1 mm deviation ranges covers 100% of the upper and lower surface. The transition areas are in (-0.348 to -0.1) mm deviation ranges.	±0.1 mm deviation ranges covers 100% of the upper and lower surface. The transition areas are in (-0.348 to -0.1) mm deviation ranges.	±0.1 mm deviation ranges covers 100% of the upper and lower surface. The transition areas are in (-0.348 to -0.1) mm deviation ranges.	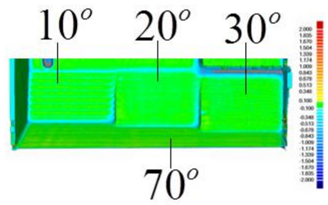	The tumbling exhibits an excellent conservation of ±0.1 mm deviation ranges on surfaces inclined at 10°, 20°, 30° and 70°. The transition areas are worn out to be in deviation range of (-0.348 to -0.1) mm.
Shot peening	Deviation ranges (-0.687 to -0.1) mm cover 30% of the surface made by series of seven thin horizontal bands, parallel to layers are observed. The remaining part of the surface is covered by a deviation range of ±0.1 mm.	Deviation ranges (-0.687 to -0.1) mm cover 10% of the surface made by two thin horizontal bands, parallel to the layers. 20% of the surface is covered by a non-uniformly distributed combination ±0.1 mm and (-0.687 to -0.1) mm deviation ranges. 70% is covered by ±0.1 mm deviation ranges.	A non-uniformly distributed combination of ±0.1 mm and (-0.687 to -0.1) mm deviation ranges cover 30% of the surface. 70% of the surface are covered by ±0.1 mm deviation ranges	Almost 100% of the surface is covered by ±0.1 mm deviation ranges.	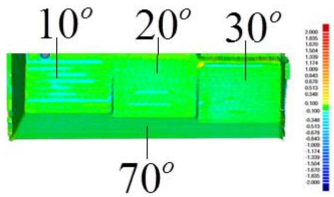	The shot peening techniques removes the hills which results from the stair-step effect of the FDM process. This is more pronounced on the surface at 10° of inclination, at 20° the effect is reduced and at 30°, the effect disappear resulting in a region of combination of ±0.1 mm and (-0.678 to -0.1) mm deviation ranges at the centre of the surface. In general, the predominance of ±0.1 mm deviation ranges increases with the increase of the inclination angle. At a surface inclined at 70°, a deviation range of±0.1 mm covers almost 100% of the surface. The shot peening techniques removes sharp corners (transition areas and hills) and conserves ±0.1 mm deviation ranges over 80% of the surfaces.

Process	Inclination angle of the surface from the horizontal				Touch probe scan picture	Conclusion
	10°	20°	30°	70°		
Hand finishing	On the left side of the surface, a series of thin horizontal bands parallel to layers are in the (0.1 to 0.348) mm deviation range. These bands extend to be covered by ±0.1 mm deviation ranges. On the right side of the surface, a series of similar bands in (-0.678 to -0.1) mm extend to the left side to present ±0.1 mm deviation ranges. At the centre of the surface, the horizontal bands made by a combinations of ±0.1 mm, (0.1 to 0.348) mm and (-0.678 to -0.1) mm are observed.	The upper and lower parts of the surface are in the (-0.678 to -0.1) mm deviation range and the remaining part which cover 80% is in the ±0.1 mm deviation range.	The upper and lower transition areas are in the (-0.678 to -0.1) mm deviation range and the remaining part which cover 90% is in the ±0.1 mm deviation range.	The left part (40%) is covered by a non-uniformly distributed combination of ±0.1 mm and (0.1 to 0.348) mm. The remaining right part is covered by the ±0.1 mm deviation range.	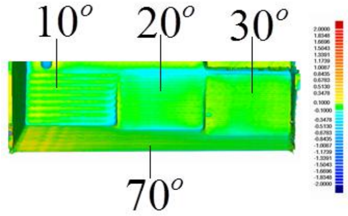	The priming adds material in the valleys and the sanding removes materials from the hills. The adding and removing of the material is not consistent across the surface, the reason why a contrast between separate areas of a given surface is observed. This is more pronounced on the surface with 10° inclination angle as a surface where the stair step effect is more dominating. The % of the areas which is covered by the deviation range of ±0.1 mm increases as the inclination angle increases. The hand finishing is not consistent in distribution of deviation ranges; however the deviation ranges of ±0.1 mm cover 70% of the surfaces.
Spray painting	A uniformly distributed (0.1 to 0.513) mm deviation ranges is observed.	A uniformly distributed (0.1 to 0.513) mm deviation ranges is observed.	A uniformly distributed (0.1 to 0.513) mm deviation ranges is observed.	A uniformly distributed (0.1 to 0.513) mm deviation ranges is observed.	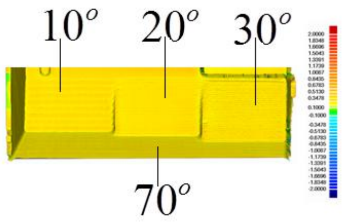	The spray painting technique displays a good consistence in (0.1 to 0.513) mm deviation ranges.

Process	Inclination angle of the surface from the horizontal				Touch probe scan picture	Conclusion
	10°	20°	30°	70°		
Chemical treatment	Non-uniformly distributed combinations of (-0.348 to 0.1) mm, ±0.1 mm and (0.1 to 0.348) mm appearing in the form of horizontal bands, with a high predominance of ±0.1 mm cover the surface.	Non-uniform distributed combination of (-0.348 to -0.1) mm and ±0.1 mm deviation ranges, with a high predominance of the latter, covers the surface. It can be said that almost 100% of the surface is covered by the ±0.1 mm range.	Non- uniformly distributed combinations of (-0.348 to 0.1) mm, ±0.1 mm and (0.1 to 0.348) mm, with a high predominance of ±0.1 mm cover the surface. The (-.348 to -0.1) mm deviation ranges are pronounced on upper and lower transition areas.	Non- uniformly distributed combinations of (-0.348 to 0.1) mm, ±0.1 mm and (0.1 to 0.348) mm, with a high predominance of ±0.1 mm cover the surface. The (-.348 to -0.1) mm deviation ranges are pronounced on upper and lower edges.	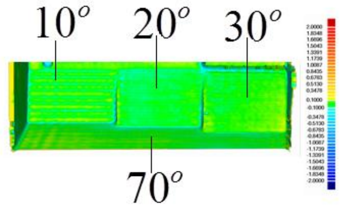	The chemical treatment with acetone produces deviation ranges in the proximity of ±0.1 mm. Immersion of ABS test piece into an acetone bath at room temperature for a period of 60s dissolved the stair stepped surface and the dimensional deviation ranges were kept in proximity of ±0.1 mm. (-0.348 to -0.1) mm deviation ranges are pronounced on upper and lower edges (sharp corners).
CNC machining	A uniformly distributed (-0.513 to -0.1) mm deviation range covers the surface up to 99%. The deviation range ±0.1 mm appears slightly at transition areas.	A uniformly distributed (-0.513 to -0.1) mm deviation range covers the surface up to 99%. The deviation range ±0.1 mm appears slightly at transition areas.	A uniformly distributed (-0.513 to -0.1) mm deviation range covers the surface up to 99%. The deviation range ±0.1 mm appears at transition areas.	A uniformly distributed (-0.733 to -1.050) mm deviation range covers the surface up to 100%.	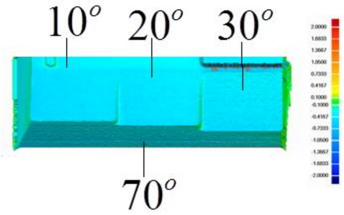	The deviation range of (-0.513 to -0.1) mm dominates the CNC machined test piece. The trend to the negative range is explained by the fact that it strongly possible that there was an error in setting up of the cutting parameters and in calibration of the machine in vertical direction. The cutting tool has a limited access to small transition areas which remains in deviation range of ±0.1 mm.

C. Surfaces inclined at 40°, 50° and 60°

Process	**Inclination angle of the surface from the horizontal**			**Touch Probe scan picture**	**Conclusion**
	40°	**50°**	**60°**		
Tumbling	±0.1 mm deviation ranges covers 100% of the upper and lower surface. The transition areas are in the (-0.348 to -0.1) mm deviation range.	±0.1 mm deviation ranges covers 100% of the upper and lower surface. The transition areas are in the (-0.348 to -0.1) mm deviation range.	±0.1 mm deviation ranges covers 100% of the upper and lower surface. The transition areas are in the (-0.348 to -0.1) mm deviation range.	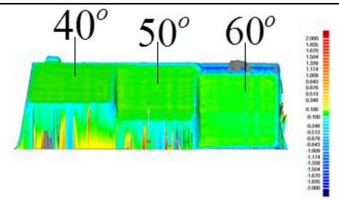	Tumbling exhibits an excellent conservation of ±0.1 mm deviation ranges on surfaces inclined at 10°, 40°, 50° and 60°. The transition areas are worn out to be in the deviation range of (-0.348 to -0.1) mm.
Shot peening	A uniformly distributed combination of (-0.348 to -0.1) mm and ±0.1 mm deviation ranges, with a high predominance of ±0.1 mm deviation range cover the surface.	A uniformly distributed combination of (-0.348 to -0.1) mm and ±0.1 mm deviation ranges, with a high predominance of ±0.1 mm deviation range cover the surface.	A uniformly distributed combination of (-0.348 to -0.1) mm and ±0.1 mm deviation ranges, with a high predominance of ±0.1 mm deviation range cover the surface.	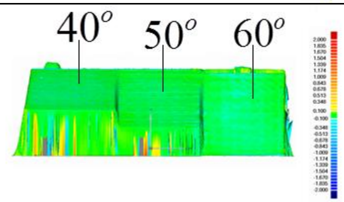	The shot peening technique conserves excellently the deviation ranges in proximity of ±0.1 mm.
Hand finishing	A uniformly distributed combination of ±0.1 mm and (0.1 to 0.348) mm, with a high predominance of ±0.1 mm cover the surface. The (-.348 to -0.1) mm deviation range is pronounced on the transition areas.	Non- uniformly distributed combination of (-0.348 to 0.1) mm, ±0.1 mm and (0.1 to 0.348) mm, with a high predominance of ±0.1 mm cover the surface. The (-0.348 to -0.1) mm deviation ranges are pronounced on upper and lower transition areas.	Non- uniformly distributed combinations of (-0.348 to 0.1) mm, ±0.1 mm and (0.1 to 0.348) mm, with a high predominance of ±0.1 mm cover the surface.	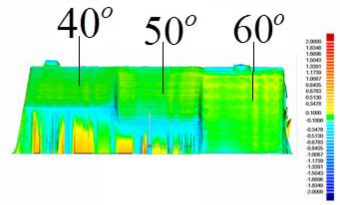	During the priming and the sanding processes, the adding and removing of the material are not consistent across an individual surface, the reason why a contrast between separate areas of a given surface is observed. This is more pronounced on the surface with 60º inclination angle as a surface where the stair step effect is less dominating. The hand finishing produces ±0.348 mm deviation ranges with non-uniform distribution over the surfaces.
Spray painting	A uniformly distributed (0.1 to 0.678) mm deviation ranges is observed	A uniformly distributed (0.1 to 0.678) mm deviation ranges is observed	A uniform distributed combination of (0.1 to 0.513) mm and (0.1 to 0.678) mm covers the surface.	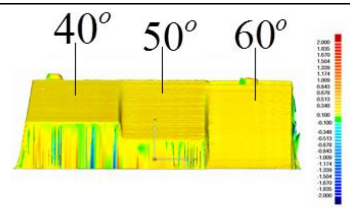	The spray painting technique displays a good consistence in (0.1 to 0.678) mm.

Process	Inclination angle of the surface from the horizontal			Touch Probe scan picture	Conclusion
	40°	**50°**	**60°**		
Chemical treatment	±0.1 mm deviation range covers the surface up to 100%.	±0.1 mm deviation range covers the surface up to 100%.	±0.1 mm deviation range covers the surface up to 80%. (-0.348 to -0.1) mm cover 10% at the upper transition area and (0.1 to -0.135) mm cover 10% at the low edge of the surface.	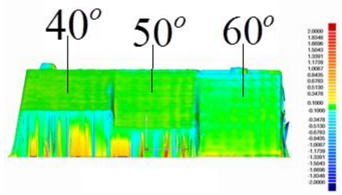	The chemical treatment with acetone produces deviation ranges in proximity of ±0.1 mm. Immersion of ABS test piece into an acetone bath at room temperature for period of 60 s dissolved the stair stepped surface and the dimensional deviation ranges were kept in proximity of ±0.1 mm. The (-0.348 to -0.1) mm deviation ranges observed on the region closed to the upper edge of a surface inclined at 60° indicates that the sharp edges are worn away by acetone.
CNC machining	A uniformly distributed (-0.513 to -0.1) mm deviation ranges cover the surface up to 99%. The deviation range ±0.1 mm appears at transition areas.	A uniformly distributed (-0.513 to -0.1) mm deviation ranges cover the surface up to 99%. The deviation range ±0.1 mm appears at transition areas.	A uniformly distributed (-0.513 to -0.1) mm deviation ranges cover the surface up to 99%. The deviation range ±0.1 mm appears at transition areas.	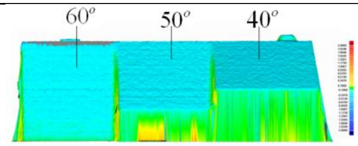	The deviation range of (-0.513 to -0.1) mm dominates the CNC machined test piece. Extra material has been removed from surfaces. The cutting tool has a limited access to small transition areas which remains in deviation range of ±0.1 mm.